UNIVERSITY OF CALIFORNIA

SANTA CRUZ

FROM CANE TO CORAL REEFS: ECOSYSTEM CONNECTIVITY AND DOWNSTREAM RESPONSES TO LAND USE INTENSIFICATION

A dissertation submitted in partial satisfaction
of the requirements for the degree of

DOCTOR OF PHILOSOPHY

in

ECOLOGY AND EVOLUTIONARY BIOLOGY

by

Stacy D. Jupiter

September 2006

The Dissertation of Stacy D. Jupiter is approved:

Professor Laurel R. Fox, Chair

Professor Donald C. Potts

Professor Daniel F. Doak

Professor Stuart R. Phinn

Lisa C. Sloan
Vice Provost and Dean of Graduate Studies

Table of Contents

Chapter 1. Connectivity in Natural versus Anthropogenic Systems

Chapter 2. Land Use in the Pioneer Catchment: Changes in Cleared and Riparian Areas Interpreted in a Historical Context

(Chapter 2 cont.)

Chapter 3. Natural and Anthropogenic Changes to Mangrove Distributions in the Pioneer River Estuary

Chapter 4. Geochemical Proxies for Delivery of Suspended Sediment to Nearshore Waters off Mackay

(Chapter 4 cont.)

Chapter 5. Coral Rare Earth Elements and Yttrium (REY) from Inshore and Midshelf Islands off Mackay

Chapter 6. A Synthesis of Land Cover Change, Water Quality Proxies and Reef Communities: Are Mackay Coral Reefs in Jeopardy?

(Chapter 6 cont.)

List of Tables

List of Figures

Abstract

From Cane to Coral Reefs: Ecosystem Connectivity and Downstream Responses to Land Use Intensification

Stacy D. Jupiter

Clearing of catchments draining into the Great Barrier Reef Lagoon (Queensland, Australia) has increased sediment and nutrient loads in river runoff. The extent of land cover change and the intensification of land use were analyzed for the Pioneer River catchment near Mackay (from Landsat images, 1972-2004), and for the estuary (from aerial photographs, 1948-2002), to determine whether and how loss of natural vegetation has affected sediment delivery to nearshore waters and adjacent coral reefs. Geochemical proxy records of weathering and sediment delivery to the sea, deposited in skeletons of living *Porites* corals from inshore (5 km from Pioneer mouth) and midshelf (32-51 km offshore) reefs, were analyzed to determine the spatial and temporal extent of terrestrial impacts. High-temporal resolution (~weekly) concentrations of barium (Ba), yttrium (Y) and calcium (Ca) were measured by laser ablation inductively-coupled mass spectrometry (LA-ICP-MS), while annual samples of rare earth elements and yttrium (REY) were measured by solution ICP-MS. Major trends emerging from integration of contemporaneous terrestrial changes, marine geochemical proxies and climate records include: 1. A 33% net decline (1972-2004) of forests on alluvial plains as farms encroached into riparian zones; and a 22% net decline (1948-2002) of tidal mangroves in the estuary. 2. Ba/Ca correlations with Pioneer River discharge were influenced by wind direction and strength; but there was no apparent temporal change in Ba/Ca since 1946. The absence of enrichment in mean inshore Ba/Ca ratios (versus midshelf reefs) may be due to biological recycling by phytoplankton, which may restrict Ba availability. 3. Mean Y/Ca ratios from inshore (5 km) corals were 3.1 and 3.6 times higher than from midshelf (32 and 51 km) corals, and inshore REY abundances were ~2-5 times higher than from mishelf reefs. Inter-annual REY variation on both inshore and midshelf sites was correlated significantly with year and discharge, while long-term temporal trends in maximum annual Y/Ca, normalized to Pioneer River discharge, appear to reflect both agricultural expansion and changing management practices. 4. The combination of high turbidity and high nutrient discharge from the Pioneer River may be affecting benthic community composition on both inshore and midshelf reefs.

Acknowledgements

First and foremost, I dedicate my thesis to Maureen Cooper of Padaminka Nature Refuge in Walkerston, Queensland, Australia. I have never met a more perseverant environmentalist or gracious human being. She has been a wonderful inspiration to my research and an overly generous host during my often lengthy field visits to Mackay. It is because of her that I consider Mackay another home.

Because my research has been a truly integrative effort across disciplines, I have many people to thank for their patience while I learned new fields and for their eagerness to participate. Above all, I thank Guy Marion for his willingness to embark upon a major collaboration that allowed us to produce a story that really goes beyond the sum of its parts. And through our tag-team science we have built a lasting friendship.

Special appreciation goes to the Australian-American Fulbright Foundation who made all of my connections in Australia possible at the University of Queensland (UQ), the Australian National University (ANU) and in Mackay. At the University of Queensland, I thank my supervisor, Stuart Phinn, for his tolerance of my unpredictable fieldwork schedules, his ability to return a draft by the next day and his unflagging support of my project. Norm Duke, in the Marine Botany Group, motivated me to choose Mackay as a study region through his enthusiasm for mangroves and his dedication to environmental causes. Ove Hoegh Guldberg, director of the Centre for Marine Studies, kept me passionate about coral reefs and

showed me that working hard and playing hard *always* go together. Both Balz Kamber and Michael Lawrence at the Advanced Centre for Queensland University Research Excellence (ACQUIRE) facility patiently gave support and answered my many questions as I struggled to master rare earth element geochemistry. I thank Alan Grieg at ACQUIRE, and Jurgen Overhue and Alan Victor at the Centre for Remote Sensing and Spatial Information Science (CRSSIS), for technical laboratory and computing support; and I thank the students and staff in the CRSSIS, Marine Botany and Centre for Marine Studies research groups for making me feel welcome and giving feedback on my project.

At the Australian National University, above all I am enormously grateful to Malcolm McCulloch at the Research School of Earth Sciences (RSES) for sharing his laboratory and expert knowledge of coral geochemistry. Without assistance from Les Kinsley, I would never have been able to operate the mass spectrometers. Tim Wyndham, Sam Burgess and Bridget Ayling helped introduce me to the art of making sense out of laser ablation data and provided moral support during 3 am laser runs. I am also grateful to the RSES workshop staff for all of the coring gear and assistance with the “Grunter”, and to Stuart Hay at ANU Photography for his ingenuity in photographing coral luminescence bands.

None of my work in the field would have been accomplished without teams of loyal volunteers and dedicated citizens of Mackay. Foremost, I thank Warren and Barbara Hill of Queensland Trochus and Diving Ltd. for their intimate knowledge of the Mackay section of the Great Barrier Reef. Warren pulled us through some hairy weather conditions on his workhorse of a boat, the Lara Star, while Barbara kept us well fed and smiling after every dive. We would never have been able to locate the vessel without the help of resident dive guru, Mark Earney, who always provided dive contacts for me and filled my tanks at the fire station when all of the dive shops disappeared from Mackay. Ian “Cap’n Havachat” Finnel, Jim Ryman, Eddie Roggenveen and Bruce Pettingal also provided critical dive assistance with boats and gear. Andrew Christian, Maoz Fine, Meegan Henderson, Michelle Jonkers, Paulina Kaniewska, Diana Kleine, Kate Moore, Jill Quaintance, Verena Schrameyer, and Chris Shaw all assisted on diving trips and were great companions aboard the Lara Star. For my mangrove work, I am indebted to Judith Wake (from Central Queensland University), Greg Tooth, Judith Johnstone, members of the Mackay Conservation Group (particularly Patricia Julien and Maureen Cooper for slogging through the mud), and Noel Whitehead (of Sunfish Mackay) for updating me on the history of the mangrove dieback.

Through our Australian Research Council (ARC) Linkage grant LP0560896, I received both financial and expert assistance from the Great Barrier Reef Marine Park Authority (GBRMPA), the Mackay-Whitsunday Natural Resource Management Group (MWNRM) and the Mackay City Council (MCC). I would like to thank the individuals that helped secure the successful partnerships: David Haynes and Lawrence McCook (GBRMPA); Julia Carpenter and Ray Allen (MWNRM); and Stuart Holley and Stuart Fyfe (MCC). I also am indebted to Bronwyn Masters, Ed Oldmeadow and other members of the Mackay branch of the Queensland Department of Natural Resources Mines and Water (QDNRMW) for advice and field assistance; and to Nick Cuff at the Queensland Herbarium for providing data on the regional ecosystems of the Pioneer catchment. It is my sincere hope that the results from my study will help improve local and regional management plans supported by these agencies to reduce land pollution into the Great Barrier Reef Lagoon.

Through the course of my degree, many people have given advice and helped with data analysis. Bill Pickles, Eli Silver, Karen Joyce, Chris Roelfsema, Peter Scarth, Kasper Johnanssen and Liane Guild all aided with my remote sensing analyses, and I thank Liane in particular for serving as my mentor at NASA Ames for the duration of my Graduate Student Researchers Program fellowship. I am especially grateful for the expert MATLAB skills of Curt Storlazzi and Mike Hutnak that were instrumental for finding long-term trends in the coral data related to river discharge and wind.

Additional funding for my project and during my tenure at Santa Cruz was provided by: the PADI Foundation, the UCSC Center for the Dynamics and Evolution of the Land-Sea Interface (C.DELSI), the American Geophysical Union (AGU), Lawrence Livermore National Laboratories (LLNL), Pacific Gas and Electric (PG&E), Monterey Bay Aquarium Research Institute (MBARI), the Cooperative Institute for Coastal and Estuarine Environmental Technology (CICEET), and the Dr. Earl H. Myers and Ethel M. Myers Oceanographic and Marine Biology Trust.

Last, but by no means least, I would like to extend my gratitude to people who have provided me encouragement and moral support along my journey. For several years in Australia, I lived essentially as a nomad, so I thank those who hosted me as I roamed up and down the coast: Kathryn McMahon; Chris Roelfsema, Diana Kleine, Djoy and Anouk; Simon Albert and Joelle Prange; Jeanine and Glenn Alemany; Sharon and Nathan Berenger; Ray Martin; and Jocelyn Davies. I also extend a huge thank you to Mark Talkovic and Amy West, who took me in to their home in Aptos, gave me access to their wonderfully large desk, and put up with me while I holed up writing. I thank my labmates at UCSC, both current and former, for their encouragement and readiness to lend an ear: Wendy Cover, Daria Siciliano, Erin McCarthy, Rebecca Johnson, Steve Lonhart, Allison Gong, Becky Jacobs and Cris Vaughan. In the EEB department, I am very grateful to Annie Town, Ashley Vizurraga, Susie Canora and Susan Thuringer for keeping me in line and enrolled, especially as I was hardly ever in Santa Cruz, and I reserve an enormous thank you to Susan for convincing Don to accept me as a graduate student and welcoming me at UCSC.

To my committee (Don Potts, Laurel Fox, Dan Doak, Stuart Phinn), I thank you all for your patience and persistence reading through my many drafts and long chapters. Your insights have vastly improved my work. And to Don, thank you for continuing to believe in me from start to finish and for providing guidance along the way. To Brigette Martini, Mimi D'Iorio and Julio Harvey, thank you for the sanity checks, the good times in the Cruz and Australia, and for showing me that it can be done. To Becky Stamski, Kena Fox-Dobbs, Carissa Carter, and Jennifer O'Leary, thank you for the breaks to run and surf and feel the sunshine. To my Peace Corps family, thank you for keeping me down to earth. And finally, to my mother, father, and brother, your love and support have carried me through. Thank you for always being there.

Chapter 1. Connectivity in Natural versus Anthropogenic Systems

Introduction

During the past century, human population growth has been explosive, and increasing rates of environmental modification from anthropogenic activities have been largely unchecked. Global population has increased nearly 4-fold since 1900 and is predicted to reach 9 billion by 2050 (Cohen 1995; Tilman et al. 2001). To support the population boom, humans currently use more than one third of terrestrial primary production and over half of accessible freshwater runoff (Vitousek et al. 1986; Postel et al. 1996; Vitousek et al. 1997a; Vitousek et al. 1997b; Tilman et al. 2001). Soil loss rates, amplified by land clearing for agriculture and development, are (at a minimum) 10 times greater than rates of soil formation (Pimentel et al. 1993). Global fertilizer consumption has increased by ~700% in the past 40 years, and anthropogenic sources of nutrients in the biosphere now exceed natural sources (Matson et al. 1997; Tilman et al. 2001; Foley et al. 2005). Atmospheric increases of CO_2 at ~3.5 Pg C yr^{-1} (Keeling et al. 1989), driven principally driven by fossil fuel combustion, will account for more than half of the anticipated global warming expected in the next century (Rodhe 1990; Vitousek 1994). Concurrently, ecological destruction of entire trophic levels by removal of top predators has reduced ecosystem resistance and resilience to disturbance (Jackson et al. 2001; Scheffer et al. 2001). No place on Earth is currently unaffected by human activity.

Any meaningful discussion about how these changes impact ecosystems, linkages between ecosystems and the value of ecosystem services, must first ask: what qualifies as an “ecosystem” and how is it maintained over time? Because the term “ecosystem” has been used in many ways, is often misunderstood and is often misapplied (Polunin and Worthington 1990; Likens 1992; Golley 1993; Willis 1997), and because science has failed to communicate the concept clearly to the public, the management and regulatory agencies responsible for protecting ecosystems and their services often lack the jurisdiction to do so. In this chapter, I briefly review the history of the ecosystem concept and stress the importance of linkages within and between ecosystems for understanding the broadscale impacts of human alterations to the planet. I outline several examples of connectivity between ecosystems and discuss how these interactions respond to anthropogenic impact. Finally, I suggest modifications to current management strategies for dealing with connectivity across traditionally recognized ecosystem boundaries (especially the land-sea interface).

This chapter provides background and conceptual contexts for a study of anthropogenic perturbations of natural ecosystem linkages within the Pioneer River catchment in Queensland, Australia, presented in later chapters. For the Pioneer catchment, I describe the temporal and spatial progressions of anthropogenic disturbance, beginning with upstream land clearing and agricultural management practices. I then relate these changes to subsequent downstream impacts on water quality around nearshore coral communities and midshelf reefs in along a distance gradient from the Pioneer River mouth.

Origins of the Ecosystem Concept

In 1935, Arthur Tansley coined the term *ecosystem* as “the basic unit of nature”, and defined it to include the abiotic and biotic elements within a physical space and the interactions between them (Tansley 1935). Tansley’s ecosystem concept was not based on field data or experiments. Instead it was a rebuttal to the “biotic community” hypothesis of his colleague John Phillips who proposed that communities were holistic in nature (Anker 2002). Phillips, building on work by American ecologist Frederic Clements and South African philosopher Jan Christian Smuts, recognized that biotic communities possess emergent properties beyond the sum of their parts (Golley 1993). He also believed the biotic community to be a “mass-entity with a destiny peculiar to itself” (Phillips 1931), arising from progressive succession to a climax state. Tansley (1935) objected to Phillips’s implied idealistic metaphors and wrote a paper, *Use and Abuse of Vegetation Concepts and Terms*, in which he emphasized that: (1) emergent properties “are *in analysis* nothing but the synthesized actions of the components in association” (i.e. interactions between abiotic and biotic components; Tansley 1935); and (2) ecosystem stability is attained through its movement toward an equilibrium (Golley 1993; Jax 1998). He borrowed the terms *system* and *equilibrium* deliberately from physics to provide a mechanistic underpinning for ecological processes (Golley 1993; Pickett and Cadenasso 2002).

Modifications and Limitations

Tansley's ecosystem concept has expanded and been modified over time, including much theoretical and empirical work defining its components, scales, and stability. Among remaining, recognized limitations of the concept, perhaps the greatest are the difficulties in specifying ecosystem boundaries. Researchers continue to redefine ecosystems based on certain characteristics detailed below to find the best ways to: describe emergent properties that arise from a system's components; specify the scale at which these properties operate; and predict the system's responses to spatial and temporal disturbances.

Components

Raymond Lindeman was the first to use an ecosystem framework in a quantitative field study of Cedar Bog Lake, Minnesota. He defined an ecosystem as "the system composed of physical-chemical-biological processes active within a space-time unit of any magnitude" (Lindeman 1942), but he went beyond Tansley to include the flow of matter and energy in his trophic-dynamic approach for explaining the ecosystem processes of productivity, efficiency and succession. Evans (1956) later included the rates of processes governing energy and nutrient cycling and defined ecosystems as the interactions of biological processes (e.g. photosynthesis, decomposition, herbivory, predation, parasitism, etc.) with the physical processes (e.g. evaporation, precipitation, erosion, deposition, etc.) that move matter. The functions of the ecosystem (e.g. productivity) are then defined by the rates of energy flow and nutrient cycling, and by the strength of competition among the component species for energy and nutrients (O'Neill 2001).

Emergent properties of ecosystems are often estimated by constructing energy and nutrient budgets. In one of the first examples, the high rate of primary productivity on Eniwetok Atoll was attributed to the high efficiency of energy exchange and nutrient cycling between corals and their symbiotic zooxanthellae (Odum and Odum 1955; Odum 1977). The Odum and Odum (1955) study was applauded for its novel application of the ecosystem concept to coral reefs, but it was also criticized for assuming the ecosystem was closed to external material exchanges. Fifty years later we know that almost all ecosystems are intimately inter-connected by the pathways for gaining, losing and replacing of energy and matter, and through dispersal of organisms, and so they must be open at many levels (Holt 2004).

Scale

The ecosystem concept is scale-independent, meaning that it can be applied at multiple levels: from an organism to an entire planet or beyond. Consequently, ecosystems form nested hierarchies in which they “overlap, interlock and interact with one another” (Tansley 1935). It is this connectivity that often makes determining ecosystem limits difficult, particularly when there is no clear physical boundary between systems. This problem is analogous in some ways to the issues of delimiting a single species from its ancestral and sister taxa when there are continuous gradients of morphological or molecular differences (Evans 1956). As

Tansley himself pointed out, the ecosystem concept, like the species concept, is a mental construct created for the purpose of study, rather than a concrete natural entity.

For practical purposes, an ecosystem needs to be specified with appropriate boundaries in space and time for the goals and questions of a particular study (Likens 1992; Willis 1997; Jax 1998). For example, a watershed model can focus on the entire drainage basin or on the sub-regions that produce or capture runoff and the interactions between sub-regions to assess relative system stability on different scales (Pickett and Cadenasso 2002). Where the limits should be drawn depends largely on the scale of the research questions. In the Pioneer catchment system, I am studying the linkages between catchment runoff and water quality at adjacent coral habitats, and so the system is largely bounded by hydrodynamic forces that influence the sources of runoff and the potential geographical range over which the freshwater and suspended sediments are redistributed in the nearshore.

If the study is focused on stability dynamics, the scale of an ecosystem must be large enough to include all the main processes affecting ecosystem stability at the largest scale. For example, recruitment of individuals into an ecosystem is often critical for recovery from disturbance (Huffaker 1958), particularly in highly variable environments (Roff 1974a, 1974b). The boundaries of a local ecosystem must therefore be scaled to include the dispersal ranges of the main component species: there ranges are determined by (a) biotic and abiotic environmental constraints; (b) dispersal barriers; and (c) species dispersal mechanisms (O'Neill 2001). The potential dispersal ranges may also change in response to environmental shifts and disturbances (O'Neill 2001).

Ecosystem stability

Central to Tansley’s concept is the development of ecosystems (i.e. succession) as a progression toward stable states, and he described a climax community as “the highest stage of integration and nearest approach to perfect dynamic equilibrium that can be attained in a system developed under the given conditions and with the available components” (Tansley 1935). The concept of “stability” is also very difficult to define, and many ecologists now feel that Tansley’s equilibrial, integrated, climax ecosystems do not exist (e.g. Soulé 1995). Even highly “stable” systems have fluctuations caused by internal dynamics, such as species interactions and demographic stochasticity, and/or by external dynamics, such as environmental changes (Loreau et al. 2002; Scheffer and Carpenter 2003). In some cases (e.g. Huisman and Weissing's (1999) simulations of resource-limited phytoplankton communities), population oscillations promote higher-level stability (e.g. species co-existence, or stabilization of such ecosystem properties as total biomass).

Ecologically, “stability” usually accepts fluctuations within some defined boundaries (Vogt et al. 1997). Ecosystem stability is often described by measuring several components, which may include: the rate of return to a previous steady state after perturbation (*resilience*); the capacity to absorb perturbations without change (*resistance*); the amount of perturbation tolerated before switching to an alternate state (*robustness*); and the length of time a system remains in one state (*persistence*) (Pimm 1984; Vogt et al. 1997; McCann 2000; Loreau et al. 2002). Stability depends partly on the length of intervals between disturbance relative to recovery rates, and on the spatial extent of disturbances relative to the spatial extent of the effective dispersal range (Turner et al. 1993). Stability also reflects evolutionary history: the degree to which an ecosystem can respond to and recover from disturbance is constrained by how natural selection has influenced the component species in the past (Holling 1973; O'Neill 2001).

Significant positive associations between ecosystem stability and biodiversity have been demonstrated in both small-scale, highly controlled microcosms and in large-scale field experiments (Naeem et al. 1994; Tilman and Downing 1994; Naeem et al. 1995; Tilman et al. 1996; McGrady-Steed et al. 1997; Naeem and Li 1997; Tilman et al. 1997; Tilman et al. 2002), although the links are debatable because the mechanisms generating the relationships are not always documented adequately (McCann 2000), and because some studies have inverse relationships between species richness and resistance to environmental perturbation (Zhang and Zhang 2006). In some long-term grassland experiments, both the number of plant species *and* the species composition of functional groups significantly affected aspects of ecosystem function (e.g. above ground biomass, root biomass, carbon storage in living plant biomass, concentration of unconsumed soil nitrate; Tilman et al. 2002). Redundancy within functional groups (i.e. species with similar ecological roles) is believed to maintain persistence of ecosystem functions by providing “insurance” against unpredictable environmental changes that may cause extinctions of individual species (Walker 1992; Lawton and Brown 1993; Chapin et al. 1997; Naeem and Li 1997). For example, from paleontological records of African savannas, Harris (1993) concluded that redundancy within mammalian guilds facilitated the system’s survival through a severe climatic period 1.5 million years ago. Loreau et al. (2003a) suggest that these insurance effects are greatest at intermediate dispersal rates, which tends to maximize local species diversity, while both high and low dispersal rates can lead to competitive exclusion and less ecological redundancy of species (Mouquet and Loreau 2002).

Ecosystem Connectivity

Historically, terrestrial, freshwater and marine ecosystems have been studied separately because they have very different physical conditions, productivities and food webs. But if ecosystems really are open to external fluxes of material, energy and dispersing individuals, all of which are influenced to varying degrees by disturbances in space and time, then some of these ecosystems should be strongly linked. For example, the productivity and diversity of one ecosystem may be sustained by nutrient subsidies from an adjacent system, and these subsidies often cross traditional terrestrial-aquatic boundaries (Bormann and Likens 1967; Polis et al. 1997; Likens 2004; Polis et al. 2004). Loreau et al. (2003b) proposed the meta-ecosystem concept to provide a theoretical framework for emergent properties arising from such spatial coupling (e.g. diversity-productivity patterns, global source-sink constraints, and stabilization processes). They defined a meta-ecosystem as “a set of ecosystems connected by spatial flows of energy, materials and organisms across ecosystem boundaries” (Loreau et al. 2003b). This meta-ecosystem concept extends existing metacommunity theory, which focuses on the broad-scale properties that result from reciprocal biotic connections among component local communities (Wilson 1992; Holt 1993; Hubbell 2001), by placing the communities within an ecosystem context. Abiotic constraints and feedbacks are included as additional determinants of higher order properties that emerge from coupled systems (Loreau et al. 2003b).

In the following sections I discuss several types of ecosystem linkages within meta-ecosystems in natural environments. I first treat the linkages resulting from biotic pathways (e.g. predator-prey interactions, nutrient subsidies, life history movements) separately from those based on abiotic pathways (e.g. material transport by wind, water or gravity), even though several types of processes probably interact to produce overall emergent effects. I then consider how these linkages are being affected by anthropogenic global changes.

Linkages through biotic pathways

Individuals moving across ecosystem boundaries to disperse, forage or occupy different ontogenetic niches can substantially alter the properties of adjacent ecosystems by changing food web dynamics, which in turn affects rates of primary production, herbivory, predation and biomass accumulation, and all of which will influence rates of nutrient cycling (Werner and Gilliam 1984; Polis and Strong 1996; Polis et al. 1997). In terrestrial systems, top-down nutrient subsidies delivered by winged animals (e.g. birds, bats, insects) may be sufficient to cause landscape-level changes in ecosystem chemistry, productivity and species composition (Weir 1969; Wainright et al. 1998; Anderson and Polis 1999; Kitchell et al. 1999; Wait et al. 2005). For instance, guano deposition may increase heterogeneity in soil chemistry (e.g. pH, salinity), which in turn may impact species richness (Anderson and Polis 1999; Wait et al. 2005). Multiple studies from the Gulf of California have found fewer plant species on bird islands versus non-bird islands (Anderson and Polis 1999; Wait et al. 2005).

Nutrients can be moved by animals across traditionally recognized ecosystem boundaries (e.g. freshwater-terrestrial, marine-terrestrial, marine-freshwater). Nutrient translocation by bats may export stream-derived nutrients to upslope communities (Power et al. 2004). In Sonoran Desert streams, 97% of aquatic insect biomass, largely derived from algal carbon (Mayer and Likens 1987), is exported by bats to the watershed (Jackson and Fisher 1986). These aquatic insects also contribute to higher densities of terrestrial arthropods and lizards, although transfer of nutrients to these higher level consumers is less likely to induce landscape effects than deposition of bat guano (Sabo and Power 2002; Power et al. 2004).

Similarly, birds may supply marine-derived nutrient subsidies to terrestrial and coastal zones. Seabirds may remove between 10-30% of marine production from their feeding grounds (Weir 1969; Furness 1978; Wainright et al. 1998), some of which is later deposited as nutrient additions (e.g. guano) in terrestrial roosting and breeding areas where increasing soil nutrients may alter both landscape structure and ecosystem processes, and may increase plant biomass and productivity (Anderson and Polis 1999; Wait et al. 2005). Bird guano has also been associated with intertidal community changes (Bosman et al. 1986; Wooten 1991) and coastal phytoplankton blooms (Wainright et al. 1998).

Habitat requirements of many animals change substantially during different phases of their development. For example, anadromous fish move from marine to freshwater habitats as they return to their natal watersheds where they impact stream food webs by seasonal inputs of allochthonous marine nutrients, from both their eggs and their carcasses (Ben-David et al. 1998; Wipfli et al. 1999; Minakawa et al. 2002; Willson et al. 2004). Movements in the opposite direction include many species of coral reef fish that rely on mangroves as juvenile nurseries, but later help to maintain coral dominance on reefs through herbivory of macroalgae (Hughes 1994; Jackson et al. 2001). By increasing the survivorship of many species, the protective mangrove habitat increases herbivore biomass on neighboring reefs (Mumby et al. 2004; Manson et al. 2005).

Linkages through abiotic pathways

Physical transport mechanisms, including gravity, winds and water currents, may transport large quantities of materials, often for great distances, across the same traditionally recognized ecosystem boundaries. Many studies document the movement and impacts of terrigenous materials into freshwater (Bormann and Likens 1967; Fisher and Likens 1973; Webster and Meyer 1997; Caraco and Cole 2004) and marine ecosystems (Nugues and Roberts 2003; Darnaude et al. 2004; Beman et al. 2005). Although only ~1% of terrestrial production is exported to aquatic systems (Ludwig et al. 1997), allochthonous inputs concentrated in watershed drainages may provide disproportionate nutrient sources (Caraco and Cole 2004). Some material, such as leaf litter, breaks down rapidly into biologically-accessible inorganic compounds and subsidizes stream food webs through bottom-up effects (Meyer and Johnson 1983; Wallace et al. 1997), but because residence times in streams are usually short, much organic matter (both dissolved and particulate) is transported to and deposited in larger aquatic systems, such as lakes or reservoirs, where it may increase rates of ecosystem respiration and secondary production (Caraco and Cole 2004; Lennon and Pfaff 2005), and exert changes in community structure (Paterson et al. 1997).

Marine systems are currently being severely impacted by terrestrial nutrient fluxes from combinations of river runoff and wind-blown terrestrial dust on local to regional scales. A model by Lenes et al. (2005) suggests that cyanobacterial blooms off Barbados are driven by phosphorus additions from South American river plumes and iron additions from wind-blown Saharan dust. These surface blooms may potentially impact benthic as well as pelagic communities: e.g. coral deaths off the

Sumatran coast in 1997 were attributed to anoxia from red tide blooms fertilized by fallout of airborne terrestrial iron from widespread wildfires (Abram et al. 2003).

Coastal, pelagic and benthic marine subsystems are often treated as separate ecosystems because they differ considerably in productivity, trophic structure and physical environments, and are usually studied in very different ways, but they are coupled by the physical forcing of gravity and upwelling (Loreau et al. 2003b). In the deep-sea, benthic community ecosystem processes (e.g. secondary production) are often stimulated by localized, episodic pulses of kelp (Harrold et al. 1998), whale carcasses (Baco and Smith 2003), and particulate organic carbon (POC) (Smith et al. 1992). These allochthonous energy sources may be a driving force for diversification of deep-sea faunas: average numbers of species living on a single whale skeleton in the deep sea approaches that known globally from all cold-seeps combined (Baco and Smith 2003).

Marine detritus (e.g. algal drift, animal carcasses) also subsidizes many terrestrial food webs, after it is washed ashore by currents and tides (Polis et al. 2004). Polis and Hurd (1995, 1996) found higher arthropod densities associated with high levels of marine detritus, and these arthropod sources were important foods for higher order consumers, such as coyotes, whose populations along the Gulf of California coast are 2-13 times denser in regions that receiving marine inputs than in adjacent areas without such inputs (Rose and Polis 1998).

All of the above examples of ecosystem linkages come from natural systems, in the sense that they operate in the absence of direct anthropogenic inputs, but the concept of “natural” systems in today’s world may be a fallacy (Vitousek et al. 1997a). Although some regions of the globe are less disturbed by human activity, current ecosystem processes and linkages are impacted by indirect effects, lagged effects and historical legacies of anthropogenic disturbance (McDonnell and Pickett 1994). The next section addresses how some of these linkages are currently being directly and indirectly disturbed by human modification to Earth’s resources.

Anthropogenic Effects on Ecosystem Connectivity

Although current rates and scales of anthropogenic change are unprecedented in Earth’s history, and although some types of human disturbance (e.g. industrial pollution) are novel, human beings are a species that is now an integral component of many modern ecosystems. Humans are a keystone species (*sensu* Paine 1969) able to impact ecosystem structure, function and stability on all scales by altering the physical environment, biological components and disturbance regimes (O'Neill 2001). Even Tansley (1935) recognized that “anthropogenic” and “natural” ecosystems consist of the same processes emerging from interactions of biotic organisms with their abiotic environments, but that “anthropogenic” systems have higher levels of disturbance resulting in reduced resilience and resistance, and greater instability.

Most human impacts on the environment fall into three broad, overlapping categories: land cover change; climate change; and biodiversity change. Changes within any one category influence the others: for example, increased albedo and reduced evapotranspiration following deforestation in Central Africa has substantially altered rainfall and water retention patterns, with the likelihood of major effects on local biodiversity (Semazzi and Song 2001). I describe examples to illustrate each category below, and then discuss how each type of change leads to cascading effects in other ecosystems.

Land cover changes: An estimated 39-50% of the Earth's land has been transformed or degraded by man (Vitousek et al. 1986; Daily 1995; Kates et al. 1995; Vitousek et al. 1997a; Foley et al. 2005). These changes have altered the structure and functioning of terrestrial ecosystems and their interactions with the atmosphere, with aquatic systems and with adjacent terrestrial regions (Vitousek et al. 1997b; O'Neill 2001). In the Hubbard Brook Experimental Forest, watershed-scale deforestation changed rates of both physical and biological processes: decomposition and nitrification were greatly accelerated; soil erodibility increased; and the severe reduction in evapotranspiration translated into increased runoff of water (Likens 2004). These changes led to marked chemical changes (e.g. >40-fold increases in nitrate concentrations in streams, and depleted soil nitrogen, compared to undisturbed drainages; Likens et al. 1970). Deforestation is often accompanied by land conversion to intensive agriculture requiring fertilizer application, which further changes the nutrient cycling regime and usually leads to heavy losses of nitrogen and phosphorus through runoff or leaching (Matson et al. 1997). Agricultural sources of phosphorus lead to eutrophication in many freshwater systems, such as lakes (Schindler 1977; Matson et al. 1997), where experimental phosphorus additions have caused harmful cyanobacterial blooms (Schindler 1977), which release toxins upon death or ingestion and contribute to fish kills (Carpenter et al. 1998). Nutrient accumulation has been implicated in reduced ecosystem resilience, leading to catastrophic shifts to alternate states in lakes, from submerged vegetation to phytoplankton dominance (Scheffer et al. 1993), and in coral reefs, from coral to fleshy macroalgal dominance (Nystrom et al. 2000).

Land cover changes also impact ecosystem stability through habitat fragmentation, which creates barriers to dispersal, interrupts energy and nutrient exchanges, and often restricts ecosystem recovery from disturbance (Gardener et al. 1993; Loreau et al. 2003b). For example, dams may cause instability in upstream ecosystems by preventing repopulation by fishes or other organisms that must migrate back upstream to initiate recovery from disturbance (O'Neill 2001). Anthropogenic climate change may intensify effects of habitat fragmentation by indirectly creating barriers to dispersal as the potential range of organisms are shifting in response to changed environmental conditions (Opdam and Wascher 2004).

Climate changes: Because predicted changes in Earth’s thermal and precipitation regimes, ocean circulation and carbon budgets are so rapid and occur on global scales, they are likely to substantially modify ecosystems. Average global air temperature has increased by 0.6 ºC, and tropical ocean sea surface temperatures (SSTs) have gained 1-2 ºC, over the past 100 years (Hoegh-Guldberg 1999; Walther et al. 2002). Even modest temperature changes have the potential to shift entire ecosystems to new states. Mass bleaching events on coral reefs typically occur when SSTs exceed long-term summer extremes by >1 ºC for several weeks (Glynn 1991; Hoegh-Guldberg 1999), and they are often followed by phase shifts from coral to macroalgal dominance as the algae colonize dead coral skeletons (McCook et al. 2001). In 1998, an estimated 16% of global reef-building corals died after bleaching (Wilkinson 2000), with severe consequences on fisheries: in Kenya, fishermen increased their effort by 17% while the total demersal catch declined by 8% and the catch per man declined by 21% (McClanahan et al. 2002).

Diversity changes: Global warming trends may also cause phase shifts through climate-linked invasions. The recent and rapid spread of the invasive macroalgae *Caulerpa taxifolia* and *C. racemosa* in the Mediterranean may have been triggered by climate shifts that favored their reproduction, while populations of the native seagrass *Posidonia oceanica* declined due to combined effects of long-term SST increases, increased bottom trawling and coastal pollution from runoff (Duarte et al. 1999; Walther et al. 2002; Occhipinti-Ambrogi and Savini 2003). Many invasions, particularly in the coastal and marine environment, have been facilitated by human activity: either as intentional introductions for commercial aquaculture or fisheries; or unintentionally via release from ships' ballast (Grosholz 2002). Some successful invading species alter the structure and functions of entire ecosystems (Alpine and Cloern 1992; Cordell and Morrison 1996; Vitousek et al. 1997a; D'Iorio 2003; Belnap et al. 2005; Batten et al. 2006), and after land transformation, invasions are the next most important driver of species extinctions (Vitousek et al. 1996).

Accumulating evidence suggests that anthropogenic influence from global climate change and coastal eutrophication is also leading to increased prevalence of existing diseases and the emergence of new diseases. Recent outbreaks of arthropod-borne diseases like malaria, dengue and Rift Valley fever at higher elevations have been linked to warmer, wetter conditions associated with more frequent El Niño-Southern Oscillation (ENSO) events (Epstein et al. 1998; Harvell et al. 2002). Coastal eutrophication may impair host resistance to pathogens: field experiments from the Caribbean found nutrient enrichment associated with increased amounts of coral tissue loss from yellow band disease and increasing severity of outbreaks of aspergillosis in sea fans (Bruno et al. 2003). Such types of epizootic outbreaks have appeared with increasing frequency over the past 20 years (Harvell et al. 1999), and may, in some cases, causes phase shifts within ecosystems (e.g. the decimation of the urchin, *Diadema antillarum*, and the major reef building corals, *Acropora cervicornis* and *A. palmata*, which may have been pathogen-mediated, facilitated a shift to macroalgal dominance in the Caribbean in the 1980s; Lessios 1988; Aronson and Precht 2001; Bruno et al. 2003). When such diseases impact keystone species, they have the potential ability to alter not only their own ecosystems, but may also cause subsequent cascading effects in adjacent systems.

Land use, climate change and species introductions all impact global biodiversity patterns (Sala et al. 2000), and changes in membership of biotic communities are likely to alter ecosystem functioning (Chapin et al. 1997). Eliminating higher level consumers can impact ecosystems at a landscape-level: for example, the onset of chronic anoxia, hypoxia and eutrophication in Chesapeake Bay coincided with the collapse of the oyster fishery—previously, huge oyster populations had maintained water quality through their filter feeding (Jackson et al. 2001). Conversely, the introduction of arctic foxes to Aleutian islands effectively added a new keystone predator that reduced allochthonous marine subsidies by preying on seabirds, and thereby altered landscape structure by transforming grasslands into shrub/forb dominated systems (Croll et al. 2005). Such alterations of plant biodiversity can have other effects on such ecosystem functions as productivity, CO_2 capture, and community respiration (Naeem et al. 1994).

Conservation from the Ecosystem Level

Determining priorities for conservation is a complex task, complicated by disagreements among scientists working on different spatial and temporal scales about the best ways to approach environmental protection. This lack of consensus makes it difficult to convey to policy makers the importance of protecting ecosystem structure and function before the systems shift to less desirable states and lose the economic and aesthetic functions that we value. Many conservation groups concentrate on protecting a few charismatic species (e.g. conservation literature has 10 times as many references for mammals than more speciose groups, such as amphibians or insects; Clark and May 2002). While this approach brings critical funds into conservation organizations, protection of these species *per se* may do little unless the featured organisms are also keystone species in their ecosystems.

Walker's (1995) concept of ecosystem conservation emphasizes the importance of first determining which processes are critical for maintaining ecosystem function and persistence, and then protecting the groups of functionally redundant species carrying out these ecosystem processes. Preservation of functional redundancy increases ecosystem resilience to disturbance, as minor species may emerge as keystone species if environmental conditions change (Walker 1995; Naeem 1998). In this model, priority should be given to important functional groups with the fewest number of species (Walker 1995). An alternate approach focuses on protecting the ecosystem processes themselves and thereby protecting functional diversity (Silver et al. 1996). For conservation of functional diversity within tropical forest ecosystems, Silver et al. (1996) identified important interfaces (atmosphere-terrestrial; plant-soil; terrestrial-hydrologic) where it is essential for the flow of nutrients and energy to be maintained for healthy ecosystem functioning. The two approaches are not mutually exclusive: conservation of organisms within important functional groups is likely to preserve the processes of nutrient cycling and energy flow, though it is wise to first assess which organisms overlap at the most critical interfaces.

In a practical sense, policy makers and managers need to evaluate the sizes of areas needed to preserve ecosystem functions. Because local ecosystem diversity, processes, and stability are determined partly by the amount of dispersal into that system, knowing the dispersal patterns of organisms in critical functional groups is needed when designing reserve networks across fractured landscapes (Loreau et al.

2003a). For marine reserve networks, this requires considering not only the dispersal distances of different species, but also the hydrological factors determining local replenishment of species and the potential human activities "upstream" of a reserve that may alter these patterns (Allison et al. 1998).

Managing ecosystems becomes especially challenging when important processes controlling ecosystem functions are driven by the fluxes of organisms and materials across ecosystem boundaries from other regions that may be under different management practices, because they fall under the jurisdiction of a separate agency, state or even country. In Australia, water quality is one major focus of the Great Barrier Reef Marine Park Authority (GBRMPA), but the Great Barrier Reef Marine Park Act 1975, which created the agency to protect the reef, did not give GBRMPA the authority to control land-based activities in the catchments draining into the GBR Lagoon (Wachenfeld et al. 1998; Haynes and Michalek-Wagner 2000). Management of catchment activities is primarily regulated through the Environmental Protection Act 1994, overseen by the Queensland Environmental Protection Agency, and the Water Resources Act 1989, overseen by the Queensland Department of Natural Resources. In addition, local city councils and regional management groups may enact their own policies, which are not necessarily consistent throughout the entire Great Barrier Reef catchment or congruent with GBRMPA's goals. The Queensland Government sought to remedy this divide across the land-sea interface by setting up Integrated Catchment Management (ICM) groups, composed of representative members from all local interests; however, the program is voluntary, receives only limited state funding, and there is no evidence that ICM strategies have improved water quality (Brodie et al. 2001). This case highlights the need to invest more authority and legislative backing in umbrella agencies that are charged to manage systems from an ecosystem perspective (Rosenberg and McLeod 2005).

Conclusions

Although the ecosystem concept is applicable across many scales, all definitions of ecosystems should include the major abiotic and biotic components and the interactions between them that yield the biological and physical processes that determine ecosystem function. Ecosystems are variably open to the flux of materials, energy and individuals from other ecosystems, but each system must be sensibly bounded to address particular questions. While ecosystem boundaries delimited for study can be physical, such as the topography defining a drainage system, all considerations of ecosystem functions, services and stability should include the dispersal ranges of important component species. Ecosystem stability is determined by partly by duration of intervals between disturbances relative to recovery rates, and partly by the spatial extent of disturbances relative to effective dispersal ranges. Intimate connectivity between ecosystems, driven by both biotic and abiotic pathways, not only changes the stability of one ecosystem, but may also affect adjacent ecosystems. Anthropogenic activities have decreased the stability of many natural ecosystems through habitat destruction/fragmentation (which limits dispersal), climate change, trophic level elimination, and species introductions and extinctions. Preservation of ecosystem functions by protecting important species, functional groups and processes should be a global conservation priority and may require boosting the authority of regulatory agencies with the jurisdiction to manage ecosystems at a regional to global scale.

In the following chapters, I explore ecosystem connectivity across the land-sea interface near Mackay in Queensland, Australia, in a region of heavy anthropogenic impact. Throughout the Great Barrier Reef catchment (Figure 1.1), forests have been converted to agricultural activities (e.g. grazing, cropping) since the onset of European settlement, while riparian and wetland areas have been cleared and filled. This study describes how loss of ecosystem functions, from conversion of catchment lands from forest to agriculture, has changed the downstream movements of materials (e.g. water, sediments, nutrients) to estuarine and coastal mangroves, and onwards to nearshore coral reefs, largely via abiotic pathways (e.g. erosion, river transport, deposition), but also through changing biotic processes (e.g. nutrient cycling by phytoplankton blooms). I integrate several approaches (from community ecology, landscape ecology, geomorphology, and geochemistry) to evaluate whether water quality has changed as a result of land cover change, and whether the magnitudes of these changes have been sufficient to perturb adjacent coral reef ecosystems. In Chapter 2, I describe how land cover in the Pioneer River catchment has changed since European settlement (1862), and then evaluate its impacts on soil erosion. In Chapter 3, I explore in detail changes in mangrove distributions in the Pioneer River estuary since 1948 and discuss impacts of mangrove loss on nearshore water quality. In Chapters 4 and 5, I present historical records of nearshore water quality derived from geochemical proxy data taken from corals sampled at increasing distances from the Pioneer River mouth. Lastly, in Chapter 6, I analyze and integrate the long-term trends to separate anthropogenic impacts from natural variation and then assess whether past changes in water quality have impacted present day coral reef communities.

References

Abram, N.J., Gagan, M.K., McCulloch, M.T., Chappell, J. and Hantoro, W.S. 2003. Coral reef death during the 1997 ocean dipole linked to Indonesian wildfires. Science 301.

Allison, G.W., Lubchenco, J. and Carr, M. 1998. Marine reserves are necessary but not sufficient for marine conservation. Ecological Applications 8: S79-S92.

Alpine, A.E. and Cloern, J.E. 1992. Trophic interactions and direct physical effects control biomass and production in an estuary. Limnology and Oceanography 37: 946-955.

Anderson, W.B. and Polis, G.A. 1999. Nutrient fluxes from water to land: seabirds affect plant nutrient status on Gulf of California islands. Oecologia 118: 324-332.

Anker, P. 2002. The context of ecosystem theory. Ecosystems 5: 611-613.

Aronson, R.B. and Precht, W.F. 2001. White-band disease and the changing face of Caribbean coral reefs. Hydrobiologia 460: 25-38.

Baco, A.R. and Smith, C.R. 2003. High species richness in deep-sea chemoautotrophic whale skeleton communities. Marine Ecology Progress Series 260: 109-114.

Batten, K.M., Scow, K.M., Davies, K.F. and Harrison, S.P. 2006. Two invasive plants alter soil microbial community composition in serpentine grasslands. Biological Invasions 8: 217-230.

Belnap, J., Phillips, S.L., Sherrod, S.K. and Moldenke, A. 2005. Soil biota can change after exotic plant invasion: does this affect ecosystem processes? Ecology 86: 3007-3017.

Beman, J.M., Arrigo, K.R. and Matson, P.A. 2005. Agricultural runoff fuels large phytoplankton blooms in vulnerable areas of the ocean. Nature 434: 211-214.

Ben-David, M., Hanley, T.A. and Schell, D.M. 1998. Fertilization of terrestrial vegetation by spawning Pacific salmon: the role of flooding and predator activity. Oikos 83: 47-55.

Bormann, F.H. and Likens, G.E. 1967. Nutrient cycling. Science 155: 424-429.

Bosman, A.L., Du Toit, J.T., Hockey, P.A.R. and Branch, G.M. 1986. A field experiment demonstrating the influence of seabird guano on intertidal primary production. Estuarine, Coastal and Shelf Science 23: 283-294.

Brodie, J.E., Christie, C., Devlin, M., Haynes, D., Morris, S., Ramsay, M., Waterhouse, J. and Yorkston, H. 2001. Catchment management and the Great Barrier Reef. Water Science and Technology 43: 203-211.

Bruno, J.F., Petes, L.E., Harvell, C.D. and Hettinger, A. 2003. Nutrient enrichment can increase the severity of coral diseases. Ecology Letters 6: 1056-1061.

Caraco, N.F. and Cole, J. 2004. When terrestrial organic matter is sent down the river: the importance of allochthonous carbon inputs to the metabolism of lakes and rivers. *In*: Polis, G.A., Power, M.E. and Huxel, G.R. (eds.), Food Webs at the Landscape Level. pp. 301-316. The University of Chicago Press, Chicago.

Carpenter, S.R., Caraco, N.F., Correll, D.L., Howarth, R.W., Sharpley, A.N. and Smith, V.H. 1998. Nonpoint pollution of surface waters with phosphorus and nitrogen. Ecological Applications 8: 559-568.

Chapin, F.S., III, Walker, B.H., Hobbs, R.J., Hooper, D.U., Lawton, J.H., Sala, O.E. and Tilman, D. 1997. Biotic control over the functioning of ecosystems. Science 277: 500-504.

Clark, J.A. and May, R.M. 2002. Taxonomic bias in conservation research. Science 297: 191-192.

Cohen, J.E. 1995. How Many People Can the Earth Support? Norton, New York.

Cordell, J.R. and Morrison, S.M. 1996. The invasive Asian copepod *Pseudodiaptomus inopinus* in Oregon, Washington, and British Columbia estuaries. Estuaries 19: 629-638.

Croll, D.A., Maron, J.L., Estes, J.A., Danner, E.M. and Byrd, G.V. 2005. Introduced predators transform subarctic islands from grasslands to tundra. Science 307: 1959-1961.

Daily, G.C. 1995. Restoring value to the world's degraded lands. Science 269: 250-254.

Darnaude, A.M., Salen-Picard, C., Polunin, N.V.C. and Harmelin-Vivien, M.L. 2004. Trophodynamic linkage between river runoff and coastal fishery yield by stable isotope data in the Gulf of Lions (NW Mediterranean). Oecologia 138: 325-332.

D'Iorio, M.M. 2003. Mangroves and shoreline change on Molokai, Hawaii: assessing the role of introduced *Rhizophora mangle* in sediment dynamics and coastal change using remote sensing and GIS. Ph.D. Dissertation. University of California, Santa Cruz, Santa Cruz, USA.

Duarte, C.M., Agustí, S., Kennedy, H. and Vaqué, D. 1999. The Mediterranean climate as a template for Mediterranean marine ecosystems: the example of the northeast Spanish littoral. Progress in Oceanography 44: 245-270.

Epstein, P.R., Diaz, H.F., Elias, S., Grabherr, G., Graham, N.E., Martens, W.J.M., Mosley-Thompson, E. and Susskind, J. 1998. Biological and physical signs of climate change: focus on mosquito-borne diseases. Bulletin of the American Meteorological Society 79: 409-417.

Evans, F.C. 1956. Ecosystem as the basic unit in ecology. Science 123: 1127-1128.

Fisher, S.G. and Likens, G.E. 1973. Energy flow in Bear Brook, New Hampshire: an integrative approach to stream ecosystem metabolism. Ecological Monographs 43: 421-439.

Foley, J.A., DeFries, R.S., Asner, G.P., Barford, C., Bonan, G., Carpenter, S.R., Chapin, F.S., Coe, M.T., Daily, G.C., Gibbs, H.K., Helkowski, J.H., Holloway, T., Howard, E.A., Kucharik, C.J., Monfreda, C., Patz, J.A., Prentice, I.C., Ramankutty, N. and Snyder, P.K. 2005. Global consequences of land use. Science 309: 570-574.

Furness, R.W. 1978. Energy requirements of seabird communities: a bioenergetic model. Journal of Animal Ecology 47: 39-53.

Gardener, R.H., O'Neill, R.V. and Turner, M.G. 1993. Ecological implications of landscape fragmentation. *In*: McDonnell, M.J. and Pickett, S.T.A. (eds.), Humans as Components of Ecosystems. pp. 208-226. Springer-Verlag, New York.

Glynn, P.W. 1991. Coral reef bleaching in the 1980s and possible connections with global warming. Trends in Ecology and Evolution 6: 175-179.

Golley, F.B. 1993. A History of the Ecosystem Concept in Ecology: More than the Sum of the Parts. Yale University Press, New Haven. 254 pp.

Grosholz, E. 2002. Ecological and evolutionary consequences of coastal invasions. Trends in Ecology and Evolution 17: 22-27.

Harris, J. 1993. Ecosystem structure and growth of the African savana. Global and Planetary Change 8: 231-248.

Harrold, C., Light, K. and Lisin, S. 1998. Organic enrichment of submarine-canyon and continental-shelf benthic communities by macroalgal drift imported from nearshore kelp forests. Limnology and Oceanography 43: 669-678.

Harvell, C.D., Mitchell, C.E., Ward, J.R., Altizer, S., Dobson, A.P., Otsfeld, R.S. and Samuel, M.D. 2002. Climate warming and disease risks for terrestrial and marine biota. Science 296: 2158-2162.

Harvell, C.D., Kim, K., Burkholder, J.M., Colwell, R.R., Epstein, P.R., Grimes, D.J., Hofmann, E.E., Lipp, E.K., Osterhaus, A.D.M.E., Overstreet, R.M., Porter, J.W., Smith, G.W. and Vasta, G.R. 1999. Emerging marine diseases--climate links and anthropogenic factors. Science 285: 1505-1510.

Haynes, D. and Michalek-Wagner, K. 2000. Water quality in the Great Barrier Reef World Heritage Area: past perspectives, current issues and new research directions. Marine Pollution Bulletin 41: 428-434.

Hoegh-Guldberg, O. 1999. Climate change, bleaching and the future of the world's coral reefs. Marine and Freshwater Research 50: 839-866.

Holling, C.S. 1973. Resilience and stability of ecological systems. Annual Review of Ecology and Systematics 4: 1-23.

Holt, R.D. 1993. Ecology at the mesoscale: the influence of regional processes on local communities. *In*: Ricklefs, R.E. and Schluter, D. (eds.), Species Diversity in Ecological Communities: Historical and Geographical Perspectives. pp. 77-88. The University of Chicago Press, Chicage.

Holt, R.D. 2004. Implications of system openness for local community structure and ecosystem function. *In*: Polis, G.A., Power, M.E. and Huxel, G.R. (eds.), Food Webs at the Landscape Level. pp. 96-114. The University of Chicago Press, Chicago.

Hubbell, S.P. 2001. The Unified Neutral Theory of Biodiversity and Biogeography. Princeton University Press, Princeton. 375 pp.

Huffaker, C.B. 1958. Experimental studies on predation: dispersion factors and predator-prey oscillations. Hilgardia 27: 343-383.

Hughes, T.P. 1994. Catastrophes, phase shifts, and large-scale degradation of a Caribbean coral reef. Science 265: 1547-1551.

Huisman, J. and Weissing, F.J. 1999. Biodiversity of plankton by species oscillations and chaos. Nature 402: 407-410.

Jackson, J.B.C., Kirby, M.X., Berger, W.H., Bjorndal, K.A., Botsford, L.W., Bourque, B.J., Bradbury, R.H., Cooke, R., Erlandson, J., Estes, J.A., Hughes, T.P., Kidwell, S., Lange, C.B., Lenihan, H.S., Pandolfi, J.M., Peterson, C.H., Steneck, R.S., Tegner, M.J. and Warner, R.R. 2001. Historical overfishing and the recent collapse of coastal ecosystems. Science 293: 629-638.

Jackson, J.K. and Fisher, S.G. 1986. Secondary production, emergence, and export of aquatic insects of a Sonoran Desert stream. Ecology 67: 629-638.

Jax, K. 1998. Holocoen and ecosystem--on the origin and historical consequences of two concepts. Journal of the History of Biology 31: 113-142.

Kates, R.W., Turner, B.L., II and Clark, W.C. 1995. The great transformation. *In*: Turner, B.L., II, Clark, W.C., Kates, R.W., Richards, J.F., Mathews, J.T. and Meyer, W.B. (eds.), The Earth as Transformed by Human Action. Cambridge University Press, Cambridge, UK.

Keeling, C.D., Bacastrow, R.B., Carter, A.F., Piper, S.C., Whorf, T.P., Heiman, M., Mook, W.G. and Roeloffzen, H. 1989. A three-dimensional model of atmospheric CO_2 transport based on observed winds: 1. Analysis of observational data. *In*: Peterson, D.H. (ed.), Aspects of climate variability in the Pacific and the western Americas. Geophysical Monographs. pp. 165-236. American Geophysical Union, Washington DC.

Kitchell, J.F., Schindler, D.E., Herwig, B.R., Post, D.M., Olson, M.H. and Oldham, M. 1999. Nutrient cycling at the landscape scale: the role of diel foraging migrations by geese at the Bosque del Apache National Wildlife Refuge, New Mexico. Limnology and Oceanography 44: 828-836.

Lawton, J.H. and Brown, V.K. 1993. Redundancy in ecosystems. *In*: Shulze, E.D. and Mooney, H.A. (eds.), Biodiversity and Ecosystem Function. pp. 255-270. Springer-Verlag, Berlin, Germany.

Lenes, J.M., Walsh, J.J., Otis, D.B. and Carder, K.L. 2005. Iron fertilization of *Trichodesmium* off the west coast of Barbados: a one-dimensional numerical model. Deep-Sea Research Part I Oceanographic Research Papers 52: 1021-1041.

Lennon, J.T. and Pfaff, L.E. 2005. Source and supply of terrestrial organic matter affects aquatic microbial metabolism. Aquatic Microbial Ecology 39: 107-119.

Lessios, H.A. 1988. Mass mortality of *Diadema antillarum* in the Caribbean: what have we learned? Annual Review of Ecology and Systematics 19: 371-393.

Likens, G.E. 1992. The Ecosystem Approach: Its Use and Abuse. Excellence in Ecology. Ecology Institute, Oldendorf, Germany. 166 pp.

Likens, G.E. 2004. Some perspectives on long-term biogeochemical research from the Hubbard Brook ecosystem study. Ecology 85: 2355-2362.

Likens, G.E., Bormann, F.H., Johnson, N.M., Fisher, D.W. and Pierce, R.S. 1970. Effects of forest cutting and herbicide treatment on nutrient budgets in the Hubbard Brook watershed-ecosystem. Ecological Monographs 40: 23-47.

Lindeman, R.L. 1942. The trophic-dynamic aspect of ecology. Ecology 23: 399-417.

Loreau, M., Mouquet, N. and Gonzalez, A. 2003a. Biodiversity as spatial insurance in heterogeneous landscapes. Proceedings of the National Academy of Sciences 100: 12765-12770.

Loreau, M., Mouquet, N. and Holt, R.D. 2003b. Meta-ecosystems: a theoretical framework for a spatial ecosystem ecology. Ecology Letters 6: 673-679.

Loreau, M., Downing, A., Emmerson, M., Gonzalez, A., Hughes, J., Inchausti, P., Joshi, J., Norberg, J. and Sala, O. 2002. A new look at the relationship between diversity and stability. *In*: Loreau, M., Naeem, S. and Inchausti, P. (eds.), Biodiversity and Ecosystem Functioning. pp. 79-91. Oxford University Press, New York.

Ludwig, W., Probst, J.-L. and Kempe, S. 1997. Predicting the oceanic input of organic carbon by continental erosion. Global Biogeochemical Cycles 10: 23-41.

Manson, F.J., Lonergan, N.R., Harch, B.D., Skilleter, G.A. and Williams, L. 2005. A broad-scale analysis of links between coastal fisheries production and mangrove extent: a case-study for northeastern Australia. Fisheries Research 74: 69-85.

Matson, P.A., Parton, W.J., Power, A.G. and Swift, M.J. 1997. Agricultural intensification and ecosystem properties. Science 277: 504-509.

Mayer, M.S. and Likens, G.E. 1987. The importance of algae in a shaded headwater stream as food for an abundant caddisfly (Trichoptera). Journal of the North American Benthological Society 6: 262-269.

McCann, K.S. 2000. The diversity-stability debate. Nature 405: 228-233.

McClanahan, T.R., Maina, J. and Pet-Soede, L. 2002. Effects of the 1998 coral mortality event on Kenyan coral reefs and fisheries. Ambio 31: 543-550.

McCook, L.J., Jompa, J. and Diaz-Pulido, G. 2001. Competition between corals and algae on coral reefs: a review of evidence and mechanisms. Coral Reefs 19: 400-417.

McDonnell, M.J. and Pickett, S.T.A. 1994. Introduction: scope and need for an ecology of subtle human effects and populated areas. *In*: McDonnell, M.J. and Pickett, S.T.A. (eds.), Humand as Components of Ecosystems. pp. 1-5. Springer-Verlag, New York.

McGrady-Steed, J., Harris, P.M. and Morin, P.J. 1997. Biodiversity regulates ecosystem predictability. Nature 390: 162-165.

Meyer, J.L. and Johnson, C. 1983. The influence of elevated nitrate concentration on rate of leaf decomposition in a stream. Freshwater Biology 13: 177-183.

Minakawa, N., Gara, R.I. and Honea, J.M. 2002. Increased individual growth rate and community biomass of stream insects associated with salmon carcasses. Journal of the North American Benthological Society 21: 651-659.

Mouquet, N. and Loreau, M. 2002. Coexistence in metacommunities: the regional similarity hypothesis. The American Naturalist 159: 420-426.

Mumby, P.J., Edwards, A.J., Arias-González, J.E., Lindeman, K.C., Blackwell, P.G., Gall, A., Gorczynska, M.I., Harborne, A.R., Pescod, C.L., Renken, H., Wabnitz, C.C.C. and Llewellyn, G. 2004. Mangroves enhance the biomass of coral reef fish communities in the Caribbean. Nature 427: 533-536.

Naeem, S. 1998. Species redundancy and ecosystem reliability. Conservation Biology 12: 39-45.

Naeem, S. and Li, S. 1997. Biodiversity enhances ecosystem reliability. Nature 309: 507-509.

Naeem, S., Thompson, L.J., Lawler, S.P., Lawton, J.H. and Woodfin, R.M. 1994. Declining biodiversity can alter the performance of ecosystems. Nature 368: 734-737.

Naeem, S., Thompson, L.J., Lawler, S.P., Lawton, J.H. and Woodfin, R.M. 1995. Empirical evidence that declining species diversity may alter performance of terrestrial ecosystems. Philosophical Transactions: Biological Sciences 347: 249-262.

Nugues, M.M. and Roberts, C.M. 2003. Partial mortality in massive reef corals as an indicator of sediment stress on coral reefs. Marine Pollution Bulletin 46: 314-323.

Nystrom, M., Folke, C. and Moberg, F. 2000. Coral reef disturbance and resilience in a human-dominated environment. Trends in Ecology and Evolution 15: 413-417.

Occhipinti-Ambrogi, A. and Savini, D. 2003. Biological invasions as a component of global change in stressed marine environments. Marine Pollution Bulletin 46: 542-551.

Odum, E.P. 1977. The emergence of ecology as a new integrative discipline. Science 4284: 1289-1293.

Odum, H.T. and Odum, E.P. 1955. Trophic structure and productivity of a windward coral reef community on Eniwetok Atoll. Ecological Monographs 25: 291-320.

O'Neill, R.V. 2001. Is it time to bury the ecosystem concept? (With full military honors, of course!). Ecology 82: 3275-3284.

Opdam, P. and Wascher, D. 2004. Climate change meets habitat fragmentation: linking landscape and biogeographic scale levels in research and conservation. Biological Conservation 117: 285-297.

Paine, R.T. 1969. A note on trophic complexity and community stability. The American Naturalist 103: 91-93.

Paterson, M.J., Findlay, D.L., Beaty, K., Findlay, W., Schindler, E.U., Stainton, M. and McCullough, G. 1997. Changes in the planktonic food web of a new experimental reservoir. Canadian Journal of Fisheries and Aquatic Sciences 54: 1088-1102.

Phillips, J. 1931. The biotic community. Journal of Ecology 19: 1-24.

Pickett, S.T.A. and Cadenasso, M.L. 2002. The ecosystem as a multidimensional concept: meaning, model and metaphor. Ecosystems 5: 1-10.

Pimentel, D., Allen, J., Beers, A., Guinand, L., Hawkins, A., Linder, R., McLaughlin, P., Meer, B., Musonda, D., Perdue, D., Poisson, S., Salazar, R., Siebert, S. and Stoner, K. 1993. Soil erosion and agricultural productivity. *In*: Pimentel, D. (ed.), World Soil Erosion and Conservation. pp. 277-292. Cambridge University Press, Cambridge, UK.

Pimm, S.L. 1984. The complexity and stability of ecosystems. Nature 307: 321-326.

Polis, G.A. and Hurd, S.D. 1995. Extraordinarily high spider densities on islands: flow of energy from the marine to terrestrial food webs and the absence of predation. Proceedings of the National Academy of Sciences 92: 4382-4386.

Polis, G.A. and Hurd, S.D. 1996. Linking marine and terrestrial food webs: allochthonous input from the ocean supports high secondary productivity on small islands and coastal land communities. The American Naturalist 147: 396-423.

Polis, G.A. and Strong, D.R. 1996. Food web complexity and community dynamics. The American Naturalist 147: 813-846.

Polis, G.A., Anderson, W.B. and Holt, R.D. 1997. Toward an integration of landscape and food web ecology: the dynamics of spatially subsidized food webs. Annual Review of Ecology and Systematics 28: 289-316.

Polis, G.A., Sanchez-Pinero, F., Stapp, P.T., Anderson, W.B. and Rose, M.D. 2004. Trophic flows from water to land: marine inputs affects food webs of islands and coastal ecosystems worldwide. *In*: Polis, G.A., Power, M.E. and Huxel, G.R. (eds.), Food Webs at the Landscape Level. pp. 200-216. The University of Chicago Press, Chicago.

Polunin, N. and Worthington, E.B. 1990. On the use and misuse of the term 'ecosystem'. Environmental Conservation 17: 274.

Postel, S.L., Daily, G.C. and Ehrlich, P.R. 1996. Human appropriation of renewable fresh water. Science 271: 785-788.

Power, M.E., Rainey, W.E., Parker, M.S., Sabo, J.L., Smyth, A., Khandwala, S., Finlay, J.C., McNeely, F.C., Marsee, K. and Anderson, C. 2004. River-to-watershed subsidies in an old-growth conifer forest. *In*: Polis, G.A., Power, M.E.

and Huxel, G.R. (eds.), Food Webs at the Landscape Level. pp. 217-240. The University of Chicago Press, Chicago.

Rodhe, H. 1990. A comparison of the contributions of various gases to the greenhouse effect. Science 248: 1217-1219.

Roff, D.A. 1974a. Spatial heterogeneity and the persistence of populations. Oecologia 15: 245-258.

Roff, D.A. 1974b. The analysis of a population model demonstrating the importance of dispersal in a heterogeneous environment. Oecologia 15: 259-275.

Rose, M.D. and Polis, G.A. 1998. The distribution and abundance of coyotes: the effects of allochthonous food subsidies from the sea. Ecology 79: 998-1007.

Rosenberg, A.A. and McLeod, K.L. 2005. Implementing ecosystem-based approaches to management for the conservation of ecosystem services. Marine Ecology Progress Series 3000: 270-274.

Sabo, J.L. and Power, M.E. 2002. River-watershed exchange: effects of riverine subsidies on riparian lizards and their terrestrial prey. Ecology 83: 1860-1869.

Sala, O.E., Chapin, F.S., III, Armesto, J.J., Berlow, E., Bloomfield, J., Dirzo, R., Huber-Sanwald, E., Huenneke, L.F., Jackson, R.B., Kinzig, A., Leemans, R., Lodge, D.M., Mooney, H.A., Oesterheld, M., Poff, N.L., Sykes, M.T., Walker, B.H., Walker, M. and Wall, D.H. 2000. Global biodiversity scenarios for the year 2100. Science 287: 1770-1774.

Scheffer, M. and Carpenter, S.R. 2003. Catastrophic regime shifts in ecosystems: linking theory to observation. Trends in Ecology and Evolution 18: 648-656.

Scheffer, M., Hosper, S.H., Meijer, M.-L., Moss, B. and Jeppesen, E. 1993. Alternative equilibria in shallow lakes. Trends in Ecology and Evolution 8: 275-279.

Scheffer, M., Carpenter, S., Foley, J.A., Folkes, C. and Walker, B. 2001. Catastrophic shifts in ecosystems. Nature 413: 591-596.

Schindler, D.W. 1977. Evolution of phosphorus limitation in lakes. Science 195: 260-262.

Semazzi, F.H.M. and Song, Y. 2001. A GCM study of climate change induced by deforestation in Africa. Climate Research 17: 169-182.

Silver, W.L., Brown, S. and Lugo, A.E. 1996. Effects of changes in biodiversity on ecosystem function in tropical forests. Conservation Biology 10: 17-24.

Smith, K.L., Jr., Baldwin, R.J. and Williams, P.M. 1992. Reconciling particulate organic carbon flux and sediment community oxygen consumption in the deep North Pacific. Nature 359: 313-317.

Soulé, M.E. 1995. The social siege of nature. *In*: Soulé, M.E. and Lease, G. (eds.), Reinventing Nature? pp. 137-170. Island Press, Washington DC.

Tansley, A.G. 1935. The use and abuse of vegetational concepts and terms. Ecology 16: 284-307.

Tilman, D. and Downing, J.A. 1994. Biodiversity and stability in grasslands. Nature 367: 363-365.

Tilman, D., Wedin, D. and Knops, J. 1996. Productivity and sustainability influenced by biodiversity in grassland ecosystems. Nature 379: 718-720.

Tilman, D., Knops, J., Wedin, D., Reich, P., Ritchie, M. and Siemann, E. 1997. The influence of functional diversity and composition on ecosystem processes. Science 277: 1300-1302.

Tilman, D., Fargione, J., Wolff, B., D'Antonio, C., Dobson, A., Howarth, R., Schindler, D., Schlesinger, W.H., Simberloff, D. and Swackhamer, D. 2001. Forecasting agriculturally driven global environmental change. Science 292: 281-284.

Tilman, D., Knops, J., Wedin, D. and Reich, P. 2002. Plant diversity and composition: effects on productivity and nutrient dynamics of experimental grasslands. *In*: Loreau, M., Naeem, S. and Inchausti, P. (eds.), Biodiversity and Ecosystem Functioning. pp. 21-35. Oxford University Press, New York.

Turner, M.G., Romme, W.H., Gardener, R.H., O'Neill, R.V. and Kratz, T.K. 1993. A revised concept of landscape equilibrium: disturbance and stability on scaled landscapes. Landscape Ecology 8: 213-277.

Vitousek, P.M. 1994. Beyond global warming: ecology and global change. Ecology 75: 1861-1876.

Vitousek, P.M., Ehrlich, P.R., Ehrlich, A.H. and Matson, P.A. 1986. Human appropriation of the products of photosynthesis. BioScience 36: 368-373.

Vitousek, P.M., D'Antonio, C., Loope, L. and Westbrooks, R. 1996. Biological invasions as global environmental change. American Scientist 84: 468-478.

Vitousek, P.M., Mooney, H.A., Lubchenco, J. and Melillo, J.M. 1997a. Human domination of Earth's ecosystems. Science 277: 494-499.

Vitousek, P.M., Aber, J.D., Howarth, R.W., Likens, G.E., Matson, P.A., Schindler, D.W., Schlesinger, W.H. and Tilman, D.G. 1997b. Human alteration of the global nitrogen cycle: sources and consequences. Ecological Applications 7: 737-750.

Vogt, K.A., Gordon, J.C., Wargo, J.P., Vogt, D.J., Asbjornsen, H., Palmiotto, P.A., Clark, H.J., O'Hara, J.L., Patel-Weynand, T., Larson, B., Tortoriello, D., Perez, J., Marsh, A., Corbett, M., Kaneda, K., Meyerson, F. and Smith, D. 1997. Ecosystems: Balancing Science With Management. Springer, New York. 470 pp.

Wachenfeld, D.R., Oliver, J.K. and Morrissey, J.I. 1998. State of the Great Barrier Reef World Heritage Area. Great Barrier Reef Marine Park Authority, Townsville.

Wainright, S.C., Haney, J.C., Kerr, C., Golovkin, A.N. and Flint, M.V. 1998. Utilization of nitrogen derived from seabird guano by terrestrial and marine plants at St. Paul, Pribilof Islands, Bering Sea, Alaska. Marine Biology 131: 62-71.

Wait, D.A., Aubrey, D.P. and Anderson, W.B. 2005. Seabird guano influences on desert islands: soil chemistry and herbaceous species richness and productivity. Journal of Arid Environments 60: 681-695.

Walker, B. 1992. Biodiversity and ecological redundancy. Conservation Biology 6: 18-23.

Walker, B. 1995. Conserving biological diversity through ecosystem resilience. Conservation Biology 9: 747-752.

Wallace, J.B., Eggert, S.L., Meyer, J.L. and Webster, J.R. 1997. Multiple trophic levels of a forest stream linked to terrestrial litter inputs. Science 277: 102-104.

Walther, G.-R., Post, E., Convey, P., Menzel, A., Parmesan, C., Beebee, T.J.C., Fromentin, J.-M., Hoegh-Guldberg, O. and Bairlein, F. 2002. Ecological responses to recent climate change. Nature 416: 389-395.

Webster, J.R. and Meyer, J.L. 1997. Organic matter budgets for streams: a synthesis. Journal of the North American Benthological Society 16: 141-161.

Weir, J.S. 1969. Importation of nutrients into woodlands by rooks. Nature 221: 487-488.

Werner, E.E. and Gilliam, J.F. 1984. The ontogenetic niche and species interactions in size-structured populations. Annual Review of Ecology and Systematics 15: 393-425.

Willis, A.J. 1997. The ecosystem: an evolving concept viewed historically. Functional Ecology 11: 268-271.

Willson, M.F., Gende, S.M. and Bisson, P.A. 2004. Anadromous fishes as ecological links between ocean, fresh water, and land. *In*: Polis, G.A., Power, M.E. and Huxel, G.R. (eds.), Food Webs at the Landscape Level. pp. 284-300. The University of Chicago Press, Chicago.

Wilson, D.S. 1992. Complex interactions in metacommunities, with implications for biodiversity and higher levels of selection. Ecology 73: 1984-2000.

Wipfli, M.S., Hudson, J.P., Chaloner, D.T. and Caouette, J.P. 1999. Influence of salmon spawner densities on stream productivity in southeast Alaska. Canadian Journal of Fisheries and Aquatic Sciences 56: 1600-1611.

Wooten, J.T. 1991. Direct and indirect effects of nutrients on intertidal community structure: variable consequences of seabird guano. Journal of Experimental Marine Biology and Ecology 151: 139-153.

Zhang, Q.-G. and Zhang, D.-Y. 2006. Species richness destabilizes ecosystem functioning in experimental aquatic microcosms. Oikos 112: 218-226.

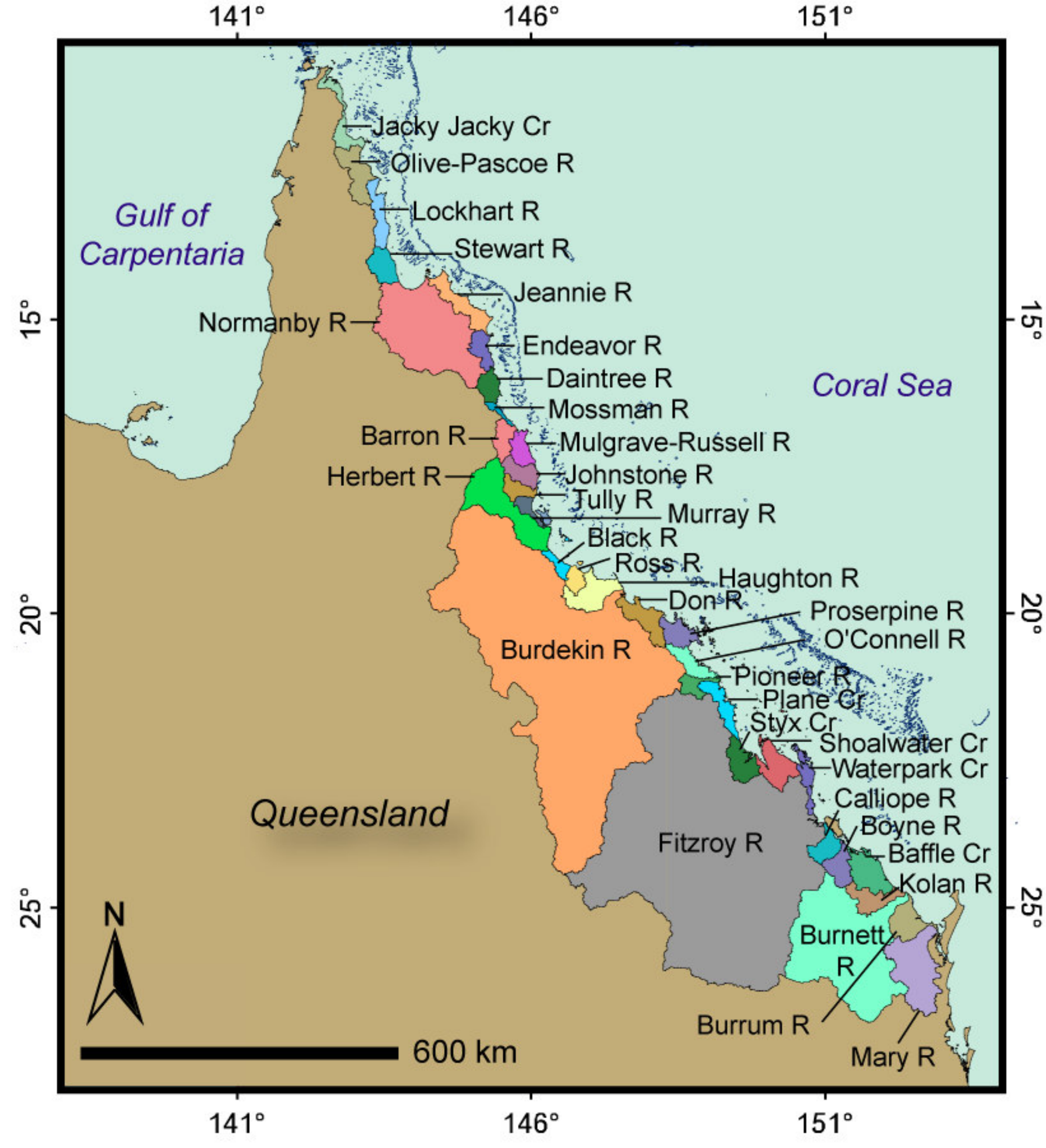

Figure 1.1. Catchments of the Great Barrier Reef Lagoon, Queensland, Australia.

Chapter 2. Land Use in the Pioneer Catchment: Changes in Cleared and Riparian Areas Interpreted in a Historical Context

Introduction

Conversion of natural forests to agriculture is a global phenomenon with croplands and pastures now occupying ~40% of terrestrial regions worldwide (Daily 1995; Ramankutty and Foley 1999; Asner et al. 2004; Foley et al. 2005). Degradation of water quality is one major consequence of such land use (Matson et al. 1997; Bennett et al. 2001). Intensive agriculture increases rates of soil erosion on land and suspended sediment loads in waterways, while fertilizers and pesticides applied to cultivated areas leach into ground and surface waters (Matson et al. 1997; Vitousek et al. 1997a; Vitousek et al. 1997b; Foley et al. 2005). Agricultural activities are now the largest sources of excess total nitrogen (N) and phosphorus (P) to the coastal zone (Carpenter et al. 1998; Bennett et al. 2001).

Relationships between vegetation cover, runoff and soil erosion are well documented for many systems around the world (Douglas 1967; Bormann and Likens 1979; Evans 1980; Trimble 1990; Viles 1990). Forest ecosystems affect water flux via: (1) transpiration, which affects soil moisture and streamflow; (2) dissipation of raindrop energy, which affects runoff rates; (3) decomposition of organic matter, which facilitates infiltration and increases soil water storage; and (4) export of logs and debris, which affects streamflow (Bormann and Likens 1979; Evans 1980; Viles 1990). These processes, along with soil binding by roots, also modify rates of erosion and particulate matter export from the catchments (Bormann and Likens 1979; Viles 1990). In general, surface runoff and erosion rates increase when natural forest stands are cleared and/or overgrazed (Likens et al. 1970; Lusby 1970; Reed 1979; Gupta 1981; Mitchell 1990; Sahin and Hall 1996; Costa et al. 2003; Houser et al. 2006). Major changes in rates of sediment yield and runoff occur mainly with remnant vegetation cover <30%; changes of cover usually have little effect in areas with >30% remnant vegetation (Nortcliff et al. 1990).

When land is grazed or tilled, soil compaction leads to increasing erosion and runoff as infiltration declines (Trimble 1990; Pimentel et al. 1993; Robertson et al. 1996; Roth 2004). In Australia, soil erosion rates from catchments under grazing and cropping have been estimated or measured at 2.6-20 $t\ ha^{-1}\ yr^{-1}$ and <5 - >500 $t\ ha^{-1}\ yr^{1}$, respectively, far above the baseline range (<0.1-5 $t\ ha^{-1}\ yr^{-1}$) estimated for pristine catchments (Douglas 1967; Sallaway 1979; Matthews and Makepeace 1981; Capelin and Prove 1983; Mullins et al. 1984; Prove et al. 1986; Prove and Hicks 1991; Prove 1992). The large range of values for cultivated lands reflects regional differences in rainfall intensity and frequency, slope, geology, total vegetation cover and agricultural management practices (Gourlay and Hacker 1986; Furnas and Mitchell 2001; Neil et al. 2002). While eroded material is redeposited and/or trapped on floodplains before reaching catchment waterways (Gourlay and Hacker 1986), substantial amounts enter streams and are transported towards the sea.

Within zones of riparian vegetation, sediments from both overland wash and streamflow can be trapped by roots, trunks and branches, which dampen water velocity and shear, reduce scour, and increase particle settlement (Kirkby and Morgan 1980; Thorne 1990; Norris 1993). In addition, riparian vegetation buffers filter nutrients and chemical pollutants directly from runoff through vegetative uptake and indirectly via microbial cycling (Cooper et al. 1987; Dillaha et al. 1989; Norris 1993; Hubbard and Lowrance 1994; Arthington et al. 1997; Lowrance et al. 1997; Verhoeven et al. 2006), although Osborne and Kovacic (1993) found total and dissolved P may be re-released to waterways during the dormant season. Expanding land use activities have greatly reduced the total area of riparian vegetation worldwide; and within northeastern Australia, a large percentage of riparian losses have occurred within the past 50 years (Johnson et al. 2001). Yet in most regions of the world, changes to riparian vegetation have not been quantified systematically because of the labor required to map narrow riparian strips when using the traditional approach of visual interpretation from aerial photographs (Goetz 2006).

The principal objective of this chapter is to use images from the series of multispectral sensors on the Landsat satellites to map recent changes (between 1972 and 2004) in forest cover on both a basin-wide scale and within the riparian zones of the intensively farmed Pioneer River catchment surrounding the city of Mackay, Queensland, Australia. These data will be used to identify recent periods and spatial patterns of vegetation loss with the potential to affect catchment water quality, particularly sediment delivery to nearshore marine waters. Records of land clearing will be used, at least partially, to fill gaps in knowledge of catchment land use changes since European land-clearing began. Currently, available data on land use change from the Pioneer catchment include: (1) historical accounts of widespread catchment clearing following the settlement of Mackay in 1862; (2) district sugarcane harvest records on industry expansion since 1930; (3) clearing rates of woody vegetation since 1988, compiled by the Queensland Department of Natural Resources, Mines and Water's (QDNRMW) Statewide Landcover and Trees Survey (SLATS); and (4) current maps and pre-clearing estimates of riparian vegetation from the Queensland Environmental Protection Agency (QEPA). While the Queensland Department of Primary Industries has identified severe riverbank erosion as a major concern in the Pioneer catchment (QDPI 1993), and Brodie (2004) described the condition of the riparian vegetation as "severely disrupted or non-existent", no previous survey has mapped changing riparian area at <10 year intervals. These chronologies, combined with other available land cover change data for the Pioneer catchment, will be compared with coral proxy records of nearshore water quality in Chapter 6 to determine whether temporal changes in the proxy records of sediment delivery to the coast can be related to land use change over the past 60 years.

Methods

Study region

The Pioneer River catchment (Figure 2.1; 21^{o} – $21^{o}25'$S; $148^{o}30'$ – $149^{o}15'$E) covers 1570 km^2 within the Central Queensland Coast Bioregion (QDNRM 2001; Furnas 2003). It is bounded by the steep slopes of the Clarke Range to the northwest and the Connors Range to the southwest, both of which are composed largely of granites and granodiorites of the Carboniferous-Mesozoic Urannah Complex, the dominant geological unit within the catchment (Figure 2.2). Most of the lower elevation regions lie on Quaternary alluvium, which covers an underlying fault, the Pioneer lineament, along which the Pioneer River has developed (Gourlay and Hacker 1986).

The Pioneer catchment has four main sub-basins varying in topography, lithologies, vegetation, and land use: (1) Cattle Creek, (2) Upper Pioneer, (3) McGregor Creek, and (4) Lower Pioneer (QDNRM 2001). The headwaters of Cattle Creek begin at 700 m in Eungella National Park and drain rainforests on the steep terrain of the igneous Urannah Complex before reaching heavily cropped regions in the valley floor. The main tributaries of the Upper Pioneer subcatchment, Teemburra and Blacks Creeks, extend into the Clarke, Connors and Pinnacle Ranges where they drain open grassy to closed woodlands dominated by species of *Corymbia* and *Eucalyptus*. The lower portion of Blacks Creek passes through heavily grazed lands and carries a sandy sediment load from weathering of the granitic Urannah Complex source (QDNRM 2001). McGregor Creek, in the north central region of the catchment, drains *Corymbia/Eucalyptus* woodland and rainforest on the Urannah Complex and on the Permian volcanic and sedimentary units of the Middle Plains Range down to a valley floor that has been extensively cleared for sugarcane. Finally, the Lower Pioneer River, extending east from the confluence of Cattle Creek and the Upper Pioneer River, drains small catchments to the north with remnants of rainforest and open to wooded *Corymbia/Eucalyptus* areas largely on Permian volcanic and metamorphosed sediments. The Lower Pioneer River once overflowed across the floodplain (now largely converted to agriculture) into Sandy and Bakers Creeks during major flooding, but this has not occurred within the past 150 years (QDNRM 2001).

The Pioneer Valley has high natural rates of erosion from several factors: (1) deep weathering horizons due to its history of lush vegetation cover; (2) relatively rapid breakdown of granitic source rocks; (3) steep topography, with 27% (423 km^2) of the catchment on >20% slopes, leading to landslides during heavy rains; and (4) high flood runoff per unit area coupled with highly variable flow rates (Gourlay and Hacker 1986). Clearing vegetation for agricultural activities likely increased catchment sediment yield, which was estimated in the 1980s to be two to four-fold greater than the pre-clearing value (Gourlay and Hacker 1986; Hacker 1988). As evidence supporting increased yield, the -3 m contour of the sand bar at the mouth of the Pioneer River prograded 600 m seaward between its initial charting in 1886-87 and 1979, due to accumulation of 3.5×10^6 m^3 of fluvial sediment (Hacker 1988).

Sugarcane history

European exploration of the Pioneer River began in 1860 during a cattle run led by John Mackay (Gourlay and Hacker 1986). Mackay returned to settle the region in 1862, and by 1865, the first experimental sugarcane plot was planted (Kerr 1980; Manning 1983). In 1870, 400 ha of sugarcane were farmed, and by 1872, the Mackay district led Australian sugarcane production (Kerr 1980). Land clearing of native vegetation for agricultural production continued rapidly: there were 25 operational mills in 1883, and by 1902, most lands available for sugarcane were already being cropped (Bolton 1963).

Although the forested hillslopes were initially thought unsuitable for planting, lands north of the river were quickly cleared when the soil was deemed to be fertile (Manning 1983). Several mills, including The Cedars (Figure 2.3), expanded into the higher country, where stones were used to form broken terraces for erosion control (Manning 1983). According to *The Daily Mercury*'s 1967 centenary feature on the sugar industry, "most of the steep hillside paddocks were thrown out of cultivation . . . late in 1902, when field cultivation techniques made weed and moisture control on the flat country more positive."

Beginning in the late 1930s, applying fertilizer to sugarcane paddocks led to rapid development of the industry (Rolleston 1987), with a peak cane harvest of 77,766 km^2 within the Mackay district in 1998 (Figure 2.4). Similar heavy applications of pesticides and herbicides also increased yields; for example, cane production rose steadily from ~1948, when farmers first applied gammexane to control wireworm damage (Rolleston 1987). By 1996, the Central Queensland region (including Mackay) had the highest statewide application rate per ha of the herbicides diuron, ametryn and glyphosate (Brodie 2004). Since most (>90%) farmers switched harvesting methods to green cane harvesting and trash blanketing (GCTB) in the mid-1990s, runoff rates of sediments, nutrients and agrichemicals have likely declined (Mitchell et al. 2005). Under conventional tillage and harvesting (including burning), measured soil erosion rates from sugarcane paddocks in the Mackay region ranged between 42-227 t ha^{-1} yr^{-1} (Sallaway 1979). Following adoption of GCTB and minimum tillage, soil erosion rates have dropped to ~5-15 t ha^{-1} yr^{-1} (Rayment and Neil 1997; Rayment 2003; Mitchell et al. 2005).

Landsat imagery pre-processing

I subset seven Landsat Multispectral Scanner (MSS: 1972, 1978, 1984), Thematic Mapper (TM: 1990, 1995, 2004) and Enhanced Thematic Mapper Plus (ETM+: 2000) scenes to map land clearing and riparian change in the Pioneer River catchment (Table 2.1). All scenes (except 1990) were acquired during dry season months. I downloaded the 1990 and 2000 scenes as orthorectified products from the University of Maryland's Global Land Cover Facility (http://glcf.umiacs.umd.edu). The 1972, 1978, 1984 and 2004 scenes were purchased as Level-1G radiometrically and geometrically corrected products from the USGS National Land Archive Production System (NLAPS). The 1995 scene was purchased through QDNRMW's SLATS program and delivered as a radiometrically corrected product, georeferenced to Map Grid of Australia coordinates.

I applied a dark pixel subtraction to each image subset, with dark pixels defined by the average values within a region of interest covering ~7-8 ha selected from clear waters within Kinchant or Teemburra Dams. As the 1972 image was captured prior to completion of these dams, I selected pixels from Eungella Dam, approximately 9 km west of the Pioneer Catchment (see Figure 2.7a). This widely used approach attributes the minimum digital number (DN) values for each spectral band to atmospheric effects that are subsequently subtracted from each pixel within the scene (Chavez 1989). For post-classification change-detection applications, where each image date is classified independently, further atmospheric correction was unnecessary (Singh 1989; Song et al. 2001).

Because the delivered NLAPS Landsat scenes had considerable positional registration error, I further georectified the image subsets to the orthorectified 2000 Landsat ETM+ subset of the Pioneer catchment (Table 2.1). Following rectification, I used the Pioneer catchment boundary, defined by digital data provided by QDNRMW, to mask out all area outside of the Pioneer catchment management region for each image. All processing was done using ENVI v. 4.1 software.

Riparian vegetation mapping

Riparian zones are defined as the vegetation at the interface between terrestrial and aquatic systems, and may occupy a variety of landforms and communities across sharp environmental gradients (Gregory et al. 1991). For this study, the riparian zone was considered to be any forested area within a defined buffer region (see below), although this will necessarily included some purely terrestrial forest systems and may have excluded shrub and grassy area that also function to trap sediment and filter nutrients. I manually digitized riparian zones on the orthorectified 2000 Landsat ETM+ subset of the Pioneer catchment, using an assortment of groundtruth data to identify these areas: georeferenced 1998 and 2002 aerial photographs (estuary only); photographs taken coincidentally with GPS readings adjacent to catchment waterways; Australian Surveying and Land Information Group (AUSLIG) topographic maps; and a slope map calculated (kernel size = 10) from a NASA Shuttle Radar Topography Mission (SRTM) 3 arc-second digital elevation model (DEM) (~90 m horizontal data) subset to the Pioneer catchment. I added a five pixel buffer zone (~150 m) to the digitized riparian zones, and used this region to mask out all other catchment area from subsequent classifications of each dataset.

To standardize classification results, I spatially resampled all masked TM and ETM+ images to match MSS spatial resolution (57 m x 57 m pixels), and spectrally subset to four band files by omitting the larger infrared bands at 1.55-1.75 µm and 2.08-2.35 µm (for ETM+: 2.09-2.35 µm) wavelengths. Then I applied the MSS Tasseled Cap (TC) transformation to each scene to maximize discrimination of target landcover classes. The TC transformation reorients the data along a plane that typically contains >95% of all variation, with major axes relating to soil (Brightness) and vegetation (Greenness) reflectance characteristics (Kauth and Thomas 1976; Crist and Kauth 1986). Although the spectral coverage for the subset TM (0.45-0.53 µm, 0.52-0.60 µm, 0.63-0.69 µm, 0.76-0.90 µm) and ETM+ bands (0.45-0.515 µm, 0.525-0.605 µm, 0.63-0.69 µm, 0.75-0.90 µm) is slightly different from the MSS bands (0.5-0.6 µm, 0.6-0.7 µm, 0.7-0.8 µm, 0.8-1.1 µm), the transformed TC Greenness and Brightness features are nearly identical across datasets (Crist and Cicone 1984; Crist and Kauth 1986). I performed unsupervised ISODATA (Iterative

Self-Organizing Data Analysis Technique) classifications on each TC transformed dataset with the following input parameters: 100 iterations; 7 maximum classes; a convergence threshold of 95%; and a minimum of 500 pixels per class. Classes were merged into “riparian” and “non-riparian” based on evaluation of mean spectra and distributions across the catchment.

Land clearing mapping

I followed a similar protocol to map cleared land from the masked Pioneer catchment regions in the 2004 Landsat TM and 1972 Landsat MSS images. Because ISODATA classifications of TC transformed data initially did not produce coherent classes, I divided the catchment area into two subregions: (A) slope ≤ 10 degrees on terrain below 500 m elevation, which contained all of the sugarcane regions and alluvial plains; and (B) slope > 10 degrees and/or areas above 500 m, which largely encompassed the mountain ranges and high plateaus. To subset the data to divisions based on slope and elevation, I spatially resampled both the 2004 TM and 1972 MSS data to match the SRTM DEM resolution (86.5 m x 92.27 m). For the 2004 TM data, regions A and B were separately subset to the first four bands and TC transformed, followed by classification with the ISODATA unsupervised algorithm using the following input parameters: 300 iterations; 7 maximum classes; a convergence threshold of 95%; and a minimum of 1000 pixels per class. I applied the same processing steps to the 1972 MSS data, except for the spectral subset. Classes were merged into “cleared” and “forest” based on evaluation of mean spectra and distributions across the catchment. Because the aspect angles of northeast-facing slopes caused some sun-illuminated forested lands to be misclassified as cleared lands, these areas were contextually edited following classification. Contextual editing, commonly applied in both marine and terrestrial environments, requires defining logical rules for the distributions of identified classes and reclassifying pixels that have been assigned to an "out-of-context" class (Groom et al. 1996; Mumby et al. 1998).

Accuracy assessments

Accuracy assessments were performed on 2004 Landsat classifications of riparian/non-riparian area and cleared/forest lands. In March 2005 and March 2006, I collected field validation points by stratified random sampling in the Pioneer catchment using visual assessments of ground cover, and I recorded all locations with a 12 channel handheld GPS (measurement accuracy <20 m). I assessed the accuracy of land clearing using a 2 x 2 normalized error matrix (Congalton 1991), with 170 and 130 reference points for the "cleared" and "forest" classes respectively. To determine whether spatial resampling impacted classification accuracy of the often narrow riparian habitat strip, I also used 2 x 2 error matrices to compare field reference points (118 riparian, 94 non-riparian) to classifications from both 28.5 m and resampled 57 m spatial resolutions. The error matrices report the overall accuracy, as well as the commission, omission, user's and producer's accuracies. Commission errors are those that misclassify a pixel to another class, while omission errors occur when pixels are erroneously excluded from a class (Congalton and Green 1999). The user's accuracy, calculated by dividing the number of correctly classified pixels in a class by the total number of pixels assigned to that class, is the probability that the mapped class (e.g. riparian, forest) correctly represents its ground distribution. The producer's accuracy, calculated by dividing the total number of correctly classified pixels in a class by the total number of reference measurements of that class, is the probability that a class identified from the reference data is correctly classified on the map. Errors of commission reduce user's accuracy while errors of omission reduce producer's accuracy (Stehman 1997). In addition to these values, K_{hat} statistics (an estimate of Kappa) were also calculated using the formula from Congalton and Green (1999):

$$\hat{K} = \frac{N \sum_{i=1}^{k} x_{ii} - \sum_{i=1}^{k} x_{i+} x_{+i}}{N^2 - \sum_{i=1}^{k} x_{i+} x_{+i}} \tag{2.1}$$

where N is the total number of reference points, x_{ii} is an error matrix diagonal, x_{i+} is the row total and x_{+i} is the column total. Kappa analysis, a standard feature of most remote sensing accuracy assessments, provides a measure of how many more pixels were correctly classified than expected by chance and can be used to statistically determine significant differences between error matrices (Congalton et al. 1983; Congalton 1991; Congalton and Green 1999).

Data integration

To evaluate the erosion potential for cleared land in the Pioneer catchment, classifications of cleared land from 1972 and 2004 were exported as shapefiles into a geographic information system (GIS) in ArcView 3.2 software and overlaid with maps of slope, geology and pre-clearing vegetation classes. I constructed the Pioneer catchment geologic map using Geoscience Australia (GA) vector digital geoscience data (1: 100,000 scale) for the Mackay (8755), Mirani (8655) and Hillalong (8555) map tile coverages (Figure 2.2). I used ArcView 3.2a software to merge polygons (assigned by GA) to reflect the major geologic units. I used the SRTM DEM (~90 m pixel) to construct a slope map in ENVI v. 4.1 software, where slope regions (<2º, 2-5º, 5-10º, 10-20º, 20-30º, >30º) were defined using band thresholds and exported as shapefiles into the GIS (Figure 2.1). I created pre-clearing and 2001 vegetation maps (1: 100,000 scale) using Queensland Environmental Protection Agency (QEPA) digital regional ecosystem (RE) data. I merged polygons of mixed categories with the dominant RE cover classes that are listed in Appendix A. Current RE distributions were mapped by QEPA from high resolution, stereo aerial photographs, combined with additional reference data from topographic charts, digital elevation models, geologic maps and Landsat TM scenes (Neldner et al. 2005). Distributions of pre-clearing RE classes were determined by QEPA by extrapolation from the earliest available photographs covering the entire catchment (1962), guided by land forms (see Neldner 1993; Fensham and Fairfax 1997; Neldner et al. 2005). The 2004 cleared areas were integrated in a GIS with QEPA's preclearing RE distributions to determine which REs have been most affected by clearing

Results

Classification accuracies

The 2004 riparian zone classification at 28.5 m resolution had an overall accuracy of 73.1% ($K_{\text{hat}} = 0.474$; Table 2.2). Of the 118 riparian reference points, 38.1% were misclassified as non-riparian regions (error of omission), resulting in a low producer's accuracy of 61.9%, while only 12.8% of the non-riparian reference points were misclassified. Resampling the data to 57 m did not change the overall accuracy, which remained at 73.1% ($K_{\text{hat}} = 0.469$; Table 2.2), but fewer errors of omission for the riparian class were offset by more errors of commission, as more non-riparian reference points were misclassified as riparian areas. The 2004 catchment land cover classification had an overall accuracy of 78.7% ($K_{\text{hat}} = 0.558$; Table 2.3), with the largest error coming from misclassification of forest as cleared land that resulted in a 31.5% omission error for the forest class.

Riparian vegetation change

The total forested area within the delineated riparian buffer zone declined by 32% from 175 km^2 in 1972 to 118.5 km^2 in 2004, with most losses occurring on the lower elevation alluvial plains in sugarcane growing regions (Figure 2.5, Table 2.4). While most losses came from reductions in the width of the riparian zone, other changes followed hydrologic manipulations, such as construction of Teemburra Dam in 1997. Annual net rates of change of forested riparian area varied from +1.77 km^2 yr^{-1} between 1972 and1978 to -4.45 km^2 yr^{-1} between 1978 and 1984.

Catchment land cover change

The total area of cleared land in the 1972 MSS data (539.5 km^2) was very similar to that in the 2004 TM data (524 km^2; Table 2.4), which was only slightly more than the area of cleared land reported for 2001 by QEPA (509.9 km^2, Appendix A). While the percentage of cleared land on slopes > 2º was higher in 1972 (38.8%) than in 2004 (33.4%; Figure 2.6), this was due to the large burn scars (32 km^2) from wildfires in the 1972 image (Figure 2.7). There was no general trend of expansion or contraction of clearing across the catchment related to elevation, although in some regions (e.g. confluence of Blacks Creek and Upper Pioneer River), the cleared regions appeared to move upslope over time, while in others (e.g. Finch Hatton Creek) cleared regions may have been replaced by secondary forest. The most notable new cleared land in the 2004 image is from the Teemburra Dam region (Figure 2.8).

Current cleared areas are mainly found in regions that probably were occupied by *Melaleuca* (REs: 8.3.2, 8.3.11) and *Corymbia/Eucalypt* (REs: 8.3.5, 8.3.6a) woodlands, closed forests, and grasslands (RE: 8.3.12) on alluvial plains and terraces (Figure 2.9). Each of these REs now occupies <10% of its estimated original distribution (Appendix A). Small, sensitive coastal dune ecosystems, including grasslands and beach scrub (REs: 8.2.6a; 8.2.9), have also been reduced considerably through harbor and coastal development.

Discussion

Assessment of mapping techniques

The overall accuracies for mapping riparian vegetation (73.1%) and land cover (78.7%) in the Pioneer catchment were within the ranges reported in other studies that used Landsat satellite imagery. Johansen and Phinn (2006) had >80% accuracies when they mapped riparian areas in the tropical savannah in North Queensland using Landsat ETM+: riparian zones >50 m wide (spanning both sides of a creek) were accurately mapped, but strips <10 m wide could not be identified with this sensor (Johansen and Phinn 2006). Congalton et al. (2002) noted other sources of error when the Landsat TM pixels (28.5 m x 28.5 m) were larger than many ground features, which resulted in mixing of substrate spectra within pixels (pixel mixing). When they classified riparian vegetation from Landsat TM data within 15.25 m and 61 m (ground width) buffer strips along sections of the Yaquina River basin, Oregon, there was only 25% and 36% correspondence with classifications from aerial photography, although a substantial portion of the error resulted from misregistration of the photographs, causing vertical displacement of streams relative to their true field positions (Congalton et al. 2002). Using the same mapping technique as in this study (Tasseled Cap transformation followed by an ISODATA unsupervised classification), Manson et al. (2001) found 27.9-46.6% correspondence between maps of the linear extent of mangroves in northern Australia using Landsat TM and aerial photographs. Like Congalton et al. (2002), they attributed the mismatch to the unsuitability of Landsat data for accurate mapping of narrow fringes, and to positional errors of up to 60 m between the aerial photographs and Landsat imagery (Manson et al. 2001). This is consistent with assessments from the Pioneer catchment: I abandoned accuracy assessments for this study using georeferenced aerial photographs because of misregistration errors (> 150 m in some cases) that exceeded the width of the riparian zone in most areas in 2004.

Using reference data from field-checked locations can also introduce error. Because access is restricted on privately held lands, which comprise a large proportion of the Pioneer catchment, riparian areas were accessed largely from main roads and bridges. To avoid trespassing, field locations for sugarcane and grazed paddocks were collected from the peripheries. Field validation points from these marginal locations are likely to involve a considerable amount of pixel mixing. Therefore, the reported accuracies are more reflective of how well the boundaries between classes have been mapped, rather than an estimate of classification within habitat patches: true accuracies of the classifications are probably higher than those reported here. Ideally, reference points should be taken from a representative distribution of locations both distant and adjacent to class borders.

Classification error can also result from a failure to distinguish different vegetation classes. In one study of the Yellowstone region, land cover classifications based on tasseled cap transformed Landsat TM and MSS data often resulted in mismatches between agricultural and vegetation classes, although the producer's and user's accuracies for both classes still exceeded 84% (Parmenter et al. 2003). Vina et al. (2004) also found high misclassification rates for agricultural classes ($K_{\mathrm{hat}} = 0.69$) mapped using ISODATA unsupervised classifications of Landsat TM data from the Colombia-Ecuador border region. Because the agricultural class was a heterogeneous mixture of land-cover categories with different amounts and types of vegetation cover and canopy architecture in different stages of growth, that class often was not distinguished from young secondary growth forest (Vina et al. 2004). While all vegetation classes contain some amount of spectral variability, they also share similar biophysical properties (e.g. photosynthetic pigments, vegetation cellular structure) that cause predictable and similar reflectance patterns (Crist and Kauth 1986), and this may lead to misclassification (particularly with sensors like Landsat MSS that have fairly low spectral resolution). Classification errors may also be introduced by the presence of different phenological stages of one vegetation type within the same scene, which can cause within-class spectral variability to exceed among-class variability (Price 1994; Lunetta et al. 2002), or by differences among scenes in rainfall and tidal height that may affect vegetation greenness and soil moisture (Khorram et al. 1999).

Despite these potential errors, vegetation mapping from moderately high resolution (20-30 m) satellite multispectral data can be both cost-effective and reliable for estimating stream and riparian conditions over large regions such as entire watersheds or watershed networks (Lattin et al. 2004; Van Sickle et al. 2004; Goetz 2006), although mapping accuracies could be improved with higher resolution (spatial, radiometric, and spectral) data and/or integration with data from active sensors, such as light and ranging (Lidar) systems (Goetz 2006; Johansen and Phinn 2006). In the present study, even though the catchment-scale Landsat data were resampled to ~90 m resolution for integration with elevation features from the SRTM DEM, the estimated area of cleared land in 2004 in the Pioneer catchment (524 km^2) was still very close to the Queensland Herbarium results (509.9 km^2) for 2001 based on regional ecosystem mapping (QEPA, unpublished data). Similarly, the total changes in riparian forested areas (20.3 km^2) between 1990 and 2004, mapped in the present study from resampled 57 m Landsat TM data, is almost the same as the 19.92 km^2 loss of woody foliage cover in the Pioneer catchment mapped from 28.5 m Landsat TM and ETM+ data by SLATS (QDNRM 2006). These similar results support the conclusion that clearing within the Pioneer watershed in recent decades occurred mainly in riparian areas of the floodplains.

Implications of land cover change for water quality

Catchment runoff and erosion rates are influenced not only by vegetation cover and land use type, but also by rainfall erosivity, slope, soil weathering (i.e.

underlying geology) and sediment transport of catchment waterways (Braud et al. 2001; Prosser et al. 2001; Neil et al. 2002; McKergow et al. 2005a). In the Pioneer River catchment, changing erosion and runoff rates between 1972 and 2004 are unlikely to have been affected by underlying geology or slope. The rocks are almost uniformly of granitic origin over the Upper Cattle Creek sub-catchment, which produces 80% of total discharge (Gourlay and Hacker 1986). Clearing steep slopes can result in elevated erosion rates (e.g. >4000 mg/L of total suspended solids (TSS) from the highly disturbed, developing urban Airlie Creek sub-catchment in the Whitsunday region; Rohde et al. 2006). Since initial clearing in the Pioneer catchment was in the late 19th and early 20th centuries, it is likely that current erosion and runoff rates from high slopes probably exceed preclearing baselines, but these rates are unlikely to have changed substantially since 1972. There is no evidence of expanded clearing on hillslopes in the Pioneer catchment between 1972 and 2004: the area of cleared land on slopes > 2º is not substantially different between 1972 and 2004 after the areas affected by wildfires (32 km^2) are subtracted from the 1972 total.

Because clearing by fire is a natural process that often results in rapid regrowth, the SLATS project generally does not map fire-affected areas as vegetation clearing (QDNRM 2006). Regeneration following burning can affect catchment runoff by reducing streamflow through increased transpiration rates (Langford 1976), yet, since flows from the Upper Pioneer subcatchment comprise only ~20% of the total catchment runoff (Credlin 1973), it is unlikely that fires in that region would have had a substantial effect on the total volume of water discharged by the Pioneer River.

By contrast, the substantial loss of riparian area and the reduced widths of the buffer zone across most of the catchment are more likely to have influenced runoff and erosion rates than changes in higher elevation regions. The overall area of riparian vegetation within the Pioneer catchment declined by approximately 56.4 km^2 (32% of the 1972 baseline). This loss is consistent with recent changes in riparian vegetation in other parts of Queensland, such as the Herbert River and Johnstone River catchments, where 80% and 60% of riparian and freshwater wetlands, respectively, have been lost since 1943 and 1951 (Johnson et al. 1999). In all the above cases, sugarcane is now planted on alluvial floodplains formerly occupied largely by *Melaleuca* stands (Arthington et al. 1997; Johnson et al. 1999).

Because most losses of riparian vegetation within the Pioneer catchment have occurred adjacent to sugarcane paddocks, water draining from these regions is likely to have higher suspended sediment and nutrient loads (Dillaha et al. 1989; Norris 1993). In a comparison of sub-catchments from the Mackay and Whitsunday regions, average storm maximum and ambient baseflow levels of total suspended solids (TSS) in January 2005 were two and eleven-fold greater, respectively, from sub-catchments cleared for sugarcane than from forested sub-catchments (Rohde et al. 2006). Simultaneously, maximum storm levels of total N and P in runoff from sugarcane sub-catchments were approximately twice as high as those from forested sub-catchments, while ambient levels were four to six-fold greater from the cultivated areas (Rohde et al. 2006). In March 2006, I conducted (with G. Marion) a more complete survey of ambient water nutrient concentrations from Pioneer catchment waterways draining different land use types: when these data are available they will be used to assess correlations between stream and riparian conditions.

Conclusions

Moderately high resolution Landsat satellite imagery was a cost-effective and efficient data source for mapping changes to land cover within the Pioneer River catchment. Between 1972 and 2004, the total area of cleared land remained relatively constant, while the area of riparian vegetation declined by 56.5 km^2 (32% net loss), mainly through reduced width of riparian buffer zones. Most riparian losses occurred on alluvial floodplains where riparian stands dominated by *Melaleuca* spp. have been replaced by sugarcane or weeds. The reduced width of riparian zones is likely to have major consequences for the quality of water draining off agricultural regions, in addition to decreasing the area of habitat for associated faunal communities. In Chapter 6, these temporal records of land cover change, in combination with records of mangrove change (Chapter 3), will be compared with proxy records of variations in nearshore and midshelf water quality (Chapters 4 and 5) to determine whether there have been changes in the magnitude of terrestrial influences on coral reef environments near Mackay.

References

Arthington, A.H., Marshall, J.C., Rayment, G.E., Hunter, H.M. and Bunn, S.E. 1997. Potential impact of sugarcane production on riparian and freshwater environments. *In*: Keating, B.A. and Wilson, J.R. (eds.), Intensive Sugarcane Production: Meeting the Challenges Beyond 2000. pp. 403-421. CAB International, Wallingford, UK.

Asner, G.P., Elmore, A.J., Olander, L.P., Martin, R.E. and Harris, A.T. 2004. Grazing systems, ecosystem responses, and global change. Annual Review of Environment and Resources 29: 261-299.

Bennett, E.M., Carpenter, S.R. and Caraco, N.F. 2001. Human impact on erodable phosphorus and eutrophication: a global perspective. BioScience 51: 227-234.

Bolton, G.C. 1963. A Thousand Miles Away. Jacaranda, Brisbane, Australia. 366 pp.

Bormann, F.H. and Likens, G.E. 1979. Pattern and Process in a Forested Ecosystem: Disturbance, Development, and the Steady State Based on the Hubbard Brook Ecosystem Study. Springer-Verlag, New York. 253 pp.

Braud, I., Vich, A.I.J., Zuluaga, J., Fornero, L. and Pedrani, A. 2001. Vegetation influence on runoff and sediment yield in the Andes region: observation and modelling. Journal of Hydrology 254: 124-144.

Brodie, J. 2004. Mackay Whitsunday Region State of the Waterways Report 2004. ACTFR Report Number 02/03, Australian Centre for Tropical Freshwater Research, Townsville, Australia.

Capelin, M.A. and Prove, B.G. 1983. Soil conservation problems of the humid coastal tropics of North Queensland. Proceedings of the Australian Society of Sugar Cane Technology 5: 87-93.

Carpenter, S.R., Caraco, N.F., Correll, D.L., Howarth, R.W., Sharpley, A.N. and Smith, V.H. 1998. Nonpoint pollution of surface waters with phosphorus and nitrogen. Ecological Applications 8: 559-568.

Chavez, P.S., Jr. 1989. Radiometric calibration of Landsat Thematic Mapper multispectral images. Photogrammetric Engineering and Remote Sensing 55: 1285-1294.

Congalton, R.G. 1991. A review of assessing the accuracy of remotely sensed data. Remote Sensing of Environment 37: 35-46.

Congalton, R.G. and Green, K. 1999. Assessing the Accuracy of Remotely Sensed Data: Principles and Practices. Lewis Publications, Boca Raton. 137 pp.

Congalton, R.G., Oderwald, R.G. and Mead, R.A. 1983. Assessing Landsat classification accuracy using discrete multivariate statistical techniques. Photogrammetric Engineering & Remote Sensing 49: 1671-1678.

Congalton, R.G., Birch, K., Jones, R. and Schriever, J. 2002. Evaluating remotely sensed techniques for mapping riparian vegetation. Computers and Electronics in Agriculture 37: 113-126.

Cooper, J.R., Gilliam, J.W., Daniels, R.B. and Robarge, W.P. 1987. Riparian areas as filters for agricultural sediment. Soil Science Society of America Journal 51: 416-420.

Costa, M.H., Botta, A. and Cardille, J.A. 2003. Effects of large-scale changes in land cover on the discharge of the Tocantins River, Southeastern Amazonia. Journal of Hydrology 283: 206-217.

Credlin, B.L. 1973. Water resources of Mackay district. Producers Review 63: 9-15.

Crist, E.P. and Cicone, R.C. 1984. Comparisons of the dimensionality and features of simulated Landsat-4 MSS and TM data. Remote Sensing of Environment 14: 235-246.

Crist, E.P. and Kauth, R.J. 1986. The tasseled cap de-mystified. Photogrammetric Engineering & Remote Sensing 52: 81-86.

Daily, G.C. 1995. Restoring value to the world's degraded lands. Science 269: 250-254.

Dillaha, T.A., Reneau, R.B., Mostaghimi, S. and Lee, D. 1989. Vegetative filter strips for agricultural nonpoint source pollution control. Transactions of the American Society of Agricultural Engineers 32: 513-519.

Douglas, I. 1967. Man, vegetation and the sediment yields of rivers. Nature 215: 925-928.

Fensham, R.J. and Fairfax, R.J. 1997. The use of the land survey record to reconstruct pre-European vegetation patterns in the Darling Downs, Queensland, Australia. Journal of Biogeography 24: 827-836.

Foley, J.A., DeFries, R.S., Asner, G.P., Barford, C., Bonan, G., Carpenter, S.R., Chapin, F.S., Coe, M.T., Daily, G.C., Gibbs, H.K., Helkowski, J.H., Holloway, T., Howard, E.A., Kucharik, C.J., Monfreda, C., Patz, J.A., Prentice, I.C., Ramankutty, N. and Snyder, P.K. 2005. Global consequences of land use. Science 309: 570-574.

Furnas, M. and Mitchell, A. 2001. Runoff of terrestrial sediment and nutrients into the Great Barrier Reef World Heritage Area. *In*: Wolanski, E. (ed.), Oceanographic Processes of Coral Reef: Physical and Biological Links in the Great Barrier Reef. pp. 37-51. CRC Press, Boca Raton.

Goetz, S.J. 2006. Remote sensing of riparian buffers: past progress and future prospects. Journal of the American Water Resources Association 42: 133-143.

Gourlay, M.R. and Hacker, J.L.F. 1986. Pioneer River Estuary Sedimentation Studies. University of Queensland, Department of Civil Engineering, St. Lucia, Australia. 207 pp.

Gregory, S.V., Swanson, F.J., McKee, W.A. and Cummins, K.W. 1991. An ecosystem perspective of riparian zones. BioScience 41: 540-551.

Groom, G.B., Fuller, R.M. and Jones, A.R. 1996. Contextual correction: techniques for improving land cover mapping from remotely sensed images. International Journal of Remote Sensing 17: 69-89.

Gupta, R.K. 1981. Ecological consequences of irrational land uses on loss of productive soil. *In*: Tingsanchali, T. and Eggers, H. (eds.), Proceedings of the South East Asian Regional Symposium on Problems of Soil Erosion and Sedimentation, Bangkok, Thailand, pp. 219-230.

Hacker, J.L.F. 1988. Rapid accumulation of fluvially derived sands and gravels in a tropical macrotidal estuary: the Pioneer River at Mackay, North Queensland, Australia. Sedimentary Geology 57: 299-315.

Houser, J.N., Mulholland, P.J. and Maloney, K.O. 2006. Upland disturbance affects headwater stream nutrients and suspended sediments during baseflow. Journal of Environmental Quality 35: 352-365.

Hubbard, R.K. and Lowrance, R.R. 1994. Riparian forest buffer system research at the coastal plain experiment station, Tifton, GA. Water, Air, and Soil Pollution 77: 409-432.

Johansen, K. and Phinn, S. 2006. Mapping structural parameters and species composition of riparian vegetation using IKONOS and Landsat ETM+ data in Australian tropical savannahs. Photogrammetric Engineering & Remote Sensing 72: 71-80.

Johnson, A.K.L., Ebert, S.P. and Murray, A.E. 1999. Distribution of coastal freshwater wetlands and riparian forests in the Herbert River catchment and implications for management of catchments adjacent the Great Barrier Reef Marine Park. Environmental Conservation 26: 229-235.

Johnson, A.K.L., Bramley, R.G.V. and Roth, C.H. 2001. Landcover and water quality in river catchments of the Great Barrier Reef Marine Park. *In*: Wolanski, E. (ed.), Oceanographic Processes of Coral Reef: Physical and Biological Links in the Great Barrier Reef. pp. 19-35. CRC Press, Boca Raton.

Kauth, R.J. and Thomas, G.S. 1976. The Tasseled Cap--a graphic description of the spectral-temporal development of agricultural crops as seen by Landsat. *In*: Proceedings of the Symposium on Machine Processing of Remotely Sensed Data, Purdue University, West Lafayette, pp. 4B41-44B51.

Kerr, J.D. 1980. Pioneer Pageant--a History of the Pioneer Shire. Pioneer Shire Council, Mackay, Australia. 232 pp.

Khorram, S.K., Biging, G.S., Chrisman, N.R., Colby, D.R., Congalton, R.G., Dobson, J.E., Ferguson, R.L., Goodchild, M.F., Jensen, J.R. and Mace, T.H. 1999. Accuracy Assessment of Remote Sensing-Derived Change Detection. American Society for Photogrammetry and Remote Sensing, Bethesda. 64 pp.

Kirkby, M.J. and Morgan, R.P.C. 1980. Soil Erosion. Wiley-Interscience, New York, USa. 312 pp.

Langford, K.J. 1976. Change in yield of water following a bushfire in a forest of *Eucaplyptus regnans*. Journal of Hydrology 29: 87-114.

Lattin, P.D., Wigington, P.J., Jr., Moser, T.J., Peniston, B.E., Lindeman, D.R. and Oetter, D.R. 2004. Influence of remote sensing imagery source on quantification of riparian land cover/land use. Journal of the American Water Resources Association 40: 215-227.

Likens, G.E., Bormann, F.H., Johnson, N.M., Fisher, D.W. and Pierce, R.S. 1970. Effects of forest cutting and herbicide treatment on nutrient budgets in the Hubbard Brook watershed-ecosystem. Ecological Monographs 40: 23-47.

Lowrance, R.R., Altier, L.S., Newbold, J.D., Schnabel, R.R., Groffman, P.M. and Denver, J.M. 1997. Water quality functions of riparian forest buffer systems in the Chesapeake Bay Watershed. Environmental Management 21: 687-712.

Lunetta, R.S., Ediriwickrema, J., Johnson, D.M., Lyon, J.G. and McKerrow, A. 2002. Impacts of vegetation dynamics on the identification of land-cover change in a biologically complex community in North Carolina, USA. Remote Sensing of Environment 82: 258-270.

Lusby, G.C. 1970. Hydrologic and biotic effects of grazing versus non-grazing near Grand Junction, Colorado. U. S. Geological Survey Professional Paper 700B.

Manning, K.W. 1983. In Their Own Hands. Farleigh Co-op Sugar Milling Association Ltd., Farleigh, Australia.

Manson, F.J., Lonergan, N.R., McLeod, J.M. and Kenyon, R.A. 2001. Assessing techniques for estimating the extent of mangroves: topographic maps, aerial photographs and Landsat TM images. Marine and Freshwater Research 52: 787-792.

Matson, P.A., Parton, W.J., Power, A.G. and Swift, M.J. 1997. Agricultural intensification and ecosystem properties. Science 277: 504-509.

Matthews, A. and Makepeace, P. 1981. A new slant on soil erosion control. Cane Growers Quarterly Bulletin 45: 43-47.

McKergow, L.A., Prosser, I.P., Hughes, A.O. and Brodie, J. 2005. Regional scale nutrient modelling: exports to the Great Barrier Reef World Heritage Area. Marine Pollution Bulletin 51: 186-199.

Mitchell, C., Brodie, J. and White, I. 2005. Sediments, nutrients and pesticide residues in event flow conditions in streams of the Mackay Whitsunday Region, Australia. Marine Pollution Bulletin 51: 23-36.

Mitchell, D.J. 1990. The use of vegetation and land use parameters in modelling catchment sediment yields. *In*: Thornes, J.B. (ed.), Vegetation and Erosion: Processes and Environments. pp. 289-316. John Wiley and Sons Ltd., New York.

Mullins, J.A., Truong, P.N. and Prove, B.G. 1984. Options for controlling soil loss in canelands -- some interim values. Proceedings of the Australian Society of Sugar Cane Technology 6: 95-100.

Mumby, P.J., Clark, C.D., Green, E.P. and Edwards, A.J. 1998. Benefits of water column correction and contextual editing for mapping coral reefs. International Journal of Remote Sensing 19: 203-210.

Neil, D.T., Orpin, A.R., Ridd, P.V. and Yu, B. 2002. Sediment yield and impacts from river catchments to the Great Barrier Reef lagoon. Marine and Freshwater Research 53: 733-752.

Neldner, V.J. 1993. Vegetation survey and mapping in Queensland. Queensland Herbarium Bulletin, No.12, Department of Environment and Heritage, Brisbane, Australia.

Neldner, V.J., Wilson, B.A., Thompson, E.J. and Dillewaard, H.A. 2005. Methodology for survey and mapping of regional ecosystems and vegetation communities in Queensland. Version 3.1. Updated September 2005 Queensland Herbarium, Environmental Protection Agency, Brisbane, Australia.

Norris, V. 1993. The use of buffer zones to protect water quality: a review. Water Resources Management 7: 257-272.

Nortcliff, S., Ross, S.M. and Thornes, J.B. 1990. Soil moisture, runoff and sediment yield from differentially cleared tropical rainforest plots. *In*: Thornes, J.B. (ed.), Vegetation and Erosion: Processes and Environments. pp. 419-436. John Wiley and Sons Ltd., New York.

Osborne, L.L. and Kovacic, D.A. 1993. Riparian vegetated buffer strips in water-quality restoration and stream management. Freshwater Biology 29: 243-258.

Parmenter, A.W., Hansen, A., Kennedy, R.E., Cohen, W., Langer, U., Lawrence, R., Maxwell, B., Gallant, A. and Aspinall, R. 2003. Land use and land cover change in the greater Yellowstone ecosystem: 1975-1995. Ecological Applications 13: 687-703.

Pimentel, D., Allen, J., Beers, A., Guinand, L., Hawkins, A., Linder, R., McLaughlin, P., Meer, B., Musonda, D., Perdue, D., Poisson, S., Salazar, R., Siebert, S. and Stoner, K. 1993. Soil erosion and agricultural productivity. *In*: Pimentel, D. (ed.), World Soil Erosion and Conservation. pp. 277-292. Cambridge University Press, Cambridge, UK.

Price, J.C. 1994. How unique are spectral signatures? Remote Sensing of Environment 49: 181-186.

Prosser, I.P., Rutherfurd, I.D., Olley, J.M., Young, W.J., Walbrink, P.J. and Moran, C.J. 2001. Large scale patterns of erosion and sediment transport in river networks, with examples from Australia. Marine and Freshwater Research 52: 81-99.

Prove, B.G. 1992. Long term erosion rates in semiarid grazing lands. Erosion Research Newletter 8: 1-2.

Prove, B.G. and Hicks, W.S. 1991. Soil and nutrient movements from rural lands of north Queensland. *In*: Yellowlees, D. (ed.) Proceedings of the Land Use Patterns and Nutrient Loading of the Great Barrier Reef Region: Workshop at James Cook University, Townsville, Australia, pp. 67-76.

Prove, B.G., Truong, P.N. and Evans, D.S. 1986. Strategies for controlling caneland erosion in the wet tropical coasts of Queensland. Proceedings of the Australian Society of Sugar Cane Technology 8: 77-84.

Pulsford, J.S. 1996. Historical nutrient usage in coastal Queensland river catchments adjacent to the Great Barrier Reef Marine Park. Research Publication No. 40 Great Barrier Reef Marine Park Authority, Townsville, Australia.

QDNRM 2001. Pioneer Valley Water Resource Plan -- Current environmental conditions and impacts of existing water resource development. Queensland Department of Natural Resources and Mines, Brisbane, Australia.

QDNRM 2006. Land cover change in the Mackay-Whitsunday Natural Resource Management region 2003-2004. Addendum No. 8 to Land cover change in Queensland 2003-2004: a Statewide Landcover and Trees Study (SLATS) Report. Department of Natural Resources and Mines, Brisbane, Australia.

QDPI 1993. The condition of river catchments in Queensland: a broad overview of catchment management issues. Queensland Department of Primary Industries, Brisbane, Australia.

QEPA 2005. Regional Ecosystem Description Database (REDD). Version 5.0. Updated December 2005

Ramankutty, N. and Foley, J.A. 1999. Estimating historical changes in global land cover: croplands from 1700 to 1992. Global Biogeochemical Cycles 13: 997-1028.

Rayment, G.E. 2003. Water quality in sugar catchments of Queensland. Water Science and Technology 48: 35-47.

Rayment, G.E. and Neil, D.T. 1997. Sources of material in river discharge. *In*: Proceedings of the The Great Barrier Reef: Science, Use and Management, Townsville, Australia, pp. 42-58. Great Barrier Reef Marine Park Authority.

Reed, A.H. 1979. Accelerated erosion of arable soils in the United Kingdom by rainfall and runoff. Outlook on Agriculture 10: 41-48.

Robertson, A.I., Lee Long, W.J., Coles, R.G., Pearson, R.G. and Hegerl, E.J. 1996. Impacts of land and water use practices on riparian areas, wetlands, estuaries and coastal seagrasses. *In*: Hunter, H.M., Eyles, A.G. and Rayment, G.E. (eds.), Downstream Effects of Land Use. pp. 45-47. Queensland Department of Natural Resources, Brisbane, Australia.

Rohde, K., Masters, B., Brodie, J., Faithful, J., Noble, R. and Carroll, C. 2006. Fresh and marine water quality in the Mackay Whitsunday region 2004/2005. Mackay Whitsunday Natural Resource Management Group, Mackay, Australia.

Rolleston, F. 1987. The Defiance. North Eton Co-operative Sugar Milling Association Limited, North Eton, Australia.

Sahin, V. and Hall, M.J. 1996. The effects of afforestation and deforestation on water yields. Journal of Hydrology 178: 293-309.

Sallaway, M.M. 1979. Soil erosion studies in the Mackay district. *In*: Egan, B.T. (ed.) Proceedings of the Proceedings of the Australian Society of sugar cane technologists, pp. 322-327.

Singh, A. 1989. Digital change detection techniques using remotely-sensed data. International Journal of Remote Sensing 10: 989-1003.

Song, C., Woodcock, C.E., Seto, K.C., Lenney, M.P. and Macomber, S.A. 2001. Classification and change detection using Landsat TM data: when and how to correct atmospheric effects? Remote Sensing of Environment 75: 230-244.

Stehman, S.V. 1997. Selecting and interpreting measures of thematic classification accuracy. Remote Sensing of Environment 62: 77-89.

Thorne, C.R. 1990. Effects of vegetation on riverbank erosion and stability. *In*: Thornes, J.B. (ed.), Vegetation and Erosion: Processes and Environments. pp. 125-144. John Wiley and Sons Ltd., New York.

Trimble, S.W. 1990. Geomorphic effects of vegetation cover and management: some time and space considerations in prediction of erosion and sediment yield. *In*: Thornes, J.B. (ed.), Vegetation and Erosion: Processes and Environments. pp. 55-65. John Wiley and Sons Ltd., New York.

Van Sickle, J., Baker, J., Herlihy, A., Bayley, P., Gregory, S., Haggerty, P., Ashkenas, L. and Li, J. 2004. Projecting the biological condition of streams under alternative scenarios of human land use. Ecological Applications 14: 368-380.

Verhoeven, J.T.A., Arheimer, B., Yin, C. and Hefting, M.M. 2006. Regional and global concerns over wetlands and water quality. Trends in Ecology and Evolution 21: 96-103.

Viles, H.A. 1990. 'The agency of organic beings': a selective review of recent work in biogeomorphology. *In*: Thornes, J.B. (ed.), Vegetation and Erosion: Processes and Environments. pp. 5-24. John Wiley and Sons Ltd., New York.

Vina, A., Echavarria, F.R. and Rundquist, D.C. 2004. Satellite change detection analysis of deforestation rates and patterns along the Colombia-Ecuador border. Ambio 33: 118-125.

Vitousek, P.M., Mooney, H.A., Lubchenco, J. and Melillo, J.M. 1997a. Human domination of Earth's ecosystems. Science 277: 494-499.

Vitousek, P.M., Aber, J.D., Howarth, R.W., Likens, G.E., Matson, P.A., Schindler, D.W., Schlesinger, W.H. and Tilman, D.G. 1997b. Human alteration of the global nitrogen cycle: sources and consequences. Ecological Applications 7: 737-750.

Table 2.1. Specifications of Landsat satellite acquisitions and image georectification. (GCP = ground control points for rectification selected from Landsat 2000 image; RMSE = root mean squared error, calculated as the square root of the sum of the deviations of each pixel from the reference GCP)

Date	Platform	Product	Path	Row	# GCPs	RMSE
04 Aug 2004	Landsat 5	TM	93	75	60	0.527
16 Jul 2000	Landsat 7	ETM+	93	75	orthorectified	
27 Jul 1995	Landsat 5	TM	93	75	orthorectified	
04 Apr 1990	Landsat 5	TM	93	75	orthorectified	
22 Sep 1984	Landsat 4	MSS	93	75	20	0.456
16 Aug 1978	Landsat 3	MSS	99	75	10	0.593
29 Aug 1972	Landsat 1	MSS	99	75	10	0.474

Table 2.2. Error matrices and accuracy assessments of 2004 Landsat TM riparian zone classifications at 28.5 m (top) and resampled 57 m (bottom) resolution. Riparian and non-riparian Landsat classes were compared to 118 riparian and 94 non-riparian field-validated sites.

Image	Class	Field-validated Sites		Error (%)		Accuracy (%)			$\hat{K}$
		Riparian	Non-riparian	Commission	Omission	Producer's	User's	Overall	
Landsat 28.5 m	**Riparian**	73	12	14.1	38.1	61.9	85.9	73.1	0.474
	Non-riparian	45	82	35.4	12.8	87.2	64.6		
Landsat 57 m	**Riparian**	78	17	17.9	33.9	66.1	82.1	73.1	0.469
	Non-riparian	40	77	34.2	18.1	81.9	65.8		

Table 2.3. Error matrix and accuracy assessment of 2004 Landsat TM catchment land cover classification at ~90 m resolution. Cleared and forest Landsat classes were compared to 170 cleared and 130 forest field-validated sites.

Image	**Class**	**Field-validated Sites**		**Error (%)**		**Accuracy (%)**			$\hat{K}$
		Cleared	**Forest**	**Commission**	**Omission**	**Producer's**	**User's**	**Overall**	
Landsat ~90 m	**Cleared**	147	41	21.8	13.5	86.5	78.2	78.7	0.558
	Forest	23	89	20.5	31.5	68.8	79.5		

Table 2.4. Changes in riparian zone and catchment land cover (to nearest 0.1 km^2) mapped from Landsat satellite data between 1972 and 2004. Annual rates of riparian change are reported for each time interval.

Year	Riparian Zone		Catchment	
	Forest (km^2)	Change km^2/yr	Forest (km^2)	Cleared (km^2)
1972	175.0		1032.0	539.5
1978	185.6	+1.8		
1984	158.9	-4.5		
1990	138.9	-3.3		
1995	133.5	-1.1		
2000	126.2	-1.5		
2004	118.6	-1.9	1046.1	524.0
Net Change 1972-2004	-56.4		14.1	-15.5

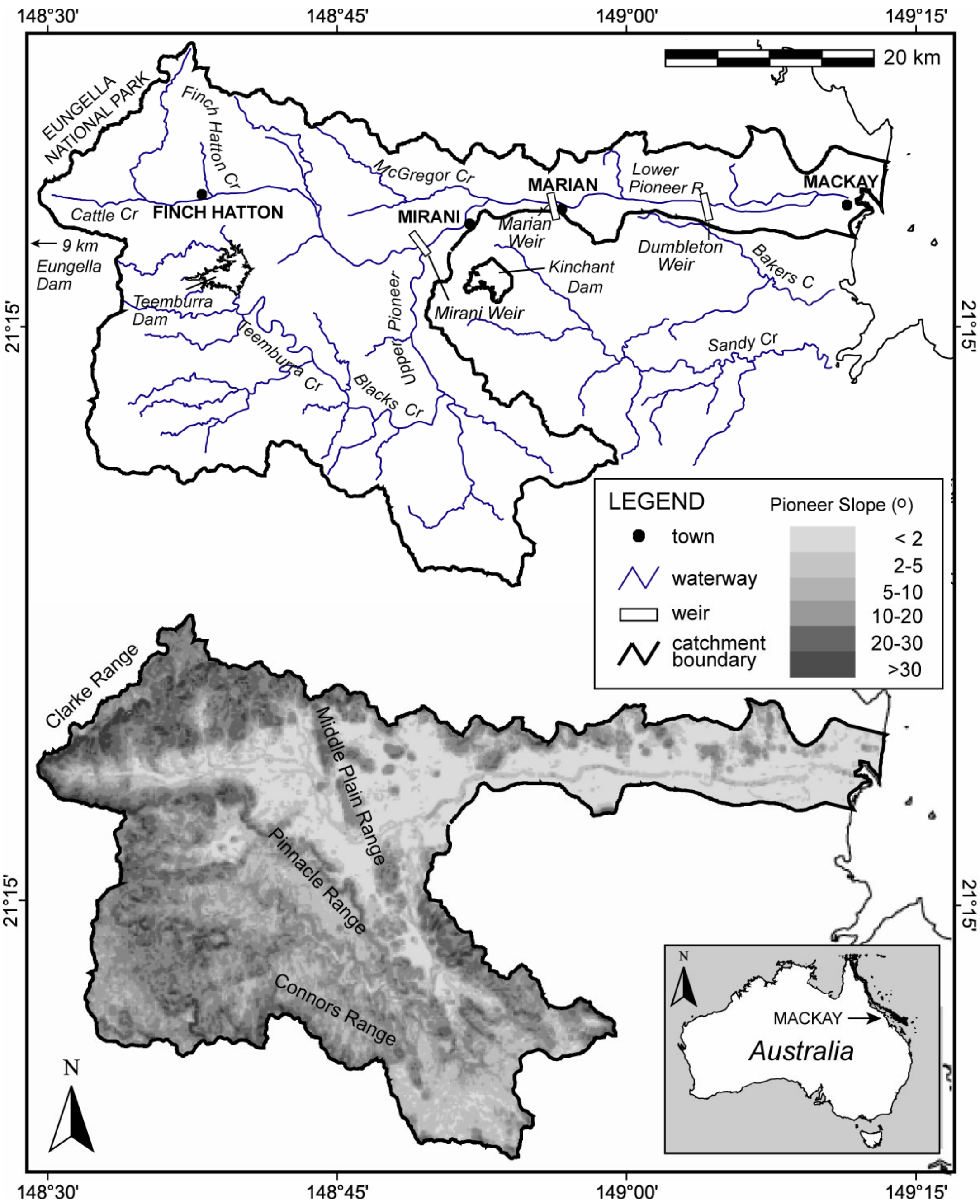

Figure 2.1. Major waterways and hydrological features (e.g. weirs, dams) of the Pioneer River, Sandy Creek and Bakers Creek catchments. Major mountain ranges are displayed below on a slope image calculated from an SRTM DEM.

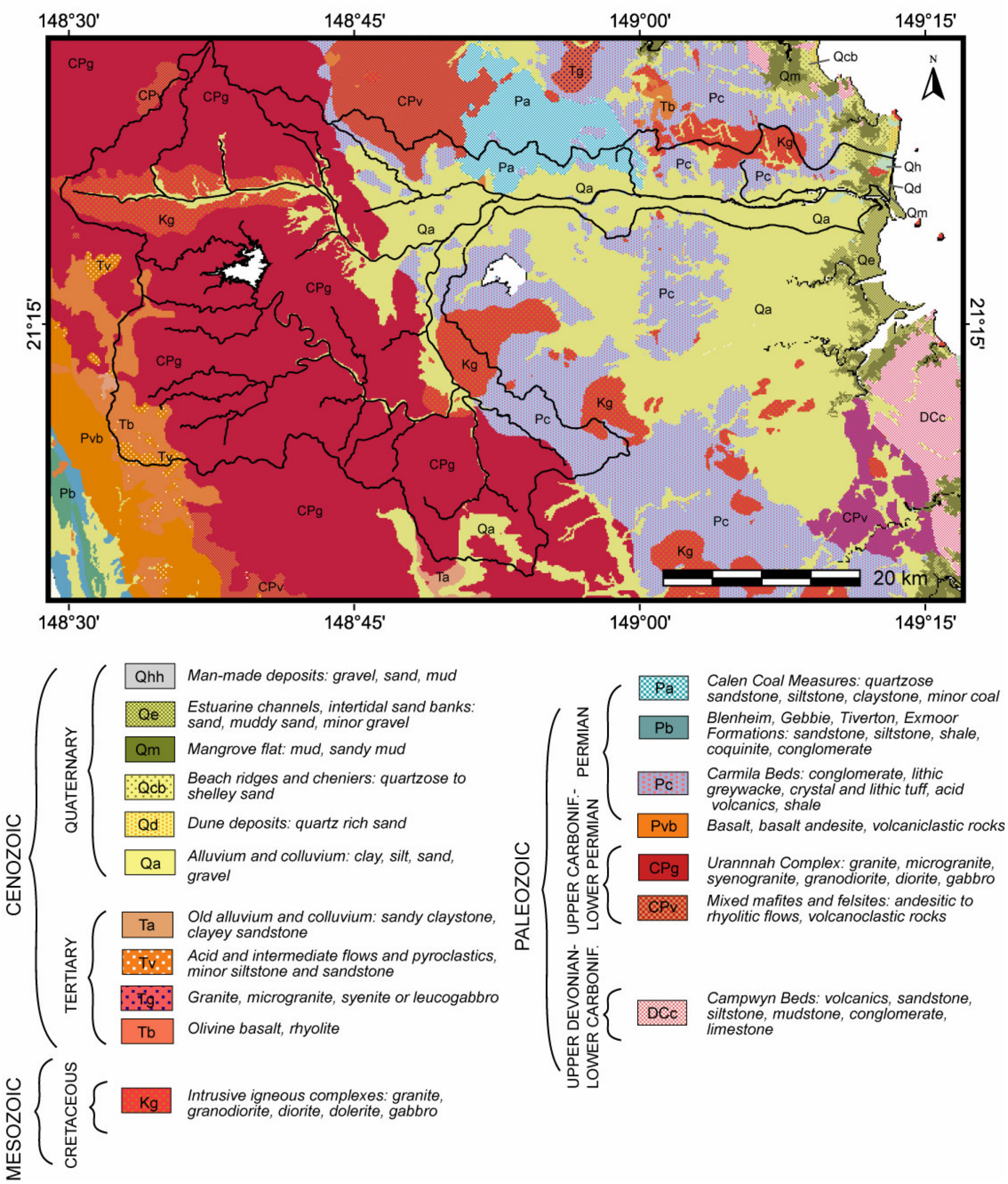

Figure 2.2. Geologic map of the Pioneer catchment region with major rock units (constructed using digital data from Geosciences Australia).

Figure 2.3. Photographs of early sugarcane expansion in the Mackay district, courtesy of John Oxley Library, Brisbane, Australia. (a) Cleared hillsides behind The Cedars plantation, c. 1878. (b) Workers harvesting sugarcane on steep slopes, c. 1910-12.


a


b

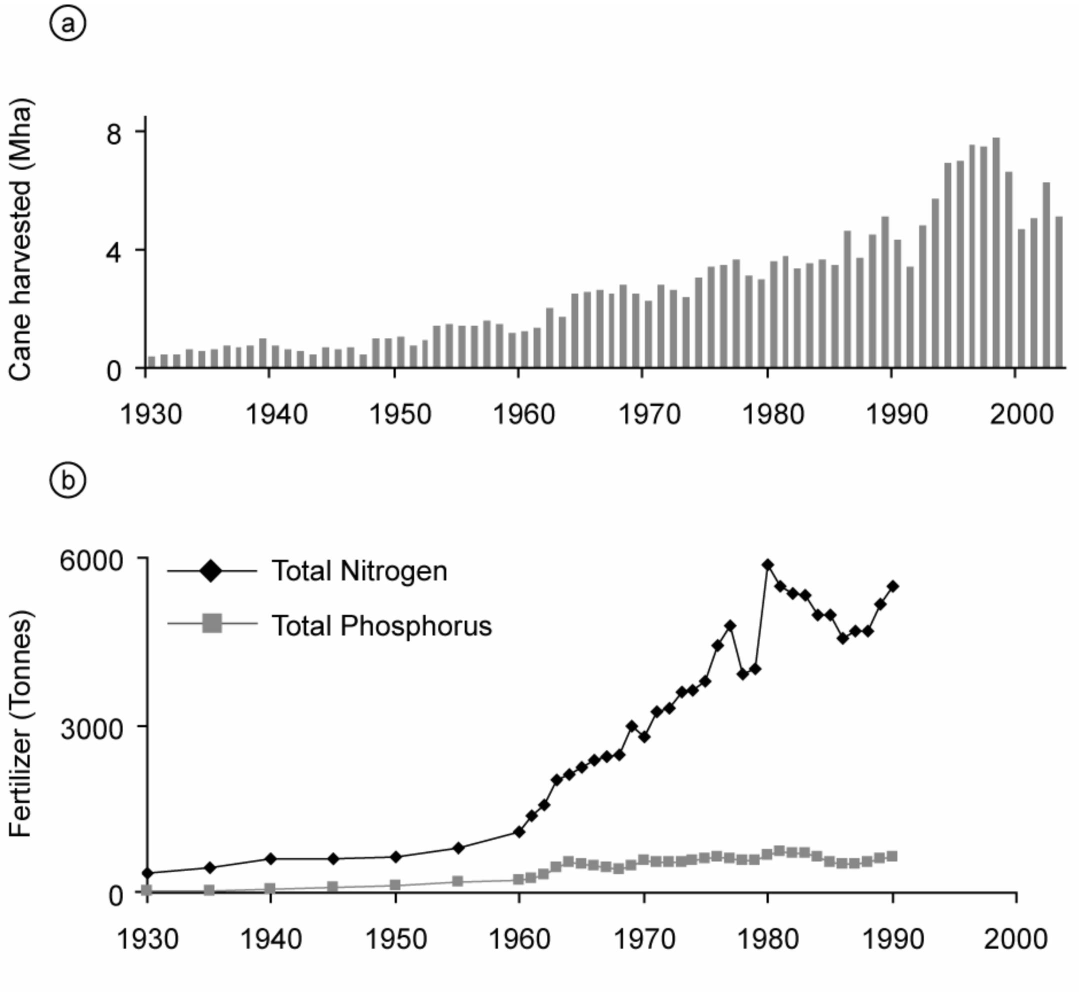

Figure 2.4. Mackay district sugarcane industry trends since 1930. (a) Area of sugarcane harvested (megahectares) within the Mackay district, 1930-2003. Data supplied by Queensland Cane Growers Organisation Ltd. (b) Annual tonnes of nitrogen and phosphorus fertilizer applied within the Pioneer catchment, 1930-1990, from Pulsford (1996). Data between 1930 and 1960 are estimates of average annual usage over each five year interval, based on cropped areas, census data and fertilizer industry records.

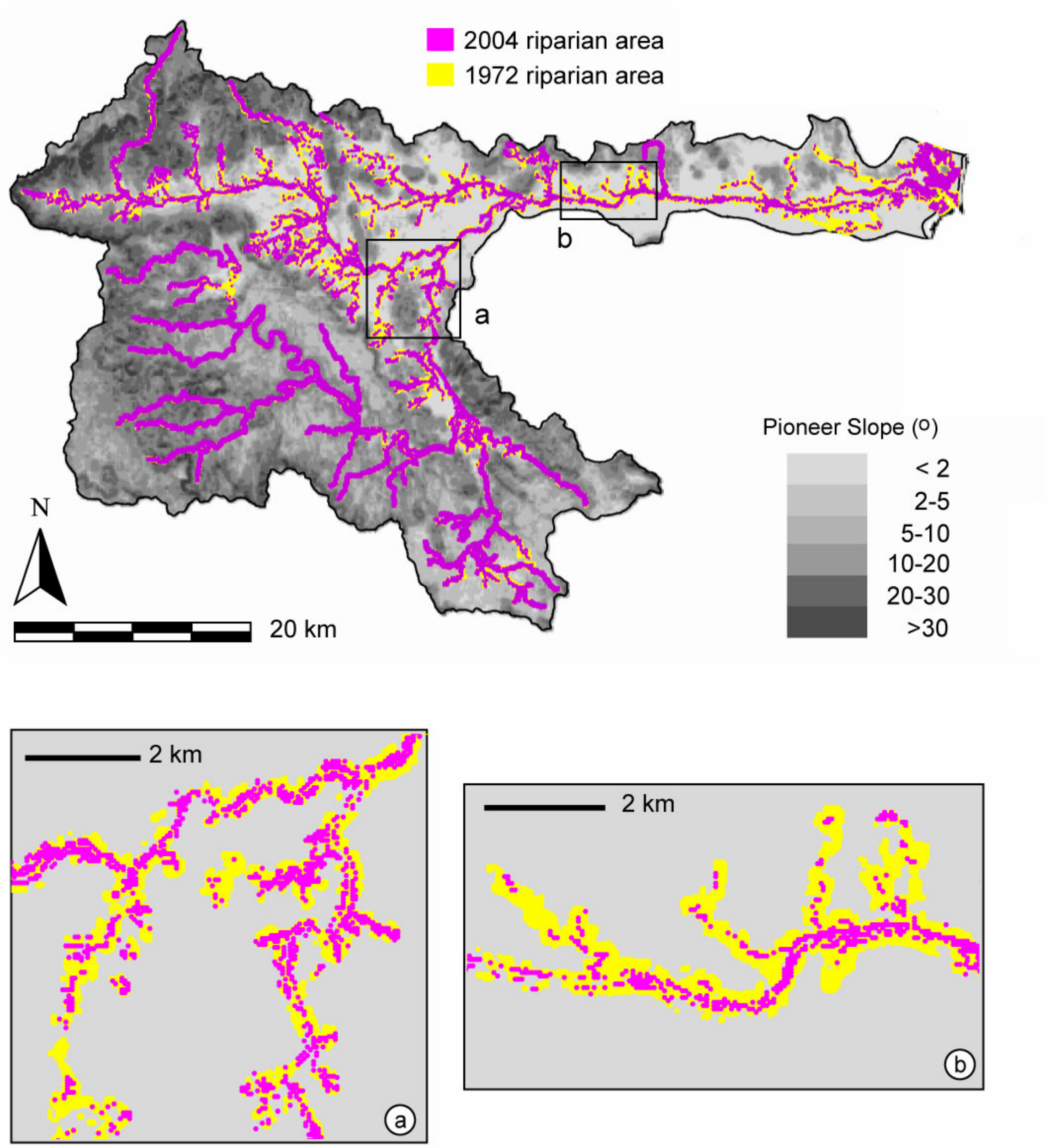

Figure 2.5. Forested area within the riparian zone of the Pioneer catchment mapped from 1972 Landsat MSS (yellow) and 2004 Landsat TM (magenta) images. The two enlarged subsets are examples that show reduced width of the riparian zone on the alluvial plains between 1972 and 2004.

Figure 2.6. Distributions of cleared land within the Pioneer catchment on slopes > 2º. (a) 1972 cleared land (aqua) mapped from Landsat MSS data. (b) 2004 cleared land (orange) mapped from Landsat TM data. (c) Changes to distributions on slopes > 2º. Magenta areas are regions on > 2º slope mapped as cleared area in 1972 that changed to regrowth forest by 2004. Green areas are regions on > 2º slope cleared since 1972.

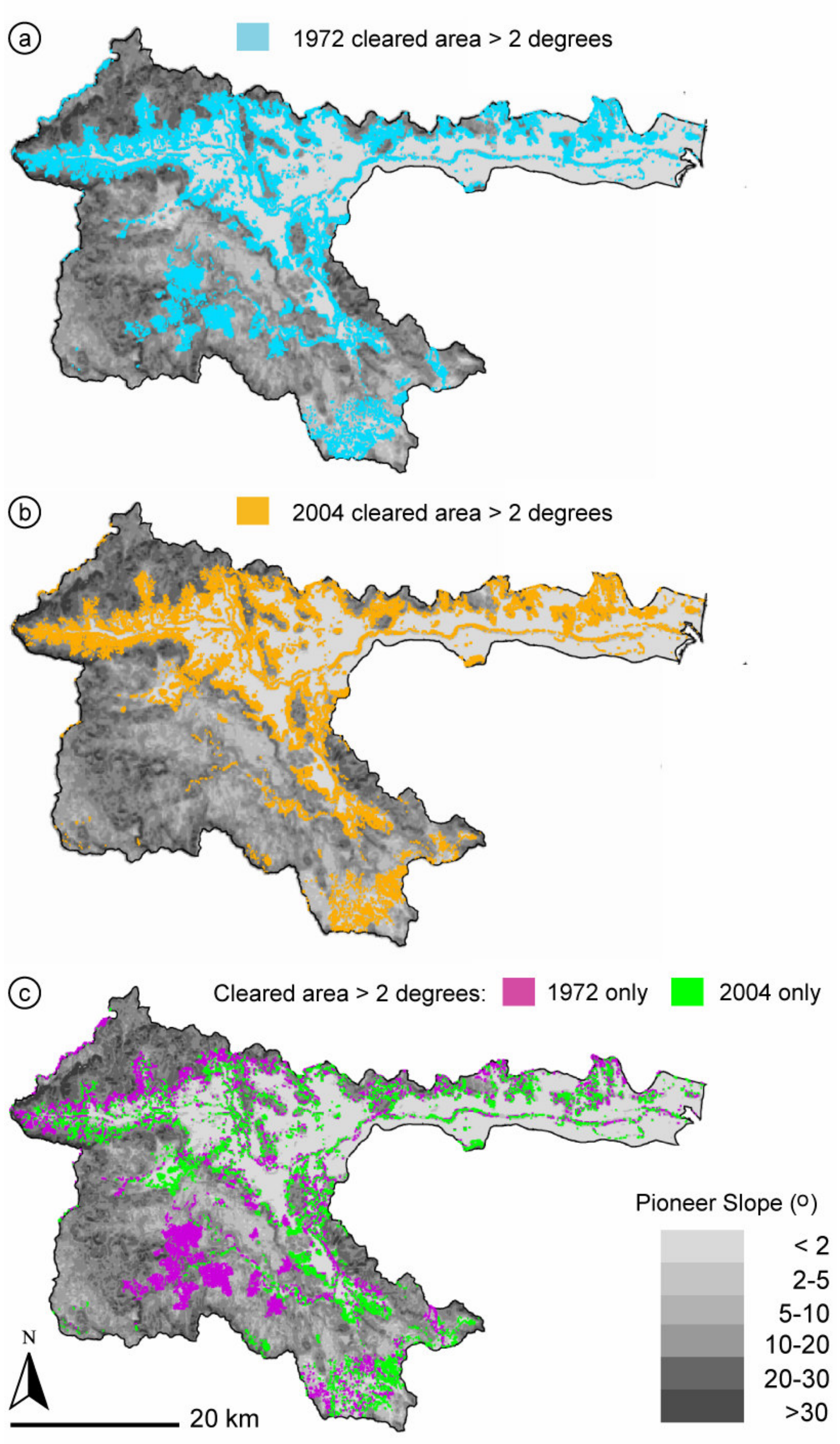
a
1972 cleared area > 2 degrees
b
2004 cleared area > 2 degrees
c
Cleared area > 2 degrees:
1972 only
2004 only
Pioneer Slope (°)
< 2
2-5
5-10
10-20
20-30
>30
N
20 km

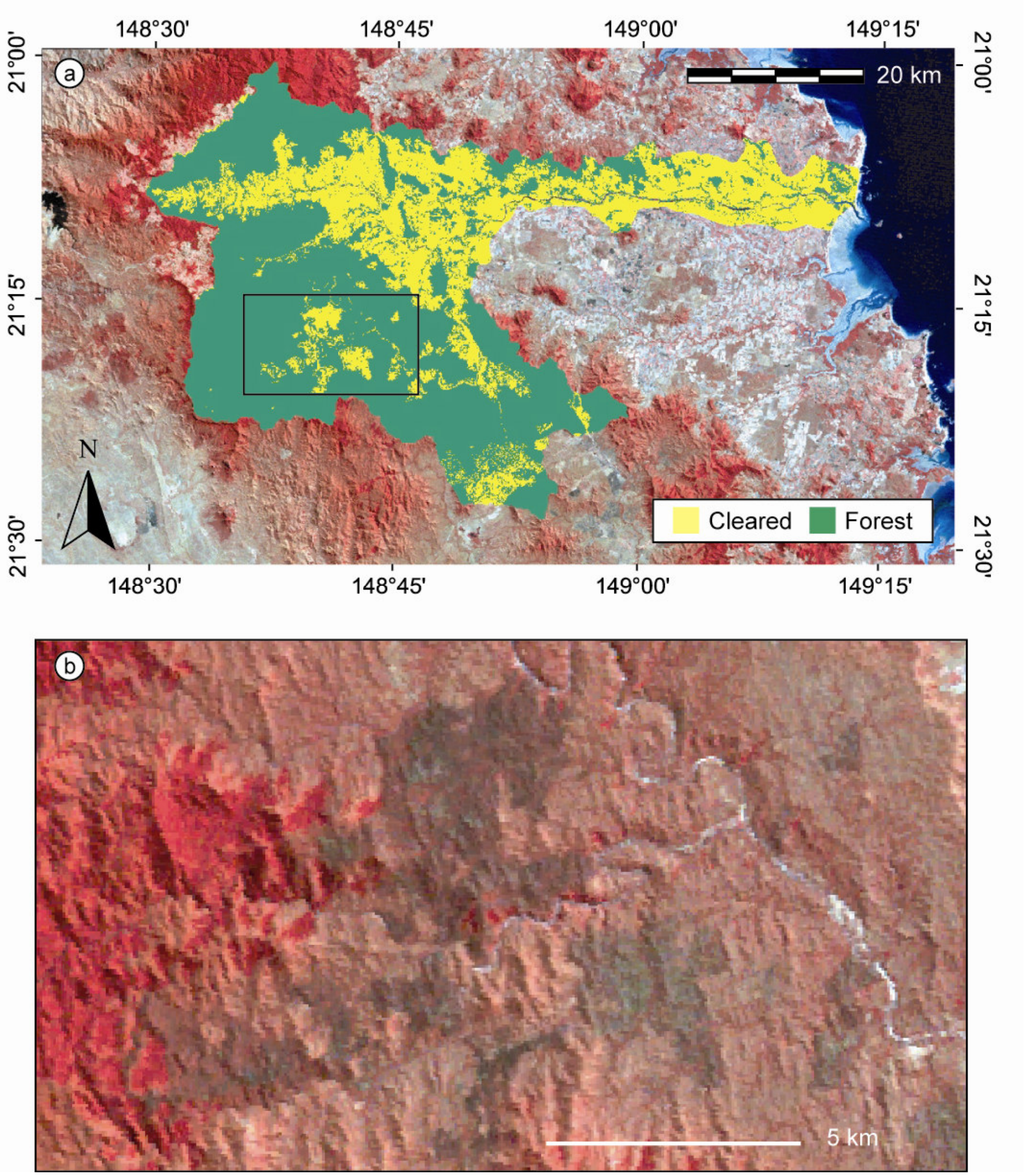

Figure 2.7. (a) 1972 classification of cleared (yellow) and forested (green) areas within the Pioneer catchment on a Landsat MSS image displayed in near-infrared, red and green bands. Agricultural areas in the eastern half of the image are pink, white and grey. Forested areas are bright red to reddish-brown. The rectangle encloses natural clearings from wildfires, whose burn scars are shown in (b).

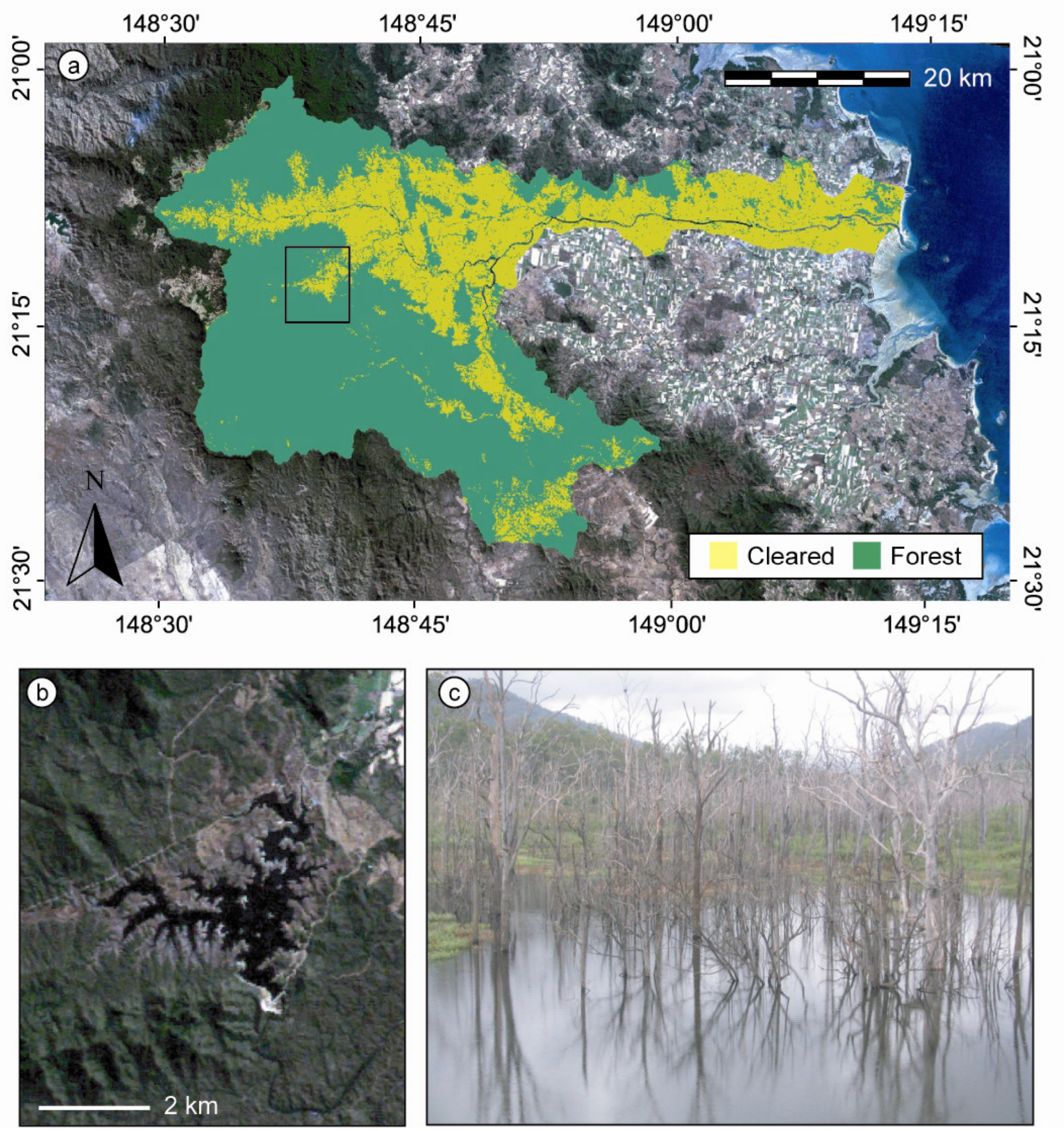

Figure 2.8. (a) 2004 classification of cleared (yellow) and forested (green) areas within the Pioneer catchment on a Landsat TM image displayed in red, green and blue (RGB) bands. Agricultural areas in the eastern half of the image are light green and white. Forested areas are dark green to light-brown. The inset indicates Teemburra Dam, shown as an enlarged subset in (b). (c) Photograph taken in March 2005 showing tree death from waterlogging within the dam.

Figure 2.9. Pre-clearing distributions of regional ecosystems within the Pioneer catchment (constructed using digital data from QEPA). Descriptions of the dominant vegetation types, land forms and underlying geology are listed in Appendix A.

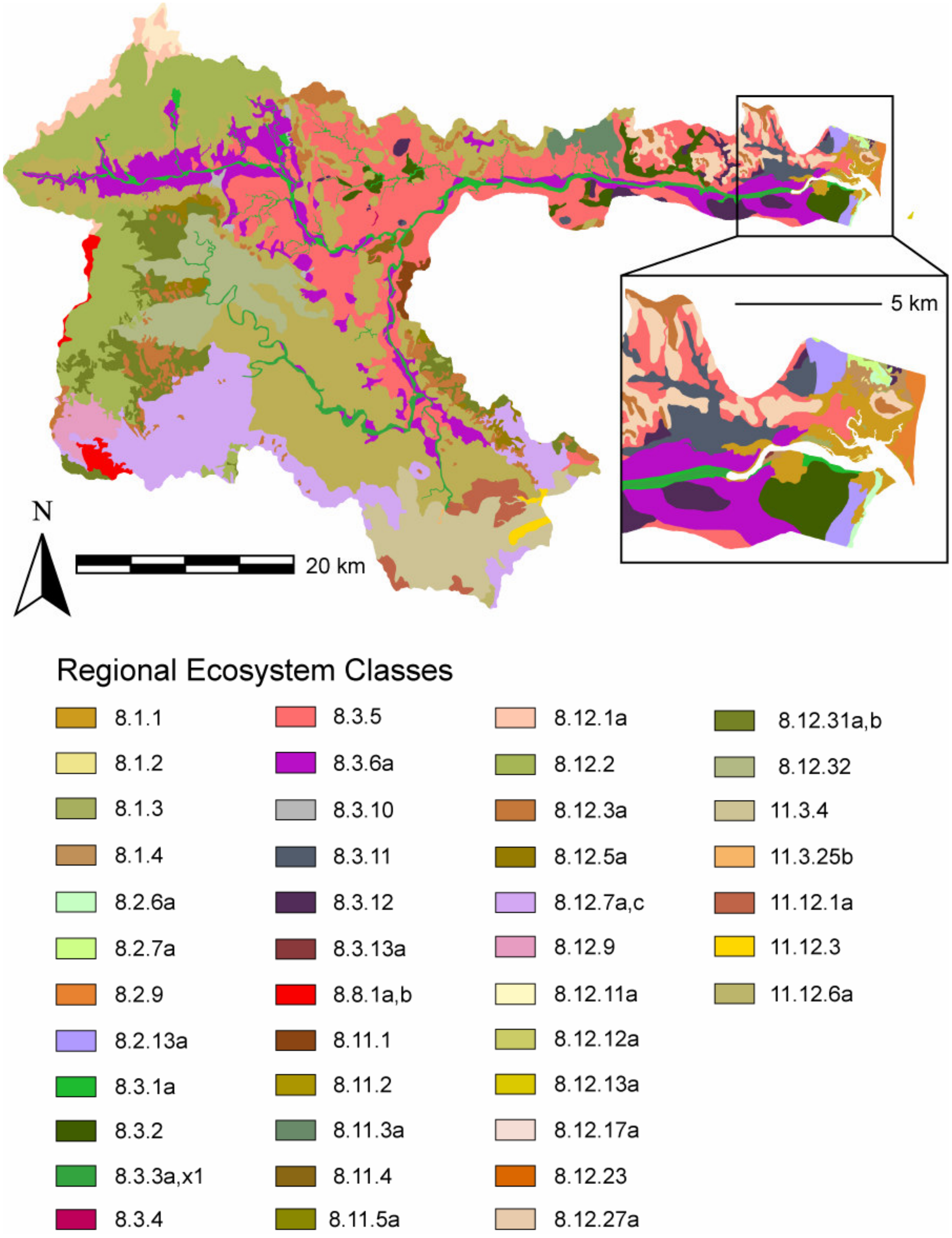
N
20 km
5 km
Regional Ecosystem Classes
8.1.1
8.1.2
8.1.3
8.1.4
8.2.6a
8.2.7a
8.2.9
8.2.13a
8.3.1a
8.3.2
8.3.3a,x1
8.3.4
8.3.5
8.3.6a
8.3.10
8.3.11
8.3.12
8.3.13a
8.8.1a,b
8.11.1
8.11.2
8.11.3a
8.11.4
8.11.5a
8.12.1a
8.12.2
8.12.3a
8.12.5a
8.12.7a,c
8.12.9
8.12.11a
8.12.12a
8.12.13a
8.12.17a
8.12.23
8.12.27a
8.12.31a,b
8.12.32
11.3.4
11.3.25b
11.12.1a
11.12.3
11.12.6a

Chapter 3. Natural and Anthropogenic Changes to Mangrove Distributions in the Pioneer River Estuary

Introduction

Globally, about one third of mangrove forests have been lost within the past 50 years (Alongi 2002). This has resulted in growing concern over the coincident decline of important mangrove ecosystem services, such as filtering river runoff. In Queensland, Australia, runoff from Great Barrier Reef (GBR) catchments is now regarded as the principal anthropogenic threat to water quality in the GBR lagoon (Haynes and Michalek-Wagner 2000; Brodie et al. 2001; Haynes et al. 2001; Devlin and Brodie 2005). For many catchments, modeled increases of sediment/nutrient exports are associated with a net loss of mangroves (Duke and Wolanski 2001; Neil et al. 2002); and mangrove loss is now central to concerns about the health of adjacent marine ecosystems.

While mangroves and tidal flats comprise only a small portion of the GBR catchment area, they trap and store disproportionate amounts of suspended particles, nutrient-rich organic matter, and associated pollutants from catchment runoff (Woodroffe 1992; Tam and Wong 1995; Furukawa and Wolanski 1996; Kitheka 1997; Haynes and Johnson 2000; Victor et al. 2004; Alongi and McKinnon 2005; Alongi et al. 2005). Mangroves typically establish in areas of mud deposition where they accelerate sediment accretion rates by reducing water velocities (e.g. through creek meanders and root baffles), and by trapping aggregates of suspended particles

(Furukawa and Wolanski 1996; Furukawa et al. 1997). Suspended particles in river runoff tend to aggregate after mixing with brackish estuarine water, either through salt flocculation caused by changes in the electrostatic stability of their coatings (Gibbs 1983), or through contact with abundant mucus produced by high bacterial populations in mangrove swamps (Alongi 1988). Because of tidal asymmetries in some regions such sediment flocs are more likely to be carried further upstream on flood tides to sites where particles become trapped in the fine root systems of inshore mangroves (Scoffin 1970; Spenceley 1982; Young and Harvey 1996), than downstream on ebb tides (Wolanski 1995). Activities affecting mangrove and wetland conditions change the flux of materials into and out of estuaries (Arthington et al. 1997; Johnson et al. 2001); and changing estuarine water quality may ultimately impact downstream marine ecosystems (Duke and Wolanski 2001).

To assess potential impacts of recent mangrove loss on adjacent ecosystems, it is necessary to quantify the magnitude of anthropogenic change relative to natural changes as because some processes are more likely to permanently alter mangrove ecosystem condition and affect ecosystem services. With synoptic, non-intrusive, data collection over large areas, remote sensing offers distinct advantages for quantifying vegetation changes over time and for examining the biophysical properties of mangroves in regions where fieldwork is difficult (Green et al. 1996; Green et al. 1997). Aerial photography has been used not only to map broad-scale mangrove distributions (Saintilan and Wilton 2001), but also to classify dominant species and assemblages (Sulong et al. 2002; Verheyden et al. 2002), evaluate tree density (Verheyden et al. 2002), and then to monitor these parameters over time (Dahdouh-Guebas et al. 2000; Lucas et al. 2002; D'Iorio 2003; Dahdouh-Guebas et al. 2004). Despite recent advances in sensor technology, the labor intensity required for digitization, and the subjectivity of photo-interpretation, aerial photography remains a preferred platform for mapping mangrove distributions, particularly in developing countries (Dahdouh-Guebas 2002).

Data from multispectral satellite sensors such as SPOT (Système Pour l'Observation de la Terre) and Landsat Thematic TM and ETM+ are also useful for discriminating mangrove from non-mangrove zones (Rasolofoharinoro et al. 1998; Gao 1999; Blasco and Aizpuru 2002; Haito et al. 2003) and are often more cost-effective than aerial photographs due to high processing efficiency (Mumby et al. 1999). In addition, multi-band spectral data, unlike traditional aerial photographs, can be used to calculate vegetation indices based on differences in reflectance properties of vegetation in different wavelengths, typically between the red and near-infrared (NIR) wavelengths. These differences have been correlated with biophysical properties of the mangrove canopy; for example, mangrove Normalized Difference Vegetation Index (NDVI) values have been correlated with biomass, canopy cover and leaf area index (LAI) (Jensen et al. 1991; Ramsey and Jensen 1996; Green et al. 1997, 1998; Green and Mumby 2000). Change detection analysis using NDVI calculated from satellite data is applied routinely in forest and agricultural management (Washmon et al. 2002; Wilson and Sader 2002; Zhan et al. 2002), and change detection has been used successfully with visual interpretation techniques to track mangrove loss in the Ganges Delta (Blasco et al. 2001) and in French Guiana (Fromard et al. 2004).

In this chapter, I quantify mangrove loss in the Pioneer River estuary and identify drivers of mangrove distribution changes at decadal intervals from aerial photographs spanning 54 years (1948-2002) to assess the magnitudes of both anthropogenic and natural changes. I specifically focus on documenting changes to mangrove areas that are hydrologically connected to the Pioneer River flow and therefore potentially act as sinks for material contained in catchment runoff and sources of eroded sediments following mangrove loss. Mangroves in the Pioneer estuary, near Mackay on the central Queensland coast, were especially appropriate for this study because the estuary: (1) has a long history of anthropogenic modification, beginning in 1887 with the construction of training walls to stabilize the river channel (Gourlay and Hacker, 1986); and (2) has recently experienced high mortality (dieback) of trees, with the dominant and normally broadly tolerant mangrove, *Avicennia marina* (Forssk.) Vierh., being the most obviously affected species (Duke et al. 2005). Because the mangrove dieback near Mackay reduces both canopy cover and LAI in small patches (<100 m^2) that are difficult to digitize manually, I also investigate using NDVI from Landsat Thematic Mapper (TM) and Enhanced Thematic Mapper Plus (ETM+) imagery for monitoring the spatial and temporal progression of canopy loss associated with tree death throughout the Pioneer estuary. Finally, I use the results from this study to formulate testable predictions about expected changes in biogeochemical proxies of nearshore water quality likely to be preserved in coral skeletons collected from adjacent downstream ecosystems.

Methods

Study site

On geological time scales, the Pioneer estuary is relatively young: thin Holocene deposits and well-developed estuaries to the south with no direct river input today suggest that the Pioneer River mouth moved to its current position within the past 3000 years (Gourlay and Hacker 1986). Such river capture has been documented in both the Burdekin and Barron river deltas north of the Pioneer catchment (Pringle 1984; Gourlay and Hacker 1986). Once the Pioneer River settled in its present location, deposition from successive floods caused the shoreline to prograde into extensive tidal flats, with outer beach ridges formed by sands accumulating under the actions of the large tidal range and prevailing south-east trade winds. Mangroves colonized the sheltered areas behind the outer beach ridges, where later floods deposited fine muds and silts (Gourlay and Hacker 1986). Although data are not sufficient to reconstruct historic mangrove distributions, it is likely that they fluctuated steadily in response to natural drivers of change similar to those at work in present times (e.g. shifting protection from wave exposure, sea level fluctuations, climate variations).

Since the beginning of European settlement in the region (1862), both natural changes and hydrological modifications to the Pioneer estuary have influenced mangrove distributions (Table 3.1). For example, training wall construction (1887-1927) on the north bank of the Pioneer River stabilized and deepened the main Pioneer River channel, but also increased mangrove area in Bassett Basin by restricting its tidal circulation and accelerating sediment deposition on muddy banks (Gourlay and Hacker 1986). Major floods have altered channel bank morphology through erosion and deposition: e.g. in 1898, the Pioneer River broke through East Point to create a new mouth; and mangroves were cleared around Alligator Creek to reduce future floodwaters after a major flood in 1958 (Gourlay and Hacker 1986). Although there was considerable mangrove regrowth after 1958, a large area in Alligator Creek was subsequently filled for construction of the Caneland Central Shopping Centre in 1978 (Gourlay and Hacker 1986).

Replacement of tidal wetlands with landfill for development has averaged 5-6 ha/yr since 1948 (Duke and Wolanski 2001), largely due to expanding urban pressures from the city of Mackay, which had a population of ~63,000 in 2001 (ABS 2002) and a 2.2% annual growth rate (Furnas 2003). Other mangrove areas have been isolated from the main network of creeks and removed from the tidal flux of the Pioneer River by construction of the railway to the outer harbor (1978-1981) which cut off northern Vines and Bassett Creeks from the Harbour Wetlands, leaving remnant mangrove patches that no longer receive regular tidal flushing (Norman 1989). Similarly, a culvert, levee and tidal gates, built in 1993-94, substantially reduced the flux of water and materials into the Sandfly Creek system (especially since the gates were not opened until 1996) (B. Discher, personal communication).

While remnant mangroves patches still persist in these regions, they can now only act as part of the estuarine filtering system during exceptional floods.

There are at least 17 different mangroves species present within the Pioneer estuary, with communities dominated by *Avicennia marina*, *Rhizophora stylosa* and *Ceriops australis* (Finglas et al. 1995; Duke et al. 2001). Local citizens first expressed concerns about mangrove dieback in the Pioneer estuary in the early 1990s (N. Whitehead, personal communication) when dieback became obvious. The dieback predominantly affected the grey mangrove, *Avicennia marina*, known for its broad latitudinal and salinity tolerances and high resilience to physical damage (Tomlinson 1986; Duke 1991; Duke et al. 1998). As of 2002, moderate to severe dieback of *A. marina* affected 58% of mangrove area in the region, including the Pioneer estuary (Duke et al. 2005). Preliminary observations suggest that erosion and bank destabilization in tidal creeks has accelerated in dieback regions (Duke et al. 2005), amplified by strong tidal currents from up to 6.5 m tides.

Mapping mangrove change through time

Black and white (1948, 1962, 1972, 1982, 1991) and color (1998, 2002) aerial photographs covering the Pioneer estuary and the city of Mackay (Figure 3.1), at scales of 1:10,000-1:30,000, were borrowed from Queensland Department of Natural Resources, Mines and Water (QDNRMW) and the Marine Botany Group at the University of Queensland (Table 3.2). Individual photographs were scanned at 600 dpi and mosaicked using Adobe Photoshop Elements 2.0. The 1998 mosaic was georeferenced to part of a Landsat ETM+ map product image captured on 16 July 2000 using ENVI 3.6 software. The Landsat ETM+ image data were previously georeferenced to 1:250,000 topographical map sheets by the data provider. All other mosaics were georeferenced to the 1998 mosaic. Output pixel resolution for each mosaic was standardized to 1.2 x 1.2 m. Mangrove distributions (to nearest ha) for each delineated sub-region within the Pioneer estuary (Figure 3.1) were manually digitized (for each year except 1998) based on tone, texture, contrast with adjacent substrates, and *a priori* field knowledge, using ArcView 3.2 software. Mangrove regions cut off from the main tidal flow as a result of hydrological modifications to the estuary were categorized as non-tidal. These regions are reported, but unlike new mangrove areas, they were not included in the overall total of mangrove area available for filtering catchment runoff. Probable drivers of change were identified after visually comparing successive maps from each region (Table 3.3).

Correction for misregistration error

Misregistration occurs when a pixel's location on a rectified image does not match its reference position on the ground. I assessed the magnitude of misregistration in each aerial photomosaic by calculating the average root mean squared error (RMSE; determined by taking the square root of the sum of the squared deviations of each pixel from its reference location) relative to the 1998 mosaic (Phinn and Rowland 2001). Because RMSE values were high (between 17.4 and 48.7m; n = 20), scale factors were applied to mapped areas of the major mangrove sub-regions (Alligator Creek, Barnes Creek, Bassett Creek, Fursden Creek, Main Pioneer, Sandfly Creek, Town Beach, Vines Creek) to correct for the distortion. Scale factors were calculated by dividing the area of a fixed polygon (e.g. a city block) adjacent to each sub-region in the 1998 mosaic by the area of the same polygon in each of the other mosaics.

Normalized Difference Vegetation Index

The Pioneer estuary subset of the 2000 Landsat ETM+ image (16 July 2000) was radiometrically matched to a 1990 Landsat TM image (24 April 1990) using an empirical line calibration to correct for differences in solar irradiance and atmospheric path radiance (Yuan et al. 1998). A mask exposing only the mangrove areas within the Pioneer estuary was created by digitizing the 1990 Landsat TM image, and then used to define the estuary area in the corrected 2000 Landsat ETM+ image. NDVI images for the identical areas in 1990 and 2000 Landsat images were then produced. The unitless NDVI (ranging from –1 to +1) was calculated as:

$$\text{NDVI} = (\text{NIR} - \text{Red})/(\text{NIR} + \text{Red}) \tag{3.1}$$

where NIR is the % reflectance in the near infrared (Landsat Band 4; 0.76-0.90 μm) and Red is the % reflectance in the visible red (Landsat Band 3; 0.63-0.69 μm) (Rouse et al. 1974).

Correlations between field and satellite data

To determine whether NDVI is an acceptable proxy measure of dieback in the Pioneer estuary, the variance of the 2000 Landsat ETM+ image NDVI values (dependent variable) was partitioned between field measures of live mangrove density and dead basal area (independent variables) in a multiple regression analysis (Sokal and Rohlf 1995). Field data were collected between May 2003 and March 2004 in 5 m x 5 m plots from five creek regions: Barnes Creek A, Barnes Creek B, Bassett Creek, Fursden Creek and Vines Creek. Species, stem circumference and health status (alive/dead) were recorded for all trees ≥ 1 m high. I scored each live *A. marina* tree visually for: leaf damage (high/medium/low); leaf color (green/green-yellow/yellow); canopy density (high/medium/low); % dead canopy exposed to sunlight (0, 25, 50, 75); A tree was considered subject to dieback if: leaf damage was high; leaf color was green-yellow or yellow; canopy density was low; % dead canopy was ≥50%; there were major dead branches; and pneumatophores were irregularly shaped. *A. marina* trees were considered sick if at least three signs of dieback were noted and/or if there were adventitious roots present along the main trunk, which has been demonstrated to be a response to stress (Tomlinson 1986; Snedaker et al. 1992; Boer 1993). To assess differences in the abundance of dieback-affected *A. marina* throughout the estuary, I performed one-way ANOVA on arcsine square-root transformed proportions of sick and dead trees from each creek region. To evaluate the magnitude of *A. marina* dieback within the estuary, health status was matched with importance values (based on relative dominance, density and frequency), calculated for all observed species in each creek region (Cintron and Novelli 1984). Due to difficulties obtaining good GPS signals beneath the mangrove canopy, only 16 of 37 plots sampled could be reliably matched with pixels in the Landsat image.

Change detection from satellite data

A difference image was calculated from the 1990 and 2000 NDVI images: for each pixel

$$D = (NDVI_{1990} + 1) - (NDVI_{2000} + 1) \tag{3.2}$$

with 1 added to all NDVI values to avoid subtraction of negative values. The change for each pixel in the difference image was classified as “NDVI lower” ($D < -0.05$), “no change” ($D = -0.05$-0.30) or “NDVI higher” ($D > 0.30$). Correlations between NDVI change classes and changes in mangrove canopy density were assessed in a normalized 2 x 2 error matrix (Congalton 1991). Georeferenced aerial photographs from 1991 and 1998, the two closest dates for which aerial photographs were available within the bounds (1990-2000) of the change detection analysis, served as reference images for canopy change estimation. One hundred and fifty points were selected for comparisons using a stratified random sampling design. Paired points (1991, 1998) on the aerial photographs were visually assessed for increases or decreases in mangrove canopy density and compared against the calculated NDVI class. The "no change" class was not included in the overall matrix because I was unable to determine reliably if the corresponding paired points had no visual change in canopy density. The error matrix summarizes the overall correlation between the NDVI map and reference data. Percent commission error, omission error, producer's accuracy and user's accuracy, defined in Chapter 2, are reported in addition to the overall accuracy.

Results

Mangrove distribution changes, 1948-2002

From 1948 to 2002, the total area of tidally-flushed mangroves mapped from aerial photographs within the Pioneer estuary decreased by 22% from 634 to 497 ha, principally from such anthropogenic activities as clearing, filling and altering the natural hydrodynamic structure of the estuary (Figure 3.2). The proportions of mangrove changes attributed to clearing/natural loss, tidal isolation from hydrological manipulations and new growth are summarized in Table 3.4. Mangroves were cleared at an average rate of ~4 ha/yr for both agricultural and urban expansion, although large-scale changes were typically episodic in frequency. New highways, levees and a railway line isolated patches of persistent non-tidal mangroves that were treated as permanent exclusions from the total hectares available for filtration of runoff. The total loss of tidal mangroves (274 ha) was partially offset by 137 ha of new growth (Figure 3.2, Table 3.4).

Mangrove distribution change by sub-region

The eight sub-regions of the Pioneer estuary had different drivers of change, and they varied across decadal intervals (Tables 3.5 and 3.6). Most new mangrove growth was in Barnes Creek and at river bends (by Fursden Creek, the southwest bank of Bassett Basin, and the south bank near the Pioneer River mouth), where decreased velocity facilitated recent sediment deposition. Although mangroves prograded rapidly from Town Beach across the south bank of the river mouth, net mangrove gain was reduced by losses from increased exposure to wave action as protective sand banks shifted to the north (Figure 3.3). Along the main channel of the Pioneer, mangrove areas eroded during flooding events and expanded during drier periods, with some net displacement due to changes in channel bank morphology. While mangroves were also cleared in every sub-region of the estuary, most clearing occurred during short, discrete intervals in Alligator Creek, Bassett Creek, Vines Creek, and Sandfly Creek; each sub-region (except Main Pioneer and Barnes Creek) now contains persistent remnant stands of non-tidal mangroves, isolated from the main channels.

Distribution change from mangrove dieback

Although visible in the field wherever *A. marina* present, mangrove dieback was quantifiable only in the 2002 aerial photomosaic, and only in the following regions: Fursden Creek, Barnes Creek, Vines Creek and Bassett Creek. Dieback appears in aerial photographs as small canopy gaps, either as light brown areas of visible muddy substrate or as dark patches caused by tree shadows (Figure 3.4a). Due to the labor and time required to accurately digitize every gap, estuary-scale mapping of mangrove distribution from visual interpretation of aerial photographs underestimated the magnitude of mangrove loss (S. Jupiter, personal observation). Fortunately, mangrove dieback can be mapped much more quickly (hours vs. weeks) from satellite imagery. The NDVI analysis applied to Landsat satellite images integrated proportions of different surfaces (e.g. bare ground, thin canopy, thick canopy) within each 28.5 m x 28.5 m image pixel. Pixels with exposed mud, thinner canopies and/or large proportions of defoliated, dead trees (more dieback) had lower NDVI values than pixels with only dense mangrove canopy (Figure 3.4b).

NDVI declined significantly with increased dead basal area (univariate $r = 0.59$, $p = 0.047$; Figure 3.5a, Table 3.7), but did not change significantly with live mangrove density (univariate $r = 0.36$; $p = 0.553$; Table 3.7). However, the latter result is probably biased by the 3 year temporal lag between the 2000 Landsat ETM+ image and the collection of field data: the NDVI values from the easternmost Bassett Creek site were higher than expected because, by 2003-04, severe dieback had spread from west to east across the estuary, thinning canopies and opening gaps as *Avicennia marina* died and became uprooted. When pixels from Bassett Creek were excluded from the analysis, the correlation between NDVI and live tree density was significant ($r = 0.738$, $p < 0.01$, $n = 12$; Figure 3.5b).

In the alternative approach to mapping dieback using change detection of the 1990 and 2000 NDVI images, 44 ha (543 pixels) were classified as lower NDVI in 2000, and 56 ha (687 pixels) were classified as higher NDVI (Figure 3.6). Dieback was most pronounced around creek margins, where the density and size of *A. marina* contributed to high importance values in every creek region surveyed (Table 3.8). Sick and dead *A. marina* occurred relatively uniformly across all lower intertidal creek regions surveyed (one-way ANOVA, p = 0.997; Table 3.9). In the error analysis, the overall accuracy (98%) indicates a very strong association between NDVI change calculated from Landsat images and canopy density changes from aerial photographs (Table 3.10).

Discussion

Drivers of mangrove change in the Pioneer estuary

In the past few decades, there has been a surge of studies documenting changes in global mangrove distributions (Spalding et al. 1997). Certain changes are directly anthropogenic in origin and result in both gains (e.g. large-scale mangrove afforestation in Bangladesh; Saenger and Siddiqi 1993) and losses (e.g. mangrove conversion to shrimp aquaculture in SE Asia; Spalding et al. 1997; Tong et al. 2004). Other changes to mangroves result from indirect effects of human activity such as hydrological alterations: for example, leaf shedding from *Heritiera fomes* in the Ganges Delta is likely to be a result of construction of embankments and dams upstream from mangrove regions (Spalding et al. 1997). Additional changes result from distinctly natural processes, such as extensive mangrove loss in the Lesser Antilles from hurricane damage (Imbert et al. 1996; Imbert et al. 2000) or rapid losses/gains from cycles of erosion and accretion at the Amazon River delta (Fromard et al. 2004). However, as current coastal population densities (within 100 km of shorelines and 100 m sea level) are nearly 3 times greater than the global average (Small and Nicholls 2003), most natural changes to mangrove distributions coincide with anthropogenic pressures that have the potential to slow rates of recovery from disturbance. Because some types of change are more likely than others to destabilize mangrove ecosystems and impact mangrove ecosystem services (e.g. sediment trapping), it is important to determine the magnitudes of each type of disturbance and the projected rates of recovery before we can assess potential impacts to adjacent ecosystems (e.g. seagrass beds, coral reefs).

Different dominant processes can be ascribed to four distinct periods of change in the distribution of Pioneer estuary mangroves in the past sixty years (Figure 3.7). During the first period (1948-1962), large-scale clearing in Alligator Creek (in response to the extreme 1958 flood) and Bassett Creek (for harbor expansion) was effectively matched by rapid mangrove expansion elsewhere to yield little net change. Two mechanisms drove mangrove expansion during this period: wetter climate and newly deposited substrate on which to colonize. Natural rates of mangrove expansion and contraction are highly sensitive to climatic variation. For example, the proportion of mangroves relative to saltpans in unaltered estuaries can be reliably predicted from the mean annual rainfall alone (Fosberg 1961; Bucher and

Saenger 1994). Indeed, the rapid growth of mangroves during the 1950's in Barnes Creek corresponded with a period of increased rainfall that may have reduced salinity and facilitated colonization (Gourlay and Hacker 1986). Similarly, new deposits of fine muds and silts along river bends facilitated rapid mangrove settlement of pioneer species onto previously unavailable substrate, particularly along the south bank of the Pioneer River mouth, where mangroves expanded northeastward from Town Beach.

During the second period (1962-1972), new mangrove growth outpaced clearing activities; mangroves continued to expand in Barnes Creek, where established trees probably provided shade and encouraged new growth by limiting evaporation (Gourlay and Hacker 1986), and along newly deposited sediments along river bends (e.g. at Fursden, into Bassett Basin, at the south mouth of the Pioneer). Mangroves also recolonized some previously cleared areas, such as along Alligator Creek. While these new mangroves may have provided additional filtration of catchment runoff and buffering of hydraulic erosion, the accelerated rate of mangrove expansion may itself be symptomatic of changes in upstream land use. Rapid mangrove expansion can reflect increased sediment and nutrient concentrations in estuarine waters (Gourlay and Hacker 1986; Duke and Wolanski 2001); thus, the new growth in the Pioneer estuary, along with mangrove expansion in other GBR catchments, such as the Johnstone and Moresby (with 14.8% and 28.7% respective increases in mangrove area from 1951 to 1992), may be a response to catchment degradation, particularly given their locations in regions of high rainfall (Duke and Wolanski 2001).

The third period (1972-1991) was characterized by the highest rate of mangrove loss. By 1972, mangroves had already saturated most available habitat. New mangrove growth in the Pioneer estuary is probably constrained by habitat availability, which is limited by training walls built along much of the north and south banks of the Pioneer River. There was little new expansion to replace losses from the major development activities of the 1970s and 1980s (e.g. railway, shopping center, port expansion) that claimed 110 ha of mangroves and isolated another 38 ha from regular tidal flushing. This mangrove loss substantially reduced (by 21% from 1972) the mangrove area available to function as sediment and nutrient sinks, and infilling of many of the cleared areas prevented any future recovery of mangroves in those regions.

The fourth period of mangrove change (1991-2002) was dominated by the onset of the mangrove dieback. Although proportionately less mangrove was lost during this period than in 1972-1991, *Avicennia marina* is a dominant species with large individuals located along creek margins and tidal banks, so the effects of *A. marina* dieback on estuarine sediment retention, bank destabilization, and sediment remobilization may be greater than from mangrove losses at the extremities of the creek systems. Within large gaps created from decomposition of dead *A. marina*, previously deposited sediments are remobilized, actively eroded and potentially redeposited in nearshore environments (Figure 3.8). In such areas as Fursden Creek, this may be due to changes to tidal creek morphology: since 1991, the amount of open space (from dieback) in the main drainage channel from the mangroves has increased by 10 times (Figure 3.8a,b), which may increase water velocity and increase scour, resulting in bank destabilization and slumping (Figure 3.8c,d). Exposed cable roots of dead *A. marina* trees suggest that sediments eroded following decomposition of live fibrous roots (Figure 3.8e-f), which may lose 30-52% of original mass after 154 days following death (Albright 1976). Losses of live fine roots may additionally lead to nutrient leaching from dead roots bound within the sediment matrix, which are thought to comprise the major nutrient reserve for *A. marina* stands (Alongi et al. 2003). Although there is clear visual evidence of bank destabilization in regions of severe dieback and sediment loss associated with uprooted trees, the direct fate of this material is heavily influenced by regional hydrological dynamics that have not yet been fully described. In the next section, the benefits and limitations of the two methods for identifying mangrove dieback are discussed.

Assessment of techniques for mapping mangrove dieback

The value of aerial surveys for studies of mangrove ecosystems has long been recognized, since many forests are impenetrable. But while aerial photographs effectively capture detailed changes in mangrove distributions, they have several disadvantages (e.g. misregistration problems, high processing time, low spectral sampling) compared with newer satellite and airborne sensors for mapping changes within the canopy, caused by natural or anthropogenic stresses. First, unless data are available to orthorectify historical aerial photographs to their true ground positions, any change detection analyses using these sources may encounter substantial misregistration between sets of photographs that results from radial displacement and variations in flying altitudes and look angles (Townshend et al. 1992; Phinn and Rowland 2001). Misregistration errors are minimal for satellite sensors, particularly those with sun-synchronous orbits, such as Landsat or SPOT, that pass over target locations at regular intervals, at the same time of day, and with the same look angle. The 2000 Landsat ETM+ image selected for this study had a root mean square error (RMSE) of 0.25 pixels (pixel size = 28.5 m x 28.5 m; n = 20) relative to the 1990 Landsat TM image, which is within the acceptable limits for geometric accuracy (0.5 to 1.0 pixels) recommended for change detection analyses (Jensen 2000; Phinn and Rowland 2001). By contrast, RMSE's for the aerial photomosaics ranged between 14.5 and 40.6 pixels (pixel size = 1.2 m x 1.2 m; n = 20), prohibiting change detection of mangrove classifications between successive datasets.

Secondly, though the high spatial resolution of aerial photographs can facilitate identification of small features, such as narrow mangrove strips (Manson et al. 2001) and patchy dieback areas, this benefit was offset in this study by the time costs of the manual digitization. Mapping estuary-scale dieback with reasonable efficiency required sacrificing some accuracy: dieback was only delineated from regions containing at least 10 pixels identified as bare ground. These tradeoffs have been noted in other studies comparing the costs and benefits of mapping mangrove distributions using different sensors and techniques. Mangrove maps from the Turks and Caicos Islands delineated from aerial photographs required four times as many person-days as maps constructed from Landsat data (Mumby et al. 1999). Similarly, due to the large number of person-hours required to pre-process and digitize aerial photographs and the high costs of acquisition, D'Iorio et al. (2006) found that mangrove maps of south Molokai, Hawaii, created from unsupervised classifications of multi-spectral satellite data had more favorable cost:benefit ratios than maps manually digitized from aerial photographs.

Processing time for classifying dieback zones from aerial photographs may be reduced by using unsupervised classifications based on textural analysis, in which the dieback gaps may separate from the unaffected canopy due to increased "roughness" (Lillesand and Kieffer 1987), but NDVI applied to satellite imagery, using spectral bands unavailable from aerial photographs, is a far quicker method for mapping dieback. The significant correlations of NDVI with dead basal area and live tree density (after excluding Bassett sites), plus the 98% correspondence with observed changes in canopy cover (from aerial photography) between 1990 and 2000, indicate that NDVI is an effective method for identifying dieback areas in this region, though its application may not be universal. Despite a significant relationship with NDVI, dead basal area only explains 28% of the variation in NDVI values. The high unexplained variation could be attributed to many factors, including the low sample size, the discrepancy in size between field plots (5 m x 5m) and Landsat pixels (28.5 m x 28.5 m), and the lag time between image acquisition and field data collection, which particularly affected the plots in Bassett Creek. The weak correlation between NDVI and live tree density (before excluding Bassett Creek sites), which explained only 2% of the variation, would probably increase if data were weighted by size of trees: the model used assumes equal sizes for all trees measured, even though larger trees have higher leaf production (Coulter et al. 2001) and therefore exert proportionally greater influence on NDVI values than smaller trees.

Using airborne or satellite sensors with higher spatial resolutions and spectral sampling intervals (e.g. IKONOS, Quickbird, IRS, SPOT 5, HyMap) should also strengthen correlations between NDVI and mangrove dieback. For example, mangrove mapping in the Turks and Caicos Islands using the multispectral Compact Airborne Spectrographic Instrument (CASI) (1m x 1m pixel; 8 user-defined bands) improved the accuracy of a regression model converting NDVI to leaf area index (within a 95% confidence interval) from 88% (Green et al. 1997) with the SPOT XS satellite (20 m x 20 m pixel; 3 bands) to 94% (Green et al. 1998). The improved spatial resolution of the CASI sensor, as well as the choice of spectral bands, also led to mangrove classifications based on height, density and dominant species with reasonable accuracy (78% for six mangrove classes; 86% for four classes; Green et al. 1998). Similar results have also been achieved with very high spatial resolution multispectral data (e.g. IKONOS, Quickbird; Wang et al. 2004) and high spatial hyperspectral integrated with radar (e.g. CASI and AIRSAR; Held et al. 2003), each of which offers advantages in high diversity ecosystems. Radar has also proven valuable to discriminate degraded mangroves (open canopy) from intact forest (closed canopy) based on increased backscatter from C-, L- and P-band frequencies

(Proisy et al. 2002), and its integration with optical data should improve dieback classifications.

Predicted links to nearshore water quality

In each of the four time periods described in this chapter, mangrove change was driven by different mechanisms that are likely to have affected the composition of dissolved molecules and suspended sediment loads, and thus nearshore water quality, in different ways. If these changes were recorded in biological or geological records of environmental conditions, there is a real potential to document environmental changes during the past 60 years, and to identify causal factors for some of these changes. Specific hypotheses can be formulated for each period that predict contemporaneous trends in geochemical proxies measured from coral core records: (1) when mangrove loss is offset by mangrove expansion, changes in the proxies are likely to be driven by catchment land use changes alone and/or by climatic variability; (2) when mangrove expansion exceeds mangrove loss, variation in proxies may be buffered and may reflect prevailing climatic or oceanographic conditions; (3) when mangrove loss exceeds mangrove expansion, changes to the coral record may be affected by both land use and mangrove loss; and (4) the severity of the recent dieback and its effects on sediment mobility, compounded by the continued wetland infilling for urban development, may be reflected in the biogeochemical record at levels above and beyond impacts from agricultural expansion. Alternatively, effects of mangrove loss on water quality, if present, may have been stronger prior to 1948: the Queensland Environmental Protection Agency (QEPA) estimated that mangroves covered 973 ha prior to European land clearing (Appendix A), which means that net mangrove change between 1862 and 1948 was over twice as great as the net change between 1948 and 2002. In Chapter 6, I will address these hypotheses when I compare trends in mangrove change to trends observed in upstream land use practices, downstream water quality (as measured from proxy coral core records) and climate.

If linkages can be demonstrated that relate proxy records of sediment concentrations in nearshore waters to historical records of mangrove change, then mapping changes in mangrove condition by remote sensing can be a powerful tool for early detection of potential threats to nearshore marine habitats. Rapid mangrove progradation, as observed from aerial photography, can indicate muddying of catchment waters. Health indices, developed from multi- or hyper-spectral data, can be applied to mangrove habitats to target areas for restoration before predicted loss of the buffer zone. These remote sensing techniques become especially valuable in highly turbid coastal regions where high and variable total suspended sediments along with suspended and dissolved organic matter concentrations complicate mapping of benthic marine habitats.

References

ABS 2002. Census of population and housing. Mackay Statistical Division 340, Commonwealth of Australia, Australian Bureau of Statistics, Canberra, Australia.

Albright, L.J. 1976. *In situ* degradation of mangrove tissues. New Zealand Journal of Marine and Freshwater Research 10: 385-389.

Alongi, D.M. 1988. Bacterial productivity and microbial biomass in tropical mangrove sediments. Microbial Ecology 15: 59-79.

Alongi, D.M. 2002. Present state and future of the world's mangrove forests. Environmental Conservation 29: 331-349.

Alongi, D.M. and McKinnon, A.D. 2005. The cycling and fate of terrestrially-derived sediments and nutrients in the coastal zone of the Great Barrier Reef shelf. Marine Pollution Bulletin 51: 239-252.

Alongi, D.M., Clough, B.F., Dixon, P. and Tirendi, F. 2003. Nutrient partitioning and storage in arid-zone forests of the mangroves *Rhizophora stylosa* and *Avicennia marina*. Trees 17: 51-60.

Alongi, D.M., Pfitzner, J., Trott, L.A., Tirendi, F., Dixon, P. and Klumpp, D.W. 2005. Rapid sediment accumulation and microbial mineralization in forests of the mangrove *Kandelia candel* in the Jiulongjiang Estuary, China. Estuarine, Coastal and Shelf Science 63: 605-618.

Arthington, A.H., Marshall, J.C., Rayment, G.E., Hunter, H.M. and Bunn, S.E. 1997. Potential impact of sugarcane production on riparian and freshwater environments. *In*: Keating, B.A. and Wilson, J.R. (eds.), Intensive Sugarcane Production: Meeting the Challenges Beyond 2000. pp. 403-421. CAB International, Wallingford, UK.

Blasco, F. and Aizpuru, M. 2002. Mangroves along the coastal stretch of the Bay of Bengal: Present status. Indian Journal of Marine Sciences 31: 9-20.

Blasco, F., Aizpuru, M. and Gers, C. 2001. Depletion of the mangroves of Continental Asia. Wetlands Ecology and Management 9: 245-256.

Boer, B. 1993. Anomalous pneumatophores and adventitious roots of *Avicennia marina* (Forssk.) Vierh. mangroves two years after the 1991 Gulf War oil spill in Saudi Arabia. Marine Pollution Bulletin 27: 207-211.

Brodie, J.E., Christie, C., Devlin, M., Haynes, D., Morris, S., Ramsay, M., Waterhouse, J. and Yorkston, H. 2001. Catchment management and the Great Barrier Reef. Water Science and Technology 43: 203-211.

Bucher, D. and Saenger, P. 1994. A classification of tropical and subtropical Australian estuaries. Aquatic Conservation: Marine and Freshwater Ecosystems 4: 1-19.

Cintrón, G. and Novelli, Y.S. 1984. Methods for studying mangrove structure. *In*: Snedaker, S.C. and Snedaker, J.G. (eds.), The Mangrove Ecosystem: Research Methods. pp. 91-113. UNESCO, Paris, France.

Congalton, R.G. 1991. A review of assessing the accuracy of remotely sensed data. Remote Sensing of Environment 37: 35-46.

Coulter, S.C., Duarte, C.M., Tuan, M.S., Tri, N.H., Ha, H.T., Giang, L.H. and Hong, P.N. 2001. Retrospective estimates of net leaf production in *Kandelia candel* mangrove forests. Marine Ecology Progress Series 221: 117-124.

Dahdouh-Guebas, F. 2002. The sustainable management of tropical coastal ecosystems. Environment, Development and Sustainability 4: 93-112.

Dahdouh-Guebas, F., Verheyden, A., De Genst, W., Hettiarachchi, S. and Koedam, N. 2000. Four decadal vegetation dynamics in Sri Lankan mangroves as detected from sequential aerial photography: a case study in Galle. Bulletin of Marine Science 67: 741-759.

Dahdouh-Guebas, F., Van Pottelbergh, I., Kairo, J.G., Cannicci, S. and Koedam, N. 2004. Human-impacted mangroves in Gazi (Kenya): predicting future vegetation based on retrospective remote sensing, social surveys, and tree distribution. Marine Ecology Progress Series 272: 77-92.

Devlin, M. and Brodie, J. 2005. Terrestrial discharge into the Great Barrier Reef Lagoon: nutrient behavior in coastal waters. Marine Pollution Bulletin 51: 9-22.

D'Iorio, M.M. 2003. Mangroves and shoreline change on Molokai, Hawaii: assessing the role of introduced *Rhizophora mangle* in sediment dynamics and coastal change using remote sensing and GIS. Ph.D. Dissertation. University of California, Santa Cruz, Santa Cruz, USA.

D'Iorio, M.M., Jupiter, S.D., Cochran, S.A. and Potts, D.C. 2006. Optimizing remote sensing and GIS tools for mapping and managing the spread of an invasive mangrove (*Rhizophora mangle*) on Molokai, Hawaii. Marine Geodesy *in review*.

Duke, N.C. 1991. A systematic revision of the mangrove genus *Avicennia* (Avicenniaceae) in Australasia. Australian Systematics Botany 4: 299-324.

Duke, N.C. and Wolanski, E. 2001. Muddy coastal waters and depleted mangrove coastlines--depleted seagrass and coral reefs. *In*: Wolanski, E. (ed.), Oceanographic Processes of Coral Reefs: Physical and Biological Links in the Great Barrier Reef. pp. 77-91. CRC Press, Boca Raton.

Duke, N.C., Ball, M.C. and Ellison, J.C. 1998. Factors influencing biodiversity and distributional gradients in mangroves. Global Ecology and Biogeography Letters 7: 27-47.

Duke, N.C., Roelfsema, C.M., Tracey, D. and Godson, L.M. 2001. Preliminary investigation into dieback of mangroves in the Mackay region. Marine Botany Group, The University of Queensland, Brisbane, Australia.

Finglas, A.P., Winter, D. and Wild, A. 1995. Current distribution and historical comparisons of intertidal vegetation communities and saltpans in the Mackay region (Shoal Point to Hay Point). Queensland Department of Primary Industries.

Fosberg, F.R. 1961. Vegetation-free zone on dry mangrove coastline. U.S. Geological Society Professional Papers 424: 216-218.

Fromard, F., Vega, C. and Proisy, C. 2004. Half a century of dynamic coastal change affecting mangrove shorelines of French Guiana. A case study based on remote sensing data analyses and field surveys. Marine Geology 208: 265-280.

Furnas, M. 2003. Catchments and Corals. Australian Institute of Marine Science, Townsville, Australia. 334 pp.

Furukawa, K. and Wolanski, E. 1996. Sedimentation in mangrove forests. Mangroves and Salt Marshes 1: 3-10.

Furukawa, K., Wolanski, E. and Mueller, H. 1997. Currents and sediment transport in mangrove forests. Estuarine, Coastal and Shelf Science 44: 301-310.

Gao, J. 1999. A comparative study on spatial and spectral resolutions of satellite data mapping in mangrove forests. International Journal of Remote Sensing 20: 2823-2833.

Gibbs, R.J. 1983. Effect of natural coatings on the coagulation of particles. Environmental Science and Technology 17: 237-240.

Gourlay, M.R. and Hacker, J.L.F. 1986. Pioneer River Estuary Sedimentation Studies. University of Queensland, Department of Civil Engineering, St. Lucia, Australia. 207 pp.

Green, E. and Mumby, P. 2000. Mapping mangroves. *In*: Edwards, A.J. (ed.), Remote Sensing Handbook for Tropical Coastal Management. pp. 183-198. UNESCO, Paris, France.

Green, E.P., Mumby, P.J., Edwards, A.J. and Clark, C.D. 1996. A review of remote sensing for the assessment and management of tropical coastal resources. Coastal Management 24: 1-40.

Green, E.P., Mumby, P.J., Edwards, A.J., Clark, C.D. and Ellis, A.C. 1997. Estimating leaf area index of mangroves from satellite data. Aquatic Botany 58: 11-19.

Green, E.P., Mumby, P.J., Edwards, A.J., Clark, C.D. and Ellis, A.C. 1998. The assessment of mangrove area using high resolution multispectral airborne imagery. Journal of Coastal Research 14: 433-443.

Haito, H., Bellan, M.F., Al-Habshi, A., Aizpuru, M. and Blasco, F. 2003. Mangrove research and coastal ecosystem studies with SPOT-4 HRVIR and TERRA ASTER in the Arabian Gulf. International Journal of Remote Sensing 24: 4073-4092.

Haynes, D. and Michalek-Wagner, K. 2000. Water quality in the Great Barrier Reef World Heritage Area: past perspectives, current issues and new research directions. Marine Pollution Bulletin 41: 428-434.

Haynes, D. and Johnson, J.E. 2000. Organochlorine, heavy metal and polyaromatic hydrocarbon pollutant concentrations in the Great Barrier Reef (Australia) environment: a review. Marine Pollution Bulletin 41: 267-278.

Haynes, D., Bass, D., Brodie, J., Christie, C., Devlin, M., Michalek-Wagner, K., Morris, S., Ramsay, M., Storrie, J., Waterhouse, J. and Yorkston, H. 2001. Great Barrier Reef water quality: current issues. Great Barrier Reef Marine Park Authority, Townsville, Australia.

Held, A., Ticehurst, C., Lymburner, L. and Williams, N. 2003. High resolution mapping of tropical mangrove ecosystems using hyperspectral and radar remote sensing. International Journal of Remote Sensing 24: 2739-2759.

Imbert, D., Labbe, P. and Rousteau, A. 1996. Hurricane damage and forest structure in Guadaloupe, French West Indies. Journal of Tropical Ecology 12: 663-680.

Imbert, D., Rousteau, A. and Scherrer, P. 2000. Ecology of mangrove growth and recovery in the Lesser Antilles: state of knowledge and basis for restoration projects. Restoration Ecology 8: 230-236.

Jensen, J.R. 2000. Remote Sensing of the Environment: An Earth Resource Perspective. Prentice Hall, Upper Saddle River, New Jersey, 544 pp.

Jensen, J.R., Ramsey, E., Davis, B.A. and Thoemke, C.W. 1991. The measurement of mangrove characteristics in south-west Florida using SPOT multispectral data. Geocartography International 2: 13-21.

Johnson, A.K.L., Bramley, R.G.V. and Roth, C.H. 2001. Landcover and water quality in river catchments of the Great Barrier Reef Marine Park. *In*: Wolanski, E. (ed.), Oceanographic Processes of Coral Reef: Physical and Biological Links in the Great Barrier Reef. pp. 19-35. CRC Press, Boca Raton.

Kitheka, J.U. 1997. Coastal tidally-driven circulation and the role of water exchange in the linkage between tropical coastal ecosystems. Estuarine, Coastal and Shelf Science 45: 177-187.

Lillesand, T.M. and Kieffer, R.W. 1987. Remote Sensing and Image Interpretation, 2nd edition. John Wiley & Sons, New York. 721 pp.

Lucas, R.M., Ellison, J.C., Mitchell, A., Donelly, B., Finlayson, M. and Milne, A.K. 2002. Use of stereo aerial photography for quantifying changes in the extent and height of mangroves in tropical Australia. Wetlands Ecology and Management 10: 161-175.

Manson, F.J., Lonergan, N.R., McLeod, J.M. and Kenyon, R.A. 2001. Assessing techniques for estimating the extent of mangroves: topographic maps, aerial photographs and Landsat TM images. Marine and Freshwater Research 52: 787-792.

Mumby, P.J., Green, E.P., Edwards, A.J. and Clark, C.D. 1999. The cost-effectiveness of remote sensing for tropical coastal resources assessment and management. Journal of Environmental Management 55: 157-166.

Neil, D.T., Orpin, A.R., Ridd, P.V. and Yu, B. 2002. Sediment yield and impacts from river catchments to the Great Barrier Reef lagoon. Marine and Freshwater Research 53: 733-752.

Norman, J. 1989. Mackay Harbour History. Maritime Archaeological Association, Mackay, Australia. 44 pp.

Phinn, S.R. and Rowland, T. 2001. Quantifying and visualizing geometric misregistration from Landsat Thematic Mapper imagery and its effects on change detection in a rapidly urbanizing catchment. Asian-Pacific Remote Sensing and GIS Journal 14: 41-54.

Pringle, A.W. 1984. Evolution of the East Burdekin Delta coast, Queensland, Australia 1940-1980. Zeitschrift fuer Geomorphologie 28: 129-154.

Proisy, C., Mougin, E., Fromard, F., Trichon, V. and Karam, M.A. 2002. On the influence of canopy structure on the radar backscattering of mangrove forests. International Journal of Remote Sensing 23: 4197-4210.

Ramsey, E.W., III and Jensen, J.R. 1996. Remote sensing of mangrove wetlands: relating canopy spectra to site-specific data. Photogrammetric Engineering and Remote Sensing 62: 939-948.

Rasolofoharinoro, M., Blasco, F., Bellan, M.F., Aizpuru, M., Gauquelin, T. and Denis, J. 1998. A remote sensing based methodology for mangrove studies in Madagascar. International Journal of Remote Sensing 19: 1873-1886.

Rouse, I.W., Haas, R.H., Schell, I.A. and Deering, D.W. 1974. Monitoring vegetation systems in the Great Plains with ERTS. *In*: Proceedings of the Third Earth Resources Technology Satellite-1 Symposium, pp. 3010-3017.

Saenger, P. and Siddiqi, N.A. 1993. Land from the sea: the mangrove afforestation of Bangladesh. Ocean and Coastal Management 20: 23-39.

Saintilan, N. and Wilton, K. 2001. Changes in the distribution of mangroves and saltmarshes in Jervis Bay, Australia. Wetlands Ecology and Management 9: 409-420.

Scoffin, T.P. 1970. The trapping and binding of subtidal carbonate sediments by marine vegetation in Bimini Lagoon, Bahamas. Journal of Sedimentary Petrology 40: 249-273.

Small, C. and Nicholls, R.J. 2003. A global analysis of human settlement in coastal zones. Journal of Coastal Research 19: 584-599.

Snedaker, S.C., Jimenez, J.A. and Brown, M.S. 1992. Anomalous roots in *Avicennia germinans* (L.) in Florida and Costa Rica. Bulletin of Marine Science 31: 467-470.

Sokal, R.R. and Rohlf, F.J. 1995. Biometry: The Principles and Practice of Statistics in Biological Research, 3rd edition. W. H. Freeman and Company, New York, USA. 887 pp.

Spalding, M., Blasco, F. and Field, C. 1997. World Mangrove Atlas. The International Society for Mangrove Ecosystems, Okinawa, Japan. 178 pp.

Spenceley, A.P. 1982. Sedimentation patterns in a mangal on Magnetic Island, nr. Townsville, North Queensland, Australia. Singapore Journal of Tropical Geography 3: 100-107.

Sulong, I., Mohd-Lokman, H., Mohd-Tarmizi, K. and Ismail, A. 2002. Mangrove mapping using Landsat imagery and aerial photographs: Kemaman district, Terengganu, Malaysia. Environment, Development and Sustainability 4: 135-152.

Tam, N.F.Y. and Wong, Y.S. 1995. Mangrove soils as sinks for wastewater-borne pollutants. Hydrobiologia 295: 231-241.

Tomlinson, P.B. 1986. The Botany of Mangroves. Cambridge University Press, Cambridge, UK.

Tong, P.H.S., Auda, Y., Populus, J., Aizpuru, M., Al-Habshi, A. and Blasco, F. 2004. Assessment from space of mangroves evolution in the Mekong Delta, in relation to extensive shrimp farming. International Journal of Remote Sensing 25: 4795-4182.

Townshend, J.R.G., Justice, C.O., Gurney, C. and McManus, J. 1992. The impact of misregistration on change detection. IEEE Transactions on Geoscience and Remote Sensing 30: 1054-1059.

Verheyden, A., Dahdouh-Guebas, F., Thomaes, K., De Genst, W., Hettiarachchi, S. and Koedam, N. 2002. High-resolution vegetation data for mangrove research as obtained from aerial photography. Environment, Development and Sustainability 4: 113-133.

Victor, S., Golbuu, Y., Wolanski, E. and Richmond, R.H. 2004. Fine sediment trapping in two mangrove-fringed estuaries exposed to contrasting land-use intensity, Palau, Micronesia. Wetlands Ecology and Management 12: 277-283.

Wang, L., Sousa, W.P., Gong, P. and Biging, G.S. 2004. Comparison of IKONOS and Quickbird images for mapping mangrove species on the Caribbean coast of Panama. Remote Sensing of Environment 91: 432-440.

Washmon, C.N., Solie, J.B., Raun, W.R. and Itenfisu, D.D. 2002. Within field variability in wheat grain fields over nine years in Oklahoma. Journal of Plant Nutrition 25: 2655-2662.

Wilson, E.H. and Sader, S.A. 2002. Detection of forest harvest type using multiple dates of Landsat TM imagery. Remote Sensing of Environment 80: 385-396.

Wolanski, E. 1995. Transport of sediment in mangrove swamps. Hydrobiologia 295: 31-42.

Woodroffe, C. 1992. Mangrove sediments and geomorphology. *In*: Robertson, A.I. and Alongi, D.M. (eds.), Tropical Mangrove Ecosystems. pp. 7-36. American Geophysical Union, Washington D.C.

Young, B.M. and Harvey, L.E. 1996. A spatial analysis of the relationship between mangrove (*Avicennia marina* var. *australasica*) physiognomy and sediment accretion in the Hauraki Plains, New Zealand. Estuarine, Coastal and Shelf Science 42: 231-246.

Yuan, D., Elvidge, C.D. and Lunetta, R.S. 1998. Survey of multispectral methods for land cover change analysis. *In*: Lunetta, R.S. and Elvidge, C.D. (eds.), Remote Sensing Change Detection: Environmental Monitoring Methods and Applications. pp. 21-39. Sleeping Bear Press, Inc., Chelsea, Michigan.

Zhan, X., Sohlberg, R.A., Townshend, J.R.G., DiMiceli, C., Carroll, M.L., Eastman, J.C., Hansen, M.C. and DeFries, R.S. 2002. Detection of land cover changes using MODIS 250 m data. Remote Sensing of Environment 83: 336-350.

Table 3.1. History of modifications to the Pioneer estuary with potential or known impacts on mangrove distributions (1862-present).

Year	Modification to Pioneer Estuary	Effect on mangrove distribution
1862	City of Mackay established; harbor facilities begun along River Street (south bank of Pioneer)	Unknown[a]
1872-1885	Construction of (old) training wall along estuarine margin of East Point (to deepen and stabilize Pioneer River channel)	Silting of Bassett Basin with reduced tidal circulation and accelerated accretion[a]
1898	Catastrophic flood; sea broke through East Point creating new river mouth	Possible mangrove loss along inside of East Point[a]
1899	Old north wall raised and extended by 305 m	Increased silting in Bassett Basin[a]
1905	Construction of south wall and wall across entrance to Bassett Basin	Prevention of northward channel migration and mangrove colonization along south bank; decrease in size of Bassett Basin; deposition of sediments and mangrove colonization on Mangrove Island[a]
1920-1927	Construction of director wall downstream from Forgan Bridge to Bassett Basin (to deepen and stabilize Pioneer River channel)	Prevention of northward channel migration and mangrove colonization along north bank[a]
1958	Catastrophic flood	Mangroves cleared around Alligator Creek to reduce flood levels during next event[a]
from 1960	Construction of industrial zone near harbor facilities at northern end of Bassett Creek	Clearing of mangroves and isolation of remnant patches[b]
1978	Construction of Canelands Shopping Centre and southern approach to Ron Camm bridge	Substantial clearing of mangroves; large proportion of Alligator Creek infilled[a]
1978-1981	Construction of railway across northern end of Vines Creek	Isolation of remnant mangrove patches[b]
1986-1990	Proposed development in Sandfly Creek region	Clearing of mangroves in Sandfly Creek in preparation for development (which has not taken place)[c]
1993	Construction of culvert and levee across entrance to Sandfly Creek	Severe restriction of tidal flow entering Sandfly Creek[c]
1994	Construction of tidal gates at Sandfly Creek	Complete restriction of tidal flow until gates opened in 1996; substantial mangrove loss[c]

[a] Gourlay and Hacker (1986)
[b] Norman (1989)
[c] B. Discher, personal communication

Table 3.2. Specifications for aerial photography acquisitions.

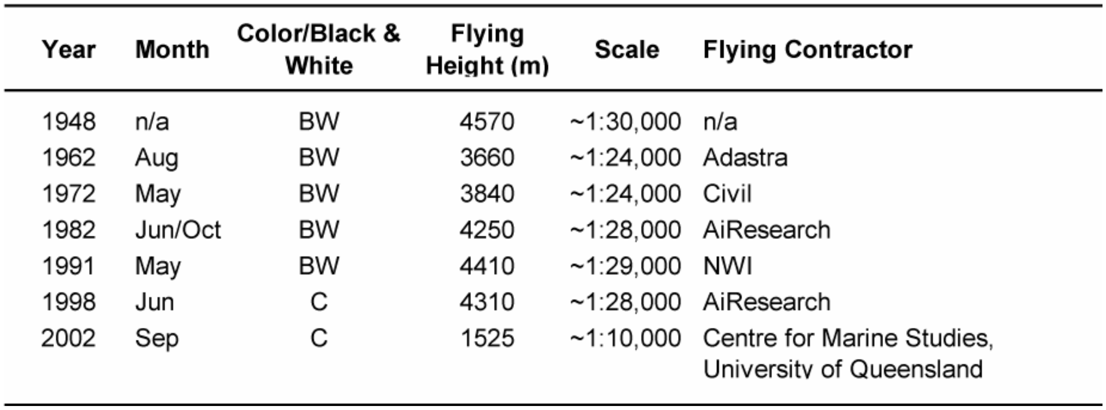

Year	Month	Color/Black & White	Flying Height (m)	Scale	Flying Contractor
1948	n/a	BW	4570	~1:30,000	n/a
1962	Aug	BW	3660	~1:24,000	Adastra
1972	May	BW	3840	~1:24,000	Civil
1982	Jun/Oct	BW	4250	~1:28,000	AiResearch
1991	May	BW	4410	~1:29,000	NWI
1998	Jun	C	4310	~1:28,000	AiResearch
2002	Sep	C	1525	~1:10,000	Centre for Marine Studies, University of Queensland

Table 3.3. Classification of drivers of mangrove change, based on definitions in Shaffelke et al. (2005).

Type of Change	Abbreviation	Evidence from the Pioneer Estuary
Direct Damage	D	Replacement of mangrove areas by agriculture or development OR saltpan formerly occupied by mangrove (and clearing reported in the literature)
Restricted Tidal Exchange	R	Remnant patches of mangroves isolated from tidal channels due to clearing or development
Species-specific Effects	S	Canopy gaps previously occupied by mangroves, most notably *Avicennia marina;* gaps distinguishable as lighter grey (B/W photographs) or lighter green (color photographs) patches
Depositional Gains and Losses	P	Mangrove loss from scour or wave action OR mangrove growth onto newly deposited substrate
Ecotone Shift	E	Replacement of saltpan by mangroves associated with wet years OR replacement of mangrove areas by saltpan (with no reported of clearing) associated with dry years
No change	N	Stable regions; any visible changes were <1 ha (approx. limit of accuracy)

Table 3.4. Changes in mangrove areas (to nearest ha) mapped from aerial photographs between 1948 and 2002. Values for non-tidal, cleared or lost, and new growth are reported relative to the previous time interval.

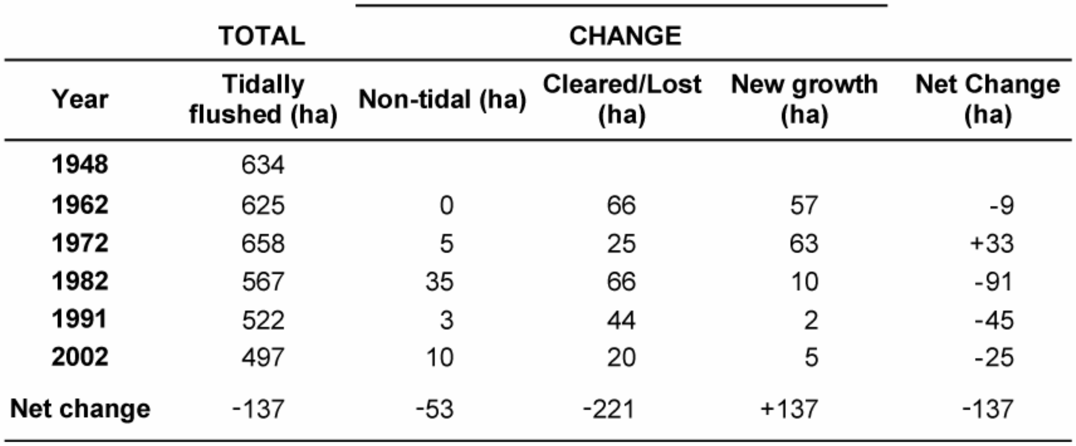

	TOTAL	CHANGE			
Year	**Tidally flushed (ha)**	**Non-tidal (ha)**	**Cleared/Lost (ha)**	**New growth (ha)**	**Net Change (ha)**
1948	634				
1962	625	0	66	57	-9
1972	658	5	25	63	+33
1982	567	35	66	10	-91
1991	522	3	44	2	-45
2002	497	10	20	5	-25
Net change	-137	-53	-221	+137	-137

Table 3.5. Mangrove areas (to nearest ha) from 1948 to 2002 in 8 sub-regions of the Pioneer estuary (mapped from aerial photographs).

REGION	**1948**	**1962**	**1972**	**1982**	**1991**	**2002**
Fursden Creek	57	57	59	52	51	46
Alligator Creek	63	20	33	4	6	5
Barnes Creek	61	93	115	116	113	109
Vines Creek/Bassett Basin W	223	218	212	165	164	153
Sandfly Creek	51	58	39	33	7	0
Main Pioneer	25	24	36	40	36	35
Bassett Creek/Bassett Basin E	154	139	143	130	123	121
South Pioneer Mouth	0	16	21	27	22	28
TOTAL TIDAL	634	625	658	567	522	497
TOTAL NON-TIDAL	N/A	0	5	40	43	53

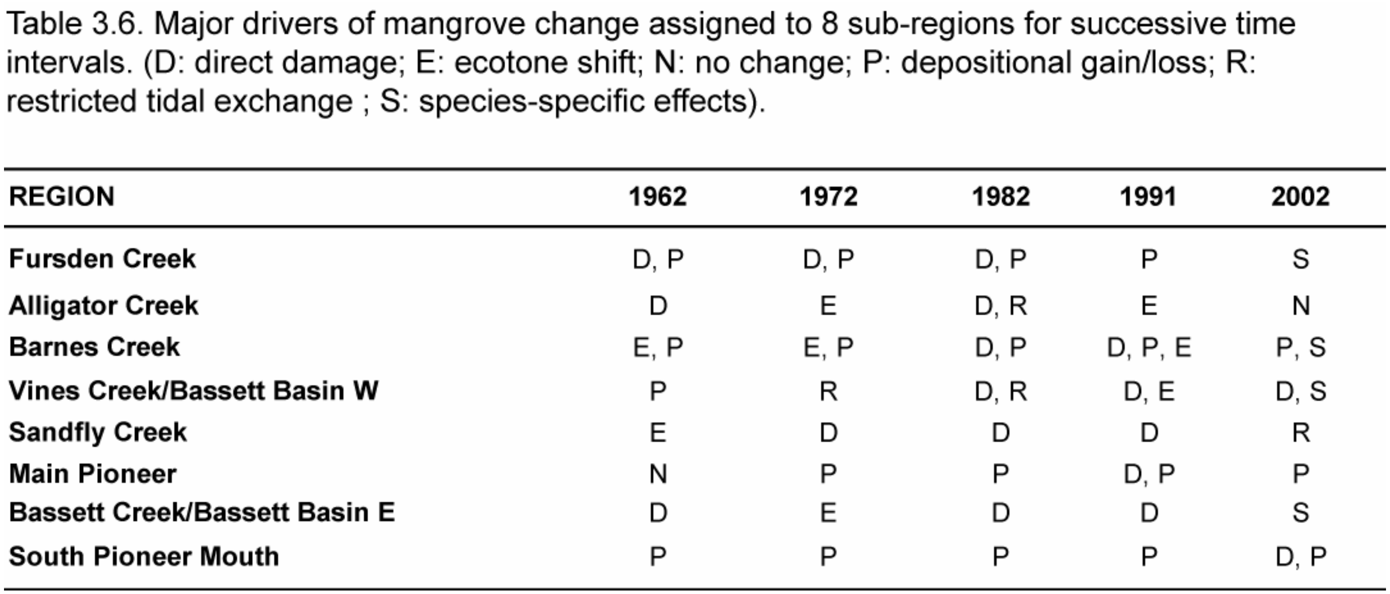

Table 3.6. Major drivers of mangrove change assigned to 8 sub-regions for successive time intervals. (D: direct damage; E: ecotone shift; N: no change; P: depositional gain/loss; R: restricted tidal exchange ; S: species-specific effects).

REGION	**1962**	**1972**	**1982**	**1991**	**2002**
Fursden Creek	D, P	D, P	D, P	P	S
Alligator Creek	D	E	D, R	E	N
Barnes Creek	E, P	E, P	D, P	D, P, E	P, S
Vines Creek/Bassett Basin W	P	R	D, R	D, E	D, S
Sandfly Creek	E	D	D	D	R
Main Pioneer	N	P	P	D, P	P
Bassett Creek/Bassett Basin E	D	E	D	D	S
South Pioneer Mouth	P	P	P	P	D, P

Table 3.7. ANOVA for a multiple regression of NDVI (from 2000 Landsat image) on live tree density (per m^2) and dead basal area (m^2). ($r^2 = 0.3682$).

Souce	*df*	*SS*	*MS*	*F*	*p*
Regression	2	0.1265	0.0632	3.707	0.053
Live tree density	1	0.0063	0.0063	0.371	0.553
Dead basal area	1	0.0821	0.0821	4.816	0.047 *
Unexplained	13	0.2218	0.0171		
Total	15	0.3482	0.0232		

*$p < 0.05$

Table 3.8. Importance values (I.V.) of the mangroves in the lower intertidal regions of the Pioneer estuary by creek region. Dominance = basal area species/basal area all trees x 100%. Density = # trees species/# trees total x 100%. Frequency = # plots species present/total # plots x 100%. I.V. = Dominance + Density + Frequency. Total number of plots: Fursden Creek = 5 (total area = 125 m^2); Barnes Creek A = 6 (total area = 150 m^2); Barnes Creek B = 5 (total area = 125 m^2); Vines Creek = 8 (total area = 200 m^2); Bassett Creek = 6 (total area = 150 m^2).

		Relative values (%)			
Creek	**Species**	**Dominance**	**Density**	**Frequency**	**I.V.**
Fursden	*Avicennia marina*	62.2	37.2	100.0	137.2
	Aegiceras corniculatum	35.8	53.7	100.0	153.7
	Rhizophora stylosa	3.4	15.2	60.0	78.7
Barnes A	*Aegiceras corniculatum*	33.1	64.8	100.0	197.9
	Avicennia marina	64.6	21.2	100.0	185.7
	Rhizophora stylosa	1.1	5.1	83.3	89.6
	Aegialitis annulata	2.9	12.1	50.0	65.0
Barnes B	*Avicennia marina*	100.0	100.0	100.0	300.0
Vines	*Aegiceras corniculatum*	27.8	37.7	100.0	165.5
	Avicennia marina	33.8	16.6	100.0	150.4
	Excoecaria agallocha	25.7	33.3	75.0	134.0
	Xylocarpus sp	3.1	3.1	100.0	106.2
	Rhizophora stylosa	2.3	4.2	87.5	94.0
	Ceriops australis	17.7	16.4	37.5	71.6
	Lumnitzera racemosa	5.0	2.3	50.0	57.3
	*Bruguiera sp***	3.1	4.7	37.5	45.4
	Osbornia octodonta	9.4	6.1	25.0	40.4
	Aegialitis annulata	2.3	6.1	37.5	45.9
	*Other****	4.2	11.1	12.5	27.8
Bassett	*Avicennia marina*	56.1	22.9	100.0	179.1
	Aegiceras corniculatum	24.1	47.5	100.0	171.6
	Osbornia octodonta	5.5	13.0	83.3	101.8
	Excoecaria agallocha	9.3	10.3	50.0	69.6
	Xylocarpus sp.	37.8	8.3	16.7	62.8
	Aegialitis annulata	1.8	8.5	50.0	60.2
	Rhizophora stylosa	8.4	10.3	33.3	52.0
	*Bruguiera sp**	1.4	1.7	16.7	19.7

**B. parviflora* ; ***B. gymnorhiza* and *B. parviflora* ; ***Unidentifiable dead trees

Table 3.9. Proportions of healthy, sick and dead *Avicennia marina* trees by site.

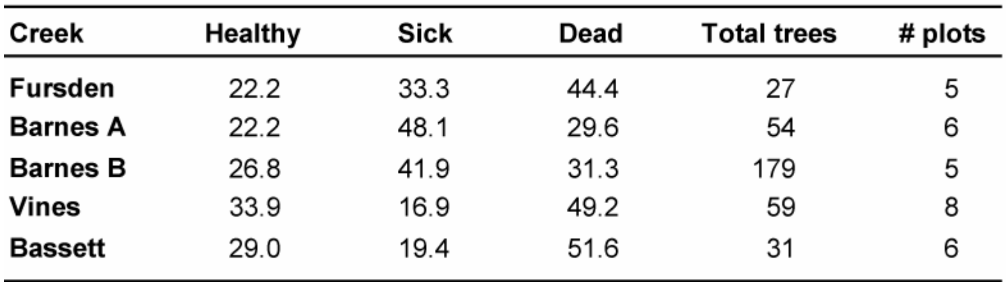

Creek	Healthy	Sick	Dead	Total trees	# plots
Fursden	22.2	33.3	44.4	27	5
Barnes A	22.2	48.1	29.6	54	6
Barnes B	26.8	41.9	31.3	179	5
Vines	33.9	16.9	49.2	59	8
Bassett	29.0	19.4	51.6	31	6

Table 3.10. Error matrix for associations between NDVI change classes (1990-2000) and canopy density changes (1991-1998). Data are the numbers (out of 150) of 28.5 x 28.5 m (Landsat-sized) pixels cross-classified between the NDVI difference image and the difference between 1991 and 1998 aerial photomosaics. The "no change" class was excluded from analysis.

Image	**Class**	**Reference Aerial Photographs Canopy Density Change (1991-1998)**		**Error (%)**		**Accuracy (%)**		
		Lower	**Higher**	**Commission**	**Omission**	**Producer's**	**User's**	**Overall**
Landsat NDVI Difference Classes (1990-2000)	**NDVI lower**	59	1	1.7	3.3	96.7	98.3	98.0
	NDVI higher	2	88	2.2	1.1	98.9	97.9	

Figure 3.1. Eight mangrove sub-regions (white) within the Pioneer estuary. Major urban features include: railway (thick dashed line), Caneland Central Shopping Centre (star), tidal gates (arrow), and training walls (thin dashed line) along the north and south banks of the Pioneer River. Small black square in the Fursden Creek (F) sub-region defines the area of dieback in Figure 3.4; larger black rectangle defines the area depicted in Figure 3.8a,b.

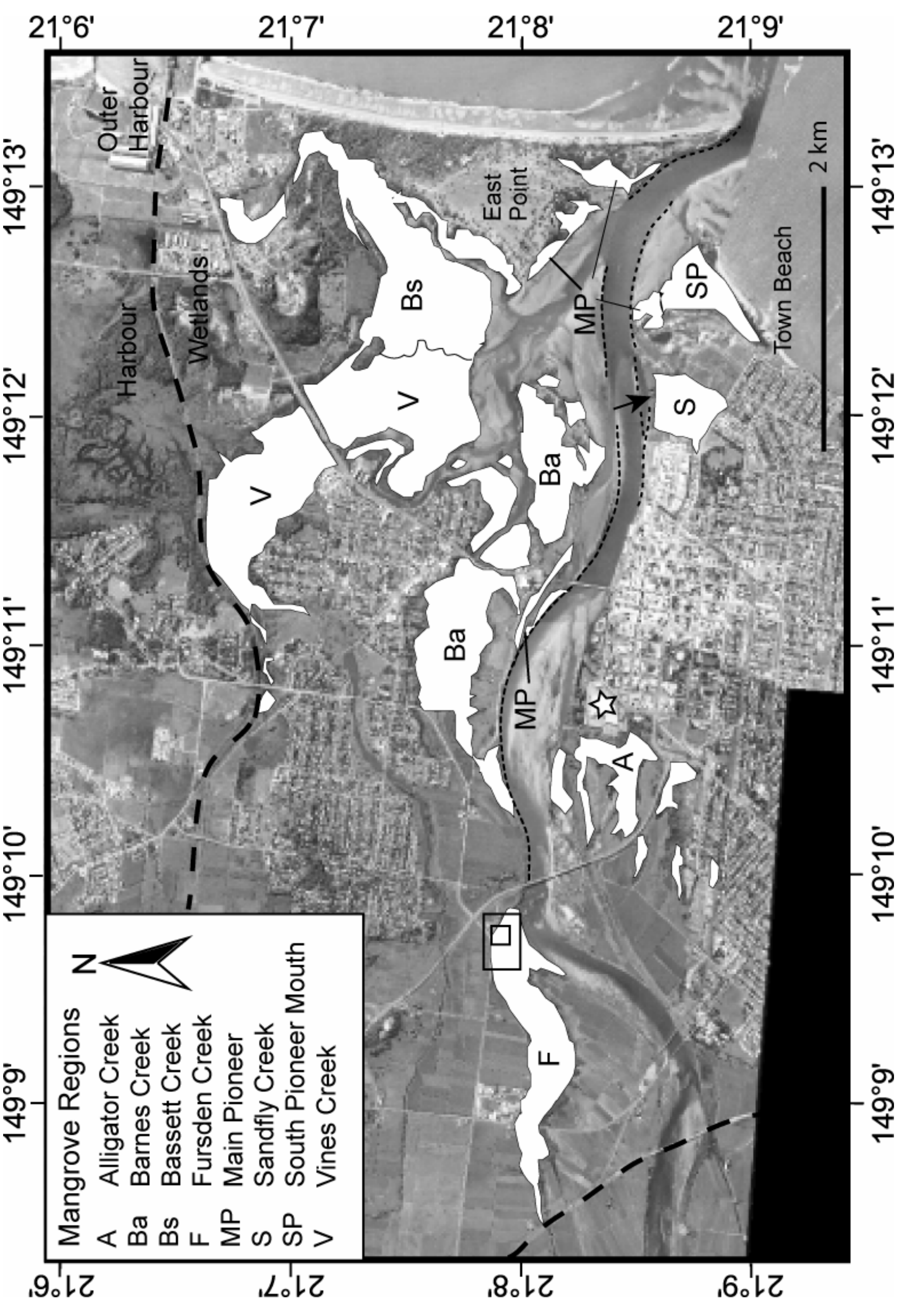
Mangrove Regions
A Alligator Creek
Ba Barnes Creek
Bs Bassett Creek
F Fursden Creek
MP Main Pioneer
S Sandfly Creek
SP South Pioneer Mouth
V Vines Creek
N
Outer Harbour
Harbour
Wetlands
East Point
Town Beach
2 km
Bs
V
V
Ba
Ba
MP
MP
A
S
SP
F
21°6'
21°7'
21°8'
21°9'
149°9'
149°10'
149°11'
149°12'
149°13'

Figure 3.2. Net changes to mangrove distributions between 1948 and 2002.

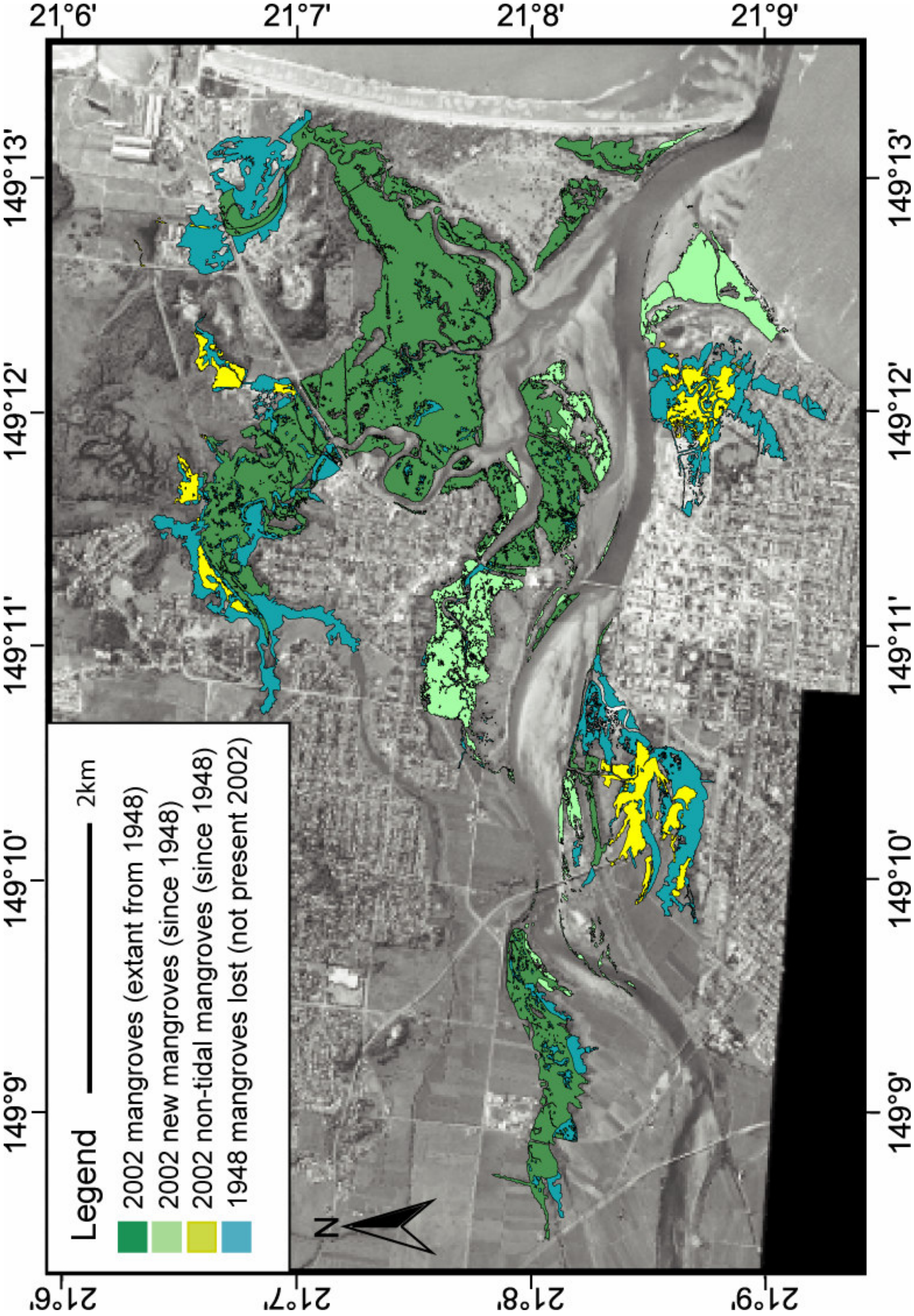
21°6'
21°7'
21°8'
21°9'
149°13'
149°12'
149°11'
149°10'
149°9'
Legend
2km
2002 mangroves (extant from 1948)
2002 new mangroves (since 1948)
2002 non-tidal mangroves (since 1948)
1948 mangroves lost (not present 2002)
N

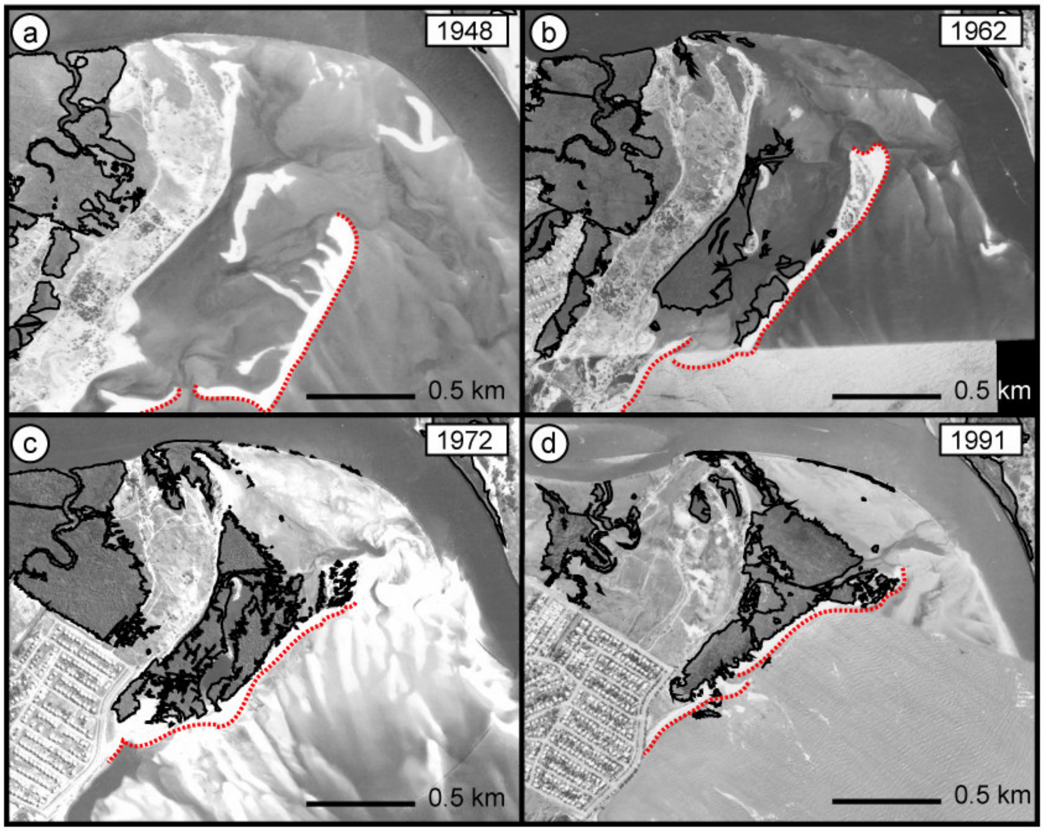

Figure 3.3. Northward shift of sand banks on the south bank of the Pioneer River mouth. (a) 1948. (b) 1962. (c) 1972. (d) 1991. Red dashed lines indicate eastern, exposed side of sand banks. Solid black lines delineate mangrove areas. Scale of photographs = 1:28,000.

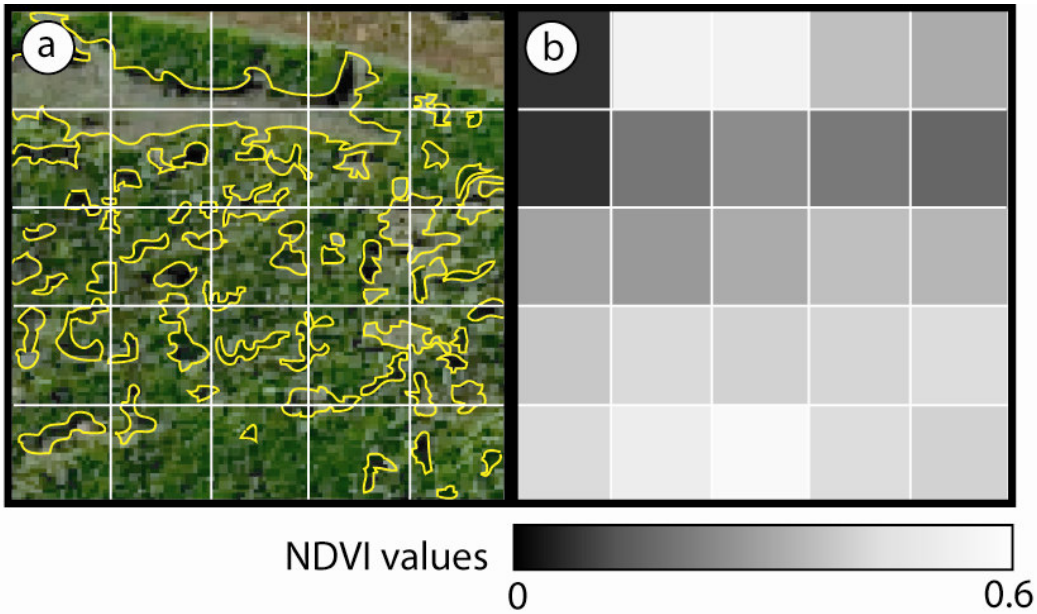

Figure 3.4. Mangrove canopy maps for approximately the same 142 x 142 m area in a region of substantial dieback within Fursden Creek. (a) Subset of a 2002 aerial photograph with digitized canopy gaps from dieback outlined in yellow. The grid represents the scale of Landsat pixels (28.5 m x 28.5 m). (b) NDVI classification of 2000 Landsat ETM+ pixels for the same region. Brighter pixels have high NDVI values (= denser, greener canopy); darker pixels have low NDVI values (= more open space).

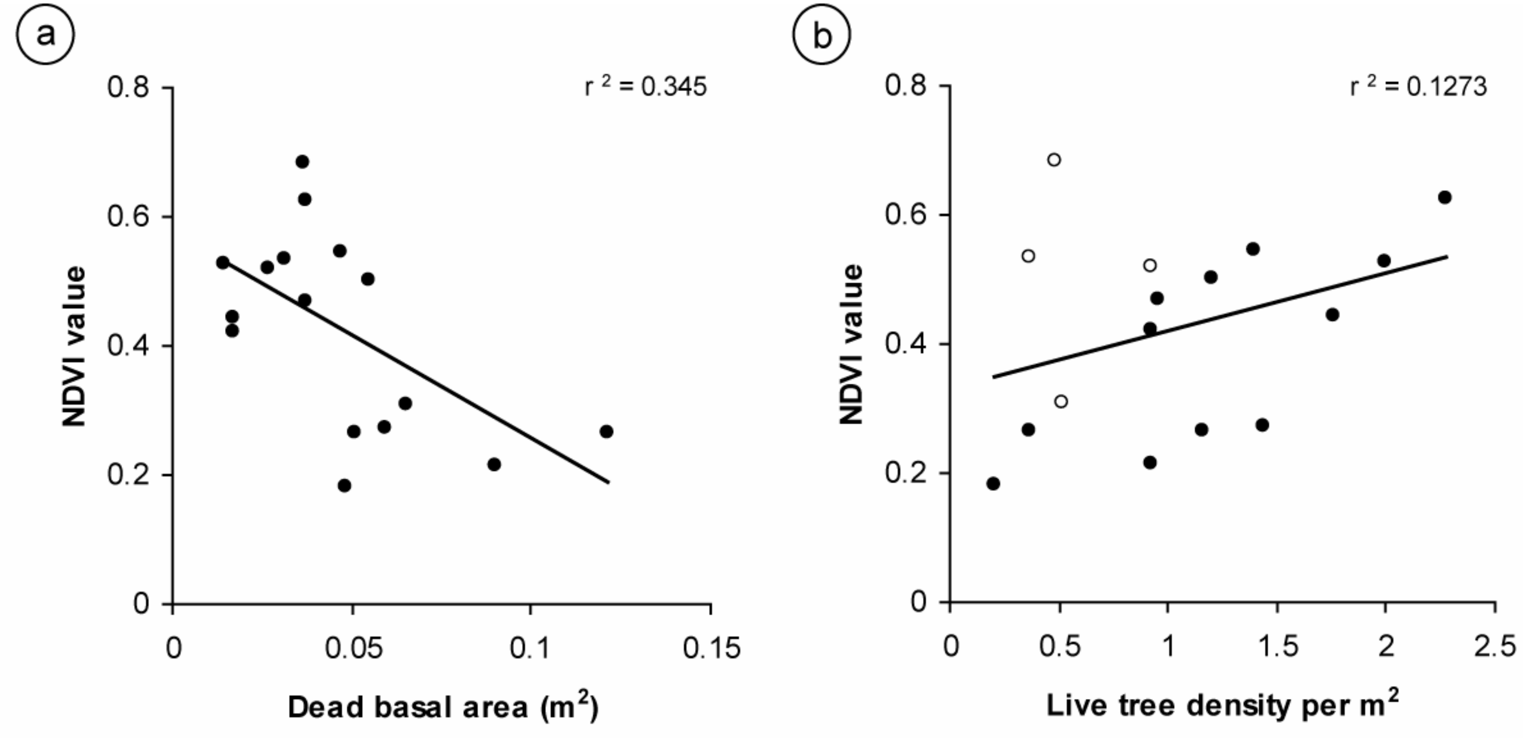

Figure 3.5. NDVI values derived from 2000 Landsat ETM+ data plotted against *in situ* measurements of: (a) dead basal area (m^2); and (b) live tree density per m^2. Closed circles are sites from Fursden, Barnes and Vines Creeks; open circles are sites from Bassett Creek.

Figure 3.6. Differences in NDVI values between 1990 and 2000. Light grey regions indicate no change. Red pixels indicate reduced NDVI values from dieback; green pixels indicate increased NDVI values from new growth and denser canopies.

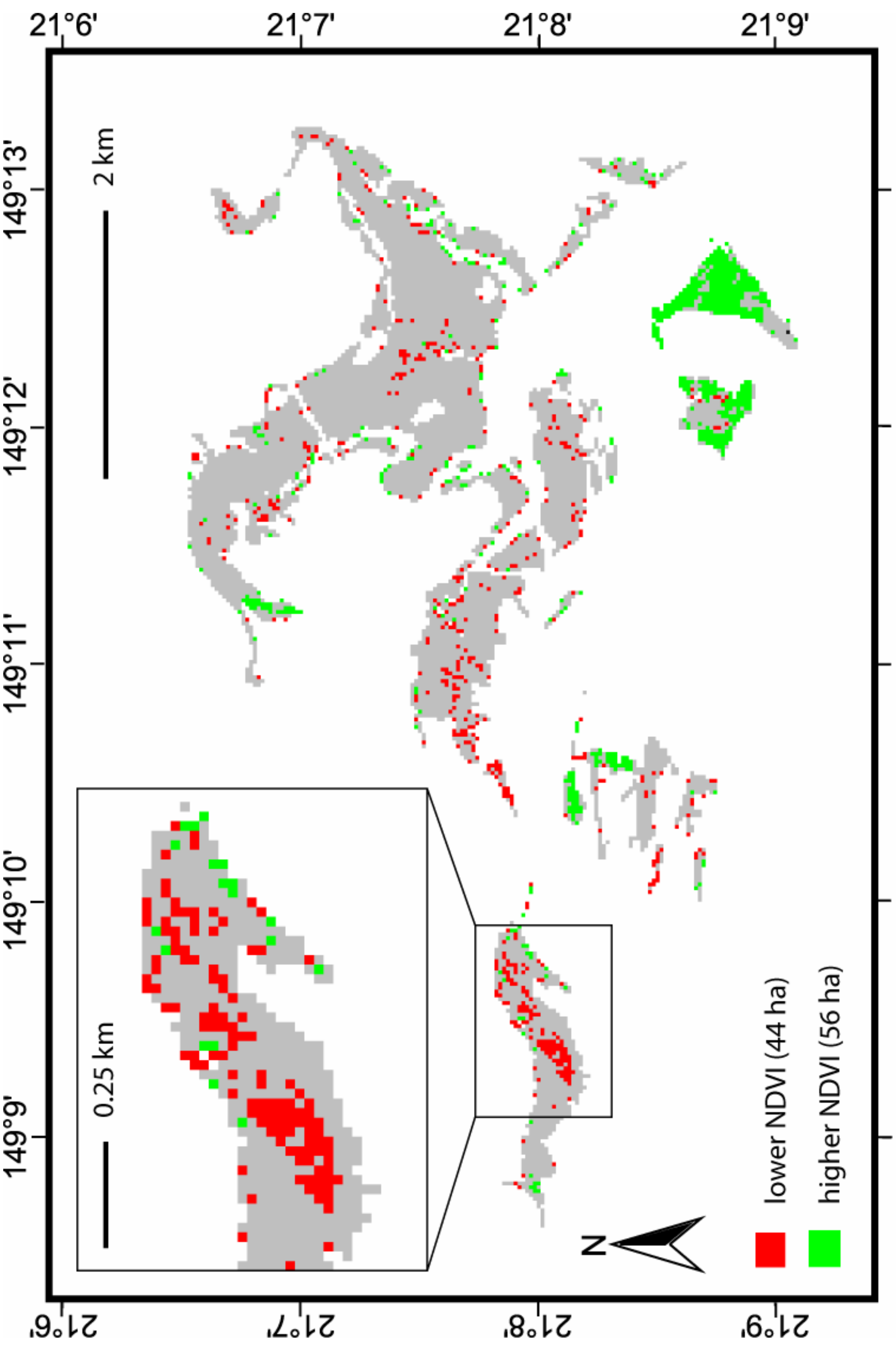
21°6'
21°7'
21°8'
21°9'
149°9'
149°10'
149°11'
149°12'
149°13'
2 km
0.25 km
N
🟥 lower NDVI (44 ha)
🟩 higher NDVI (56 ha)

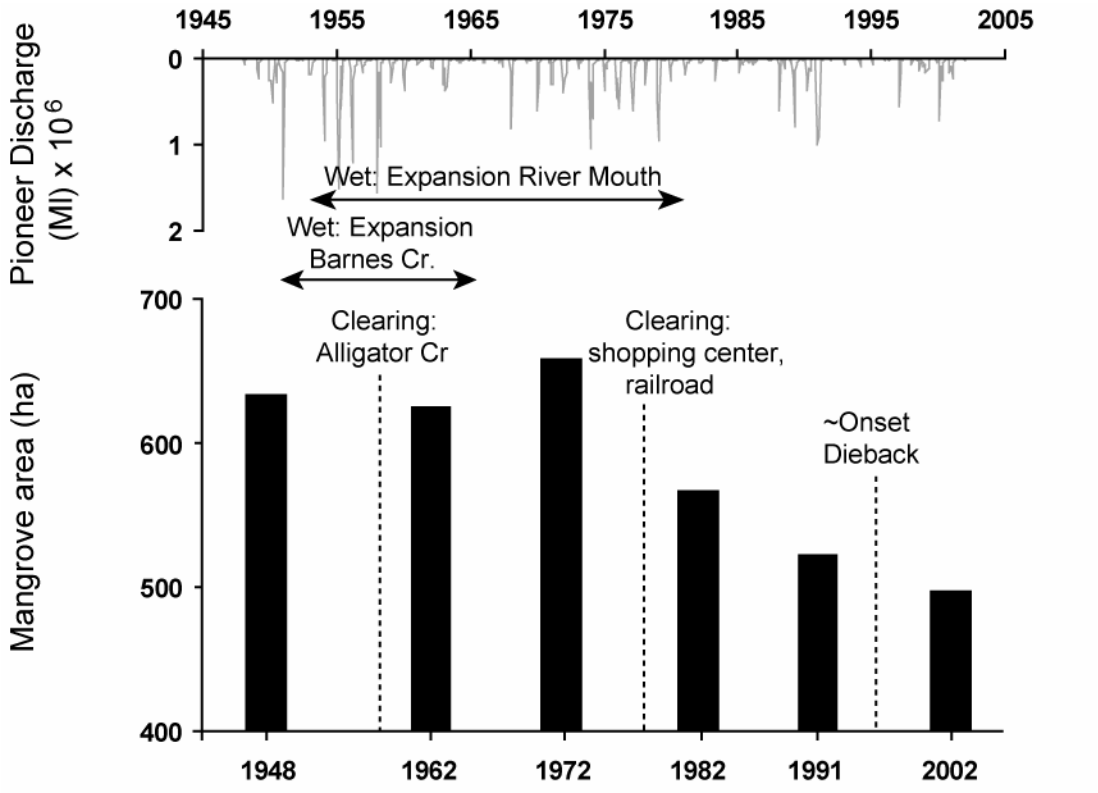

Figure 3.7. Time series of changes in Pioneer estuary mangrove area (bottom) plotted with Pioneer River discharge (top). Black bars represent the total tidal mangrove area digitized from aerial photography. Dashed lines denote approximate timing of major mangrove losses. Arrows indicate periods of major mangrove expansion.

Figure 3.8. Sediment remobilization in dieback regions. (a) Pre-dieback aerial photograph (1991) of mangrove distribution in Fursden Creek along exposed tidal drainage channel (0.0035 ha; dashed outline). (b) Post-dieback aerial photograph (2002) of mangrove distribution in Fursden Creek with large gap along same creek (0.32 ha; dashed outline). Arrow points to location of photographs in c-d. (c) Erosion monitoring site across tidal creek gully in May 2003. Dashed line outlines region of slumping in d. (d) Same bank after slumping event, March 2004. (e) Exposed cable roots of dead *Avicennia marina* near drainage channel along the north bank of the Pioneer River. (f) Exposed cable roots of dead *A. marina* in severe dieback region within Barnes Creek.

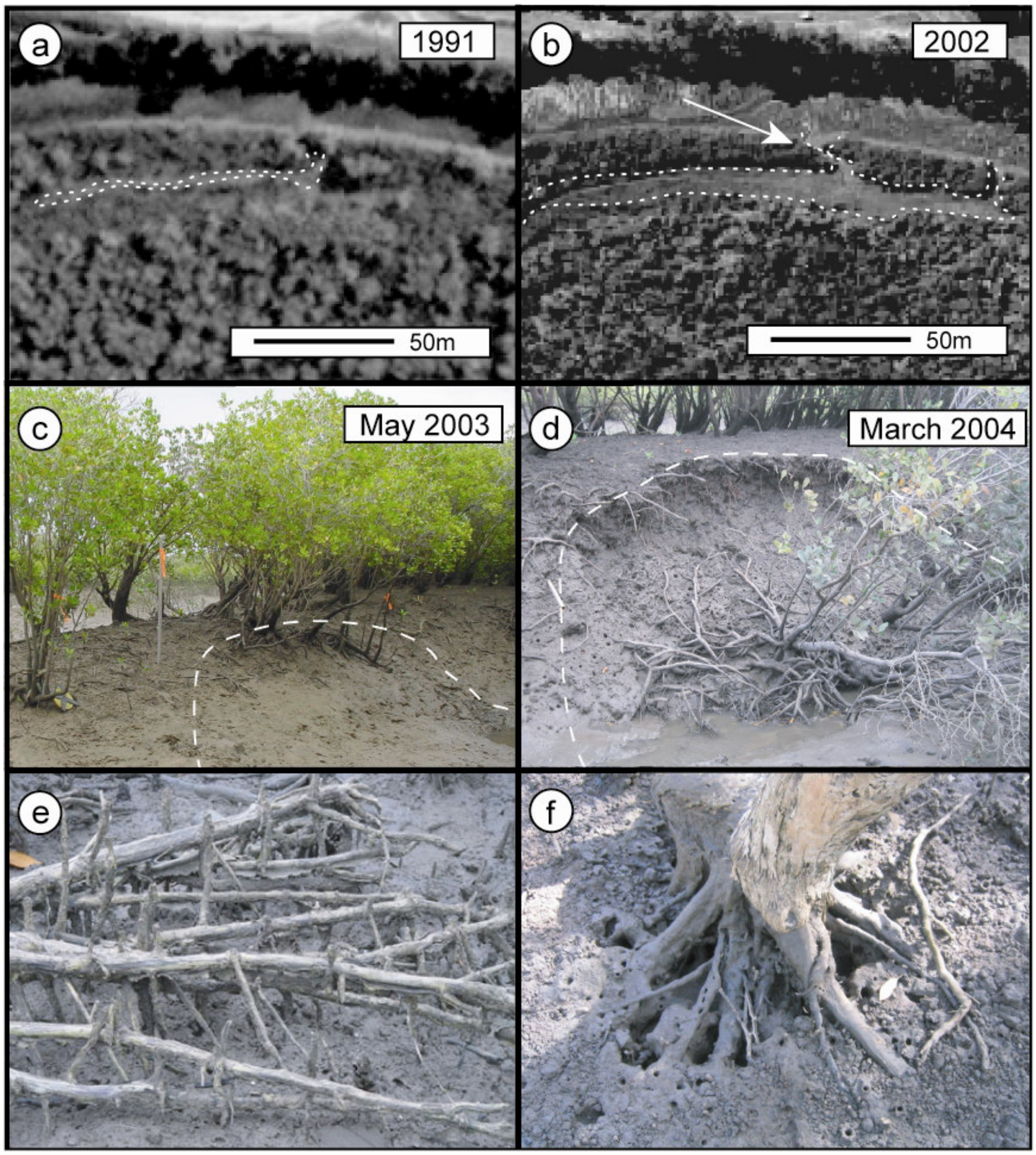
a
1991
50m
b
2002
50m
c
May 2003
d
March 2004
e
f

Chapter 4. Geochemical Proxies for Delivery of Suspended Sediment to Nearshore Waters off Mackay

Introduction

Human activity on land has increased global sediment loss by an order of magnitude over natural weathering rates (Wilkinson 2005). A substantial proportion of this material is stored in adjacent downslope regions (e.g. floodplains, reservoirs, estuaries) (Pimentel et al. 1995; Tilman et al. 2001; Vorosmarty et al. 2003; Walling and Fang 2003). For example, in the Burdekin River catchment of north Queensland, Australia, only 13% of sediment delivered to catchment waterways is exported from the river mouth to the ocean (Prosser et al. 2002). Even with so much catchment retention, sediment supply models for northeastern Australia suggest that sediment delivery loads into the Great Barrier Reef (GBR) World Heritage Area have increased approximately two to eightfold above estimated values before European land clearing (~1850) for grazing and crops (Table 4.1; Belperio 1983; Moss et al. 1992; Neil and Yu 1996; Rayment and Neil 1997; Neil et al. 2002; Prosser et al. 2002; Furnas 2003; McKergow et al. 2005a, 2005b). The most recent and spatially complex models used in Australia to predict sediment delivery to the nearshore (e.g. SedNet) are based largely on predictions of sediment loss (e.g. due to land use, vegetation cover, rainfall erosivity, soil erodibility, slope) and sediment transport capacity (e.g. as functions of discharge, river width, river slope, particle size, hydraulic roughness, floodplain/reservoir deposition) (Prosser et al. 2001; McKergow et al. 2005a). However, all of these models are sensitive to the quality of data for each input variable (Neil et al. 2002).

An alternative approach for determining temporal changes in fluvial sediment delivery is to measure empirically geochemical proxies of sediment delivery to nearshore waters from coral skeletal records (Fallon et al. 2002; Alibert et al. 2003; McCulloch et al. 2003; Sinclair and McCulloch 2004). Two elements, barium (Ba) and yttrium (Y), have been related to suspended sediment delivery. Since river waters are usually enriched in barium and yttrium and depleted in calcium (Ca), relative to nearshore marine waters, pulses of floodwater to the nearshore will increase the ratios of Ba/Ca and Y/Ca that are deposited in skeletons of massive *Porites* corals (Sinclair 1999; Fallon et al. 2002; Alibert et al. 2003; McCulloch et al. 2003; Sinclair and McCulloch 2004; Sinclair 2005a). Using a 200+ year coral record from the Burdekin River drainage region of the GBR, McCulloch et al. (2003) found both an ~30% increase in baseline Ba/Ca values timed during the rapid expansion of cattle stocking rates (~1870) and a resulting five to tenfold increase in sediment delivery rates to the nearshore since that time. In another study from Misima Island, Papua New Guinea, Fallon et al. (2002) found marked increases of Y (and other rare earth elements) in corals living close to discharge from an open-cut mine. The spikes in Y/Ca corresponded to periods of heavy discharge and they tapered off following cessation of mining operations (Fallon et al. 2002). It has yet to be determined whether these strong relationships observed from heavily grazed, dry tropics regions (e.g. Burdekin catchment) and point-sources of sediment pollution (e.g. Misima

Island mine) are also preserved in corals growing near intensive agricultural regions, where coastal eutrophication will affect biological activity and may influence trace element uptake by corals.

Sediment yield to the coast is largely determined by vegetation cover, precipitation and river transport capacity (Douglas 1967), but once fine particles are discharged into the ocean, their fate is determined mainly by electrostatic forces, gravity and flood plume dynamics (Larcombe and Woolfe 1999; Furnas 2003; Devlin and Brodie 2005). Within low salinity, freshwater-seawater mixing zones, fine particles (e.g. clays, colloids, humics) aggregate and sink (Sholkovitz 1976; Gibbs 1983, 1985; Wolanski and Gibbs 1995), resulting in deposition of most terrestrial material within a few kilometers of shore (Belperio 1983; Wolanski and Gibbs 1995; Larcombe and Woolfe 1999; Neil et al. 2002; Furnas 2003). Ba and Y, however, dissociate from the fine particles within the mixing zone (see below), remain in solution, and are advected with the river plumes. In the GBR Lagoon, the dispersal of plumes is governed by wind stress, tidal currents, wind-driven currents and geostrophic forces (Wolanski and Bennett 1983; Church et al. 1985; Wolanski and Pickard 1985; Larcombe and Woolfe 1999; Haynes et al. 2001; Neil et al. 2002; Devlin and Brodie 2005). Strong prevailing southeasterly winds produce longshore movement of inner shelf waters that, combined with Coriolis forcing, usually drive flood plumes alongshore to the north (Figure 4.1a; Wolanski and Ruddick 1981; Larcombe and Woolfe 1999; Brinkman et al. 2002; Furnas 2003; Devlin and Brodie 2005). Under these conditions, plumes are typically restricted to within 20 km of the coast (King et al. 2001; Devlin and Brodie 2005). However, when wind stress from very strong winds exceeds the Coriolis effect (Chao 1988; Wolanski 1994), or when northerly winds oppose the direction of Coriolis forcing, river plumes may spread south and east across the shelf (Figure 4.1b; Devlin et al. 2001; Furnas 2003; Devlin and Brodie 2005). Although most fine suspended sediment remains within an inshore wedge (Belperio 1983; Larcombe et al. 1995; Larcombe and Woolfe 1999), plumes dispersing across the shelf may contain dissolved nutrients and other pollutants that may affect coral reefs systems (Hutchings and Haynes 2000).

In this chapter, I investigate spatial and temporal variation in sediment delivery from the Pioneer River between 1946 and 2003, estimated from high-temporal resolution measurements of Ba/Ca and Y/Ca in coral skeletons using laser ablation inductively-coupled mass spectrometry (LA-ICP-MS). I investigate correlations of Ba/Ca and Y/Ca with fluvial discharge and wind to evaluate their utility as proxies of terrestrial runoff from the intensively cultivated Mackay-Whitsunday region, and I compare my results with those from other inshore coral records along the Queensland coast. I discuss anomalous behavior within the coral records which may be related to changing land use dynamics and El Niño-Southern Oscillation (ENSO) events.

Trace Element Incorporation

The ratios of trace elements to calcium within coral aragonitic ($CaCO_3$) skeletons are usually in equilibrium with seawater composition, and are good natural tracers of fluvial or pollutant inputs to seawater (Livingston and Thompson 1971; Flor and Moore 1977; Howard and Brown 1984; Shen and Boyle 1988; Sholkovitz and Shen 1995; Fallon et al. 2002; McCulloch et al. 2003). Several mechanisms, that are not necessarily mutually exclusive, may explain trace metal incorporation into coral skeleton: (1) trace ions can substitute for Ca^{2+} or CO_3^- in the crystal lattice (Allison 1996a; Sinclair 1999; Fallon et al. 2002), and there are numerous possible pathways by which the dissolved ions may coprecipitate into the skeletal matrix (see Sinclair 1999); (2) some ions may also precipitate directly onto the calcifying surface if a coral retracts its tissues after stress or damage (Brown et al. 1991); (3) organic matter can be trapped in skeletal cavities, either during skeletal growth when coral tissue becomes trapped during crystal formation (Barnes 1970), or through particulate detritus entering damaged cavities that becomes sealed inside as the polyp deposits new skeleton (Barnard et al. 1974); and (4) uptake of organic matter via heterotrophic feeding may release trace elements into the precipitation fluid during digestion (St. John 1974; Sinclair 1999). This particulate organic matter may be substantially enriched in certain trace elements, such as barium, which has highly elevated concentrations in certain tissues (including coral tissue), and the rare earth elements and yttrium (REY), which readily adsorb to organic surfaces of particles (Sinclair 1999).

Some variation in trace element ratios may be related to changing rates of biological processes (de Villiers et al. 1995; Cohen et al. 2001; Cohen et al. 2002; Mitsuguchi et al. 2003; Sinclair 2005b). For example, coral symbiotic activity within the cold water coral *Astrangia poculata* is responsible for up to 65% of the Sr/Ca variability within the coral skeleton (Cohen et al. 2002), while daytime symbiotic photosynthesis causes Sr/Ca incorporation in *Porites* skeletons to be five times more sensitive to sea surface temperature (SST) variations than during night-time calcification (Cohen et al. 2001). Variation introduced from such biological processes can obscure coral trace element correlations with environmental signals, and the magnitude of these effects may vary by species, location and the strength of the environmental factors.

Barium

River discharge is the main source of Ba to the nearshore, providing 50-75% of the total dissolved Ba load (Hanor and Chan 1977; Li and Chan 1979; Carroll et al. 1993). Ba transported by rivers is adsorbed to fine-grained suspended clay particles in freshwater, but it desorbs rapidly within the low salinity, high ionic strength, mixing zone of estuaries where Ba ions exchange with more abundant magnesium (Mg) and Ca ions in seawater (Hanor and Chan 1977; Edmond et al. 1978; Li and Chan 1979; Froelich et al. 1985; Carroll et al. 1993; Coffey et al. 1997; Guay and Falkner 1998; Stecher and Kogut 1999; Nozaki et al. 2001; Sinclair and McCulloch 2004). Desorption can occur at salinities between 2 and 20 ppt (though typically < 10 ppt), but the exact geographical location depends on river flow rate, suspended sediment concentration, and the length of the mixing zone (Coffey et al. 1997). Dissolved Ba then advects with river discharge into nearshore waters (Coffey et al. 1997; Stecher and Kogut 1999; McCulloch et al. 2003), where it becomes incorporated into coral aragonite in proportion to its local abundance.

Most research suggests that Ba^{2+} substitutes directly for Ca^{2+} in coral skeletons (Speer 1983; Lea et al. 1989; Sinclair 1999; Sinclair and McCulloch 2004), although experiments by Pignitore et al. (1989) indicate that a substantial proportion of Ba in *Acropora palmata* and *Montastrea annularis* skeletons may have been incorporated by occlusion (i.e. adsorbed to the surface of skeletal elements and buried by further growth). The distribution coefficient (D_{Ba}) for Ba (the ratio of Ba/Ca in coral to Ba/Ca in seawater) is usually close to 1 (Livingston and Thompson 1971; Buddemeier et al. 1981; Lea et al. 1989; Shen and Sandford 1990), which suggests that coral Ba accurately reflects ambient seawater concentrations (Livingston and Thompson 1971; Lea et al. 1989; Alibert et al. 2003; McCulloch et al. 2003; Sinclair and McCulloch 2004). In at least one case, Allison (1996b) measured enriched barium in microborings and centers of calcification within coral skeletons, which may have led to overestimates of D_{Ba}, particularly from bulk sampling techniques. Additional significant variation in Ba concentrations among individuals within a species and taxonomic groups may reflect biological influences affecting Ba partitioning (Buddemeier et al. 1981; Pignitore et al. 1989; Tudhope et al. 1996; Allison 1996a, 1996b).

Ba has been used as a geochemical proxy for several different processes. Because Ba has a typical profile for nutrients in the open ocean (i.e. surface depletion and deep-water enrichment; Bruland 1983), many studies have used coral Ba to trace upwelling of nutrient-rich waters (Lea et al. 1989; Shen and Sandford 1990; Shen et al. 1992a; Fallon et al. 1999). Links between Ba/Ca ratios and terrestrial runoff were first reported by Shen and Boyle (1988), who found enriched Ba/Ca in nearshore corals relative to those from the open ocean. This suggests that coral Ba/Ca, measured in skeletons from long-lived corals growing in coastal waters, can record historical changes in suspended sediment delivery to the nearshore (McCulloch et al. 2003), and comparisons to offshore sites may reveal the spatial impact of flood plumes.

Yttrium and rare earth elements

Because the chemistry of Y is similar to that of the lanthanides (rare earth elements), a discussion of Y behavior must include the behaviors of the rare earth elements (REE) from river to sea. Rare earth elements and yttrium (REY) can be measured independently, or together in series, to investigate patterns that may indicate sources from local geology or land use (Sholkovitz et al. 1999; Lawrence et al. 2006a). Yet, the geochemical pathways from riverine transport of Y to incorporation within coral skeletons are less well studied that those for Ba, largely because instruments that can measure aqueous concentrations of yttrium and the monoisotopic REE with precision have only recently become available (Nozaki et al. 1997; Kawabe et al. 1998; Lawrence et al. 2006b).

Fluvial discharge is the main source of marine REY (Byrne and Sholkovitz 1996), with large contributions from aeolian dust possible in some areas (Elderfield and Greaves 1982; Elderfield et al. 1988; Sholkovitz 1993; Greaves et al. 1999; Lawrence and Kamber 2006). REY come from weathered topsoil (Boiko et al. 1986; Byrne and Sholkovitz 1996; Fallon et al. 2002) and are transported in catchment waterways attached to colloidal particles (e.g. colloidal iron oxy-hydroxides, organic colloids) within the 0.45μm fraction of the suspended sediment load (Sholkovitz and Elderfield 1988; Elderfield et al. 1990; Sholkovitz 1992, 1995; Lawrence et al. 2006a). The total concentration of REY in freshwater may vary with pH and temperature, which influences the availability of colloidal particles (Elderfield et al. 1990; Gammons et al. 2005; Lawrence et al. 2006a). Because of these variations, Gammons et al. (2005) cautioned using REE as tracers of source materials. However, when Lawrence et al. (2006a) first normalized water REY samples to shale and then scaled the values to the same total concentration of REY (excluding anomalous elements), they found that REY *patterns* within the Pioneer River catchment were independent of pH and preserved within the freshwater system. It is still uncertain whether these provincial patterns persist through the estuary and into the ocean.

A large amount of REY (~60-80%) is removed in the estuarine mixing zone due to flocculation of iron-organic colloids at low salinities (Hoyle et al. 1984; Sholkovitz 1995; Lawrence and Kamber 2006), although large increases in REY abundances between ~5 to 10 ppt probably reflect REY release from river particles (Lawrence and Kamber 2006). Secondary removals occur at higher salinities and sometimes may be caused by biological uptake (Nozaki et al. 2000; Nozaki et al. 2001). Fractionation of the freshwater REY pattern also occurs within the mixing zone: light rare earth elements (LREEs) become more depleted relative to heavy rare earths (HREEs); Y fractionates relative to holmium (Ho), and a positive lanthanum (La) anomaly develops relative to its pattern in shale (Lawrence and Kamber 2006; see Chapter 5 for further discussion).

Coastal waters influenced by river discharge have concentrations and patterns of REY that are transitional between fluvial and oceanic waters (Elderfield et al. 1990; see also Chapter 5). Because corals incorporate REY into their aragonite lattice in close proportions to seawater concentrations (Sholkovitz and Shen 1995; Fallon et al. 2002; Akagi et al. 2004; Wyndham et al. 2004), REY should be appropriate geochemical proxies for river discharge. Yet, the exact mechanism of REY incorporation has not yet been described, and Akagi et al. (2004) note that within species variation in REE distribution coefficients may be related to biological factors. Whatever the mechanisms, elevated levels of Y and several REEs (e.g. lanthanum (La), cerium (Ce), gadolinium (Gd), ytterbium (Yb)) measured in corals do correlate well with magnitudes and times of fluvial discharge (Sinclair 1999; Fallon et al. 2002; Alibert et al. 2003; Wyndham et al. 2004). In this chapter I present data from high-temporal resolution records of Y/Ca, Ba/Ca, B/Ca, and Sr/Ca from corals along a gradient of distance from the Pioneer River; data from bulk annual measures of the REY series from coral cores from two of the same sites are presented in Chapter 5.

Methods

Pioneer catchment geography

The Pioneer River catchment covers 1570 km^2, within the 9031 km^2 contained within the Mackay-Whitsunday regional management area[1] (Figure 4.2). Upper catchment soils are derived largely from highly erodible granites and granodiorites of the igneous Urannah complex which forms the Clarke and Connors ranges to the W and SW (Figures 2.1 and 2.2; Gourlay and Hacker 1986). Lower catchment soils are dominated by Quaternary alluvium on the flood plain of the Pioneer River, which stretches 75 km from the ranges to the sea (Gourlay and Hacker 1986). Rainfall is highly seasonal, occurring mainly during the summer cyclone season (December-April), with severe cyclonic flooding occurring every 14-16 years (Marion et al. 2006). Mean annual rainfall[2] and discharge[3] (1586 ± 543 mm SD and 0.808 ± 0.726 km^3 SD, respectively) vary considerably among years, influenced by the strong monsoon trough and regional ENSO fluctuations that affect eastern Australia (Hacker 1988; Verdon et al. 2004). Rainfall is higher in the Pioneer catchment than in adjacent drainage systems due to topography: both the funnel shape of the lower catchment and the abrupt rise in slope contribute to orographic uplift, causing high rainfall on the ranges that drain mainly into Cattle Creek and its tributaries (Figure 2.1; Gourlay and Hacker 1986). The southwestern part of the Pioneer catchment has a much drier climate: although the Upper Pioneer branch of

---

[1] Areas were calculated from digital polygons of catchment boundaries provided by the Queensland Department of Natural Resources Mines and Water.

[2] Digital data supplied by Australian Bureau of Meteorology, 1916-2003.

[3] Digital data supplied by the Queensland Department of Natural Resources Mines and Water, 1916-2003.

the river system drains over half of the total catchment area, it produces only ~20% of the discharge (Credlin 1973).

The Pioneer catchment has the second highest proportion of cropped land (19%) among all GBR catchments, and another 74% is grazed (Rayment and Neil 1997; Haynes et al. 2001). The high percentage of cropped lands, combined with the soil composition and steep topography of the drainage, all contribute to one of the highest rates (per unit area) of sediment export from any GBR catchment (Moss et al. 1992), that reflects an estimated two to fourfold increase from pre-clearing rates (Gourlay and Hacker 1986; Hacker 1988). Two dams and three major weirs across the Pioneer River and its tributaries retain a high percentage of coarse sediment from the upper catchment (QDNRM 2001), but most fine sediment flows downstream to be deposited in and around the Pioneer estuary (Gourlay and Hacker 1986).

Pioneer River discharge

I used records of Pioneer River flow (in megaliters) between 1916 and 2003 compiled from daily hydrographic measurements taken at the Pleystowe Mill gauge (QDNRMW station 125001A; October 1916-August 1978) and the Mirani Weir gauge (QDNRMW station 125007A; November 1977-November 2003). Because Mirani Weir is approximately 19 km upstream from Pleystowe Mill (see Figure 2.1), a regression equation obtained from the temporal overlap of sites between November 1977 and August 1978 ($y = 1.3275x – 106.37206$; $r^2 = 0.981$) was used to adjust the Mirani values to Pleystowe Mill equivalents. I used TIMER software for linear interpolation of the discharge data to 52 points per year (~weekly resolution), matching the output resolution of the smoothed coral trace element data from LA-ICP-MS.

Mackay wind data

Measurements of wind speed and direction were taken between 1959 and 2003 at the Australian Bureau of Meteorology (BOM) station number 33119 at Mount Bassett in Mackay (21.1706ºS, 149.1794ºE; 30 m elevation). From October 1959 to December 1995, data were collected every three hours; after that, they were collected hourly. No wind data were available from offshore locations, and daily differences between Mackay and Scawfell Island (the outermost site at 51 km offshore) are unknown. I used the BOM data to calculate wind stress (τ), measured in dynes/cm^2, with the following equation adapted from Large and Pond (1981):

$$\tau = \tfrac{1}{2} \rho C_d V^2 \qquad (4.1)$$

where ρ is mean air density, C_d is the drag coefficient, and V is wind velocity. Alongshore wind stress was also calculated, using the velocity vectors oriented along a NW-SE axis, approximately parallel to the Mackay coastline. I interpolated the data (with TIMER software) to 52 points per year to match discharge and coral data.

Coral collection and preparation

In March-April 2004 and December 2004, 15 coral cores (5 cm diameter; 0.4-2.0 m length) were collected from massive *Porites* colonies (depths 4-10 m), using a pneumatic drill and steel coring cylinder (Table 4.2). The cores were from inshore coral communities (Round Top Island) and midshelf fringing reefs (Keswick Island, Scawfell Island) surrounding continental islands along a cross-shelf gradient beginning at the mouth of the Pioneer River (Figures 4.2 and 4.3). Massive *Porites* colonies live mainly in leeward habitats sheltered from SE swells (Done and Potts 1992). Inshore colonies tended to have a bumpier (multilobate) external morphology and more convoluted growth bands compared to midshelf colonies.

Cores were slabbed (~8 mm thick), ultrasonically cleaned in 18 MΩ water and X-radiographed to visualize annual and seasonal density banding. Slabs were then photographed under UV light with a yellow/orange filter on black and white film (Sinclair 1999; Hendy et al. 2003) to display luminescence features correlated with flood events (Isdale 1984; Barnes and Taylor 2001; Lough et al. 2002; Hendy et al. 2003). Quantitative measures of luminescence were obtained (by G. Marion, University of Queensland) for three cores (RTC, KIC and SCC) using a luminometer which illuminates the coral at 390 nm and records emission intensities at 490 nm in 0.25 mm increments (Barnes et al. 2003). Prior to ICP-MS analysis, each slab was sectioned into 24 mm x 90 mm pieces, cut parallel to the major growth axis, cleaned with an ultrasonic probe in 18 MΩ water and dried overnight at 40°C.

LA-ICP-MS analyses

I analyzed the cores with a modified VG Elemental PQ2$^+$ ICP-MS attached to an ArF excimer laser (193 nm wavelength). Specifications for the systems are described by Eggins et al. (1998), Sinclair et al. (1998) and Sinclair (1999). Coral pieces were mounted on an X-Y sample stage and placed in a sealed perspex chamber (under helium atmosphere) for analysis of tracks selected along the major growth axis. The laser was operated with an energy density of 5 Jcm^{-2} and the beam (3 cm x 1 cm) was masked with a rectangular aperture (40 µm x 600 µm) for sample cleaning and instrument preconditioning during 2 pre-ablation runs prior to data collection (see Wyndham et al. 2004). During sample ablation, the laser spot size was decreased to 40 µm x 500 µm, yielding a sampling resolution of 20 nm at 5Hz. The ablated coral skeleton was entrained in helium and argon gas for ICP-MS counts of isotopes of: ^{11}B, ^{43}Ca, ^{84}Sr, ^{89}Y, and ^{138}Ba. I corrected for instrumental drift (assumed to be linear) by bracketing each coral scan with 2 analyses each of an in-house pressed coral powder standard (for ^{11}B, ^{84}Sr, ^{138}Ba; Fallon et al. 1999) and a NIST 614 silicate glass standard for Y (Fallon et al. 2002). I then normalized all isotopic concentrations to ^{43}Ca (0.13% Ca) to account for variations due to changes in coral surface architecture and density (Sinclair et al. 1998; Fallon et al. 1999).

Data were smoothed using a 10 point running median to remove outliers (Sinclair et al. 1998), followed by a 10 point mean to reduce data volume, a necessary step for long time series analysis (Figure 4.4). I calibrated a time series for each coral from Keswick and Scawfell Islands by matching Sr/Ca maximum and minimum values to 1° gridded weekly SST records (Nov 1981-Dec 2004) (Figure 4.5; Beck et al. 1992). SST data were composites of ship, buoy and bias-corrected satellite measurements (Reynolds and Smith 1994)[4]. The Round Top Island cores did not have smooth seasonal Sr/Ca signals, possibly due to high environmental variability (e.g. light intensity, nutrients) in the nearshore that may influence Sr^{2+} transport (Sinclair 1999; Marshall and McCulloch 2002) or because they were different species. Therefore, I used the smoother B/Ca profiles as a substitute temperature proxy (Sinclair et al. 1998; Fallon et al. 1999). For data before 1981 (earliest instrumental SST records), I calculated the average week of SST summer maxima and winter minima (between 1981 and 2004) for the gridded cells encompassing Round Top Island (centered at 21.5°S, 149.5°E) and the mid-shelf islands (centered at 20.5°S, 149.5°E) and applied those weeks to the Sr/Ca or B/Ca minima and maxima for the respective cores for years prior to 1981. I also used strong luminescent bands from known years of high magnitude floods as dating markers, and verified independently that the ages of cores assigned by the number of seasonal elemental cycles matched the counts of annual density bands. Because uneven annual and seasonal growth rates result in unequal numbers of sample points

---

[4] Data were downloaded from the IRI/LDEO Climate data library at: http://iridl.ldeo.columbia.edu/SOURCES/.IGOSS/.nmc/

between years, I used TIMER software to linearly interpolate the data to 52 points per year (~weekly resolution) for statistical analyses.

Statistical analyses

I used MATLAB to calculate correlations and time lags between weekly Pioneer River discharge measurements and the full records of Ba/Ca and Y/Ca from four cores: RTC (Feb 1962-May 2003); RTF (Aug 1959-May 2003); KIC (Jan 1991-May 2003); and SCC (Jan 1989-May 2003). Lags are reported as the number of weeks by which the core records trailed behind the discharge data to achieve maximum correlations. To assess the impacts of flood events and wind on correlation strength, I repeated separate sets of correlations with data restricted to: all flood weeks; flood weeks with northwesterly wind stress (where alongshore $\tau < 0$); and weeks with strong winds. I defined flood weeks as those that exceeded the weekly mean recorded between 1916 and 2003 (16,060 Ml), and weeks with strong winds as those with wind stress (τ) $\geq$ mean + 1 SD (≥ 21.73 dynes/cm^2). To compare inshore and midshelf patterns of Ba/Ca and Y/Ca, records from inshore cores (RTC and RTF) were averaged and compared with the average of midshelf cores (KIC and SCC) for the overlapping periods of analysis (January 1991—March 2004). Averaging proxy records is a common procedure to enhance shared features (Fallon et al. 2002).

Results

Inshore correlations with river discharge and wind

Replicate cores (RTC, RTF) from Round Top Island had very similar qualitative patterns of Ba and Y throughout the time series (1962-2003; Figure 4.6). Ba/Ca and Y/Ca were most different between 1975 and 1982, although the seasonal and longer-term fluctuations remained largely consistent between cores. Baseline winter values were elevated for both elemental ratios during wetter periods (1968-1980, 1988-1991 and, to a lesser extent, 1998-2002), but were most noticeable in the Ba/Ca records (Figure 4.6e). Inshore Ba/Ca ratios had strong annual peaks (Figure 4.6e), but had low correlations with Pioneer River discharge when all weeks were compared (RTC: $r = 0.271$, RTF: $r = 0.272$; Table 4.3a). Annual peaks of Y/Ca from Round Top Island were less obvious (Figure 4.6f), and both Round Top cores had low correlations of Y/Ca with discharge when all weeks were compared (RTC = 0.282, RTF = 0.244; Table 4.3b). Correlations of inshore Ba/Ca and Y/Ca with discharge were substantially higher when only flood weeks were included in the analyses; they rose further when the analyses were restricted to flood weeks that coincided with northwest wind stress (Table 4.4a,b). Both proxies also had higher correlations with discharge during periods of strong wind stress (τ) from any direction (Table 4.4c).

Because the Y/Ca records were considerably more variable than Ba/Ca, it is easier to see their trends when the data are displayed at higher resolution. During wet years in the 1970s, most Y/Ca peaks in the Round Top RTC core coincided with luminescence maxima and B/Ca summer minima, both of which are related to summer SST maxima (Figure 4.7). The highest correlations with Pioneer River discharge for Y/Ca occurred with little to no lag (0-3 weeks; Table 4.3b). The maximum correlations for inshore Ba/C occurred with 13-14 week lags (Figure 4.7; Table 4.3a) and Ba/Ca began to increase on average about 6-7 weeks after flood events.

Spatial patterns

Correlations of Y/Ca and Ba/Ca with discharge for all weeks were slightly lower at midshelf sites, with little or no time lags (0-4 weeks; Table 4.3). At Keswick Island, the relationship between Ba/Ca with discharge was not significant ($p < 0.10$; Table 4.3a), but was significant at Scawfell Island ($p < 0.05$; Table 4.3a). Correlations between Y/Ca with discharge were significant at both midshelf sites ($p < 0.05$; Table 4.3b). As with the Round Top cores, strength of relationships with discharge increased after correlations were restricted to flood weeks and weeks of strong wind stress (Table 4.4). Although correlations were high for flood weeks with northwest wind stress in both Keswick (KIC) and Scawfell (SCC) cores, they were not significant due to the small number of events during the short time spans analyzed (KIC: 12 yrs; SCC: 13 years).

Mean Y/Ca values from inshore cores (Jan 1991-Mar 2004) were 3.1 and 3.6 times higher than mean midshelf values from Keswick and Scawfell Island cores, respectively (Figure 4.8a). In contrast, mean inshore and midshelf Ba/Ca values were similar, but the inshore records had more distinct annual peaks than those from the midshelf locations (Figure 4.8b). Both the KIC and SCC cores were highly enriched in Ba/Ca in the surface tissue layer, with less enrichment ~2 cm below the top of each core, which coincided in both cores with a layer of endolithic algae (Figure 4.8b). Some, but not all, sharp midshelf Ba/Ca spikes are coincident with peaks in total wind stress (Figure 4.8c).

Anomalous bands

Cores from all three locations had unusually bright luminescence bands dating to December 1982-early January 1983 (summer) and late June-early July 1993 (winter) (Figure 4.9a). The timing of these bands coincided with anomalously high Sr/Ca and Ba/Ca values (Figure 4.9b,c). The peak Sr/Ca value through the 1983 band was the highest recorded in the RTC core, while the Ba/Ca value was second only to the peak following the 1979 flood (Figure 4.9b). Both Sr/Ca and Ba/Ca peaks coincided with minor Pioneer River discharge, low positive SST anomalies and low positive total wind stress (τ) anomalies. The same patterns were found in the RTF core. The Sr/Ca spike in the SCC core through the 1993 band was the highest in the record (dating from 1989; Figure 4.10c), while the value of the corresponding Ba/Ca spike (Figure 4.9c) is the highest after peaks within the tissue and endolithic algae layers (where Ba is known to be enriched; Figure 4.8b). Both peaks coincided with extremely low river discharge, strong positive and rapidly rising SST anomalies, and low positive total wind stress (τ) anomalies (Figure 4.9c). Another anomalous Ba/Ca spike in both RTC and RTF in midwinter 1994 (Figure 4.8b) was not associated with strong luminescence, high Sr/Ca or high discharge, but it did occur during the lowest weekly SST (19.5 ºC) on record between November 1981 and December 2004.

Discussion

Trace element variability

Long term records (> 50 years) from massive corals are necessary for distinguishing proxy signals related to environmental and anthropogenic factors from variation in these signals introduced by other factors (Lough and Barnes 1997, 2000). While the replicate cores from Round Top Island have mostly coherent patterns throughout the period of overlap, RTF had notably lower Ba/Ca and higher Y/Ca than RTC between 1975 and 1982. Factors that could cause within site variability in trace element ratios include: location of colonies; genetic differences; and skeletal architecture (Allison 1996a; Lough and Barnes 1997; Akagi et al. 2004). Even within a single core profile, some variation may be due to: placement of sampling tracks relative to calcification centers; altered concentrations within microborings; and uneven distribution of organic material, which may affect the metal binding capacity of the skeleton (Allison 1996a, 1996b; Sinclair et al. 1998; Sinclair 2005b). Since I selected tracks for LA-ICP-MS analysis that avoided borings and discolored areas that appeared to be enriched in organic material, these were probably minor sources of longer term (> 5 year) variability. The two cores were collected from different sides of Round Top Island, and probably experienced different current vectors (both magnitude and direction) even under medium Pioneer River discharge (QEPA 2004). Current and tidal differences may have modified concentrations of suspended sediment at the two sites. 1981 and 1982 had low rainfall and discharge, suggesting minimal sediment delivery from the land, so the elevated Y/Ca values during those years in RTF (but not RTC) may also reflect strong positive wind stress anomalies (Figure 4.9b) or some form of contamination.

The correlations between Ba/Ca and weekly discharge explained only 4-8% of the variance in all of the Mackay cores, but it is likely that Ba/Ca incorporation in corals also responds to other environmental or biological effects during non-flood periods. Lea et al. (1989) suggested that part of barium variation in *Pavona clavus* from Galapagos Island cores could be attributed to temperature effects on incorporation, and Ba/Ca was more significantly correlated with instrumental temperature records in the cold water coral *Plesiastria versipora* from South Australia than the typical temperature proxies Sr/Ca, B/Ca and U/Ca (Burgess et al. 2005). On the GBR, previous Ba/Ca measurements in *Porites* Ba/Ca have not correlated with SST (Sinclair et al. 1998; Sinclair 1999), and this is supported by the present records from the inshore and midshelf sites. The midshelf Keswick (KIC) and Scawfell (SCC) cores were less influenced by the summer monsoonal discharges that often coincide with peak SSTs, and therefore should have lower Ba/Ca midsummer values and higher midwinter values if they were temperature dependent. Yet, neither core had seasonal trends in Ba/Ca, despite high frequency variation (weekly-monthly) similar to that reported from *Porites* cores from Davies reef, another midshelf reef off Townsville (Sinclair et al. 1998; Alibert et al. 2003). Sinclair (2005b) suggested that differences in Ba/Ca records at scales < 1 month are more likely due to individual differences in biomineralization chemistry between corals and/or contaminants. This may be the same for Y/Ca, although the mechanisms generating its variations have not been studied thoroughly.

Correlations with river discharge and wind

Strong correlations of Ba/Ca and Y/Ca with river discharge have been reported for other inshore reefs of the GBR (Sinclair 1999; Alibert et al. 2003; McCulloch et al. 2003; Sinclair and McCulloch 2004), but no previous study from the region has addressed the effects of wind stress on these ratios. In *Porites* from Shirigai Bay, Japan, peak values of Ba/Ca coincided with wind-forced upwelling of cold, nutrient-rich water (Fallon et al. 1999). While large upwelling events occur during summer months along the GBR, these events typically occur on the seaward margin of the outermost reefs, and the subsequent diffusion and spread of this water across the continental shelf rarely reaches inshore islands, within the 40 m isobath (Andrews and Furnas 1986; Furnas and Mitchell 1986; Sinclair 2005a). Elevated Ba/Ca related to wind in Mackay corals probably reflect north-northwesterly winds coinciding with discharge events, which tend to blow plumes offshore (Furnas 2003; Devlin and Brodie 2005); and all strong winds, generating waves that resuspend previously deposited, shallow sediment that may be remobilized and carried offshore (Orpin et al. 1999; Neil et al. 2002).

Alongshore wind stress in March 1997 largely determined the spatial extent of the Burdekin River plume associated with Cyclone Justin: it moved southeast to merge with the plumes from the Mackay-Whitsunday rivers, including the Pioneer (Devlin and Brodie 2005). During that event, the edge of the plume was between Keswick and Scawfell Islands (Devlin and Brodie 2005). Even as early as 1918, wind direction was considered responsible for a low salinity incursion over the Whitsunday reefs after an extreme cyclone hit Mackay (Rainford 1925; Devlin et al. 2001). Correspondingly, the Ba/Ca and Y/Ca records from all cores in this study had higher correlations with Pioneer River discharge during flood weeks coinciding with northwest wind stress (which is often associated with cyclonic activity; Sinclair 1999). Because river discharge can merge into continuous plumes along the coast, elevated inshore Ba/Ca and Y/Ca values during flood weeks with northwest winds may also include dissolved material from the main Whitsunday rivers (Proserpine, O'Connell) and from the Burdekin River to the north, which has approximately 10x the annual flow volume as the Pioneer (Furnas 2003). The correlations from the midshelf sites, while high, were not significant, probably due to the lack of power from too few discharge events with northwest winds since 1990. This problem can be rectified by extending the records further back in time to increase the sample size.

Since floods are episodic and infrequent, corals and other reef organisms may be more likely to experience high levels of turbidity-induced stress from resuspension of previously deposited sediment, driven by strong winds (Larcombe et al. 1995; Orpin et al. 1999; Larcombe et al. 2001; Wolanski and Duke 2002; Furnas

2003). Strong onshore surface winds are capable of causing downwelling currents that may carry sediment offshore during periods of high inshore sediment resuspension caused by wind waves (Orpin et al. 1999). In the Mackay cores, Ba/Ca and Y/Ca were strongly correlated with discharge during strong wind weeks, particularly at the midshelf sites. While some of the inshore sediment may be mobilized offshore by downwelling currents, Keswick and Scawfell Islands probably have their own pools of sediment from weathering and land use activities on the islands, especially since Keswick and St. Bees have been grazed since ~1909 (Berck 1995).

As expected from studies showing enrichment of coastal REY relative to offshore waters (Elderfield et al. 1990; Wyndham et al. 2004; see also Chapter 5), there was a three to four-fold enrichment of Y/Ca at Round Top Island compared with the midshelf sites. These results are consistent with those of Alibert et al. (2003) who found approximately five-fold enrichment of Y/Ca from coastal *Porites* corals relative to those from the midshelf off of the Burdekin River. Y/Ca from the inshore Round Top corals did not have the strong annual peaks corresponding to discharge that Ba/Ca had; rather, winter baseline values were elevated during periods of high river discharge (Figure 4.8a). As Y, like Ba, is believed to be deposited in equilibrium with seawater, the different patterns in these two elemental ratios suggests that Y and Ba may have different pathways of incorporation into coral skeletons.

Ba/Ca patterns and lags

Corals collected from reefs near the Tully River and Burdekin River catchments to the north have Ba/Ca peaks that synchronized with river discharge events, and are in phase with peaks in luminescence, Y/Ca and La/Ca (Sinclair 1999; Alibert et al. 2003; McCulloch et al. 2003; Sinclair and McCulloch 2004; Sinclair 2005a). The Tully River drains a catchment of similar size (1683 km^2) to the Pioneer, but with approximately three times the annual runoff, due to much higher annual rainfall and multiple floods per year (Furnas 2003; Devlin and Brodie 2005). The upper part of the Tully catchment is predominantly wet tropical forest with only 10% cleared for agriculture and grazing (Haynes et al. 2001). The Burdekin River system is the largest catchment (130,126 km^2) draining into the GBR Lagoon, with a drier, more seasonal wet-dry climate, and episodic flooding at 4-10 year intervals (Furnas 2003; Devlin and Brodie 2005). Grazing now occupies 95% of catchment lands, and coral Ba/Ca increases coincided with increases in cattle stock (McCulloch et al. 2003). In the Pioneer catchment, sugarcane cropping is the dominant land use, and the Mackay region has one of the highest rates per unit area of total N and total P additions from fertilizer application (Pulsford 1996). These differences in land use patterns suggest reasons why inshore coral Ba/Ca patterns might differ between systems.

Unlike inshore cores from King Reef (within reach of the Tully plume) and Havannah and Pandora Reefs (within reach of the Burdekin plume) that have sharp Ba/Ca spikes timed precisely with flood events (Sinclair 1999; Alibert et al. 2003;

McCulloch et al. 2003; Sinclair and McCulloch 2004; Sinclair 2005a), the Round Top Ba/Ca values rise slowly to peak value, remain elevated for up to several months, and drop to baseline values by midwinter. The initial rise of Ba/Ca occurs, on average, ~6-7 weeks after floods, and the best correlation between maximum annual Ba/Ca values and Pioneer discharge occurs when Ba/Ca lags discharge by ~13-14 weeks. Similar Ba/Ca lags have been reported in *Montastrea annularis* from Barbados with respect to discharge from the Amazon River (Shen and Sandford 1990). Those authors sectioned the coral slabs with a saw, and they attributed at least part of their lags to sampling errors and also to the long distance (2000 km) from the plume source to Barbados (Shen and Sandford 1990). Because the inshore Mackay cores were sampled continuously with a laser, and because Round Top Island is only 5 km from the Pioneer River mouth, neither sampling technique nor distance from source can explain their lags.

Several other possible mechanisms could explain, at least partially, the long lags. The first possibility involves the timing of skeletal deposition. After depositing new aragonite skeleton on the outer surface layer over a period of days, *Porites* corals continue to thicken their skeletons through a more diffuse process by adding layers over the course of several months (Barnes and Lough 1993; Taylor et al. 1993). This thickening process produces a smoothing effect on trace material incorporation that tends to reduce the overall amplitude and broaden the shape of a sharp environmental signature (e.g. river flood) (Barnes et al. 1995; Taylor et al. 1995). However, under this scenario, the broad slope of the trace element should appear to *precede* its environmental forcing (Taylor et al. 1995; Sinclair 1999), which is the opposite of the case for the Round Top corals where the Ba/Ca lags behind discharge events. Therefore, this does not seem to be an adequate mechanism to explain the lags.

A second possibility is that large differences in growth rates between the summer and winter affected the chronologies for the Round Top corals. All of the chronologies for the Mackay cores assumed linear growth between the annual peaks and troughs of Sr/Ca (or B/Ca) selected to match with the timing of minimum and maximum local SSTs. Fallon et al. (1999) found maximum correlations between temperature proxies (U/Ca, Sr/Ca) and SSTs in corals from Shirigai Bay, Japan, when growth was modeled with an ~2 month hiatus during cold (<18 ºC) winter months. If summer growth was actually faster than assumed by linear interpolation, this could lead to a lag in the Ba/Ca signal behind the timing of river floods, however, this is unlikely to account for the full 13-14 weeks.

A third possibility is biological recycling of Ba, whereby Ba is removed from estuarine and coastal waters in association with phytoplankton blooms and released upon their senescence (see Sinclair 1999, 2005a). Stecher and Kogut (1999) documented >90% removal of dissolved barium from a Delaware estuary in mid-May, followed by 80% recovery by early June. They proposed, based on work by Dehairs et al. (1990) and Stroobants et al. (1991), that barite precipitates within sulfate-rich detrital assemblages of senescing blooms and becomes released as the particles disaggregate upon sinking. Nozaki et al. (2000, 2001) observed a similar phenomenon in the Chao Praya Estuary, Thailand, where significant removal of barium occurred in January during a red tide bloom that was absent in either July or November when barium followed typical conservative mixing curves for mid-salinities and higher. Some removed barium may be ingested by benthic organisms: sharp barium peaks observed in several bivalve genera have been attributed to uptake of barite from phytoplankton blooms (Stecher et al. 1996; Vander Putten et al. 2000; Gillikin et al. 2006).

Tudhope et al. (1996) suggested that biological recycling also explained anomalously high Ba/Ca peaks in a *Porites* core from Oman, due to incorporation of barium from organically-bound barite released following phytoplankton blooms. Sinclair (2005a) also suggested local enrichment of dissolved barium from senescent *Trichodesmium* blooms could explain the anomalous timing of spring Ba/Ca peaks observed in a *Porites* core from Cow and Calf Island, near the Proserpine and O'Connell River drainages. *Trichodesmium* spp. are nitrogen-fixing cyanobacteria that often bloom along the GBR coast, particularly near river outlets with elevated phosphate levels (Bell 1992; Fu et al. 2005). In January 2005, a plume covering the entire Mackay-Whitsunday region (Figure 4.11) contained large quantities of *Trichodesmium* (Rohde et al. 2006). The plume appears on a MODIS satellite image as a dark green slick, which is distinctly different from the light brown, sediment-laden plume emerging from the Burdekin River to the north (Figure 4.11). Depending on regional wind conditions, plume waters from single, large events may persist for several weeks (King et al. 2001), and these periods can be extended by successive flood flows, as in 1958 and 1991, when there were 5-6 week intervals between Pioneer River flood pulses.

Enrichment of dissolved barium from senescing blooms seems a reasonable hypothesis for the nutrient-enriched coastal region near Mackay, but direct links between decaying phytoplankton and elevated dissolved barium still need to be demonstrated in this region and the timing relative to discharge needs to be quantified. Some combination of barite release and chronology construction may account for some of the observed time lags, but they do not fully explain the extended periods of elevated Ba/Ca following the initial rise. Several ideas have been proposed to explain persistence of high values. Carroll et al. (1993) suggested that barium continues to desorb from terrestrial sediments buried in the nearshore following floods, and this process increases with strong wind stress that generates sediment resuspension. Similarly, sediments deposited within the mangroves may be slowly flushed from the estuary (Alibert et al. 2003; McCulloch et al. 2003), especially in places like Mackay that have large (up to 6.5 m) tidal ranges. Groundwater additions may also be a source of elevated barium in nearshore waters (Moore 1997; Shaw et al. 1998; Swarzenski et al. 2001), but because groundwater aquifers in the Pioneer catchment are heavily used for sugarcane irrigation and town drinking water, and because coastal aquifers are being monitored for saltwater intrusion rather than freshwater export (Baskaran et al. 2001), coastal groundwater flux seems unlikely to be a major source of barium in this region.

Stress bands

The dates of the 1983 and 1993 anomalies (bright luminescence, elevated Sr/Ca and Ba/Ca) in the Mackay corals coincide with a severe El Niño (1982-83) and the longest lasting El Niño (1991-93) on record (Brassington 1997). During El Niño years, the GBR typically has reduced summer rainfall, warmer late summer SSTs and higher solar radiation (Lough 1994; Lough 2001). Anomalously high Sr/Ca values have been observed in other GBR corals during El Niño periods (McCulloch et al. 1994; Marshall and McCulloch 2002), during both extremely warm or extremely cool SSTs. Temperature stress probably results in reduced [Ca^{2+}], but not [Sr^{2+}], in the calcifying fluid, both of which would lead to higher Sr/Ca values (Sinclair 1999; Marshall and McCulloch 2002). Elevated Sr/Ca values measured during intrusion of unusually cool waters in winter 1982 (McCulloch et al. 1994) led to overestimating the negative temperature anomaly by 1ºC, compared with ship records of SST (Holbrook et al. 1993). High temperature stress may also cause Sr/Ca anomalies: e.g. a sharp elevation in Sr/Ca from a Pandora Island core followed unusually high SSTs that resulted in coral bleaching and cessation of growth in 1998 (Marshall and McCulloch 2002). The trace element anomalies in the Mackay corals took place during a summer (December 1982-January 1983) with only moderate positive temperature anomalies and a winter (late June-early July 1993) with higher than average temperatures. It is also possible that the persistence of stressful conditions through the severe 1982-83 El Niño and the long 1991-93 El Niño may have reduced the corals' resistance, so that they responded more strongly to minor disturbance, but the presence of both anomalies in all four cores suggests that some type of regional environmental signal still remains to be detected. Similar anomalous trace element enrichment, apparently not associated with SST, was also observed by Wyndham et al. (2004) in mid-1983, and they suggested that it reflected either severe stress or atypical environmental conditions.

A separate anomalous Ba/Ca peak occurred only in the Round Top Island cores in July 1994 (Figure 4.9): this peak is not associated with discharge, intense luminescence, or elevated Sr/Ca values, even though it occurred at <20 ºC winter temperatures. A strong wind stress anomaly (> 1 SD above mean) was present that week, with wind direction from the northwest, which suggests that the strong Ba/Ca peak could be the result of wind-blown dust. Continental dust is a rich source of both barium, which could get incorporated directly into corals after desorbing from the dust particles (Sinclair 1999), and iron, which is an important limiting nutrient for phytoplankton. The pool of dust within the Pioneer catchment and dry regions to the southwest of Mackay may have been elevated from several previous dry years, and augmented by burning before harvesting cane fields. Dust from a 1997 Indonesian wildfire has been invoked as a trigger for extensive red tides that led to coral reef death through anoxia (Abram et al. 2003). Trace element records from a surviving *Porites* had elevated Sr/Ca, Mn/Ca, Y/Ca and La/Ca during the event, with the high Mn and REY attributed to low oxygen levels in the water column (Abram et al. 2003). Aeolian dust from the Australian continent has been cited as a potential factor causing tight coupling of dense aerosol layers and high chlorophyll content in

Southern Ocean blooms, as measured from SeaWiFs satellite data (Gabric et al. 2002), but there has been little work thus far directly linking dust storms with blooms on the GBR.

Conclusions

Ba/Ca and Y/Ca ratios in *Porites* coral skeletons are proxies for river discharge from inshore corals in the Mackay region. Because their correlations with discharge are influenced by wind direction and magnitude, the behavior of these trace element proxies may also be used to characterize the spatial extent of past flood plumes. Results from trace metal data are consistent with coral $\delta^{15}N$ and luminescence data that suggest that Keswick and Scawfell Island reefs are less frequently affected by discharge from the Pioneer River (Marion et al. 2006), though longer records from these sites are needed to understand temporal variations on the midshelf. The observed time lags in Ba/Ca following discharge events indicates that regional differences in land use dynamics may affect trace elements records. In Chapter 6, I will synthesize the records of catchment land clearing and riparian change (from Chapter 2), mangrove change (from Chapter 3), and coral proxy records of suspended sediment delivery (this chapter and Chapter 5) to discuss temporal trends that may be influenced by land management practices.

References

Abram, N.J., Gagan, M.K., McCulloch, M.T., Chappell, J. and Hantoro, W.S. 2003. Coral reef death during the 1997 ocean dipole linked to Indonesian wildfires. Science 301.

Akagi, T., Hashimoto, Y., Fu, F.-F., Tsuno, H., Tao, H. and Nakano, Y. 2004. Variation of the distribution coefficients of rare earth elements in modern coral-lattices: Species and site dependencies. Geochimica et Cosmochimica Acta 68: 2265-2273.

Alibert, C., Kinsey, L., Fallon, S.J., McCulloch, M.T., Berkelmans, R. and McAllister, F. 2003. Source of trace element variability in Great Barrier Reef corals affected by the Burdekin flood plumes. Geochimica et Cosmochimica Acta 67: 231-246.

Allison, N. 1996a. Comparative determination of trace and minor elements in coral aragonite by ion microprobe analysis, with preliminary results from Phuket, southern Thailand. Geochimica et Cosmochimica Acta 60: 3457-3470.

Allison, N. 1996b. Geochemical anomalies in coral skeletons and their possible implications for palaeoenvironmental analyses. Marine Chemistry 55: 367-379.

Andrews, J.C. and Furnas, M.J. 1986. Subsurface intrusions of Coral Sea water into the central Great Barrier Reef--I. Structures and shelf-scale dynamics. Continental Shelf Research 6: 491-514.

Barnard, L.A., Macintyre, I.G. and Pierce, J.W. 1974. Possible environmental index in tropical reef corals. Nature 252: 219-220.

Barnes, D.J. 1970. Coral skeletons: an explanation of their growth and structure. Science 170: 1305-1308.

Barnes, D.J. and Lough, J.M. 1993. On the nature and causes of density banding in massive coral skeletons. Journal of Experimental Marine Biology and Ecology 167: 91-108.

Barnes, D.J. and Taylor, R.B. 2001. On the nature and causes of luminescent lines and bands in coral skeletons. Coral Reefs 19: 221-230.

Barnes, D.J., Taylor, R.B. and Lough, J.M. 1995. On the inclusion of trace materials into massive coral skeletons. Part II. distortions in skeletal records of annual climate cycles due to growth processes. Journal of Experimental Marine Biology and Ecology 194: 251-275.

Barnes, D.J., Taylor, R.B. and Lough, J.M. 2003. Measurement of luminescence in coral skeletons. Journal of Experimental Marine Biology and Ecology 295: 91-106.

Baskaran, S., Budd, K.L., Larsen, R.M. and Bauld, J. 2001. A Groundwater Quality Assessment of the Lower Pioneer Catchment, Qld. Bureau of Rural Sciences, Canberra, Australia.

Beck, J.W., Edwards, R.L., Ito, E., Taylor, F.W., Recy, J., Rougerie, F., Joannot, P. and Henin, C. 1992. Sea-surface temperature from coral skeletal strontium/calcium ratios. Science 257: 644-647.

Bell, P.R.F. 1992. Eutrophication and coral reefs--some examples in the Great Barrier Reef Lagoon. Water Research 26: 553-568.

Belperio, A.P. 1983. Terrigenous sedimentation in the central Great Barrier Reef Lagoon; a model from the Burdekin region. Bureau of Mineral Resources Journal of Australian Geology and Geophysics 8: 179-190.

Berck, L. 1995. St. Bees Island: It's History, Lifestyles and Tales. Boolarong Press, Mackay, Australia. 142 pp.

Boiko, T.F., Sotskov, Y.P. and Maeva, M.M. 1986. Behavior of lanthanides and yttrium during rock weathering. Litologiya i Poleznye Iskopaemye 3: 12-26.

Brassington, G.B. 1997. The modal evolution of the Southern Oscillation. Journal of Climate 10: 1021-1034.

Brinkman, R., Wolanski, E., Deleersnijder, E., McAllister, F. and Skirving, W. 2002. Oceanic inflow from the Coral Sea into the Great Barrier Reef. Estuarine, Coastal and Shelf Science 54: 655-668.

Brown, B.E., Tudhope, A.W., Le Tissier, M.D.A. and Scoffin, T.P. 1991. A novel mechanism for iron incorporation into coral skeletons. Coral Reefs 10: 211-215.

Bruland, K.W. 1983. Trace elements in sea-water. *In*: Riley, J.P. and Chester, R. (eds.), Chemical Oceanography. pp. 157-220. Academic Press, London, UK.

Buddemeier, R.W., Schneider, R.C. and Smith, S.V. 1981. The alkaline earth chemistry of corals. *In*: Proceedings of the Fourth International Coral Reef Symposium, Manila, pp. 81-85.

Burgess, S.N., McCulloch, M.T., Gagan, M.K. and Ward, T. 2005. Geochemical ecology of a high latitude coral: *Plesiastria versipora* a new paleo-environmental archive. *In*: Proceedings of the Third International Symposium on Deep-Sea Corals Science and Management, Miami, FL, USA, pp. 185. Rosenstiel School of Marine and Atmospheric Science, University of Miami.

Byrne, R.H. and Sholkovitz, E.R. 1996. Marine chemistry and geochemistry of the lanthanides. *In*: Gschneider, K.A., Jr and Eyring, L. (eds.), Handbook on the Physics and Chemistry of the Rare Earths. pp. 497-593. Elsevier, Amsterdam, The Netherlands.

Carroll, J., Falkner, K.K., Brown, E.T. and Moore, W.S. 1993. The role of the Ganges-Brahmaputra mixing zone in supplying barium and ^{226}Ra to the Bay of Bengal. Geochimica et Cosmochimica Acta 57: 2981-2990.

Chao, S.-Y. 1988. Wind-driven motion of estuarine plumes. Journal of Physical Oceanography 18: 1144-1166.

Church, J.A., Andrews, J.C. and Boland, F.M. 1985. Tidal currents in the central Great Barrier Reef. Continental Shelf Research 4: 515-531.

Coffey, M., Dehairs, F., Collette, O., Luther, G., Church, T. and Jickells, T. 1997. The behaviour of dissolved barium in estuaries. Estuarine, Coastal and Shelf Science 45: 113-121.

Cohen, A., Owens, K.E., Layne, G.D. and Shimizu, N. 2002. The effect of algal symbionts on the accuracy of Sr/Ca paleotemperatures from coral. Science 296: 331-333.

Cohen, A.L., Layne, G.D., Hart, S.R. and Lobel, P.S. 2001. Kinetic control of skeletal Sr/Ca in a symbiotic coral: implications for the paleotemperature proxy. Paleoceanography 16: 20-26.

Credlin, B.L. 1973. Water resources of Mackay district. Producers Review 63: 9-15.

de Villiers, S., Nelson, B.K. and Chivas, A.R. 1995. Biological controls on coral Sr/Ca and δ^{18}O reconstructions of sea surface temperatures. Science 269: 1247-1249.

Dehairs, F., Stroobants, N. and Goeyens, L. 1991. Suspended barite as a tracer of biological activity in the Southern Ocean. Marine Chemistry 35: 399-410.

Devlin, M. and Brodie, J. 2005. Terrestrial discharge into the Great Barrier Reef Lagoon: nutrient behavior in coastal waters. Marine Pollution Bulletin 51: 9-22.

Devlin, M., Waterhouse, J., Taylor, J. and Brodie, J. 2001. Flood plumes in the Great Barrier Reef: spatial and temporal patterns in composition and distribution. GBRMPA Research Publication No. 68 Great Barrier Reef Marine Park Authority, Townsville.

Done, T.J. and Potts, D.C. 1992. Influences of habitat and natural disturbance on contributions of massive *Porites* corals to reef communities. Marine Biology 114: 479-493.

Douglas, I. 1967. Man, vegetation and the sediment yields of rivers. Nature 215: 925-928.

Edmond, J.M., Boyle, E.A., Drummond, D., Grant, B. and Mislick, T. 1978. Desorption of barium in the plume of the Zaire (Congo) River. Netherlands Journal of Sea Research 12: 324-328.

Eggins, S.M., Kinsey, L.P.J. and Shelley, J.M.G. 1998. Deposition and element fractionation processes during atmospheric pressure laser sampling for analysis by ICP-MS. Applied Surface Science 127-129: 278-286.

Elderfield, H. and Greaves, M.J. 1982. The rare earth elements in seawater. Nature 296: 214-219.

Elderfield, H., Upstill-Goddard, R. and Sholkovitz, E.R. 1990. The rare earth elements in rivers, estuaries, and coastal seas and their significance to the composition of ocean waters. Geochimica et Cosmochimica Acta 54.

Elderfield, H., Whitfield, M., Burton, J.D., Bacon, M.P. and Liss, P.S. 1988. The oceanic chemistry of the rare-earth elements [and discussion]. Philosophical Transactions of the Royal Society of London A 325: 105-126.

Fallon, S.J., McCulloch, M.T., van Woesik, R. and Sinclair, D.J. 1999. Corals at their latitudinal limits: laser ablation trace element systematics in *Porites* from Shirigai Bay, Japan. Earth and Planetary Science Letters 172: 221-238.

Fallon, S.J., White, J.C. and McCulloch, M.T. 2002. *Porites* corals as recorders of mining and environmental impacts: Misima Island, Papua New Guinea. Geochimica et Cosmochimica Acta 66: 45-62.

Flor, T.H. and Moore, W.S. 1977. Radium/calcium and uranium/calcium determinations for western Atlantic reef corals. *In*: Proceedings of the Third International Coral Reef Symposium, Miami, FL, USA, pp. 555-561. Rosensteil School of Marine and Atmospheric Sciences, University of Miami.

Froelich, P.N., Kaul, L.W., Byrd, J.T., Andreae, M.O. and Roe, K.K. 1985. Arsenic, barium, germanium, tin, dimethylsulfide and nutrient biogeochemistry in Charlotte Harbor, Florida, a phosphorus-enriched estuary. Estuarine, Coastal and Shelf Science 20: 239-264.

Fu, F.-X., Zhang, Y., Bell, P.R.F. and Hutchins, D. 2005. Phosphate uptake and growth kinetics of *Trichodesmium* (cyanobacteria) isolates from the North Atlantic Ocean and the Great Barrier Reef, Australia. Journal of Phycology 41: 62-73.

Furnas, M. 2003. Catchments and Corals. Australian Institute of Marine Science, Townsville, Australia. 334 pp.

Furnas, M.J. and Mitchell, A.W. 1986. Phytoplankton dynamics in the central Great Barrier Reef--I. Seasonal change in biomass and community structure and their relation to intrusive activity. Continental Shelf Research 6: 363-384.

Gabric, A.J., Cropp, R., Ayers, G.P., McTanish, G. and Braddock, R. 2002. Coupling between cycles of phytoplankton biomass and aerosol optical depth as derived from SeaWiFs time series in the Subantarctic Southern Ocean. Geophysical Research Letters 29: 1112-1115.

Gammons, C.H., Wood, S.A. and Nimick, D.A. 2005. Diel behavior of rare earth elements in a mountain stream with acidic to neutral pH. Geochimica et Cosmochimica Acta 69: 3747-3758.

Gillikin, D.P., Dehairs, F., Lorrain, A., Steenmans, D., Baeyens, W. and Andre, L. 2006. Barium uptake into the shells of the common mussel (*Mytilus edulis*) and the potential for estuarine palaeo-chemistry reconstruction. Geochimica et Cosmochimica Acta 70: 395-407.

Gourlay, M.R. and Hacker, J.L.F. 1986. Pioneer River Estuary Sedimentation Studies. University of Queensland, Department of Civil Engineering, St. Lucia, Australia. 207 pp.

Greaves, M.J., Elderfield, H. and Sholkovitz, E.R. 1999. Aeolian sources of rare earth elements to the Western Pacific Ocean. Marine Chemistry 68: 31-38.

Guay, C.K. and Falkner, K.K. 1998. A survey of dissolved barium in the estuaries of major Arctic rivers and adjacent seas. Continental Shelf Research 18: 859-882.

Hacker, J.L.F. 1988. Rapid accumulation of fluvially derived sands and gravels in a tropical macrotidal estuary: the Pioneer River at Mackay, North Queensland, Australia. Sedimentary Geology 57: 299-315.

Hanor, J.S. and Chan, L.-H. 1977. Non-conservative behavior of barium during mixing of Mississippi River and Gulf of Mexico waters. Earth and Planetary Science Letters 37: 242-250.

Haynes, D., Bass, D., Brodie, J., Christie, C., Devlin, M., Michalek-Wagner, K., Morris, S., Ramsay, M., Storrie, J., Waterhouse, J. and Yorkston, H. 2001. Great Barrier Reef water quality: current issues. Great Barrier Reef Marine Park Authority, Townsville, Australia.

Hendy, E.J., Gagan, M.K. and Lough, J.M. 2003. Chronological controls of coral records using luminescent lines and evidence for non-stationary ENSO teleconnections in northeast Australia. The Holocene 13: 187-199.

Holbrook, N.J., Bindoff, N.I. and Coleman, R. 1993. Recent temperature changes in the Tasman and Coral seas. *In*: Proceedings of the Fourth International Conference on Southern Hemisphere Meteorology and Oceanography, pp. 227-228. American Meteorological Society.

Howard, L.S. and Brown, B.E. 1984. Heavy metals and reef corals. Oceanography and Marine Biology Annual Review 22: 195-210.

Hoyle, J., Elderfield, H., Gledhill, A. and Greaves, M. 1984. The behaviour of the rare earth elements during mixing of river and sea waters. Geochimica et Cosmochimica Acta 48: 143-149.

Hutchings, P. and Haynes, D. 2000. Sources, fates and consequences of pollutants in the Great Barrier Reef. Marine Pollution Bulletin 41: 265-266.

Isdale, P. 1984. Fluorescent bands in massive corals record centuries of coastal rainfall. Nature 310: 578-579.

Kawabe, I., Toriumi, T., Ohta, A. and Miura, N. 1998. Monoisotopic REE abundances in seawater and the origin of seawater tetrad effect. Geochemical Journal 32: 213-229.

King, B., McAllister, F., Wolanski, E., Done, T. and Spagnol, S. 2001. River plume dynamics in the central Great Barrier Reef. *In*: Wolanksi, E. (ed.), Oceanographic Processes of Coral Reefs: Physical and Biological Links in the Great Barrier Reef. pp. 145-160. CRC Press, Boca Raton, FL, USA.

Larcombe, P. and Woolfe, K.J. 1999. Increased sediment supply to the Great Barrier Reef will not increase sediment accumulation at most coral reefs. Coral Reefs 18: 163-169.

Larcombe, P., Costen, A. and Woolfe, K.J. 2001. Hydrodynamic and sedimentary processes associated with nearshore coral reefs, central Great Barrier Reef shelf, Australia: Paluma Shoals, a case study. Sedimentology 48: 811-835.

Larcombe, P., Ridd, P.V., Prytz, A. and Wilson, B. 1995. Factors controlling suspended sediment on inner-shelf coral reefs, Townsville, Australia. Coral Reefs 14: 163-171.

Large, W.G. and Pond, S. 1981. Open ocean momentum flux measurements in moderate to strong winds. Journal of Physical Oceanography 11: 324-336.

Lawrence, M.G. and Kamber, B.S. 2006. The behaviour of the rare earth elements during estuarine mixing--revisted. Marine Chemistry 100: 147-161.

Lawrence, M.G., Jupiter, S.D. and Kamber, B.S. 2006a. Aquatic geochemistry of the rare earth elements and yttrium in the Pioneer River Catchment, Mackay, Queensland, Australia. Marine and Freshwater Research *in review*.

Lawrence, M.G., Grieg, A., Collerson, K.D. and Kamber, B.S. 2006b. Rare earth element and yttrium variability in South East Queensland waterways. Aquatic Geochemistry 12: 39-72.

Lea, D.W., Shen, G.T. and Boyle, E.A. 1989. Coralline barium records temporal variability in equatorial Pacific upwelling. Nature 340: 373-376.

Li, Y.-H. and Chan, L.-H. 1979. Desorption of Ba and ^{226}Ra from river-borne sediments in the Hudson Estuary. Earth and Planetary Science Letters 43: 343-350.

Livingston, H.D. and Thompson, G. 1971. Trace element concentrations in some modern corals. Limnology and Oceanography 16: 786-796.

Lough, J. 2001. Climate variability and change on the Great Barrier Reef. *In*: Wolanski, E. (ed.), Oceanographic Processes of Coral Reef: Physical and Biological Links in the Great Barrier Reef. pp. 269-300. CRC Press, Boca Raton.

Lough, J.M. 1994. Climate variation and El Nino-Southern Oscillation events on the Great Barrier Reef: 1958 to 1987. Coral Reefs 13: 181-195.

Lough, J.M. and Barnes, D.J. 1997. Several centuries of variation in skeletal extension, density and calcification in massive *Porites* colonies from the Great Barrier Reef: a proxy for seawater temperature and a background of variability against which to identify unnatural change. Journal of Experimental Marine Biology and Ecology 211: 29-67.

Lough, J.M. and Barnes, D.J. 2000. Environmental controls on growth of the massive coral *Porites*. Journal of Experimental Marine Biology and Ecology 245: 225-243.

Lough, J.M., Barnes, D.J. and McAllister, F.A. 2002. Luminescent lines in corals from the Great Barrier Reef provide spatial and temporal records of reefs affected by land runoff. Coral Reefs 21: 333-343.

Marion, G.S., Hoegh-Guldberg, O., McCulloch, M.T. and Jupiter, S.D. 2006. Coral isotopic records ($\delta^{15}N$) of unprecedented land-use stress in Great Barrier Reef coastal communites. Eos Transactions of AGU, 87(36), Ocean Science Meeting Suppl., Abstract OS520-04.

Marshall, J.F. and McCulloch, M.T. 2002. An assessment of the Sr/Ca ratio in shallow water hermatypic corals as a proxy for sea surface temperature. Geochimica et Cosmochimica Acta 66: 3263-3280.

McCulloch, M., Fallon, S., Wyndham, T., Hendy, E., Lough, J. and Barnes, D. 2003. Coral record of increased sediment flux to the inner Great Barrier Reef since European settlement. Nature 421: 727-730.

McCulloch, M.T., Gagan, M.K., Mortimer, G.E., Chivas, A.R. and Isdale, P.J. 1994. A high-resolution Sr/Ca and $\delta^{18}O$ coral record from the Great Barrier Reef, Australia, and the 1982-1983 El Nino. Geochimica et Cosmochimica Acta 58: 2747-2754.

McKergow, L.A., Prosser, I.P., Hughes, A.O. and Brodie, J. 2005a. Regional scale nutrient modelling: exports to the Great Barrier Reef World Heritage Area. Marine Pollution Bulletin 51: 186-199.

McKergow, L.A., Prosser, I.P., Hughes, A.O. and Brodie, J. 2005b. Sources of sediment to the Great Barrier Reef World Heritage Area. Marine Pollution Bulletin 51: 200-211.

Mitsuguchi, T., Matsumoto, E. and Uchida, T. 2003. Mg/Ca and Sr/Ca ratios of *Porites* coral skeleton: Evaluation of the effect of skeletal growth rate. Coral Reefs 22: 381-388.

Moore, W.S. 1997. High fluxes of radium and barium from the mouth of the Ganges-Brahmaputra River during low river discharge suggest a large groundwater source. Earth and Planetary Science Letters 150: 141-150.

Moss, A.J., Rayment, G.E., Reilly, N. and Best, E.K. 1992. A preliminary assessment of sediment and nutrient exports from Queensland coastal catchments. Queensland Department of Primary Industries, Brisbane, Australia.

Neil, D.T. and Yu, B. 1996. Fluvial sediment yield to the Great Barrier Reef Lagoon: spatial patterns and the effect of land use. *In*: Hunter, H.M., Eyles, A.G. and Rayment, G.E. (eds.), Downstream Effects of Land Use. pp. 281-286. Queensland Department of Natural Resources, Brisbane, Australia.

Neil, D.T., Orpin, A.R., Ridd, P.V. and Yu, B. 2002. Sediment yield and impacts from river catchments to the Great Barrier Reef lagoon. Marine & Freshwater Research 53: 733-752.

Nozaki, Y., Zhang, J. and Amakawa, H. 1997. The fractionation between Y and Ho in the marine environment. Earth and Planetary Science Letters 148: 329-340.

Nozaki, Y., Lerche, D., Alibo, D.S. and Snidvongs, A. 2000. The estuarine geochemistry of rare earth elements and indium in the Chao Phraya River, Thailand. Geochimica et Cosmochimica Acta 64: 3983-3994.

Nozaki, Y., Yamamoto, Y., Manaka, T., Amakawa, H. and Snidvongs, A. 2001. Dissolved barium and radium isotopes in the Chao Phraya River estuarine mixing zone in Thailand. Continental Shelf Research 21: 1435-1448.

Orpin, A.R., Ridd, P.V. and Stewart, L.K. 1999. Assessment of the relative importance of major sediment-transport mechanisms in the central Great Barrier Reef lagoon. Australian Journal of Earth Sciences 46: 883-896.

Pignitore, N.E., Jr., Rangel, Y. and Kwarteng, A. 1989. Barium variation in *Acropora palmata* and *Montastrea annularis*. Coral Reefs 8: 31-36.

Pimentel, D.P., Harvey, C., Resosudarmo, K., Sinclair, K., Kurz, D., McNair, M., Crist, S., Shpritz, L., Fitton, L., Saffouri, R. and Blair, R. 1995. Environmental and economic costs of soil erosion and conservation benefits. Science 267: 1117-1123.

Prosser, I.P., Rutherfurd, I.D., Olley, J.M., Young, W.J., Walbrink, P.J. and Moran, C.J. 2001. Large scale patterns of erosion and sediment transport in river networks, with examples from Australia. Marine and Freshwater Research 52: 81-99.

Prosser, I.P., Moran, C.J., Lu, H., Scott, A., Rustomji, P., Stevenson, J., Priestly, G., Roth, C.H. and Post, D. 2002. Regional Patterns of Erosion and Sediment Transport in the Burdekin River Catchment. Technical Report 5/02 CSIRO Land and Water, Canberra, Australia.

Pulsford, J.S. 1996. Historical nutrient usage in coastal Queensland river catchments adjacent to the Great Barrier Reef Marine Park. Research Publication No. 40 Great Barrier Reef Marine Park Authority, Townsville, Australia.

QDNRM 2001. Pioneer Valley Water Resource Plan -- Current environmental conditions and impacts of existing water resource development. Queensland Department of Natural Resources and Mines, Brisbane, Australia.

QEPA 2004. Mackay Coast Study. The State of Queensland, Environmental Protection Agency, Brisbane, Australia.

Rainford, E.H. 1925. Destruction of the Whitsunday Group fringing reefs. The Australian Museum Magazine 2: 175-177.

Rayment, G.E. and Neil, D.T. 1997. Sources of material in river discharge. *In*: Proceedings of the Great Barrier Reef: Science, Use and Management, Townsville, Australia, pp. 42-58. Great Barrier Reef Marine Park Authority.

Reynolds, R.W. and Smith, T.M. 1994. Improved global sea surface temperature analyses. Journal of Climate 7: 929-948.

Rohde, K., Masters, B., Brodie, J., Faithful, J., Noble, R. and Carroll, C. 2006. Fresh and marine water quality in the Mackay Whitsunday region 2004/2005. Mackay Whitsunday Natural Resource Management Group, Mackay, QLD, Australia.

Shaw, T.J., Moore, W.S., Kloepfer, J. and Sochaski, M.A. 1998. The flux of barium to the coastal waters of the southern USA: the importance of submarine groundwater discharge. Geochimica et Cosmochimica Acta 62: 3047-3054.

Shen, G.T. and Boyle, E.A. 1988. Determination of lead, cadmium and other trace metals in annually-banded corals. Chemical Geology 67: 47-62.

Shen, G.T. and Sandford, C.L. 1990. Trace-element indicators of climate variability in reef-building corals. *In*: Glynn, P.W. (ed.), Global Consequences of the 1982-83 El Nino-Southern Oscillation. pp. 255-283. Elsevier, Amsterdam, The Netherlands.

Shen, G.T., Cole, J.E., Lea, D.W., Linn, L.J., McConnaughey, T.A. and Fairbanks, R.G. 1992a. Surface ocean variability at Galapagos from 1936-1982. Paleoceanography 7: 563-588.

Sholkovitz, E. 1993. The geochemistry of rare earth elements in the Amazon River estuary. Geochimica et Cosmochimica Acta 57: 2181-2190.

Sholkovitz, E. and Shen, G.T. 1995. The incorporation of rare earth elements in modern coral. Geochimica et Cosmochimica Acta 59: 2749-2756.

Sholkovitz, E.R. 1992. Chemical evolution of rare earth elements: fractionation between colloidal and solution phases of filtered river water. Earth and Planetary Science Letters 114: 77-84.

Sholkovitz, E.R. 1995. The aquatic chemistry of rare earth elements in rivers and estuaries. Aquatic Geochemistry 1: 1-34.

Sholkovitz, E.R. and Elderfield, H. 1988. Cycling of dissolved rare earth elements in Chesapeake Bay. Global Biogeochemical Cycles 2: 157-176.

Sholkovitz, E.R., Elderfield, H., Szymczak, R. and Casey, K. 1999. Island weathering: river sources of rare earth elements to the Western Pacific Ocean. Marine Chemistry 68: 39-57.

Sinclair, D.J. 1999. High spatial-resolution analysis of trace elements in corals using laser ablation ICP-MS. Ph.D. Thesis. The Australian National University, Canberra, Australia.

Sinclair, D.J. 2005a. Non-river flood barium signals in the skeletons of corals from coastal Queensland, Australia. Earth and Planetary Science Letters 237: 354-369.

Sinclair, D.J. 2005b. Correlated trace element "vital effects" in tropical corals: a new geochemical tool for probing biomineralization. Geochimica et Cosmochimica Acta 69: 3265-3284.

Sinclair, D.J. and McCulloch, M.T. 2004. Corals record low mobile barium concentrations in the Burdekin River during the 1974 flood: evidence for limited Ba supply to rivers? Palaeogeography, Palaeoclimatology, Palaeoecology 214: 155-174.

Sinclair, D.J., Kinsey, L.P.J. and McCulloch, M.T. 1998. High resolution analysis of trace elements in corals by laser ablation ICP-MS. Geochimica et Cosmochimica Acta 62: 1889-1901.

Speer, A.J. 1983. The kinetics of calcium carbonate dissolution and precipitation. *In*: Reeder, R.J. (ed.), Carbonates: Mineralogy and Chemistry, Reviews in Mineralogy, Volume 11. pp. 145-190. Mineralogical Society of America, Chelsea, MI, USA.

St. John, B.E. 1974. Heavy metals in the skeletal carbonate of scleractinian corals. *In*: Proceedings of the Second International Coral Reef Symposium, Brisbane, Australia, pp. 461-469.

Stecher, H.A., III and Kogut, M.B. 1999. Rapid barium removal in the Delaware estuary. Geochimica et Cosmochimica Acta 63: 1003-1012.

Stecher, H.A., III, Krantz, D.E., Lord, C.J., III, Luther, G.W., III and Bock, K.W. 1996. Profiles of strontium and barium in *Mercenaria mercenaria* and *Spisula solidissima* shells. Geochimica et Cosmochimica Acta 60: 3445-3456.

Stroobants, N., Dehairs, F., Goeyens, L., Vanderheijden, N. and Van Grieken, R. 1991. Barite formation in the Southern Ocean water column. Marine Chemistry 35: 411-421.

Swarzenski, P.W., Reich, C.D., Spechler, R.M., Kindinger, J.L. and Moore, W.S. 2001. Using multiple geochemical tracers to characterize the hydrogeology of a submarine spring off Crescent Beach, Florida. Chemical Geology 179: 187-202.

Taylor, R.B., Barnes, D.J. and Lough, J.M. 1993. Simple models of density band formation in massive corals. Journal of Experimental Marine Biology and Ecology 167: 193-125.

Taylor, R.B., Barnes, D.J. and Lough, J.M. 1995. On the inclusion of trace materials into massive coral skeletons. 1. Materials occurring in the environment in short pulses. Journal of Experimental Marine Biology and Ecology 185: 255-278.

Tilman, D., Fargione, J., Wolff, B., D'Antonio, C., Dobson, A., Howarth, R., Schindler, D., Schlesinger, W.H., Simberloff, D. and Swackhamer, D. 2001. Forecasting agriculturally driven global environmental change. Science 292: 281-284.

Tudhope, A.W., Lea, D.W., Shimmield, G.B., Chilcott, C.P. and Head, S. 1996. Monsoon climate and Arabian Sea coastal upwelling recorded in massive corals from Southern Oman. Palaios 11.

Vander Putten, E., Dehairs, F., Keppens, E. and Baeyens, W. 2000. High resolution distribution of trace elements in the calcite shell layer of modern *Mytilus edulis*: environmental and biological controls. Geochimica et Cosmochimica Acta 64: 997-1011.

Verdon, D.C., Wyatt, A.M., Kiem, A.S. and Franks, S.W. 2004. Multidecadal variability of rainfall and streamflow: Eastern Australia. Water Resources Research 40, W10201, doi:10.1029/2004WR003234, 2004.

Vorosmarty, C.J., Meybeck, M., Fekete, B., Sharma, B., Green, K. and Syvitski, J.P.M. 2003. Anthropogenic sediment retention: major global impact from registered river impoundments. Global and Planetary Change 39: 169-190.

Walling, D.E. and Fang, D. 2003. Recent trends in the suspended sediment loads of the world's rivers. Global and Planetary Change 39: 111-126.

Wilkinson, B.H. 2005. Humans as geologic agents: a deep-time perspective. Geology 33: 161-164.

Wolanski, E. 1994. Physical Oceanographic Processes of the Great Barrier Reef. CRC Press, Boca Raton. 194 pp.

Wolanski, E. and Ruddick, B. 1981. Water circulation and shelf waves in the northern Great Barrier Reef lagoon. Marine and Freshwater Research 32: 721-740.

Wolanski, E. and Bennett, A.F. 1983. Continental shelf waves and their circulation around the Great Barrier Reef. Marine and Freshwater Research 34: 23-47.

Wolanski, E. and Pickard, G.L. 1985. Long-term observations of currents on the central Great Barrier Reef continental shelf. Coral Reefs 4: 47-57.

Wolanski, E. and Duke, N.C. 2002. Mud threat to the Great Barrier Reef of Australia. *In*: Healy, T.R., Wang, Y. and Healy, J.-A. (eds.), Muddy Coasts of the World: Processes, Deposits and Function. Elsevier, Amsterdam, The Netherlands.

Wyndham, T., McCulloch, M., Fallon, S. and Alibert, C. 2004. High-resolution coral records of rare earth elements in coastal seawater: Biogeochemical cycling and a new environmental proxy. Geochimica et Cosmochimica Acta 68: 2067-2080.

Table 4.1. Modeled and estimated increases in rates of sediment delivery to the Great Barrier Reef Lagoon relative to pre-clearing conditions (~1850).

Study	**Sediment delivery increase over natural rates**	**Study Region**
Hacker 1988	2.2 - 4.0	Pioneer Catchment
Moss et al. 1992	3.0 - 5.0	Total GBR Catchment
Neil and Yu 1996	3.8	Total GBR Catchment
Neil et al. 2002	1.5 - 4.0	Range of all GBR Catchments
Prosser et al. 2002	6.0	Burdekin River Catchment
McKergow et al. 2005a	8.0	Total GBR Catchment

Table 4.2. Collection and analytical summary details for *Porites* cores, including the total length analyzed by LA-ICP-MS (presented in this chapter) and the total number of bulk annual samples used for solution ICP-MS (see Chapter 5). The distance offshore (km) and island size (ha) are reported for each island site.

Core Code	Lat °S	Lon °E	Collection Depth (m)	Length (cm)	Average Growth Rate (mm ± 1 SD)	LA-ICP-MS length (cm)	Sol'n ICP-MS (# samples)
Round Top I. (5 km; 24 ha)							
RTA	21.17058	149.26517	7	100	7.6 ± 1.2		
RTB	21.17546	149.26299	10	34	5.1 ± 1.3		
RTC	21.17546	149.26299	10	41	7.6 ± 1.9	36 *	
RTD	21.17649	149.26626	9	83	N/A		
RTE	21.17649	149.26626	8	74	N/A		
RTF	21.17084	149.26435	8	61	8.3 ± 1.8	52 *	26
Kewsick I. (32 km; 812 ha)**							
KIA	20.91769	149.41860	5	210	16.1 ± 2.2		27
KIB	20.91769	149.41778	6	42	15.7 ± 2.4		
KIC	20.91769	149.41778	6	56	15.9 ± 2.4	21	
Scawfell I. (51 km; 1441 ha)							
SCA	20.85524	149.60205	2	79	15.1 ± 3.7		
SCB	20.85524	149.60205	2	55	13.7 ± 2.8		
SCC	20.85524	149.60205	4	170	14.8 ± 2.3	25	
SCD	20.85575	149.60260	N/A	55	14.1 ± 2.8		
SCE	20.86526	149.59768	5	210	11.0 ± 2.0		
SCF	20.86526	149.59768	5	45	15.4 ± 2.4		

* Indicates whole core sampled. DIfferences between LA-ICP-MS length and total core length are due to slanted orientation of growth bands.

** Keswick is separated from St. Bees I. (1329 ha) by a narrow (< 1 km) channel.

Table 4.3. Correlations coefficients (r) of weekly Ba/Ca and Y/Ca ratios with Pioneer River discharge for the entire record from each core. n = number of weeks.

Core	# years	r	lag (wks)	n	p <
A. Ba/Ca					
RTC	44	0.271	13	2147	0.010
RTF	41	0.272	14	2272	0.010
KIC	12	0.168	4	646	0.100
SCC	13	0.213	0	747	0.050
B. Y/Ca					
RTC	44	0.282	3	2147	0.010
RTF	41	0.244	0	2272	0.020
KIC	12	0.210	0	646	0.050
SCC	13	0.215	3	747	0.050

Table 4.4. Correlation coefficients (r) of weekly Ba/Ca and Y/Ca ratios with Pioneer River discharge restricted to: (A) flood weeks (≥ mean discharge) only; (B) flood weeks coincident with northwest wind stress; and (C) strong wind weeks (≥ mean + 1 SD τ) only. n = number of weeks.

Core	# years	A. Flood Weeks			B. Flood Weeks + NW winds			C. Strong Winds		
		r	n	p <	r	n	p <	r	n	p <
Ba/Ca										
RTC	44	0.578	275	0.001	0.610	44	0.001	0.615	52	0.001
RTF	41	0.590	288	0.001	0.631	47	0.001	0.607	56	0.001
KIC	12	0.495	78	0.001	0.630	8	0.100	0.657	19	0.010
SCC	13	0.503	105	0.001	0.600	11	0.100	0.700	23	0.001
Y/Ca										
RTC	44	0.545	275	0.001	0.630	44	0.001	0.595	52	0.001
RTF	41	0.522	288	0.001	0.597	47	0.001	0.570	56	0.001
KIC	12	0.565	78	0.001	0.632	8	0.100	0.616	19	0.010
SCC	13	0.452	105	0.001	0.540	11	0.100	0.716	23	0.001

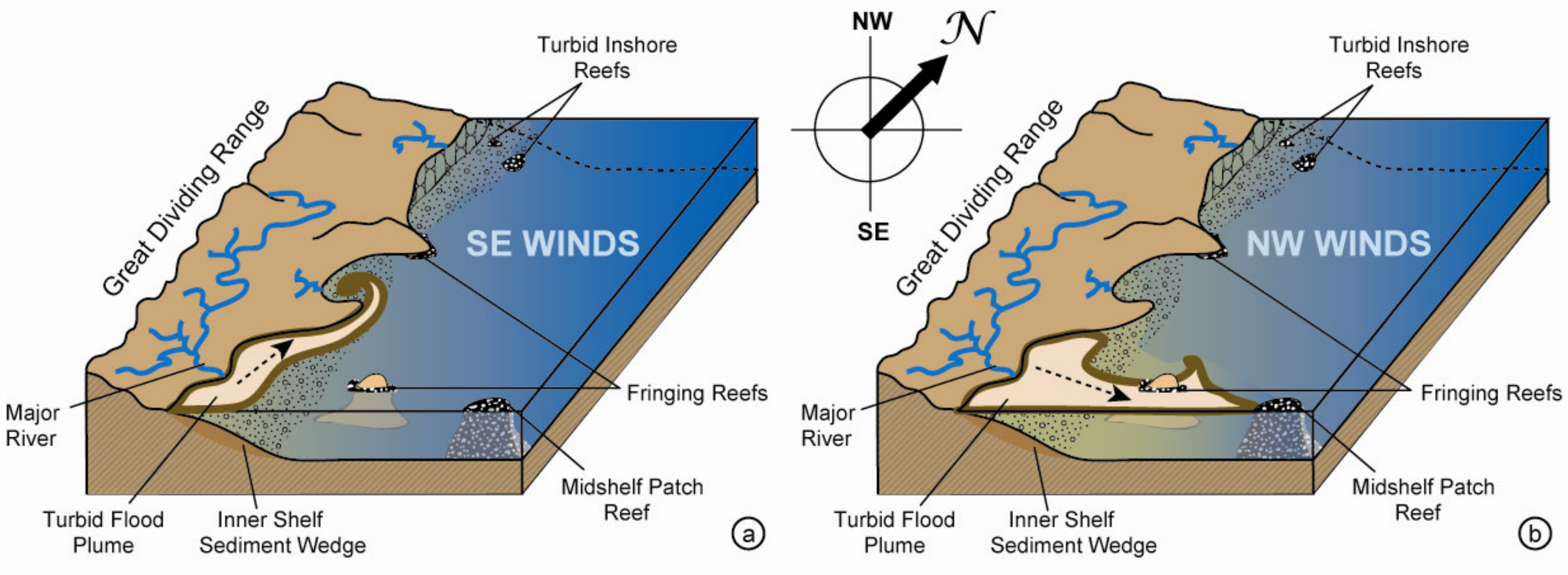

Figure 4.1. Schematic of flood plume behavior along the central Queensland coast during (a) prevailing south-easterly trade winds; and (b) northwesterly winds. Dashed arrows show net movement of flood plumes. (modified from Larcombe and Woolfe 1999).

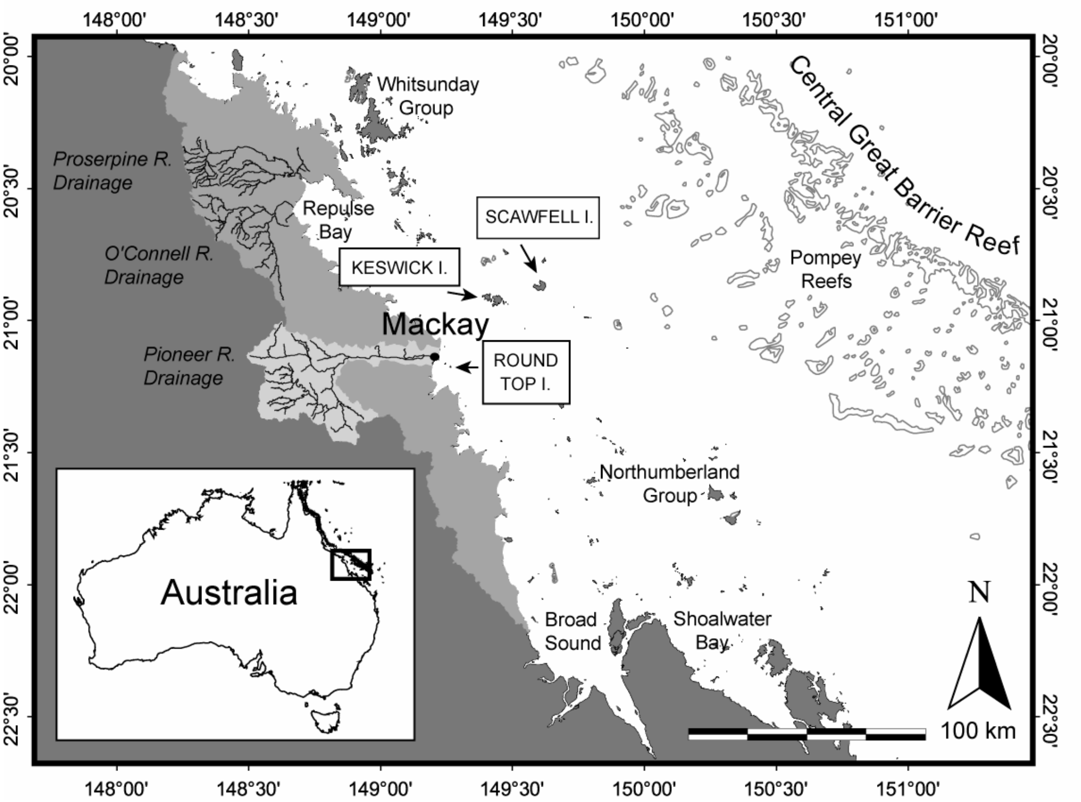

Figure 4.2. Location of the Pioneer Catchment (light grey) within the Mackay-Whitsunday management region (medium grey) along the central Queensland coast. Names in boxes indicate sites where coral cores were collected along a gradient of distance from the coast.

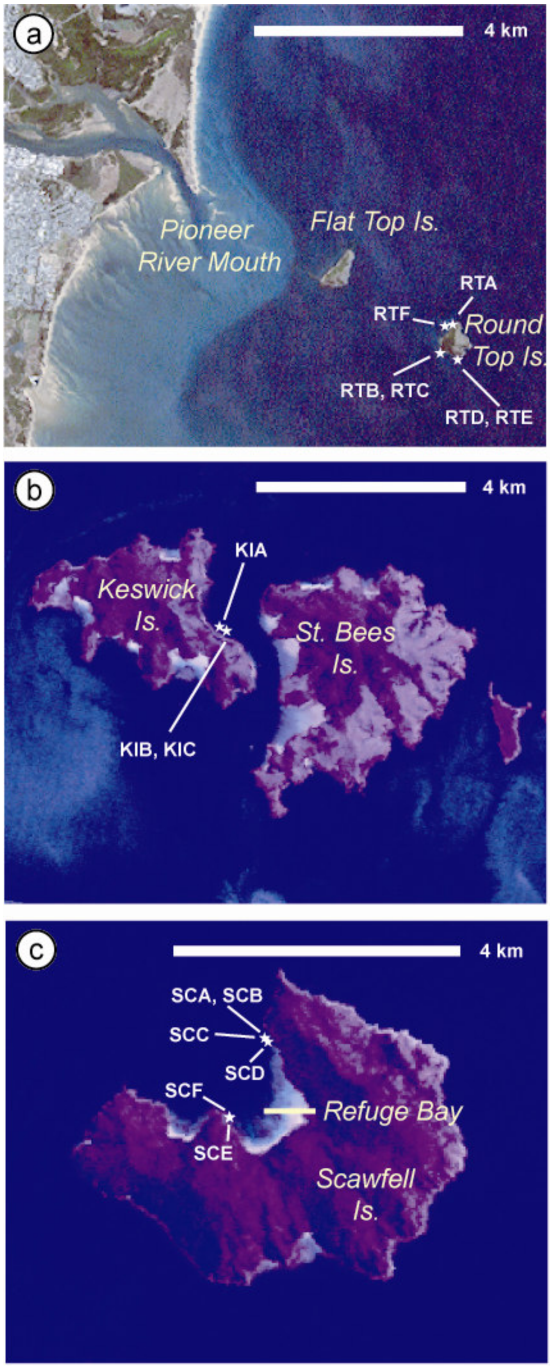

Figure 4.3. Locations of coral cores (stars) collected from (a) Round Top Island; (b) Keswick Island; and (c) Scawfell Island.

Figure 4.4. Example of effects of data smoothing on the Ba/Ca profile from Round Top core (RTC). The grey and black lines are replicate laser scans along the same track following the maximum growth axis. (a) Unfiltered Ba/Ca data for a 90 mm piece. (b) Enlargement of 20 cm following smoothing with a 10 point running median. (c) The same 20 cm smoothed with a 10 point mean.

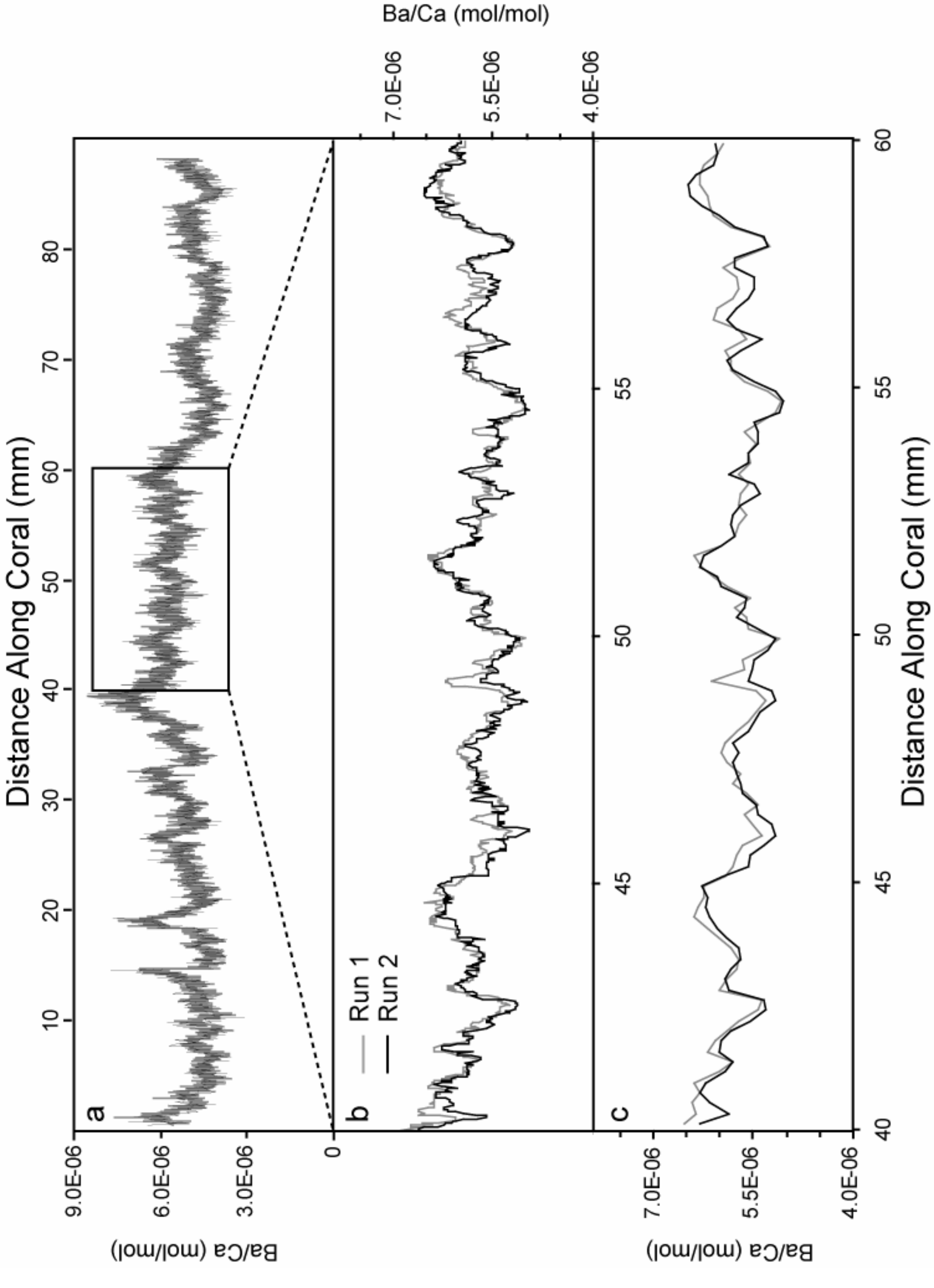
Distance Along Coral (mm)
10
20
30
40
50
60
70
80
a
b
c
Run 1
Run 2
Ba/Ca (mol/mol)
9.0E-06
6.0E-06
3.0E-06
0
7.0E-06
5.5E-06
4.0E-06
45
50
55
60
40
Distance Along Coral (mm)

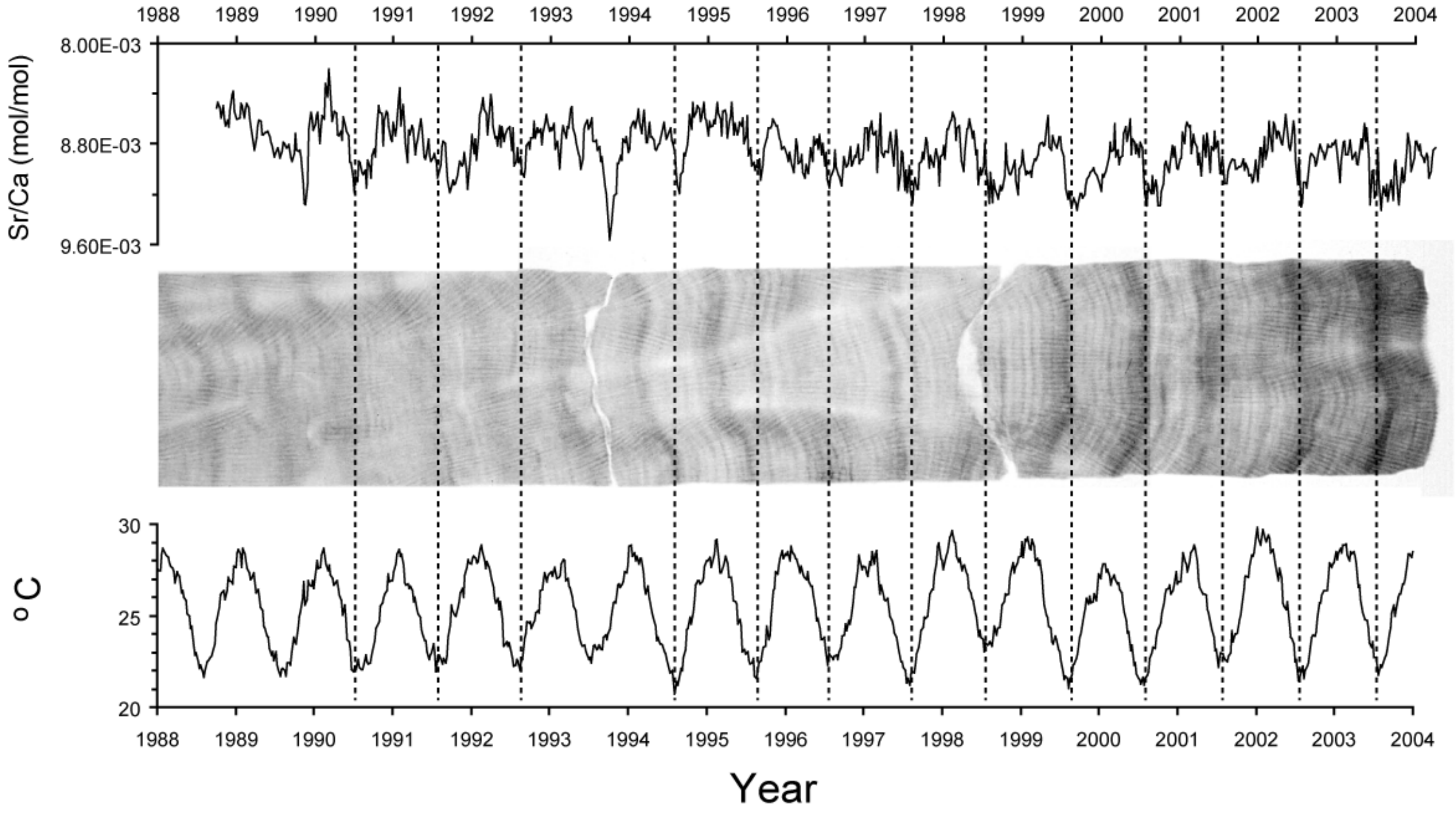

Figure 4.5. Example of chronology construction for Scawfell Island core (SCC). Dashed lines show alignment between: winter maxima of weekly Sr/Ca (above); seasonal density bands (middle); and winter SST minima (bottom).

Figure 4.6. Fluvial, anemometer, and inshore coral records from the Pioneer region, 1959-2003. (a) Pioneer River discharge. Weeks > mean (dashed line) were considered flood weeks. (b) Weekly wind vectors indicating magnitude and direction. (c) Alongshore wind stress (τ), with positive values denoting winds to the northwest. (d) Luminescence from Round Top core RTC. (e) Ba/Ca ratios from two Round Top cores (RTF = grey; RTC = red). (f) Y/Ca ratios measured from the same two cores.

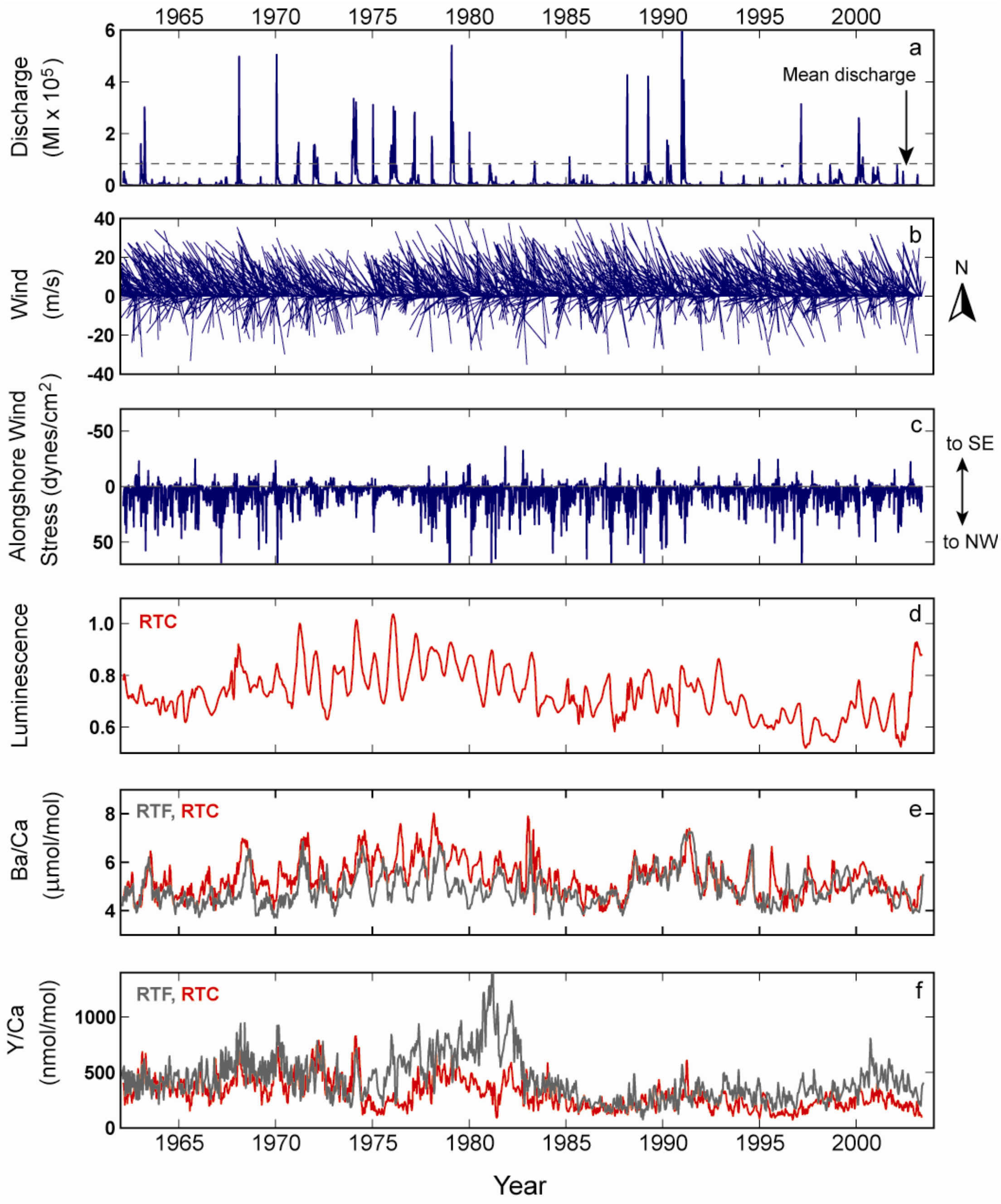

1965
1970
1975
1980
1985
1990
1995
2000
Discharge (Ml x 10^5)
6
4
2
0
a
Mean discharge
Wind (m/s)
40
20
0
-20
-40
b
N
Alongshore Wind Stress (dynes/cm^2)
-50
0
50
c
to SE
to NW
Luminescence
1.0
0.8
0.6
RTC
d
Ba/Ca (µmol/mol)
8
6
4
RTF, RTC
e
Y/Ca (nmol/mol)
1000
500
0
RTF, RTC
f
1965
1970
1975
1980
1985
1990
1995
2000
Year

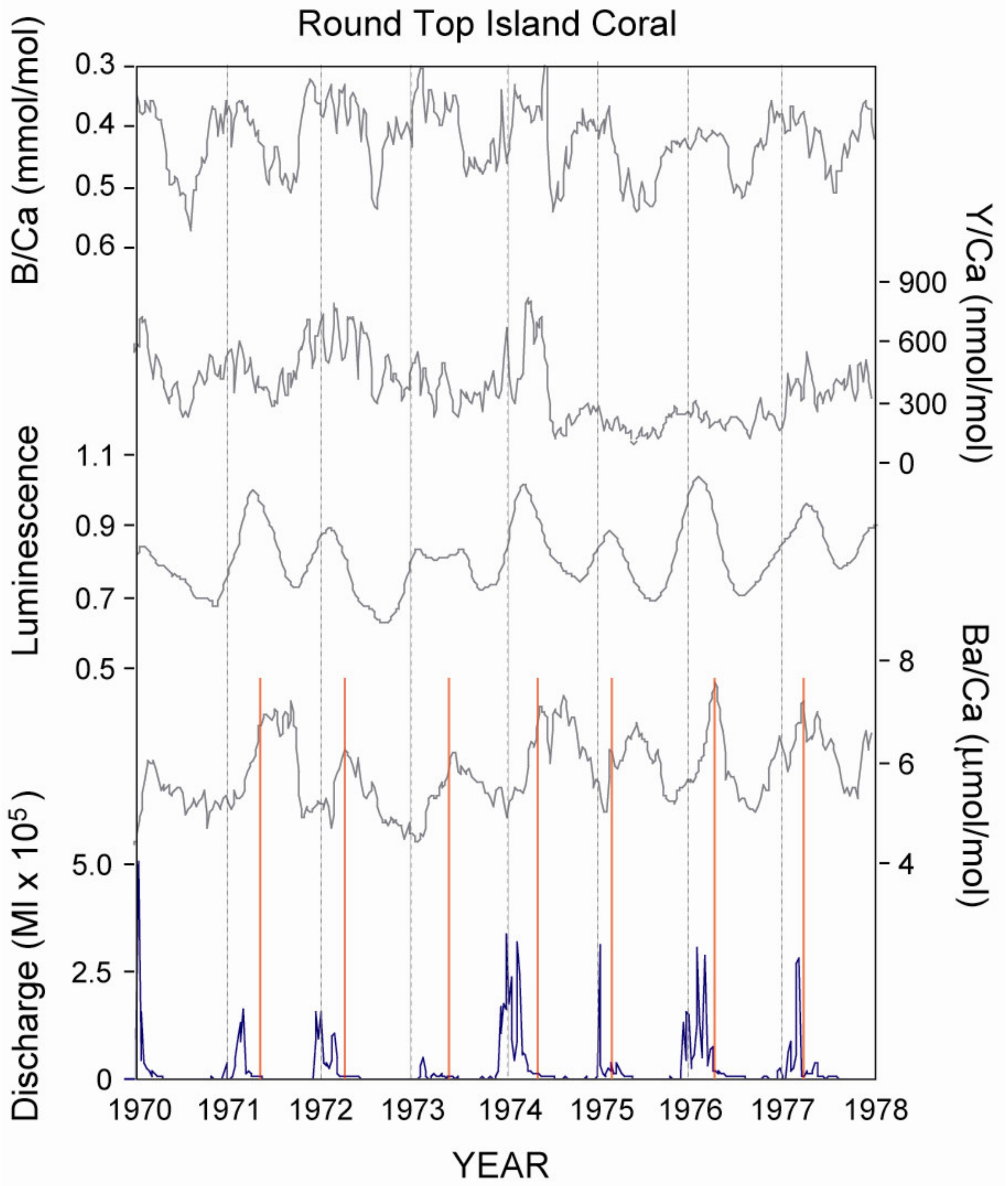

Figure 4.7. Profiles of four tracers (grey) in Round Top core (RTC) during wet years from 1970 to 1978. Vertical dashed lines are at the beginning of each year. B/Ca indicates seasonality, with peaks (minimum values) coinciding with warm summer SSTs. Luminescence and Y/Ca peaks largely coincide with discharge peaks (in blue at bottom). Ba/Ca peaks lag behind discharge by ~13 weeks, with the initial rise occurring ~6-7 weeks (on average) following maximum discharge each year (examples highlighted in red).

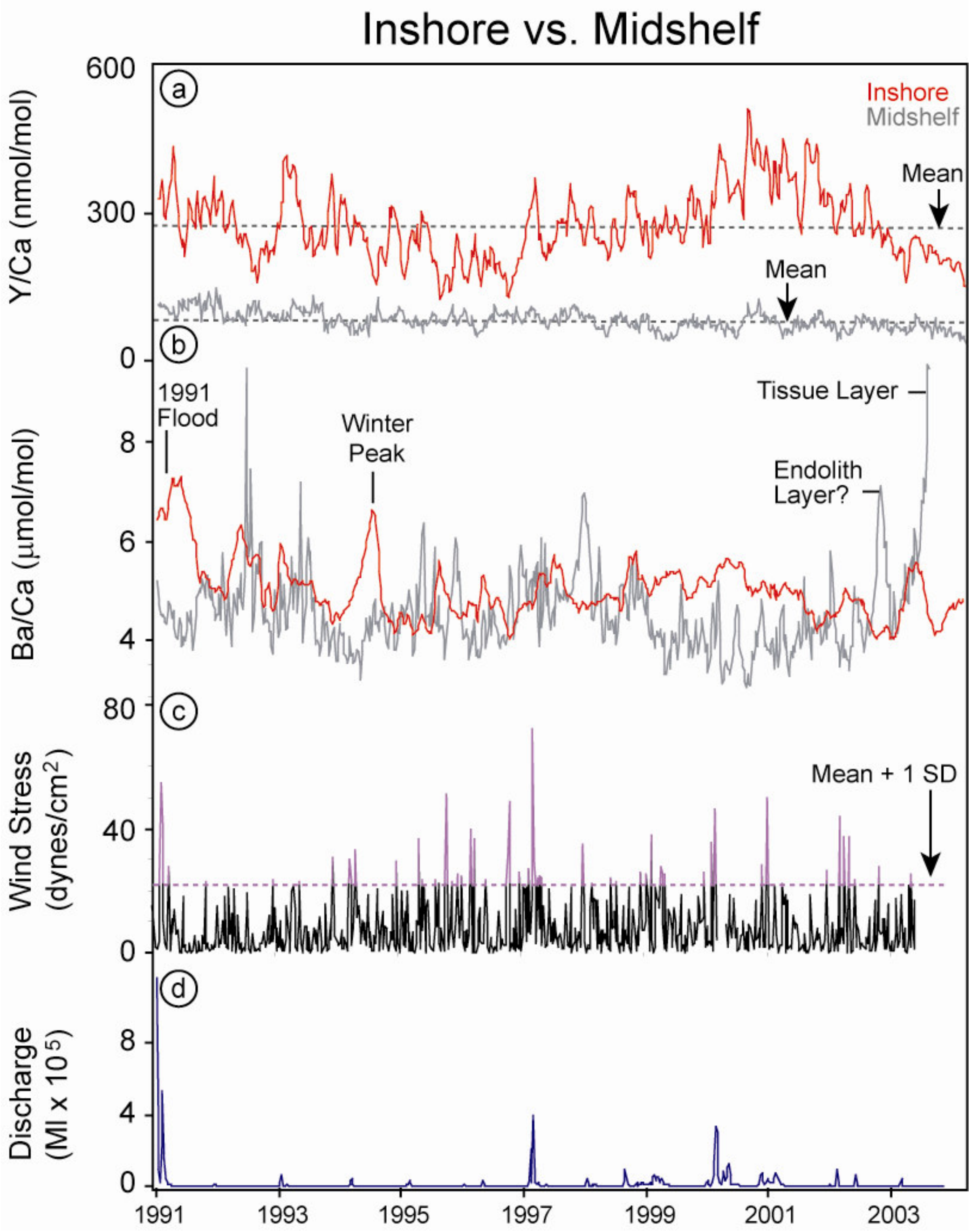

Figure 4.8. (a) Y/Ca and (b) Ba/Ca records from inshore (red) and midshelf (grey) sites. Inshore records are averages of RTC and RTF cores; midshelf records are averages of KIC and SCC. (dashed line = mean Y/Ca values). (c) Total wind stress (τ). Weeks counted as strong winds (above dashed line; > mean + 1 SD) are purple. (d) Pioneer River discharge.

Figure 4.9. (a) Luminescence bands (pale) in cores from the three sites (Round Top Island: RTC; Keswick Island: KIC; Scawfell Island: SCC) in 1983 and 1993. (b,c) Detailed (i) Sr/Ca and (ii) Ba/Ca ratios, plus (iii) discharge, (iv) SST anomalies and (v) wind stress (τ) anomalies, surrounding two luminescent bands signaling extreme events in (b) 1982-83 and (c) 1993. Anomalies were calculated by subtracted each weekly value (SST or τ) from the mean for that week over the entire record (SST: 1981-2004; τ: 1959-2003).

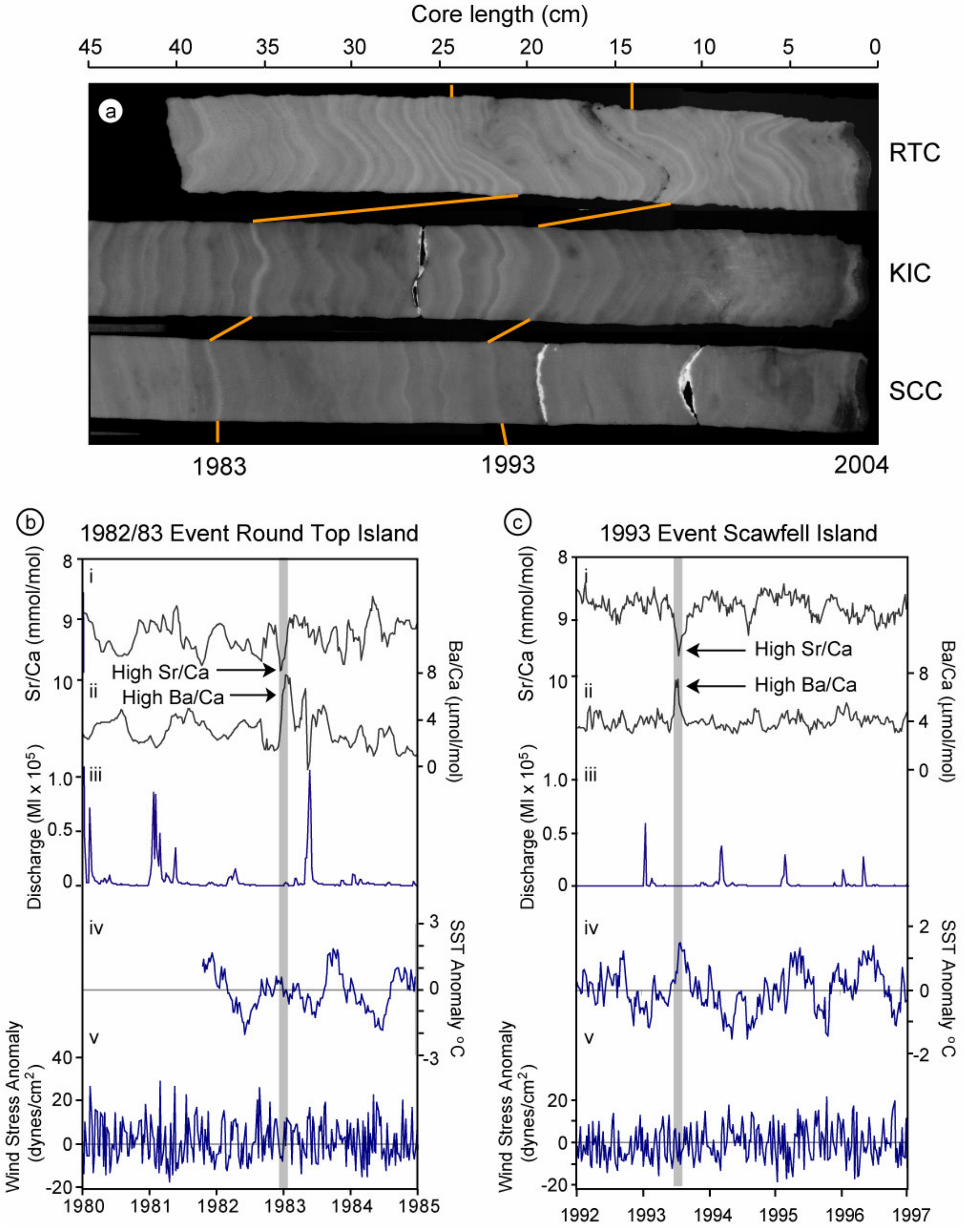
Core length (cm)
45
40
35
30
25
20
15
10
5
0
a
RTC
KIC
SCC
1983
1993
2004
b
1982/83 Event Round Top Island
Sr/Ca (mmol/mol)
8
9
10
i
ii
High Sr/Ca
High Ba/Ca
Ba/Ca (µmol/mol)
8
4
0
iii
Discharge (Ml x 10^5)
1.0
0.5
0
iv
SST Anomaly °C
3
0
-3
v
Wind Stress Anomaly (dynes/cm^2)
40
20
0
-20
1980
1981
1982
1983
1984
1985
c
1993 Event Scawfell Island
Sr/Ca (mmol/mol)
8
9
10
i
ii
High Sr/Ca
High Ba/Ca
Ba/Ca (µmol/mol)
8
4
0
iii
Discharge (Ml x 10^5)
1.0
0.5
0
iv
SST Anomaly °C
2
0
-2
v
Wind Stress Anomaly (dynes/cm^2)
20
0
-20
1992
1993
1994
1995
1996
1997

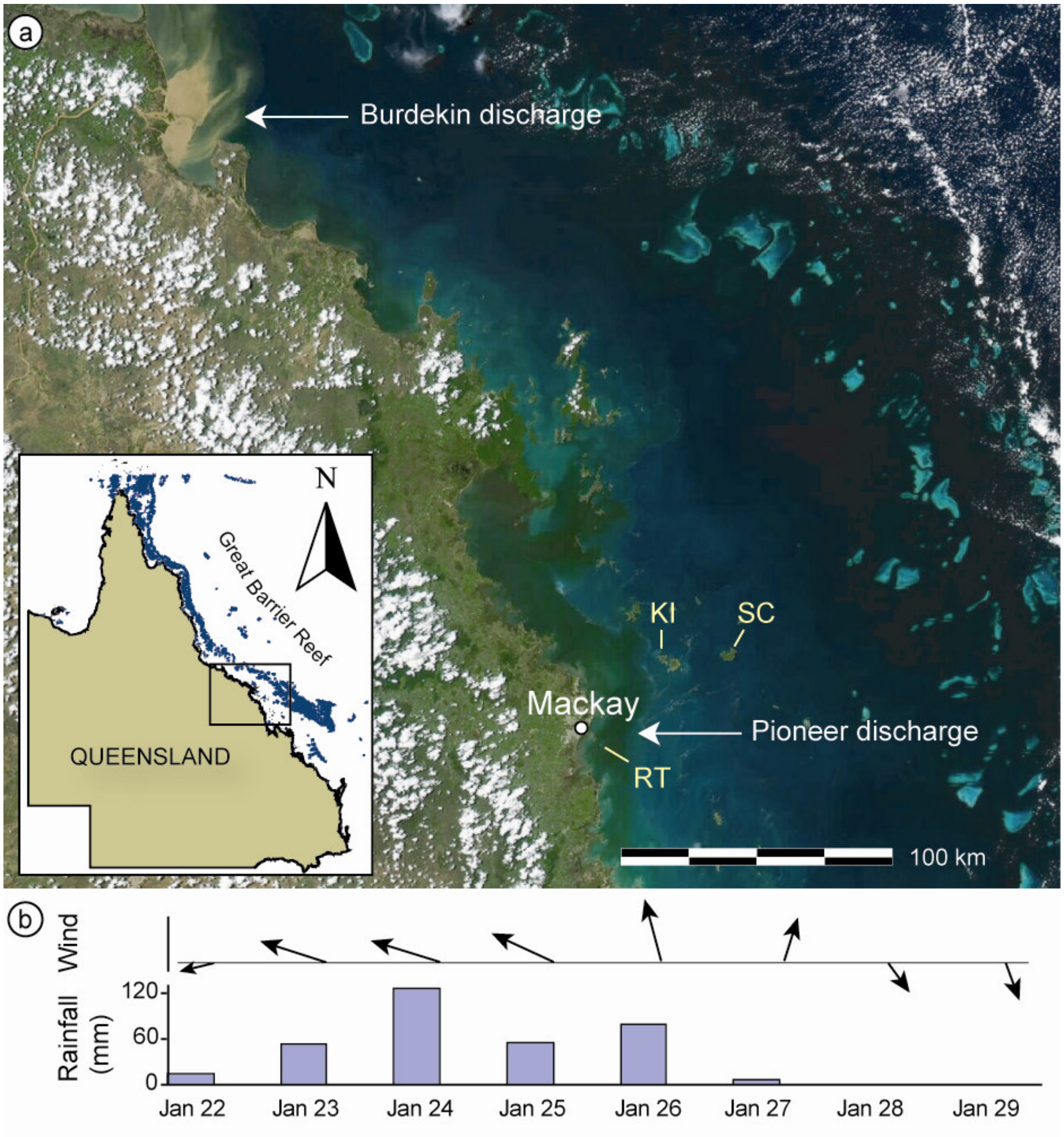

Figure 4.10. (a) MODIS satellite image of January 2005 flood (captured 29 Jan) showing distinctions between brown sediment-laden discharge from the Burdekin River and dark green plumes along the Mackay-Whitsunday coast. Lower inset shows location along Queensland coast. (b) Magnitude of rainfall and wind vectors for duration of flood to date of image capture.

Chapter 5. Coral Rare Earth Elements and Yttrium (REY) from Inshore and Midshelf Islands off Mackay

Introduction

Concentrations of rare earth elements and yttrium (REY) in coastal corals are good geochemical tracers of freshwater runoff and/or chemical weathering of continental crust because they are: (1) incorporated into coral lattices in close proportion to ambient seawater concentrations (Sholkovitz and Shen 1995; Fallon et al. 2002; Akagi et al. 2004; Wyndham et al. 2004); and (2) fractionated differentially in shales, river water and seawater (Elderfield et al. 1990; Sholkovitz 1992, 1995; Byrne and Sholkovitz 1996). For identifying potential terrestrial sources in marine REY, the data are typically normalized to a sediment or sedimentary rock (e.g. shale) composite to remove the natural "saw-tooth" distribution of absolute abundances and to describe the pattern relative to a continental source (Byrne and Sholkovitz 1996). Elemental anomalies[1] within the much smoother, normalized pattern can be used as "fingerprints" of biological and physical processes and/or provenance features (Akagi et al. 2004; Lawrence et al. 2006a). In one example, *Porites* corals living adjacent to a soft waste dump and creek delivering runoff from an open-cut mine on Misima Island, Papua New Guinea (PNG) had positive middle rare earth element (MREE) anomalies that closely resembled those from Sepik River water (Fallon et al.

---

[1] Anomalies are departures from a smooth line predicted by extrapolation from neighboring elements: values <1 are negative anomalies; values >1 are positive anomalies (Sholkovitz 1995; Lawrence et al. 2006a, 2006b).

2002), suggesting that provenance information from a strong source can be preserved through the estuarine mixing zone (Sholkovitz et al. 1999).

Shale-normalized REY patterns in coastal seawater are often intermediate between river and marine endmembers (Elderfield et al. 1990). Shale-normalized riverine REY patterns can be highly variable, and may differ considerably in magnitude and enrichments of light, middle or heavy rare earths (Goldstein and Jacobsen 1988; Elderfield et al. 1990; Sholkovitz 1992; Byrne and Sholkovitz 1996). By contrast, shale-normalized pure seawater REY patterns are consistent worldwide, and include: (1) elevated lanthanum (La); (2) depleted cerium (Ce); (3) decoupling between yttrium (Y) and holmium (Ho); and (4) enrichment of heavy rare earth elements (HREE) relative to light elements (LREE) (Elderfield and Greaves 1982; Cantrell and Byrne 1987; Elderfield et al. 1988; Byrne and Kim 1990; de Baar et al. 1991; Sholkovitz 1992; Lee and Byrne 1993; Sholkovitz 1995; Byrne and Sholkovitz 1996; Zhang and Nozaki 1996; Nozaki et al. 1997; Alibo and Nozaki 1999; Lawrence and Kamber 2006).

The changes from riverine to marine REY patterns occur both within the estuary and in adjacent coastal waters (see also Chapter 4). The elevated La anomaly in seawater is well-documented (Masuda and Ikeuchi 1979; de Baar et al. 1985; de Baar et al. 1991; Zhang et al. 1994; Lawrence and Kamber 2006): in estuaries of southeast Queensland (Australia), the anomaly is due to reduced removal (via precipitation with iron-organic colloids that flocculate at low salinities; Hoyle et al. 1984; Sholkovitz 1995) and greater remineralization of La within the mixing zone

(Lawrence and Kamber 2006). Ce is the only rare earth element known to have redox reactions in surface waters (Elderfield et al. 1988; Sholkovitz and Shen 1995; Wyndham et al. 2004): the negative Ce anomaly reflects removal of dissolved Ce^{3+} via oxidation to the highly insoluble Ce^{4+} (Elderfield et al. 1988; Sholkovitz and Schneider 1991; Sholkovitz et al. 1994), and oxidation probably occurs in coastal marine regions rather than the estuarine mixing zone (Lawrence and Kamber 2006). The decoupling of Y from Ho is the result of their different abilities to form surface and solution complexes (Byrne and Lee 1993): in low-salinity regions of estuaries, Y preferentially remains in solution while Ho is scavenged by particle aggregates (Lawrence and Kamber 2006); and the elemental fractionation between the elements is increased further in higher-salinity regions of the mixing zone where Y is preferentially released during remineralization (Lawrence and Kamber 2006). The enrichment of HREE relative to LREE reflects physical contraction of ions (decreasing radius with increasing atomic number) caused by a systematic increase from light to heavy REE^{3+} ions in REE-carbonate complexation (Cantrell and Byrne 1987; Elderfield et al. 1988; Sholkovitz 1992; Lee and Byrne 1993; Sholkovitz and Shen 1995; Byrne and Sholkovitz 1996). Differential complexation leads to preferential adsorption of LREEs to particle surfaces while HREEs remain in solution (Cantrell and Byrne 1987; Elderfield et al. 1988; Byrne and Kim 1990; de Baar et al. 1991; Sholkovitz 1992; Byrne and Li 1995).

Some deviations of REY patterns in coastal corals from typical marine REY patterns are probably due to provincial influences; and temporal changes to REY patterns are likely to reflect changing land-use patterns that alter both weathering and runoff. In this chapter, I compare REY data in cores from an inshore and a midshelf coral, from waters adjacent to the Pioneer River catchment (Queensland, Australia), to investigate both the magnitude of coastal enrichment in REY and differences in REY patterns among sites. I then describe and evaluate changes in total REY load and Y/Ho ratios in both settings. This study appears to be the first to present data on temporal variations spanning >50 years for the nearly full REY series from both inshore and midshelf corals.

Methods

Sample preparation

Two cores (RTF, KIA) were collected from massive *Porites* colonies adjacent to an inshore (Round Top) and midshelf (Keswick) islands near Mackay, Queensland, Australia (see Chapter 4 for coral collection details). I used density bands in X-rays to identify years in slabs cut from each core, from which I then drilled bulk samples from annual coral growth periods spanning many years between 1950 and 2002. For each core, I analyzed 3-5 consecutive years from each decade, avoiding years with noticeable dark staining (indicating possible inclusions of organic material). For each annual sample, I diluted approximately 5-15 µg of coral powder by 1000 with >18.2 MΩ water, added HNO_3 to a total concentration of 2%, left the samples to digest overnight, and spiked all solutions, including blanks, with 2 ppb of internal standard (indium (In), rhenium (Re), bismuth (Bi)).

Solution ICP-MS analyses

All samples were analyzed on a Thermo X-Series inductively-coupled mass spectrometer (ICP-MS), equipped with a Peltier cooled, quartz impact, bead spray chamber and a 0.4 mL/min borosilicate nebuliser. For instrument specifications, sensitivity and operating power, see Lawrence et al. (2006a) and Lawrence and Kamber (2006). Dilutions of USGS dolerite W-2, Mud of Queensland (MUQ; a composite sediment of 25 Queensland rivers Kamber et al. 2005), and JCp-1 coral reference material (collected in 1999 from Ishigaki Island, Okinawa, Japan) were measured simultaneously with the samples for machine calibration. Five repeats of 50 sweeps at three points per peak (0.02 amu spacing; 10 to 20 ms dwell time) were measured for each sample, and eight repeats were measured for blanks (Lawrence and Kamber 2006). All REY (except promethium (Pm), which does not exist naturally in measurable concentrations; Byrne and Sholkovitz 1996), zircon (Zr) and the appropriate suite of interfering isotopes were measured. All data were corrected for drift (internal and external), oxide interferences (for europium (Eu) and heavier elements), and dilution factors.

Statistical analyses and anomaly calculations

I performed a principal components analysis (PCA) using a VARIMAX rotation to compare coral REY patterns with seawater, river water and sediment. Mean coral REY from RTF and KIA (over all years analyzed) were compared with REY data from MUQ and water samples collected from: Pioneer River mouth and estuary (M. Lawrence, unpublished data); Coral Sea (Zhang and Nozaki 1996); and streams draining different regions of the Pioneer catchment (Lawrence et al. 2005a) (Table 5.1). I scaled all REY abundances to the same value of samarium (Sm), for which anomalies are not expected, and excluded Eu from the PCA because isobaric interference of BaO during ICP-MS analysis resulted in unreliable measurements of Eu from the Pioneer stream water samples (Lawrence et al. 2005a).

For visual assessment of deviations from the typical seawater pattern as indicators of terrestrial influence, I normalized mean coral sample REY concentrations (ppb) to those from terrestrial sediment (MUQ). For comparing Mackay coral REY patterns to records from other studies, I also normalized other published coral REE abundances to MUQ. To calculate the Ce anomaly, I used an equation from Lawrence et al. (2006b), Ce_n/Ce_n^*, where n refers to the shale-normalized abundances of Ce, praseodymium (Pr) and neodymium (Nd):

$$Ce_n^* = Pr_n * (Pr_n/Nd_n) \tag{5.1}$$

I assessed differences in mean Ce anomalies between RTF and KIA with two-sample t-tests, after using Cochran's test to assess homoscedasticity. To evaluate the slope of HREE, I calculated Lu_n/Er_n, where n refers to the shale-normalized abundances of lutetium (Lu) and erbium (Er). Because RTF and KIA had unequal variances in Lu_n/Er_n ratios, I used a two sample t-test with unequal variances to determine significance.

I performed multiple regressions to assess changes in total REY and Y/Ho ratios from each core over time, using year and Pioneer River discharge as the independent variables. To check for detrital contamination, which would lower the Y/Ho mass ratio closer to shale values (~26) and elevate concentrations of terrestrially derived elements such as Zr, I correlated Zr and Y/Ho ratios for each core (Webb and Kamber 2000). All statistical analyses were done with SYSTAT v.10.2 software.

Results and Discussion

General Mackay REY patterns

When the scaled REY data were ordinated along the first two principal components, which explained 67.9% and 20.8% of the total variance respectively, the data from RTF clustered tightly with water samples from the Pioneer River mouth and estuary, suggesting that the inshore coral REY pattern reflects a local source (Figure 5.1). Coastal seawater, the inshore (RTF) coral and terrestrial sediment (MUQ) all had high positive values along principal component 2, which are largely explained by differences in scaled LREE abundances (Table 5.2). LREE enrichment in the inshore coral probably relates to greater terrestrial influence, as LREEs may be more readily mobilized by weathering than HREEs (Nesbitt et al. 1990). By contrast, the midshelf coral (KIA) and the offshore seawater sample from the Coral Sea, had high positive values along principal component 1, which is largely explained by differences in scaled middle rare earth element (MREE) and HREE abundances

(Figure 5.1; Table 5.2). While HREE enrichments are typical features of normalized oceanic seawater patterns, relative HREE depletions in coastal waters probably result from fluvial discharge, biological activity or a combination of the two (see discussion of HREE below). The large differences in scaled Y abundances also contribute to principle component 2, with scaled abundances of Y strongly mirroring a gradient of terrestrial influence (MUQ < Pioneer catchment streams < Pioneer River mouth < RTF < KIA < Coral Sea). The differences in position among Pioneer stream samples along principal component 1 also reflect relative enrichments of HREE and Y from Blacks Creek and the Lower Pioneer River: this may be due to leaching from fertilizer since the REY patterns in typical fertilizers that resemble natural phosphorites are nearly indistinguishable from the marine REY pattern (Martin and McCulloch 1999; Otero et al. 2005; Lawrence et al. 2006a).

Inshore-midshelf comparisons

The presence of all of the typical marine features (La anomaly, Ce anomaly, Y/Ho fractionation, and HREE > LREE) in MUQ-normalized REY patterns from both inshore and midshelf Mackay corals supports the assertion by previous authors that corals incorporate REY in proportion to ambient seawater concentrations (Figure 5.2a,b; Sholkovitz and Shen 1995; Fallon et al. 2002; Akagi et al. 2004; Wyndham et al. 2004). However, data from the inshore Round Top Island core (RTF) differed from the midshelf Keswick Island core (KIA) in five main respects. RTF had: (1) greater total REY abundance; (2) flatter HREE patterns; (3) more negative Ce anomalies; (4) smaller Y/Ho ratios; and (5) preferential enrichment of LREEs. Each of these discrepancies will be discussed below.

REY abundances: In every decade from 1950 to 2002, REY abundances from the inshore Round Top Island core (RTF) were approximately two to five times higher than REY abundances from the midshelf Keswick Island core (KIA) (Figures 5.2 and 5.3; Tables 5.3 and 5.4). In general, the inshore Round Top Island core had MUQ-normalized REY patterns and magnitudes that were in strong agreement with other inshore GBR corals (Figure 5.4; Wyndham et al. 2004). By contrast, the midshelf Keswick Island core had lower MUQ-normalized magnitudes that were similar to values from an offshore GBR reef (Figure 5.4; Wyndham et al. 2004) and values from a *Porites astreoides* collected from Bermuda (Figure 5.4; Sholkovitz and Shen 1995), suggesting reduced terrestrial influences at these sites.

HREE patterns: While shale-normalized REY from both cores were HREE enriched, RTF was less so relative to KIA, as indicated by a significantly greater (= higher slope) mean Lu_n/Er_n ratio in KIA (1.67) than in RTF (1.11) ($t = 17.41$, $df = 43$, $p < 0.001$; Figure 5.3). This difference may be the result of terrigenous runoff, since inputs from major rivers are usually HREE depleted (relative to shale) (Goldstein and Jacobsen 1988). Alternatively, the flatter HREE patterns at Round Top Island may reflect differences in productivity between the two sites: Wyndham et al. (2004) noted seasonal HREE depletion in high resolution records of inshore corals from the Great Barrier Reef that they attributed to scavenging by organic (or organically coated) particles created through biological activity. Their observations supported previous experimental work showing HREE depletion associated with degradation of marine particles (Arraes-Mescoff et al. 2001). Evidence of summer *Trichodesmium* blooms in the Pioneer River plume inshore from Keswick Island (Rohde et al. 2006), and the lags of coral Ba/Ca peaks in Round Top Island corals following Pioneer River floods (Chapter 4), suggest there may be substantial differences in biological activity between the sites. To assess which mechanisms might act, either independently or synergistically, to produce the RTF pattern, it will be necessary to sample the cores at higher resolution to identify seasonal changes to patterns that might be related to flooding, phytoplankton blooms or other factors.

<u>Negative Ce anomaly</u>: The mean Ce anomaly (0.502) for the RTF core was significantly lower than that (0.610) from KIA samples ($t = 6.86$, $df = 51$, $p < 0.001$). This agrees with other coral (Wyndham et al. 2004) and seawater records (Nozaki et al. 2000) showing stronger Ce anomalies in coastal regions than offshore. Wyndham et al. (2004) found strong correlations between the timing of spring-summer peaks in both Mn/Ca and Ce anomalies from inshore corals. Since Ce oxidation is probably coupled with microbially-mediated Mn oxidation (Moffett 1990), Wyndham et al. (2004) suggested that Ce oxidation increased during periods of high solar radiation and temperature, and after floods, all of which increase the abundance of oxidizing bacteria. However, these authors were cautious about their interpretation, because they used anomalously positive La values in their calculations of Ce anomalies. Because the Ce anomalies for the Mackay corals were not calculated using La, I

suggest that the differences are true reflections of site-specific variability which may be linked to biological productivity.

Y/Ho fractionation: The mean Y/Ho ratio (67.3) for RTF was less than half of the mean Y/Ho (142.6) for KIA. These differences were not due to terrigenous contamination, which can lower the Y/Ho ratio and is detected by negative correlations between Zr and Y/Ho (Webb and Kamber 2000). Because there was no significant negative relationship between Zr with Y/Ho for either RTF or KIA ($r = 0.370$, $p > 0.05$ and $r = 0.045$, $p > 0.10$, respectively), the differences are likely site-specific.

Due to differing surface complex stabilities, Ho is scavenged approximately twice as fast as Y within the estuarine mixing zone (Bau 1996; Nozaki et al. 1997; Lawrence and Kamber 2006), resulting in a superchondritic marine Y/Ho mass ratio that typically varies between ~40 and 77 (Table 5.5; Zhang et al. 1994; Bau et al. 1995; Bau 1996; Zhang and Nozaki 1996; Nozaki et al. 1997; Alibo and Nozaki 1999; Nozaki et al. 2000; Lawrence and Kamber 2006). If corals incorporate REY in proportion to seawater concentrations, and if coastal seawater REY patterns are intermediate between riverine and offshore sites, then coastal corals would be more likely to have lower Y/Ho ratios than corals from further offshore. In relative terms, the data supported this hypothesis, but in terms of absolute Y/Ho values, the coral values may not reflect surface seawater conditions. While the Y/Ho ratio (40.5) in Pioneer River mouth seawater was at the lower end of seawater range, the mean RTF Y/Ho value (67.3) was near the upper end of the range (Table 5.5), suggesting that:

(1) the distribution coefficients for Y and Ho incorporation into coral may vary, as observed for REE measured from Bermuda corals (Sholkovitz and Shen 1995); or (2) seawater fractionation between Y and Ho may change between the river mouth and sites further offshore. The mean Y/Ho value (142.6) for KIA, while similar to that (150.8) from the reference coral JCp-1, was nearly double the upper measurements of seawater Y/Ho (Table 5.5). Such discrepancies in coral Y/Ho values compared to their local seawater Y/Ho ratios led Webb and Kamber (2000) to suggest that, in some cases, modern microbialites (with average Y/Ho = 56.1) may actually be a better proxy for seawater REY than skeletal carbonates.

LREE enrichment: In the Mackay corals, LREE were preferentially enriched in the inshore core (RTF) relative to the midshelf core (KIA) (Figures 5.3). LREE enrichment in corals is often associated with river runoff (Naqvi et al. 1996; Akagi et al. 2004): for example, Shioya-wan Bay (Okinawa, Japan), which receives runoff from the Taiho-o-kawa River, has flatter REY patterns (caused by LREE enrichment) and higher magnitudes of total REE in seawater and corals (including *Porites lutea*) than Sesoko-jima Island, which is distant from riverine sources (Akagi et al. 2004). When corals are sampled seasonally, LREE enrichments appear to coincide with large flood events (Naqvi et al. 1996; Wyndham et al. 2004).

Temporal change

There were two major trends in the coral REY over time in both the RTF and KIA corals: (1) increased total REY; and (2) decreased Y/Ho ratios (Figure 5.5). The rate of increase in total REY abundance was approximately three times greater in RTF than in KIA (Figure 5.5a), and was significantly related to both year and Pioneer River discharge: when combined they explained 49% and 46% of the total variance at the inshore and midshelf sites, respectively (Table 5.6). While the statistical significance of the change in the total inshore coral REY load was more affected by river discharge at Round Top Island (partial $r^2 = 0.365$, $p < 0.002$; Table 5.6a) than at Keswick Island (partial $r^2 = 0.134$, $p < 0.025$; Table 5.6b), most of the higher KIA REY values were associated with years of high annual rainfall and strong floods (1951, 1974, 1990, 2001) whose plumes probably reached the vicinity of Keswick Island. The underlying steady but small increase over time at both sites suggests diffuse inputs of REY, possibly from greater catchment erosion coincident with agricultural expansion.

The second temporal pattern in both inshore and midshelf coral records is a significant decrease of Y/Ho ratios over time, which occurred at similar rates at Round Top and Keswick Islands (Figure 5.4b; Table 5.7). In RTF, the trend was significantly related to year ($p < 0.001$) but not to discharge ($p < 0.059$), and together they explained 77% of the total variance (Table 5.7a). In contrast, Pioneer discharge had a more pronounced effect on the variability of Y/Ho in KIA: both year ($p < 0.002$) and discharge ($p < 0.035$) were negatively correlated with Y/Ho, but together they explained only 42% of the total variance (Table 5.7b). While trends of decreasing Y/Ho may be related to increasing catchment weathering and/or exposure to freshwater, further studies are needed to better determine: (1) how the seawater

Y/Ho ratio changes (at the depth of the coral colony) during flood conditions; (2) how the seawater Y/Ho ratio changes in response to remineralization of REY from resuspended sediments; and (3) how the elements are incorporated into coral skeletons.

Conclusions

This study presents the first two records of changes in coral rare earth elements and yttrium (REY) spanning >50 years from both inshore (Round Top Island) and midshelf (Keswick Island) sites adjacent to a highly agricultural catchment. There were five main differences in REY patterns between the Round Top and Keswick Island cores. The Round Top Island coral had: (1) greater total REY; (2) flatter HREE; (3) larger negative Ce anomalies; (4) lower Y/Ho ratios; and (5) preferentially enriched LREE. The differences probably reflect a combination of stronger influences of rivers and seasonal (plus flood activated) changes in biological activity. Sampling at higher resolution through the corals may enable discrimination of individual mechanisms. Total REY abundances increased over time, while Y/Ho ratios declined in both the Round Top and Keswick Island cores. This suggests increasing freshwater influence and/or catchment weathering over the past half century.

References

Akagi, T., Hashimoto, Y., Fu, F.-F., Tsuno, H., Tao, H. and Nakano, Y. 2004. Variation of the distribution coefficients of rare earth elements in modern coral-lattices: Species and site dependencies. Geochimica et Cosmochimica Acta 68: 2265-2273.

Alibo, D.S. and Nozaki, Y. 1999. Rare earth elements in seawater: particle association, shale-normalization, and Ce oxidation. Geochimica et Cosmochimica Acta 63: 363-372.

Arraes-Mescoff, R., Roy-Barman, M., Coppola, L., Souhaut, M., Tachikawa, K., Jeandel, C., Sempere, R. and Yoro, C. 2001. The behavior of Al, Mn, Ba, Sr, REE and Th isotopes during in vitro degradation of large marine particles. Marine Chemistry 73: 1-19.

Bau, M. 1996. Controls on the fractionation of isovalent trace elements in magmatic and aqueous systems: evidence from Y/Ho, Zr/Hf and the lanthanide tetrad effect. Contributions to Mineralogy and Petrology 123: 323-333.

Bau, M., Dulski, P. and Moller, P. 1995. Yttrium and holmium in South Pacific seawater: vertical distribution and possible fractionation mechanisms. Chemie der Erde 55: 1-15.

Byrne, R.H. and Kim, K.-H. 1990. Rare earth element scavenging in seawater. Geochimica et Cosmochimica Acta 54: 2645-2656.

Byrne, R.H. and Lee, J.H. 1993. Comparative yttrium and rare earth element chemistries in seawater. Marine Chemistry 44: 121-130.

Byrne, R.H. and Li, B.Q. 1995. Comparative complexation behavior of the rare earths. Geochimica et Cosmochimica Acta 59: 4575-4589.

Byrne, R.H. and Sholkovitz, E.R. 1996. Marine chemistry and geochemistry of the lanthanides. *In*: Gschneider, K.A., Jr and Eyring, L. (eds.), Handbook on the Physics and Chemistry of the Rare Earths. pp. 497-593. Elsevier, Amsterdam, The Netherlands.

Cantrell, K.J. and Byrne, R.H. 1987. Rare earth element complexation by carbonate and oxalate ions. Geochimica et Cosmochimica Acta 51: 597-605.

de Baar, H.J.W., Bacon, M.P., Brewer, P.G. and Bruland, K.W. 1985. Rare earth elements in the Pacific and Atlantic Oceans. Geochimica et Cosmochimica Acta 49: 1943-1959.

de Baar, H.J.W., Schijf, J. and Byrne, R.H. 1991. Solution chemistry of the rare earth elements in seawater. European Journal of Solid State Inorganic Chemistry 28: 357-373.

Elderfield, H. and Greaves, M.J. 1982. The rare earth elements in seawater. Nature 296: 214-219.

Elderfield, H., Whitfield, M., Burton, J.D., Bacon, M.P. and Liss, P.S. 1988. The oceanic chemistry of the rare-earth elements [and discussion]. Philosophical Transactions of the Royal Society of London A 325: 105-126.

Elderfield, H., Upstill-Goddard, R. and Sholkovitz, E.R. 1990. The rare earth elements in rivers, estuaries, and coastal seas and their significance to the composition of ocean waters. Geochimica et Cosmochimica Acta 54.

Fallon, S.J., White, J.C. and McCulloch, M.T. 2002. *Porites* corals as recorders of mining and environmental impacts: Misima Island, Papua New Guinea. Geochimica et Cosmochimica Acta 66: 45-62.

Goldstein, S.J. and Jacobsen, S.B. 1988. Rare earth elements in river waters. Earth and Planetary Science Letters 89: 35-47.

Hoyle, J., Elderfield, H., Gledhill, A. and Greaves, M. 1984. The behaviour of the rare earth elements during mixing of river and sea waters. Geochimica et Cosmochimica Acta 48: 143-149.

Kamber, B.S., Greig, A. and Collerson, K.D. 2005. A new estimate for the composition of weathered young upper continental crust from alluvial sediments, Queensland, Australia. Geochimica et Cosmochimica Acta 69: 1041-1058.

Lawrence, M.G. and Kamber, B.S. 2006. The behaviour of the rare earth elements during estuarine mixing--revisted. Marine Chemistry 100: 147-161.

Lawrence, M.G., Jupiter, S.D. and Kamber, B.S. 2006a. Aquatic geochemistry of the rare earth elements and yttrium in the Pioneer River Catchment, Mackay, Queensland, Australia. Marine and Freshwater Research *in review*.

Lawrence, M.G., Grieg, A., Collerson, K.D. and Kamber, B.S. 2006b. Rare earth element and yttrium variability in South East Queensland waterways. Aquatic Geochemistry 12: 39-72.

Lee, J.H. and Byrne, R.H. 1993. Complexation of trivalent rare earth elements (Ce, Eu, Gd, Tb, Yb) by carbonate ions. Geochimica et Cosmochimica Acta 57: 295-302.

Martin, C.E. and McCulloch, M.T. 1999. Nd-Sr isotopic and trace element geochemistry of river sediments and soils in a fertilized catchment, New South Wales, Australia. Geochimica et Cosmochimica Acta 63: 287-305.

Masuda, A. and Ikeuchi, Y. 1979. Lanthanide tetrad effect observed in marine environment. Geochemical Journal 13: 19-22.

Moffett, J.W. 1990. Microbially mediated cerium oxidation in sea water. Nature 345: 421-423.

Naqvi, S.A.S., Nath, B.N. and Balaram, V. 1996. Signatures of rare-earth elements in banded corals of Kalpeni atoll--Lakshadweep archipelago in response to monsoonal variations. Indian Journal of Marine Sciences 25: 1-4.

Nesbitt, H.W., MacRae, N.D. and Kronberg, B.I. 1990. Amazon deep-sea fan muds: light REE enriched products of extreme chemical weathering. Earth and Planetary Science Letters 100: 118-123.

Nozaki, Y., Zhang, J. and Amakawa, H. 1997. The fractionation between Y and Ho in the marine environment. Earth and Planetary Science Letters 148: 329-340.

Nozaki, Y., Lerche, D., Alibo, D.S. and Snidvongs, A. 2000. The estuarine geochemistry of rare earth elements and indium in the Chao Phraya River, Thailand. Geochimica et Cosmochimica Acta 64: 3983-3994.

Otero, N., Vitoria, L., Soler, A. and Canals, A. 2005. Fertiliser characterisation: major, trace and rare earth elements. Applied Geochemistry 20: 1473-1488.

Pulsford, J.S. 1996. Historical nutrient usage in coastal Queensland river catchments adjacent to the Great Barrier Reef Marine Park. Research Publication No. 40 Great Barrier Reef Marine Park Authority, Townsville, Australia.

Rohde, K., Masters, B., Brodie, J., Faithful, J., Noble, R. and Carroll, C. 2006. Fresh and marine water quality in the Mackay Whitsunday region 2004/2005. Mackay Whitsunday Natural Resource Management Group, Mackay, Australia.

Sholkovitz, E. and Shen, G.T. 1995. The incorporation of rare earth elements in modern coral. Geochimica et Cosmochimica Acta 59: 2749-2756.

Sholkovitz, E.R. 1992. Chemical evolution of rare earth elements: fractionation between colloidal and solution phases of filtered river water. Earth and Planetary Science Letters 114: 77-84.

Sholkovitz, E.R. 1995. The aquatic chemistry of rare earth elements in rivers and estuaries. Aquatic Geochemistry 1: 1-34.

Sholkovitz, E.R. and Schneider, D.L. 1991. Cerium redox cycles and rare earth elements in the Sargasso Sea. Geochimica et Cosmochimica Acta 55: 2737-2743.

Sholkovitz, E.R., Landing, W.M. and Lewis, B.L. 1994. Ocean particle chemistry: the fractionation of rare earth elements between suspended particles and seawater. Geochimica et Cosmochimica Acta 58: 1567-1579.

Sholkovitz, E.R., Elderfield, H., Szymczak, R. and Casey, K. 1999. Island weathering: river sources of rare earth elements to the Western Pacific Ocean. Marine Chemistry 68: 39-57.

Taylor, S.R. and McLennan, S.M. 1985. The continental crust: its composition and evolution. Blackwell, Oxford, UK. 312 pp.

Webb, G.E. and Kamber, B.S. 2000. Rare earth elements in Holocene reefal microbialites: a new shallow seawater proxy. Geochimica et Cosmochimica Acta 64: 1557-1565.

Wyndham, T., McCulloch, M., Fallon, S. and Alibert, C. 2004. High-resolution coral records of rare earth elements in coastal seawater: Biogeochemical cycling and a new environmental proxy. Geochimica et Cosmochimica Acta 68: 2067-2080.

Zhang, J. and Nozaki, Y. 1996. Rare earth elements and yttrium in seawater: ICP-MS determinations in the East Caroline, Coral Sea, and South Fiji basins of the western South Pacific Ocean. Geochimica et Cosmochimica Acta 60: 4631-4644.

Zhang, J., Amakawa, H. and Nozaki, Y. 1994. The comparative behaviors of yttrium and lanthanides in the seawater of the North Pacific. Geophysical Research Letters 21: 2677-2680.

Table 5.1. Sources of REY samples (coral, water, sediment) used as inputs for principal components analysis.

Sample #	Sample Name (Code)	Type	Lat °S	Lon °E	Source
1	Inshore coral (RTF)	Coral	21.171	149.264	This study
2	Midshelf Coral (KIA)	Coral	20.918	149.419	This study
3	Coral Sea (St.SA7, 0 m)	Seawater	14.256	154.334	Zhang and Nozaki 1996
4	Pioneer River mouth	Seawater	21.147	149.220	M. Lawrence, unpublished data
5	Pioneer River estuary	Seawater	21.129	149.196	M. Lawrence, unpublished data
6	Lower Pioneer River (S31)	Freshwater	21.142	149.026	Lawrence et al. 2006a
7	Blacks Creek (S26)	Freshwater	21.310	148.836	Lawrence et al. 2006a
8	Owens Creek (S19)	Freshwater	21.113	148.727	Lawrence et al. 2006a
9	Finch Hatton Creek (S10)	Freshwater	21.068	148.637	Lawrence et al. 2006a
10	Upper Cattle Creek (S4)	Freshwater	21.141	148.540	Lawrence et al. 2006a
11	Mud of Queensland (MUQ)	Sediment	various		Kamber et al. 2005

Table 5.2. VARIMAX-rotated factor loadings from PC analysis. PC1 and PC2 are the first two principal components.

Element	PC1	PC2
La	0.392	0.824
Ce	-0.635	0.382
Pr	-0.388	0.893
Nd	-0.154	0.929
Gd	0.978	0.054
Tb	0.960	0.038
Dy	0.987	-0.045
Y	0.907	-0.251
Ho	0.955	0.064
Er	0.967	-0.014
Tm	0.986	-0.091
Yb	0.922	-0.224
Lu	0.802	-0.294
Eigenvalue	8.72	2.70
% Variance	67.1	20.8

Table 5.3. Concentrations of rare earth element and yttrium (REY) in the inshore Round Top Island core (RTF) for 26 years between 1950 and 2002, plus rock (W-2), sediment (MUQ) and coral (JCp-1) standards. All values are in ppb, except detection limits (DL), which are in ppt (parts per trillion). Y/Ho reported as mass ratios.

Inshore -- Round Top Island core RTF

Sample	La	Ce	Pr	Nd	Sm	Eu	Gd	Tb	Dy	Y	Ho	Er	Tm	Yb	Lu	Y/Ho
RTF Year																
1950	26.579	19.763	5.270	22.294	5.113	1.399	6.749	1.024	7.729	129.405	1.709	5.650	0.839	5.564	0.910	75.71
1951	29.461	20.871	5.979	24.450	5.309	1.427	6.820	1.135	8.128	137.959	1.921	5.713	0.911	5.929	0.971	71.81
1952	14.507	10.867	2.928	12.190	2.993	0.891	4.393	0.722	5.691	121.471	1.433	4.483	0.734	4.880	0.767	84.79
1953	23.537	15.118	4.397	19.067	4.232	1.201	6.057	0.981	7.148	141.321	1.804	5.598	0.872	5.735	0.878	78.33
1960	19.962	15.937	3.874	16.813	4.175	1.295	6.371	1.003	7.583	139.271	1.803	5.523	0.842	5.999	0.988	77.24
1961	18.263	14.731	3.670	15.978	3.927	1.156	5.969	0.994	7.294	126.984	1.691	5.097	0.821	5.909	0.976	75.08
1962	17.996	14.075	3.500	14.573	3.574	0.997	5.227	0.878	6.802	120.696	1.630	4.718	0.737	4.836	0.795	74.07
1963	19.137	14.381	3.688	15.686	3.928	1.056	5.745	0.945	7.307	127.638	1.753	5.218	0.787	5.242	0.880	72.81
1970	28.967	19.785	5.536	23.671	5.217	1.543	7.910	1.263	9.226	155.463	2.211	6.591	0.997	6.231	0.997	70.32
1971	26.565	19.664	5.030	21.267	5.072	1.434	7.349	1.179	8.395	142.652	2.076	6.037	0.943	6.182	1.029	68.72
1972	21.859	15.307	4.338	29.099	3.948	1.204	5.635	1.230	6.839	124.559	1.664	4.872	0.805	5.117	0.813	74.84
1973	31.380	21.089	5.872	25.085	5.684	1.562	8.409	1.320	9.653	153.516	2.310	6.488	1.055	6.268	1.056	66.45
1974	31.154	23.183	6.105	25.961	6.090	1.808	8.565	1.402	9.996	147.283	2.366	7.083	0.997	6.138	1.025	62.25
1980	27.029	20.794	5.391	22.695	5.421	1.605	7.954	1.284	9.602	150.782	2.358	7.100	1.064	6.661	1.072	63.95
1981	29.027	22.405	5.764	24.647	5.783	1.751	8.686	1.467	10.095	154.284	2.469	7.438	1.088	6.775	1.076	62.48
1982	25.538	19.185	4.978	20.982	5.140	1.636	7.497	1.338	9.496	142.029	2.325	6.641	0.997	6.217	0.983	61.08
1983	21.564	16.801	4.282	18.148	3.994	1.333	6.603	1.125	8.567	129.134	2.034	6.136	0.908	5.824	0.945	63.49
1984	21.697	16.552	4.212	18.028	4.385	1.316	6.457	1.083	7.995	126.542	1.929	5.825	0.816	5.341	0.847	65.59
1990	36.931	25.991	7.076	29.498	6.419	1.977	9.019	1.405	10.234	149.615	2.424	7.000	1.043	6.820	1.086	61.73
1991	67.618	42.550	12.199	49.163	9.300	2.492	11.518	1.718	11.830	167.558	2.833	8.493	1.220	7.810	1.243	59.14
1992	32.493	22.504	6.513	27.204	6.272	2.340	9.063	1.436	10.472	147.448	2.381	7.111	1.111	6.758	1.126	61.94
1993	27.418	19.960	5.321	22.758	5.355	1.631	8.091	1.328	9.633	141.204	2.281	6.615	1.014	6.773	1.136	61.91
1994	25.890	20.237	5.157	21.729	5.169	1.509	7.871	1.252	9.521	136.557	2.233	6.491	1.035	6.693	1.164	61.16
2000	29.804	23.469	5.794	24.556	5.564	1.695	8.216	1.360	9.564	142.475	2.290	7.019	1.016	6.682	1.031	62.22
2001	23.263	17.782	4.528	19.340	4.385	1.354	6.863	1.123	8.275	129.392	1.993	5.878	0.951	5.919	1.006	64.93
2002	20.229	17.018	4.002	16.882	4.055	1.231	6.486	1.026	7.723	118.909	1.889	5.167	0.816	5.400	0.879	62.93
DL*	0.043	0.025	0.024	0.013	0.085	0.014	0.149	0.026	0.136	0.267	0.004	0.019	0.009	0.041	0.003	--
JCp-1	36.333	32.886	6.485	24.433	4.850	1.214	7.499	0.970	7.076	293.684	1.807	5.562	0.776	5.446	0.789	162.51
W-2a	10548	23235	3030	12919	3260	1099	3707	615	3805	20189	802	2219	325	2044	300	25.16
W-2b	10551	23371	3043	13000	3300	1095	3732	620	3864	20316	810	2258	331	2072	304	25.07
MUQ**	32510	71090	8460	32910	6880	1570	6360	990	5890	31850	1220	3370	510	3250	490	26.11

*DL = Detection Limit. Calculated as three times the standard deviation of background levels.

**source: Kamber et al. (2005)

Table 5.4. Concentrations of rare earth element and yttrium (REY) in the midshelf Keswick Island core (KIA) for 27 years between 1950 and 2002, plus rock (W-2), sediment (MUQ) and coral (JCp-1) standards. All values are in ppb, except detection limits (DL), which are in ppt (parts per trillion). Y/Ho reported as mass ratios.

Midshelf -- Keswick Island core KIA

Sample	La	Ce	Pr	Nd	Sm	Eu	Gd	Tb	Dy	Y	Ho	Er	Tm	Yb	Lu	Y/Ho
KIA Year																
1950	3.915	4.153	0.823	3.577	0.967	0.270	1.613	0.244	1.994	77.278	0.502	1.839	0.320	2.404	0.439	153.99
1951	5.893	5.414	1.224	5.266	1.380	0.360	2.047	0.352	2.319	82.963	0.627	2.192	0.391	2.847	0.515	132.41
1952	3.741	3.775	0.850	3.982	1.084	0.256	1.528	0.262	2.190	78.591	0.507	1.728	0.310	2.351	0.476	154.94
1953	4.257	4.198	0.921	3.943	1.168	0.325	1.761	0.298	2.263	80.346	0.521	1.730	0.323	2.723	0.466	154.12
1954	5.039	4.800	1.123	4.681	1.385	0.431	1.914	0.358	2.814	82.597	0.575	2.127	0.339	2.730	0.466	143.68
1960	4.249	4.732	0.967	4.358	1.153	0.372	2.232	0.319	3.268	79.581	0.518	1.883	0.362	2.825	0.479	153.73
1961	4.662	5.000	1.049	4.606	1.411	0.320	2.478	0.324	3.273	79.796	0.500	1.685	0.342	2.480	0.397	159.49
1962	5.168	4.716	1.022	4.422	1.203	0.330	2.229	0.324	3.170	77.859	0.519	1.640	0.323	2.247	0.397	150.06
1963	4.158	3.873	0.925	3.998	1.076	0.316	2.067	0.290	3.294	79.524	0.469	1.792	0.334	2.367	0.402	169.57
1970	4.549	4.516	1.088	4.244	1.282	0.380	2.069	0.316	3.436	82.577	0.565	1.927	0.353	2.256	0.439	146.19
1971	4.424	4.632	0.948	4.164	1.221	0.322	2.155	0.314	3.220	80.408	0.541	1.877	0.327	2.481	0.447	148.62
1972	4.451	4.310	0.905	3.882	1.226	0.429	1.902	0.304	3.006	80.432	0.543	1.870	0.316	2.522	0.467	148.16
1973	3.874	3.830	0.832	3.488	1.091	0.320	1.837	0.294	2.826	81.834	0.508	1.781	0.347	2.574	0.509	161.18
1974	5.479	4.766	1.179	5.312	1.586	0.470	2.403	0.376	3.469	89.374	0.680	2.328	0.447	3.113	0.587	131.47
1980	5.212	4.771	1.035	4.935	1.355	0.340	2.204	0.308	2.994	79.818	0.539	1.810	0.347	2.635	0.472	147.99
1981	4.489	4.746	0.964	4.103	1.141	0.386	1.906	0.317	2.921	82.655	0.597	1.902	0.329	2.503	0.444	138.55
1982	5.222	4.894	1.084	5.149	1.238	0.394	2.103	0.347	2.621	80.638	0.565	2.053	0.366	2.550	0.435	142.82
1983	5.043	5.018	1.166	4.973	1.362	0.429	1.995	0.312	2.922	81.477	0.583	2.119	0.366	2.709	0.483	139.78
1984	4.948	5.051	1.074	4.508	1.339	0.376	1.783	0.300	2.483	82.118	0.499	1.922	0.340	2.380	0.501	164.53
1990	8.092	7.114	1.859	7.807	2.080	0.537	2.746	0.467	3.300	93.997	0.815	2.691	0.456	3.535	0.628	115.29
1991	5.079	5.000	1.036	5.006	1.317	0.326	2.065	0.340	2.395	83.115	0.593	2.072	0.338	2.819	0.494	140.12
1992	5.261	5.625	1.147	5.001	1.606	0.345	2.042	0.358	2.543	87.345	0.675	2.123	0.419	3.103	0.591	129.42
1993	4.740	4.369	1.024	4.311	1.320	0.382	2.078	0.350	2.555	84.954	0.571	1.982	0.363	2.880	0.533	148.79
1994	4.293	3.972	0.897	3.710	1.261	0.280	1.737	0.272	2.303	83.298	0.590	2.166	0.372	2.927	0.522	141.07
2000	5.883	6.475	1.294	5.439	1.525	0.390	2.194	0.357	2.736	85.691	0.633	2.156	0.384	2.773	0.467	135.38
2001	8.309	7.166	1.879	8.344	2.214	0.564	2.923	0.475	3.440	91.243	0.793	2.639	0.430	3.224	0.556	115.07
2002	5.817	6.208	1.219	5.257	1.346	0.429	2.030	0.330	2.356	81.120	0.612	2.073	0.373	2.468	0.478	132.52
DL*	0.279	0.664	0.061	0.476	0.072	0.050	0.459	0.029	0.731	1.061	0.006	0.025	0.027	0.038	0.004	--
JCp-1**	55.277	60.043	10.308	40.292	8.400	1.620	9.641	1.543	10.366	362.372	2.542	8.039	1.234	8.338	1.374	142.53
W-2k**	10535	23272	3040	12962	3288	1097	3719	617	3823	20192	805	2233	327	2061	301	25.09
W-2l**	10509	23170	3013	12869	3248	1091	3699	613	3795	20048	802	2213	327	2056	301	24.99
MUQ***	32510	71090	8460	32910	6880	1570	6360	990	5890	31850	1220	3370	510	3250	490	26.11

*DL = Detection Limit. Calculated as three times the standard deviation of background levels

**Average for 2 separate runs on 11 Feb and 15 Feb 2005 ***source: Kamber et al (2005)

Table 5.5. Published concentrations (ppb) of Y and Ho and Y/Ho mass ratios for (a) shale, (b) river water, (c) rain, (d) seawater, (e) microbialite and (f) coral samples.

Sample	**Y**	**Ho**	**Y/Ho**	**Source**
(a) Sediments				
Mud of Queensland (MUQ)	31850	1220	26.1	Kamber et al. 2005
Post Archaean Australian Shale (PAAS)	27027	995	27.2	Taylor and McLennan 1985
(b) River water				
Pioneer Catchment, Upper Cattle Creek (1)	9.860	0.350	28.2	Lawrence et al. 2006 MFR
Pioneer Catchment, Lower Pioneer at Dumbleton (32)	21.660	0.720	30.1	Lawrence et al. 2006 MFR
Tokyo, Japan (Edogawa-1)	0.062	0.002	31.8	Nozaki et al. 1997
(c) Rain				
Tokyo, Japan (RW-940324)	0.003725	0.000089	41.8	Nozaki et al. 1997
Tokyo, Japan (RW-950122)	0.001636	0.000054	30.1	Nozaki et al. 1997
Tokyo, Japan (RW-940324)	0.007175	0.000209	34.3	Nozaki et al. 1997
(d) Seawater				
East Caroline Basin (SA-5)	0.006499	0.000091	71.6	Zhang and Nozaki 1996
Coral Sea Basin (SA-7)	0.005797	0.000076	76.4	Zhang and Nozaki 1996
East Pacific Rise (EPR)	0.004712	0.000081	58.3	Bau et al. 1995
Western North Pacific (A-LM2)	0.005690	0.000099	57.5	Nozaki et al. 1997
Western North Pacific (LM 6/11)	0.006935	0.000129	53.9	Nozaki et al. 1997
Western North Pacific (LM 9)	0.016181	0.000203	79.8	Nozaki et al. 1997
Sagami Trough, Western North Pacific	0.006348	0.000114	55.8	Alibo and Nozaki 1999
South China Sea	0.012269	0.000246	49.9	Nozaki et al. 2000
Heron Island	0.004872	0.000115	42.3	M. Lawrence, unpublished data
Pioneer River Mouth	0.044481	0.001098	40.5	M. Lawrence, unpublished data
(e) Microbialite				
Heron Island (average)	1079.154	19.296	56.1	Webb and Kamber 2001
(f) Coral				
RTF mean	134.597	2.000	67.3	This study
KIA mean	82.616	0.579	142.6	This study
JCp-1 mean	328.028	2.175	150.8	This study

Table 5.6. Multiple regressions of total REY abundance on year and Pioneer River discharge for (a) inshore Round Top Island core (RTF; Figure 5.5a) and (b) midshelf Keswick Island core (KIA; Figure 5.5a). Total r^2 is for the regression model.

Parameter	**Regression coefficient**	**Standard error**	***p***	**Partial r^2**	**Total r^2**
A. Inshore (RTF)					
Year	1.103	0.377	<0.009	0.192	0.493
Discharge	<0.001	<0.001	<0.002	0.365	
B. Midshelf (KIA)					
Year	0.318	0.076	<0.001	0.406	0.462
Discharge	<0.001	<0.001	<0.025	0.134	

Table 5.7. Multiple regressions of Y/Ho mass ratio on year and Pioneer River discharge for (a) inshore Round Top Island core (RTF; Figure 5.5b) and (b) midshelf Keswick Island core (KIA; Figure 5.5b). Total r^2 is for the regression model.

Parameter	**Regression coefficient**	**Standard error**	***p***	**Partial r^2**	**Total r^2**
A. Inshore (RTF)					
Year	-0.367	0.042	<0.001	0.771	0.769
Discharge	>-0.001	<0.001	<0.059	0.040	
B. Midshelf (KIA)					
Year	-0.481	0.126	<0.002	0.362	0.417
Discharge	>-0.001	<0.001	<0.035	0.125	

Figure 5.1. (a) Scaled REY data from coral, water and sediment samples plotted against principal components PC1 and PC2. Dashed arrows indicate directional enrichments of different groups of elements. (b) Locations of sampling sites in and adjacent to the Pioneer catchment (blue = water; red = inshore coral).

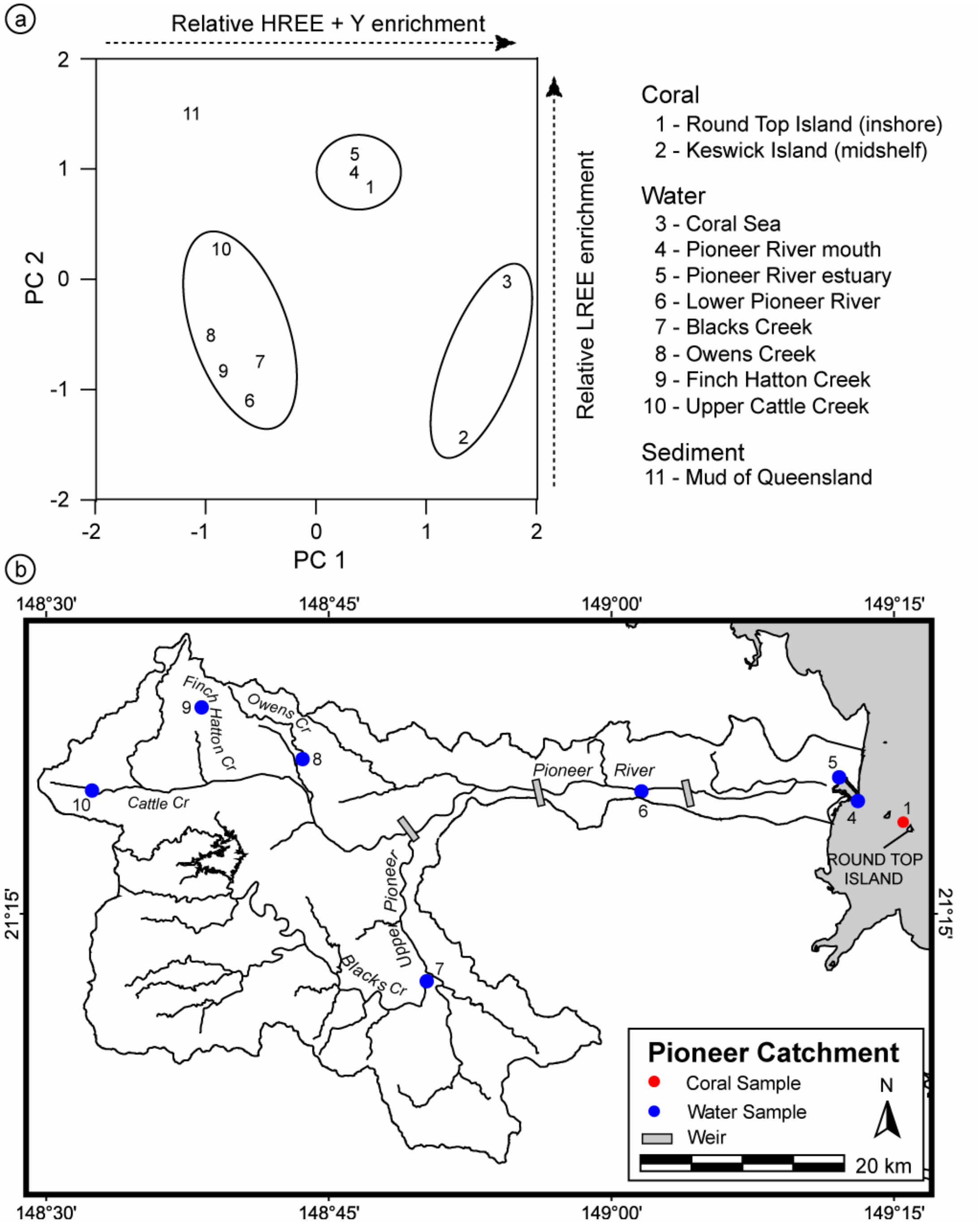a
Relative HREE + Y enrichment
Relative LREE enrichment
PC 1
PC 2
2
1
0
-1
-2
-2
-1
0
1
2
11
5
4
1
10
8
7
9
6
3
2
Coral
1 - Round Top Island (inshore)
2 - Keswick Island (midshelf)
Water
3 - Coral Sea
4 - Pioneer River mouth
5 - Pioneer River estuary
6 - Lower Pioneer River
7 - Blacks Creek
8 - Owens Creek
9 - Finch Hatton Creek
10 - Upper Cattle Creek
Sediment
11 - Mud of Queensland
b
148°30'
148°45'
149°00'
149°15'
21°15'
Finch Hatton Cr
Owens Cr
Cattle Cr
Pioneer River
Upper Pioneer
Blacks Cr
ROUND TOP ISLAND
Pioneer Catchment
● Coral Sample
● Water Sample
▭ Weir
N
20 km

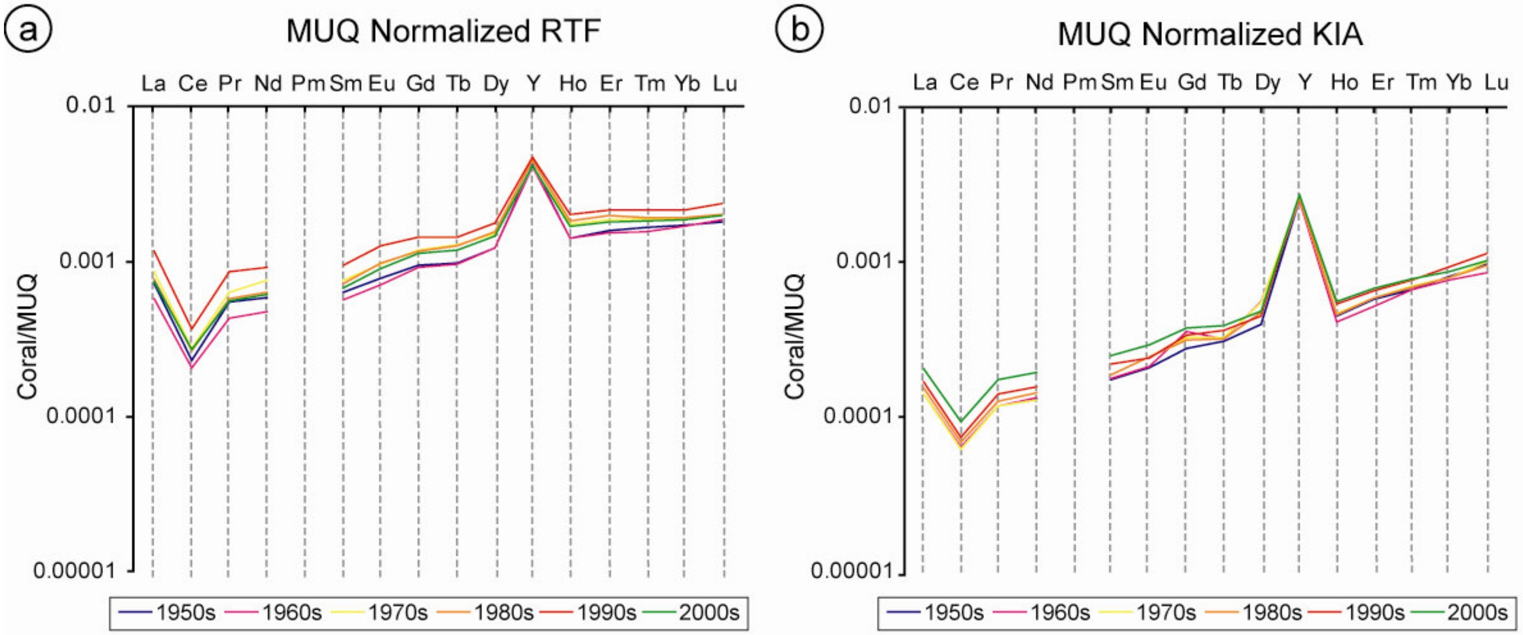

Figure 5.2. Inshore (a) and midshelf (b) coral REY normalized to MUQ, with samples grouped by decade (1950s: blue; 1960s: magenta; 1970s: yellow; 1980s: orange; 1990s: red; 2000s: green).

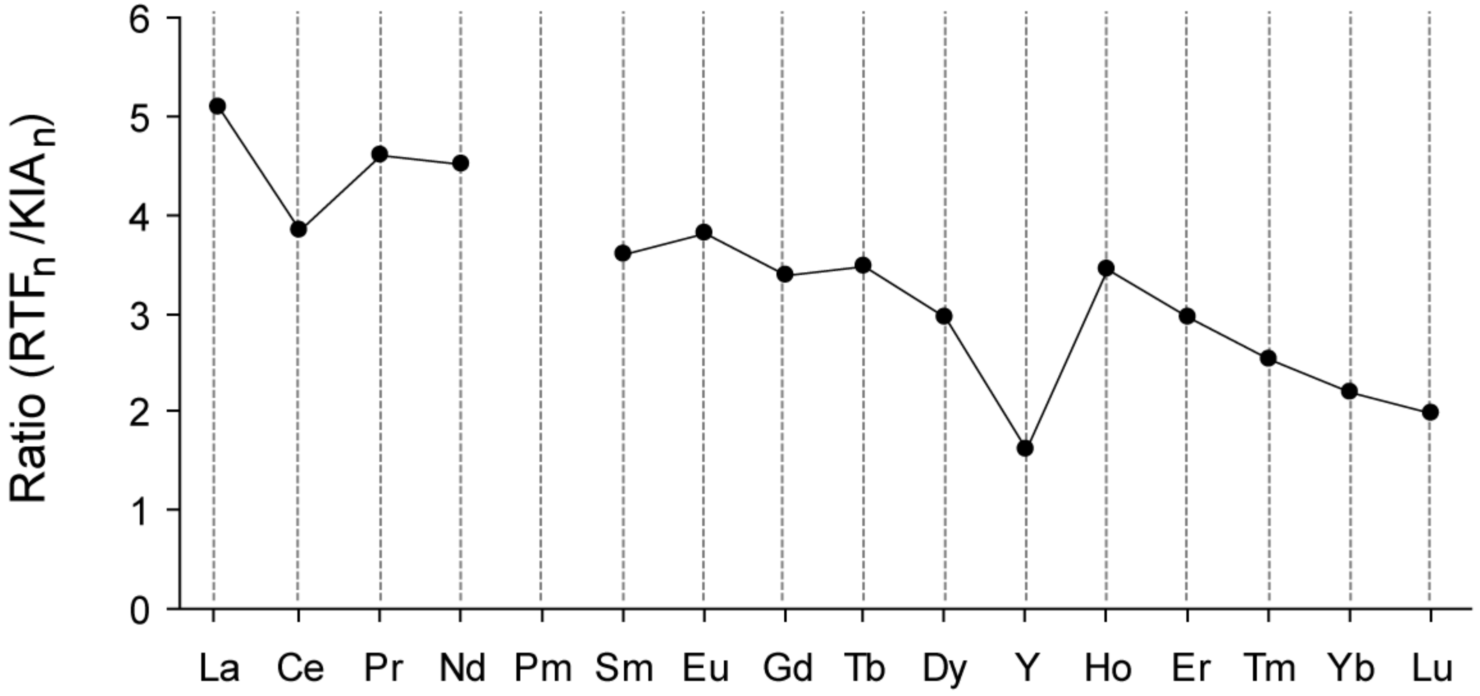

Figure 5.3. Shale-normalized inshore (RTF_n) REY data divided by shale-normalized midshelf (KIA_n) REY values.

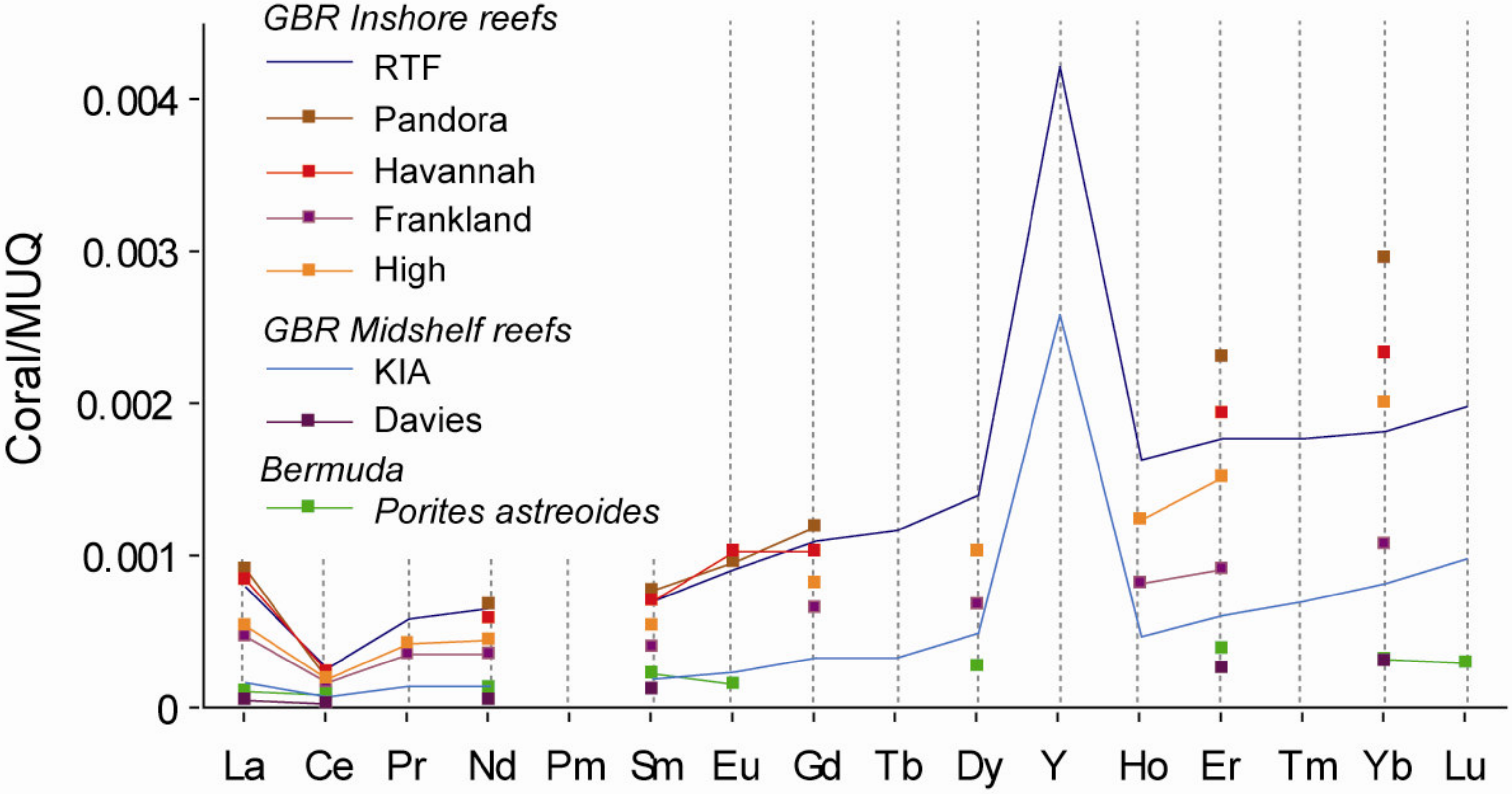

Figure 5.4. REY patterns in corals from Mackay (inshore RTF: dark blue; midshelf KIA: light blue) compared with other inshore (Pandora: brown; Havannah: red; Frankland: purple; High: orange) and midshelf (Davies: dark purple) *Porites sp.* from the Great Barrier Reef (GBR; Wyndham et al. 2004) and a *Porites astreoides* from Bermuda (Sholkovitz and Shen 1995).

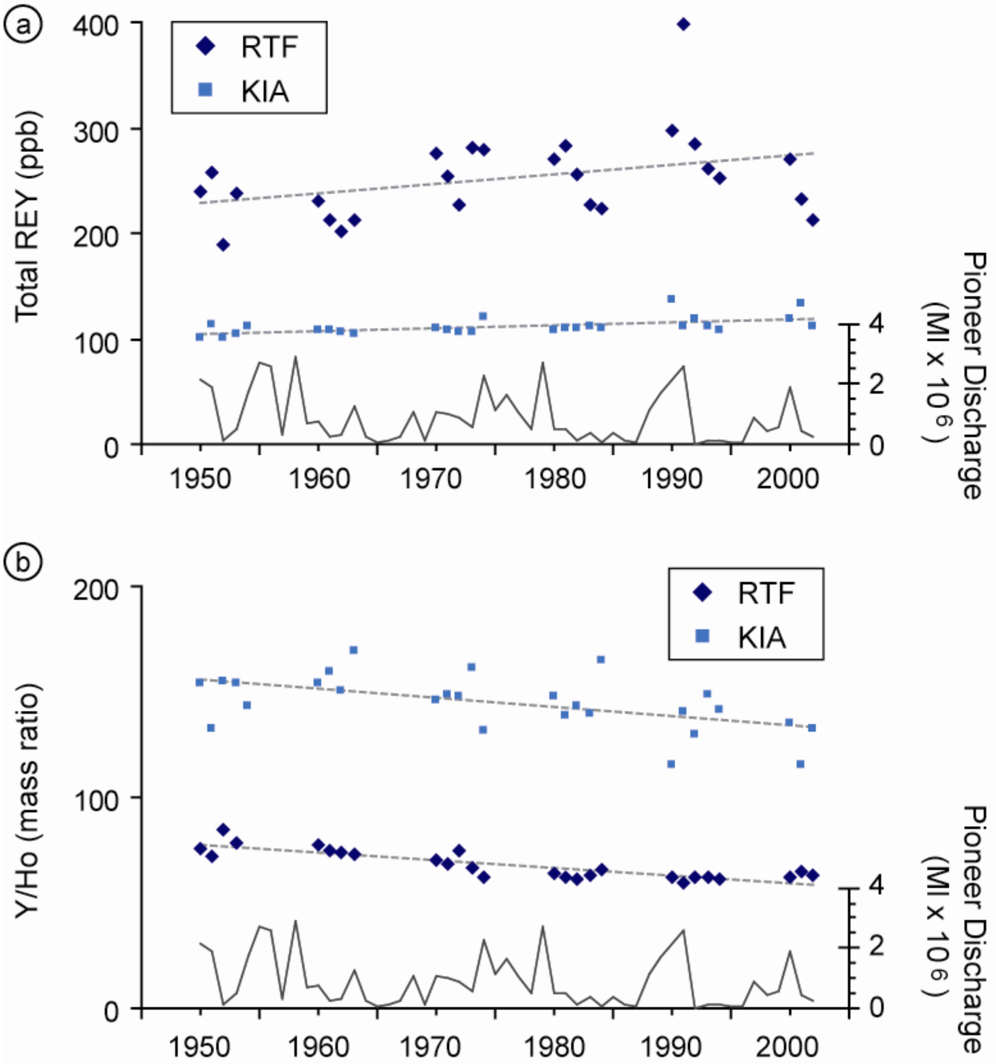

Figure 5.5. Temporal trends in (a) total REY concentration and (b) Y/Ho ratios between 1950 and 2002 for inshore RTF (diamond) and midshelf KIA (square) cores. Annual Pioneer River discharge (in megaliters) is shown with each plot.

Chapter 6. A Synthesis of Land Cover Change, Water Quality Proxies and Reef Communities: Are Mackay Coral Reefs in Jeopardy?

Introduction

Erosion and sediment delivery from drainage basins are natural processes that have occurred over millions/billions of years (Furnas 2003). While sediment supply and turbidity are limiting factors in coral reef development (Hopley 1995; Woolfe and Larcombe 1999; Smithers et al. 2006), nearshore reefs are adapted to often highly turbid conditions and, when distant from human disturbance, can be highly diverse (Figure 6.1; Veron 1995; Mallela et al. 2004; Fabricius et al. 2005). Increasing evidence (see preceding chapters) from models and empirical studies shows that land use changes since European settlement have increased the rates of sediment and nutrient delivery to the Great Barrier Reef (GBR) Lagoon. Land use changes in this region have been extensive, increasing in area and rate of change over the past 50 years because of major pressures from agriculture, grazing, mining, urban and port development, tourism and recreation (Duke and Wolanski 2001; Johnson et al. 2001). Conversion of forests to croplands causes the greatest increase in erosion rates and sediment yields, though erosion following grazing, which now dominates ~76% of all GBR catchment area, is currently the main source of sediment delivered to the GBR Lagoon (Rayment and Neil 1997; Neil et al. 2002). While it is clear that human activity has transformed the landscape of GBR catchments, the effects of land pollution on adjacent coral reefs remain largely undocumented.

To determine whether effects of land clearing on nearshore water quality can be detected against natural variation, any analysis of water quality variability must include climatic effects. Climatic effects on variation in catchment runoff and sediment yield are very pronounced in Australia: on a unit area basis, Australian rivers and streams have lower mean annual runoff and higher inter-annual variability than most other regions of the world (Gourlay and Hacker 1986; McMahon et al. 1992; Neil et al. 2002). In Queensland, the high inter-annual variability of streamflow and, to a lesser extent, wind fields, have been linked to El Niño-Southern Oscillation (ENSO) periodicity (Lough 1994). Drier, hot conditions and fewer tropical cyclones prevail during warm El Niño years, while higher rainfall, more cyclones and greater discharge occur during the cooler La Niña phase (Verdon et al. 2004; Power et al. 2005). Additionally, the negative phase of the Interdecadal Pacific Oscillation (IPO) is associated with wet conditions, that enhance streamflow, especially when in phase with coincident La Niña events (e.g. in 1949, 1954, 1955, 1970, 1971, 1973, 1975; Power et al. 1999; Verdon et al. 2004).

In the Mackay region, rapid land clearing began with European arrival in 1862 and the expansion of the sugarcane industry, while substantial losses of riparian and mangrove buffer areas have occurred mainly within the past 50 years (Chapters 2 and 3). Currently, the Pioneer River catchment is classified as “more than slightly disturbed” based on ongoing water quality surveys by the Queensland Department of Natural Resources Mines and Water (QDNRMW), in which baseflow measurements of total nitrogen (tN) generally exceeded trigger values for aquatic system protection

(Brodie 2004; Mitchell et al. 2005). While changes to terrestrial and freshwater systems in this region are well documented, several questions still need to be addressed before land use change can be linked to changes in the nearshore environment: (1) are changes in nearshore water quality associated with anthropogenic activities in the Pioneer catchment; and (2) if so, do they surpass thresholds for impacts on coral reef ecosystems?

The primary objective of this chapter is to assess how much temporal variability in freshwater runoff and suspended sediment delivery, measured from instrumental and coral proxy records, can be attributed to anthropogenic versus natural factors. I first integrate analyses of land cover changes (Chapters 2 and 3) with coral proxy records of water quality from nearshore and midshelf islands (Chapters 4 and 5) and discuss the probable drivers of change in freshwater and sediment delivery to the nearshore. I then evaluate whether water quality changes are related to present day conditions in coral communities and reefs surveyed along a gradient of distance offshore from the Pioneer River mouth. These results, in conjunction with recent catchment water quality evaluations (e.g. Brodie 2004; Rohde et al. 2006), will be used by regional management bodies to assess the relative risks of impacts from discharges of the Pioneer and adjacent rivers. With this information, managers can prioritize targets for rehabilitation to meet the stated goal of the State of Queensland and Commonwealth of Australia’s (2003) Water Quality Protection Plan to “[halt] and [reverse] the decline in water quality entering the Reef within 10 years”.

Methods

Rainfall, river discharge and coral proxy records

I compiled a record of Mackay rainfall data (in mm) between 1870 and 2006 from daily precipitation readings taken at Bureau of Meteorology (BOM) stations: the Mackay Post Office (January 1870-December 1987; station 22046; 21.1500 ºS, 149.1833 ºE; 11 m); and the Mackay Meteorological Office at Mt. Bassett (January 1959-present; station 33229; 21.1172 ºS, 149.2169 ºE; 30 m). I also used rainfall records from BOM station 33016 at Dalrymple Heights in Eungella (July 1938-present; 21.1317 ºS, 148.4922 ºE; 680 m) to compare relationships between discharge and precipitation records collected at opposite ends of the Pioneer River catchment. I constructed a composite record (details described in Chapter 4) of Pioneer River flow (in megaliters) from recorders at Pleystowe Mill (October 1916-August 1978) and Mirani weir (November 1977-November 2003).

I used the Mackay rainfall data to estimate the relationship between rainfall and discharge from 1916 to 2003, since no data from Dalrymple Heights existed prior to 1938. I used the Dalrymple Heights dataset, which has a higher correlation with discharge, to assess changes in the discharge to rainfall ratios since 1952, which I then compared with proxy records of fluvial discharge measured from coral luminescence records. Quantitative luminescence was measured by G. Marion (University of Queensland) for RTC, KIC and SCC cores (collected in 2004; Table 4.2) using a luminometer at the Australian Institute of Marine Sciences (AIMS), which illuminates the coral at 390 nm and records emission intensities at 490 nm in 0.25 mm increments along a slabbed core. Further details on the instrument and protocol are in Barnes et al. (2003). Details on coral core collection and slab preparation are in Chapter 4.

I measured Ba/Ca and Y/Ca ratios in corals at high-temporal resolution using laser ablation inductively coupled mass spectrometry (LA-ICP-MS), and used these data as proxies for sediment delivery to the nearshore. Details of instrumentation, data processing and coral chronology construction are in Chapter 4. I excluded the years 1983 and 1992 from analyses of Round Top Island core (RTF) Ba/Ca data because of anomalously high Ba/Ca peaks probably related to stress induced by El-Niño-Southern Oscillation (ENSO; Chapter 4). For analyses of Y/Ca records in RTF, I excluded 1981 and 1982 data because the maximum weekly Y/Ca in RTF values were anomalously high compared to values from RTC. While some variation between individual colonies is expected, these exceedingly high values in years with minimal runoff are more likely due to contamination from organic material inclusions that were not removed by laser pre-ablation.

Statistical analyses

To determine how variable rainfall influences discharge magnitude, I correlated total annual rainfall with total annual discharge, using the sum of weekly values between November of the preceding year and October of the listed year to include late spring-early summer rains as part of the wet season. I then focused on years with the largest positive and negative residuals from best fit linear regressions to identify factors that may have influenced large deviations from expected values. I also correlated maximum weekly values of Ba/Ca and Y/Ca (for each year) with log transformed maximum weekly discharge, then used years with large positive residuals to identify potential sources of short-term (<2.5 year) variation in delivery of trace elements to the nearshore. The discharge values were log transformed because the raw values spanned three orders of magnitude, and I assessed the significance of all correlations using Pearson's coefficient. I performed power spectrum analyses in MATLAB on linearly detrended, weekly data for (untransformed) Pioneer River discharge (Oct 1916-Nov 2003), wind speed (Aug 1959-May 2003; see Chapter 4 for details), and Ba/Ca and Y/Ca from the Round Top core RTF (Jan 1946-Nov 2004) to identify dominant, longer-term (≥2.5 year) periodicities in the core data that were likely to be related to environmental factors varying over similar temporal scales.

To assess temporal changes in runoff ratios that might reflect land cover changes (Haynes et al. 2001), I performed linear regressions of annual discharge (normalized to annual rainfall) versus year, and compared these trends to those from linear regressions of maximum annual coral luminescence intensity (using Nov-Oct years) versus year for each coral record. To determine whether temporal changes in trace element ratios (Ba/Ca, Y/Ca) were related to land use changes, I first normalized the maximum weekly Ba/Ca and Y/Ca records (from inshore corals RTF and RTC) to log transformed maximum weekly Pioneer discharge for each year to remove variation due to discharge magnitudes (related to climate variability). I then compared the remaining directional trends with the timing of trends in records of riparian zone loss (Chapter 2), tidal mangrove area loss (Chapter 3), and histories of alteration to catchment water storage obtained from the literature. All statistical analyses were performed with SYSTAT v. 10.2 software.

Benthic habitat data collection

During 6-13 March 2006, 44 transects were scored for benthic cover composition at five locations along a gradient of distance offshore from the Pioneer River mouth (Figure 6.2; Table 6.1). Transects were grouped: from Keswick and St. Bees Islands; and from Big and Little Kindemar Reefs in the Pompey Complex. At least six transects were surveyed at each location. Selection of transect locations was generally random within two constraints: (1) sites should contain hard corals to enable simultaneous assessments of incidence of coral bleaching; and (2) sites should be representative of relatively large areas to enable field validation for remote sensing analyses. All transects were within shallow water (1 to 7 m depth) and parallel to the edge of the reef flat. For surveys of the coral community (c.f. Wainright 1965; Buddemeier and Hopley 1988) at Round Top Island, which has no true reef flat, transects were laid parallel to the beach. Surveys at Scawfell Island were in Refuge Bay, which has the most extensive fringing reef development at this location (Kleypas and Hopley 1992). I used a line intercept method (Ohlhorst et al. 1988) to score every 0.5 cm along a 20 m transect tape for one of the six dominant categories: live hard coral; soft coral; turf algae/crustose coralline algae (CCA); macroalgae; sand, dead coral rubble or consolidated pavement; and other. The "other" category was dominated by giant clam (*Tridacna gigas*) and encrusting sponges, with minor contributions from large mollusks (e.g. *Trochus* sp.), hydroids, anemones, and ascidians, particularly at the outer reef. I compared gross differences in benthic habitat cover along the distance gradient with previous surveys from the Mackay-Whitsunday region and other nearshore environments on the Great Barrier Reefs to assess potential anthropogenic impacts. A more rigorous assessment of benthic habitat and coral communities (from photographs taken along each transect) will be presented in a future publication.

Results and Discussion

Changes to runoff

As discussed in Chapter 2, studies from around the world have documented increased surface runoff following clearing of natural vegetation, particularly forest, due to reduced evapotranspiration and infiltration (Douglas 1967; Likens et al. 1970; Pimentel et al. 1993; Pimentel et al. 1995; Sahin and Hall 1996; Costa et al. 2003). For example, after total deforestation of a watershed at the Hubbard Brook Experimental Forest (New Hampshire, USA), streamflow increased by 39% in the first year, and by 28% in the second year above expected values (Likens et al. 1970). Similarly, annual mean and rainy season discharge of the Tocantins River, Brazil increased by 24% and 28%, respectively, during a period in which agriculture expanded by ~19% within the catchment (Costa et al. 2003). In addition to increasing volume of discharge, catchment clearing can result in increased runoff frequency, higher maximum runoff rates and higher runoff ratios (discharge/rainfall) compared to adjacent, uncleared areas (Lawrence and Thorburn 1989).

For the Pioneer River catchment during the period where discharge records are available (1916 to present), runoff was highly variable, but there was no long-term trend in ratios of discharge-to-rainfall (Figure 6.3a). Several factors may explain the high variability. First, runoff volume is affected by soil saturation in the catchment and by scour from previous floods. Depending on the magnitude, duration and intensity of a storm event, drought-breaking rains may result in less runoff (though higher sediment yield) due to increased infiltration into the soil (Gourlay and Hacker 1986). Years with the most negative discharge residuals (1963, 1986, 1996, 1928, 1968) in the comparison of Pioneer River discharge and Mackay rainfall (Figure 6.3b) all followed periods of below-average rainfall lasting for two to six years. By contrast, a catastrophic flood with high intensity rainfall, or a rapid series of large floods may alter gully and stream hydrology by widening banks through erosion and scour, which may lead to more frequent and higher magnitude flooding than predicted from rainfall alone (Burkham 1981). After an unseasonably wet year in 1950, 1100 mm of rain fell in four days in the Pioneer catchment in 1951 (Rolleston 1987), and this resulted in higher than expected discharge. Other years with high positive discharge residuals (1991, 1955, 1947, 1946; Figure 6.3b,c) also followed periods of intense rainfall and high discharge. This suggests different flood frequency curves should be developed based on the recent history of dry or wet years (Pickup and Warner 1976).

Second, localized variation in precipitation can cause very different flow rates and suspended sediment concentrations from the same total rain falling in areas with different land uses (Mitchell et al. 2005). While annual Mackay rainfall and the composite Pioneer River discharge from 1916 to 2003 were correlated ($r = 0.80$, $p < 0.001$; Figure 6.3b), Mackay has lower mean annual rainfall and a slightly different pattern of monthly precipitation than Dalrymple Heights. Annual rainfall at Dalrymple Heights, at the head of the Cattle Creek sub-catchment with steep slopes and heavily cultivated flats, had a stronger correlation with the composite Pioneer discharge ($r = 0.92$, $p < 0.001$; Figure 6.3c).

Third, variable runoff ratios are also likely to reflect changes in intensity of land use practices and clearing in the catchment. Rapid clearing and expansion of the sugarcane industry followed the end of WWII, when soldiers returned to farms and new machinery became available (Rolleston 1987). Burning paddocks before harvesting increases surface runoff rates (and erosion) through reduced infiltration (Thornes 1980), and may have contributed to a large increase in Pioneer River discharge rates relative to rainfall through the mid-1950s. The generally lower discharge to rainfall ratios from the mid-1990s may reflect the switch to green cane harvesting and trash blanketing (GCTB) methods. For instance, 1995 had nearly comparable rainfall to 1946 and 1947, but the discharge-to-rainfall ratio was only ~6% of the post-WWII values.

Fourth, some changes to discharge volumes stem from anthropogenic alteration of the catchment's water storage system. Three weirs at Marian, Dumbleton and Mirani (constructed in 1952, 1982 and 1987 respectively) plus two dams at Kinchant and Teemburra (built in 1977 and 1997) can store 226,400 Ml of water (~25% of mean total annual runoff), primarily for irrigation (Gourlay and Hacker 1986; QDNRM 2001; Brodie 2004). Teemburra Dam has had major effects on the downstream hydrology and habitat condition of Teemburra Creek by reducing flows (QDNRM 2001), but it is unlikely to have greatly affected overall Pioneer River discharge, since Teemburra Creek is a tributary of the Upper Pioneer River, and the Upper Pioneer River contributes <20% of total runoff volume (Credlin 1973). Although Kinchant Dam falls within the boundaries of Sandy Creek catchment, it is filled with water pumped from the Pioneer River through the Mirani diversion, constructed in 1982 (Gourlay and Hacker 1986). This diversion of Pioneer River water to Kinchant Dam and the regulation of river flow at the weirs are more likely to have altered downstream discharge volumes since their construction, particularly during dry years when irrigation demands increased.

Runoff trends can also be found in coral skeletons, using two types of proxy records that have previously been correlated to river discharge from northeast Australia: coral luminescence; and coupled $\delta^{18}O$ and Sr/Ca measurements. The position and intensity of luminescent bands in coral skeletons correlate strongly with the timing and magnitude of fluvial discharge (Isdale 1984; Lough et al. 2002; Barnes et al. 2003; Hendy et al. 2003; Barnes and Taylor 2005). Reducing salinity by only ~1-2‰ causes structural changes within the coral skeleton, such as variations in pore sizes and skeletal crystals, that produce narrow luminescent bands when illuminated with UV light (Barnes and Taylor 2001; Lough et al. 2002). The intensities of these bands in the cores decrease with increasing distance from land, which is consistent with dilution of the signal with distance (Barnes and Taylor 2001; Lough et al. 2002; Barnes and Taylor 2005). Maximum annual luminescence intensities from Mackay cores have declined significantly since 1952, at approximately the same rate, at all sites (Round Top: $r^2 = 0.214$, $p = 0.003$; Keswick: $r^2 = 0.175$, $p = 0.01$; Scawfell $r^2 = 0.289$, $p < 0.001$; Figure 6.4a). Over the same time interval, the ratios of annual discharge to (Dalrymple Heights) rainfall also declined significantly ($r^2 = 0.211$, $p = 0.02$; Figure 6.4b). These declines over the past half century are consistent with several other changes: (1) most land clearing in the Pioneer catchment occurred during the late-19th century to early 20th century and there has been considerable regeneration of vegetation in parts of the catchment since then (see Chapter 2); (2) the regional climate during the past two decades has been notably drier than during the 1950s and 1970s; and (3) in the past 10-15 years, harvest practices have shifted from tilling and burning to GCTB with minimum tillage, which increases water infiltration into soils and reduces runoff.

While fifty years may be too short to determine the relative impacts of environmental versus anthropogenic factors on runoff volumes from the Pioneer catchment, both kinds of factors are likely to influence discharge to rainfall ratios and coral luminescence to some degree. To determine whether, and to what extent, early catchment land clearing affected runoff rates, modern luminescent banding intensities must be correlated with discharge records and then the relationship can be used to estimate pre-clearing discharge volumes (before stream gauging began). However, luminescence intensities, like other coral proxies for suspended sediment delivery (Chapter 4), are influenced by a combination of fluvial discharge magnitude, wind speed and wind direction during plume dispersal (Marion et al. 2006). Wind conditions were not recorded in Mackay prior to 1959, so there will always be some error associated with using luminescence to estimate discharge.

A second, more labor-intensive coral proxy of past runoff magnitudes relies on coincident, high-precision measurements of $\delta^{18}O$ and Sr/Ca. Both $\delta^{18}O$ and Sr/Ca are influenced by temperature, but only $\delta^{18}O$ is also influenced by reduced salinity from floodwaters (McCulloch et al. 1994). As salinity drops, the seawater signal incorporated in the coral skeleton becomes more negative with addition of $\delta^{18}O$-depleted freshwater ($\delta^{18}O = \sim -7$ to -8), and the resulting $\delta^{18}O$ temperature records subtracted from Sr/Ca temperature records (converted to $\delta^{18}O$ equivalents) can be used to estimate volume of river runoff (McCulloch et al. 1994). Using this method, McCulloch et al. (2003) found depletion of the $\delta^{18}O$ of coral records from the Burdekin region between 1850 and 1870. Although this period coincides with regional climate changes at the end of the Little Ice Age (Hendy et al. 2002), the timing of the $\delta^{18}O$ shift may alternatively reflect increased runoff following initial European land clearing (McCulloch et al. 2003).

Variability in proxy records of sediment delivery

Factors that introduce variability in coral proxies (Ba/Ca, Y/Ca, total REY) of suspended sediment delivery include: (1) catchment and climatic processes affecting annual sediment yield; (2) marine and oceanographic effects influencing the fate of sediments and dissolved tracers in the nearshore; and (3) coral effects (e.g. differences in skeletal architecture, tissue thickness, and cellular metabolism) that may influence the rate of trace element uptake and cause variation among colonies and among species. Categories 2 and 3 were discussed at length in Chapter 4. This section focuses on natural and anthropogenic changes within the Pioneer catchment that may have contributed to the long-term trends (or lack thereof) in trace element records of suspended sediment delivery to the nearshore.

The periodicity of climatic cycles in northeastern Australia strongly influences the frequency and magnitudes of floods and high winds (associated with cyclones) along the GBR (Lough 1994). The Southern Oscillation Index (SOI), a measure of ENSO strength, and IPO cycles strongly overlapped during some periods in the 20th century: when positive SOI coincided with negative IPO in the 1950s and 1970s, they produced very wet decades and high runoff from Queensland rivers (Power et al. 2005). The dominance of these climatic signals probably generated the strong ~19.5 year spectral cycle in the Round Top Island Ba/Ca data (1946 to 2003; Figure 6.5a). A strong ~19.5 year peak was also present in the Mackay wind data (1959 to 2003; Figure 6.5b) that cover a similar time interval, but it was much weaker in the Pioneer River discharge data (1916-2003; Figure 6.5c) that include the early 20th century when both the SOI and IPO had longer periodicity and weaker overlap (Power et al. 1999). The ~19.5 year cycle was absent in the Y/Ca record (Figure 6.5d), which instead had a high density spectral peak at approximately decadal intervals. This cycle seems to coincide with the decadal mode identified from long-term dendroclimatic records of the SOI (Lough and Fritts 1985; Brassington 1997), but because this mode has not been identified in most twentieth century reconstructions of the SOI (Brassington 1997), the coral may have responded to some other decadal environmental signal.

The inshore Ba/Ca and Y/Ca records both had spectral density peaks at approximately 4 and 2.5 year intervals (Figures 6.5a,d) corresponding to recognized quasi-quadrennial and quasi-biennial cycles of ENSO events (Rasmusson et al. 1990; Zhang and Casey 1992; Jiang et al. 1995; Brassington 1997), and suggesting that these ratios also reflect higher frequency, climatic events. Non-El Niño periods on the GBR are associated with increased rainfall, river flow, and cyclone frequency, plus higher levels of resuspension and coral disturbance from wind-generated waves (Done 1992; Lough 1994), all of which may affect Ba/Ca and Y/Ca availability. Maximum weekly Round Top Island Ba/Ca was significantly correlated with maximum weekly Pioneer River discharge ($r = 0.581$; $p < 0.001$; Figure 6.6a), and the RTF Ba/Ca record had a high spectral density peak at annual frequency (Figure 6.5a). Round Top Y/Ca was less strongly correlated with discharge ($r = 0.357$; $p < 0.01$; Figure 6.6b), and had a minor spectral peak at annual frequency (Figure 6.5d), so it may be more sensitive to wind and/or land use factors.

Some shorter-term variation in the correlations of Ba/Ca and Y/Ca with discharge may be explained by annual differences in catchment sediment storage. During dry years, the pool of sediment tends to increase within a catchment, resulting in greater sediment delivery after drought-breaking floods (Sinclair 1999; Neil et al. 2002; Alibert et al. 2003; McCulloch et al. 2003; Amos et al. 2004; Sinclair and McCulloch 2004). High rates of catchment erosion from pre-clearing periods have also been associated with drier periods, when vegetation cover would have been reduced (Thornes 1980; McCulloch et al. 2003). The height of Ba/Ca peaks associated with drought-breaking floods in the Burdekin River catchment indicate almost twice as much sediment delivery as would have been predicted from the regression across all years since European land clearing (McCulloch et al. 2003). This effect would be enhanced by rain in early November or December, which causes more erosion than storm events of similar magnitude later in the wet season (Bonnell 1988; Yu and Neil 2000; Neil et al. 2002). While Mackay rainfall in 1967 and 1971 was below or near the mean annual value, early rains at the start of the wet season in November and December 1966 and 1970 may have contributed to elevated Ba/Ca and Y/Ca values (Figure 6.6a,b). Large, infrequent storms may also enhance sediment delivery in succeeding years by mobilizing sediment from the catchment slopes to the floodplains where it can be progressively eroded by successive flows (Thornes 1980): e.g. major floods in 1964 in Oregon were followed by substantially increased sediment delivery in several successive years (Anderson 1970). This process may have contributed to higher than expected Ba/Ca peaks from Round Top Island in 1956 and 1991, and Y/Ca peaks in 1977 and 1979 (Figure 6.6a,b).

The Y/Ca record from Round Top Island (1946 to 2002) indicates a general increase in discharge-normalized values through the 1960s, high values through the 1970s, and generally lower values from the 1980s to present (except for above average values in 2000 and 2001; Figure 6.7a). Some of these variations may have been influenced by anthropogenic activities within the catchment, since alterations to catchment hydrology can affect sediment storage and yield (Gourlay and Hacker 1986; Walling 2000; Neil et al. 2002; Furnas 2003). Many agricultural drainage networks and river channels, such as those within the Pioneer River Estuary (see Chapter 3), have been engineered to prevent flooding. Where sediments and nutrients from overwash would previously have been trapped along the floodplain, they now bypass the former deposition zones (Furnas 2003). However, the training walls lining the lower reaches of the Pioneer were constructed in the late 19th and early 20th centuries (see Table 3.1), so these modifications should not have changed sediment delivery rates after 1946.

Dam and weir construction tend to increase catchment sediment storage and decrease yields to the nearshore (Walling 2000). Worldwide, more than 40% of river discharge is now interrupted by impoundments, causing global sediment retention in reservoirs to exceed 50% of the flux from catchments to the sea (Vorosmarty et al. 2003). Since construction of Mirani weir in 1987, sedimentation has filled 1000 Ml (~18%) of its water storage capacity (QDNRM 2001). Although this primarily affects the coarse-grained bedload rather than the fine-grained suspended load (Neil et al. 2002; Amos et al. 2004), the construction of two weirs during the 1980s may also have contributed to below expected sediment delivery and consequently lower Y/Ca relative to discharge.

Some variation in nearshore coral Y/Ca records of sediment delivery and weathering may be attributed to land cover change. First, while Y/Ca to discharge ratios increased following post-WWII land clearing (Figure 6.7a and 6.8d), the baseline before this agricultural expansion is unknown and needs to be established before any conclusions can be drawn. Second, I predicted high Y/Ca to discharge ratios during periods following rapid loss of riparian and mangrove areas (e.g. late-1970s to late-1980s; Figure 6.8). While discharge-normalized Y/Ca values were high in 1978 and 1979, they fell shortly thereafter (Figure 6.7a and 6.8d). Increased erosion from the cleared upstream riparian areas may have been offset by effects of the newly constructed weirs, the diversion to Kinchant Dam, and higher catchment sediment storage during the early 1980s which coincided with well below average rainfall. From existing data, fluctuations in the Y/Ca signal cannot be separated into relative gains and losses from these different influences, and consequently, it is difficult to demonstrate a direct link between vegetation loss and proxies of sediment delivery during this period. Third, the timing of the recent upswing in Y/Ca to discharge values occurred after several years of mangrove dieback. Because it takes several years for the root systems to decompose, increased erosion and scour from the estuary (accompanied by decreasing area for sediment deposition) may have been delayed for several years until the first major flushing in 2000. This effect has been termed the “historical hangover”, in which increased sediment yield following vegetation loss occurs several years later, and only after the soil-binding root systems have degraded (Douglas 1967). To demonstrate this link, it would be necessary to have evidence of significantly greater erosion from mangrove dieback regions, which could be addressed through profile measurements of environmental radionuclides, such as cesium-137 (^{137}Cs) and lead-210 (^{210}Pb), which have previously been used to identify erosional zones in cultivated lands (Walling and He 1999) and depositional zones in estuaries (Alongi et al. 2004).

Unlike the Y/Ca to discharge records, no temporal trends were detected in the ratios of annual maximum weekly Ba/Ca to discharge since 1946 (Figure 6.7b and 6.8d). This may be because Ba/Ca magnitude is more correlated to fluvial discharge and is, therefore, more influenced by climatic effects (see above). Alternatively, if phytoplankton blooms first take up large quantities of barium, then the height of the barium peaks from corals in the Mackay region may not be proportional to, nor synchronized with, sediment loads and therefore may not reliably record changes in sediment delivery within the Pioneer catchment. Preliminary results from annual skeletal δ^{15}N isotope measurements from a ~2 m core collected from Round Top Island include a distinct enrichment, beginning in the 1950s, that probably reflects increased nutrient loading in fluvial discharge (G. Marion, personal communication). Nitrogen-depleted areas of tropical and subtropical oceans are particularly vulnerable to nitrogen increases in river runoff, which initiate large phytoplankton blooms that, with increased frequency, may alter coastal marine ecosystem structure (Beman et al. 2005). Temporal patterns of elevated coral Ba/Ca (see Figure 4.6e) coincided with periods of δ^{15}N enrichment since 1946 (Marion et al. 2006). This relationship suggests that Ba/Ca ratios may reflect coastal productivity in the nearshore Mackay region. Testing this hypothesis will require measurements of changes to seawater Ba/Ca and dissolved nutrients through bloom and flood events that can be compared to ambient values.

In summary, the nearshore coral records of Y/Ca and Ba/Ca between 1946 and 2003 appear to be more influenced by climatic variations than by changes to Pioneer catchment land cover. Though there are periods in which changing values of Y/Ca relative to discharge coincided with anthropogenic activity and land cover changes within the catchment, the connection does not prove causation. More evidence would be required, specifically linking higher sediment delivery with higher ratios of Y/Ca to discharge. Such data can be gathered by deploying long-term loggers that record suspended sediment concentrations (SSCs), salinity, SSTs and tidal strength adjacent to *Porites* colonies to assess the corals' responses to high frequency variation in these environmental factors during both discharge and baseline conditions (C. Storlazzi, personal communication). Data from such instruments have been used to describe sediment resuspension and transport patterns in reef waters (Ogston et al. 2004), but not yet to refine relationships between turbidity and trace element incorporation in corals. In addition, while increases in total REY may be linked to increased catchment erosion (Chapter 5), and while the rate of increase is approximately three times greater at Round Top Island than at Keswick Island (Figure 6.8e), it will be necessary to determine if the trend still exists when all data gaps are sampled and when the record is extended back prior to European settlement.

Water quality and reef condition

Sedimentation, turbidity and fluvial discharge are major factors invoked to explain the evolution and distribution of nearshore reefs on the GBR (Done 1982; Kleypas 1996; Larcombe and Woolfe 1999; Woolfe and Larcombe 1999; Neil et al. 2002). Sediment can affect individual corals by: (1) reducing light penetration, which reduces the capacity of zooxanthellae to photosynthesize and the ability of corals to calcify; (2) physically smothering tissues, which may kill small recruits and reduce calcification of larger colonies, if energy is allocated to sediment clearing mechanisms rather than growth; and (3) reducing fecundity (see reviews in Rogers 1990 and Fabricius 2005 and references therein). Reefs that experience low hydrodynamic energy but chronic high sedimentation are more affected by settling particles, while reefs under high hydrodynamic stress, which increases particle resuspension, suffer greater impacts from light attenuation (Kleypas 1996). Freshwater flood pulses reduce photosynthesis (Moberg et al. 1997), followed by bleaching and mortality in prolonged periods of reduced salinity (Goreau 1964; Jokiel et al. 1993). There is growing concern that reef ecosystems and coral communities that are repeatedly disturbed by changing levels of freshwater, sediments and associated nutrients may be modified in ways that prevent recovery to healthy conditions (Furnas 2003). Yet, relatively few studies can cite direct causation between water quality degradation and changes to reef ecosystem state, and these tend to be examples with point-sources of eutrophication (Smith et al. 1981; Rose and Risk 1985; Loya 2004) or sedimentation (Cortes and Risk 1985).

Along natural and anthropogenically enhanced water quality gradients, scleractinian corals living closest to terrestrial and fluvial sources are generally characterized by: (1) high rates of partial mortality; (2) low rates of recruitment; (3) reduced skeletal density; (4) decreased tissue thickness; and (5) reduced depth distributions (van Woesik 1992; Kleypas 1996; Barnes and Lough 1999; van Woesik et al. 1999; Nugues and Roberts 2003; Fabricius et al. 2005; Fabricius 2005; Restrepo et al. 2006). These changes in coral communities are often associated with: increased algal cover (van Woesik et al. 1999; Fabricius et al. 2005); increased abundance and rates of bioerosion by macroborers (Sammarco and Risk 1990; Risk et al. 1995; Tribollet and Golubic 2005); and reduced octocoral abundance and diversity, particularly from zoothanthellate clades (Fabricius et al. 2005; Fabricius and McCorry 2006). Along the nearshore GBR, a study comparing community characteristics from the reefs adjacent to the highly agricultural Wet Tropics catchments and the more pristine Princess Charlotte Bay catchments found three major response variables (macroalgal cover, octocoral richness, abundance of sensitive hard coral species) that were significantly correlated with a water quality index, constructed by normalizing and summing twelve water quality variables that were sampled nine times from each reef location (Fabricius et al. 2005).

In complex ecosystems such as coral reefs, where multiple stressors (e.g. coral bleaching, overfishing, crown-of-thorns outbreaks, land pollution) have interactive effects, it is extremely difficult to prove, with traditional statistical techniques, that water quality change has caused changes in benthic habitat state (Fabricius and De'ath 2004). Documenting water quality effects from diffuse, broad-scale sources like catchment land use change may require different methodologies to evaluate changes in coral reef ecosystem health. One approach is to determine if there is a mismatch between present reef-building capacity and Holocene reef framework that increases along a gradient of declining distance from a river source (van Woesik and Done 1997; van Woesik et al. 1999). van Woesik et al. (1999) suggested that the limited reef-building at Calf Island and Pine Island in the Whitsunday Group was associated with recent increases in suspended particulate matter and nutrients delivered to Repulse Bay by the Proserpine and O'Connell rivers. However, this technique does not distinguish between effects of terrestrial runoff and other possible effects suggested by Smithers et al. (2006), such as: reduced flushing from Repulse Bay following closure of the Holocene high-energy window, when outer barrier reefs caught up with sea level (Hopley 1984); and changes to SSTs and aragonite saturation state associated with global warming that may have increased disturbance from bleaching and decreased calcification rates (Hoegh-Guldberg 1999; Kleypas et al. 1999).

Alternatively, Fabricius and De'ath (2004) used a creative approach to pinpoint ecosystem effects specifically from water quality. Borrowing techniques from epidemiology, the authors used a matrix to cross-correlate ecological attributes (e.g. benthic cover, species richness) with eight criteria (e.g. effect size, logical time sequence, consistency with other studies, specificity of response) for assessing causality between water quality and ecosystem state (see Table 4 in Fabricius and De'ath 2004). Using inshore reef ecosystem data from the Wet Tropics and Princess Charlotte Bay as an example, they found strong causal links between high nutrient loads and high macroalgal cover, as well as low octocoral diversity (Fabricius and De'ath 2004). Although hard coral cover was twice as high on Princess Charlotte Bay reefs, the epidemiological framework suggested that the difference may be related to site-specific differences in exposure to other disturbances (e.g. coral bleaching, predation by crown-of-thorns seastar; Fabricius and De'ath 2004).

Habitat surveys along the inshore to offshore transect from Mackay documented distinct differences in benthic substrate cover. In general, current benthic habitat composition in the Mackay region reflects expected inshore to offshore trends in hard coral, octocoral and algal cover. Sites within ~30 km of the coast (Round Top, Keswick and St. Bees Islands) had low mean hard coral cover (7-8%), versus 33-35% at sites further offshore (Derwent Island, Pompey Reefs; Figure 6.9a; Table 6.2). The inshore coral community at Round Top Island is dominated by rubble, pavement and sand, with higher densities of corals on the northwestern side of the Island; it is composed largely of encrusting and foliose species (e.g. *Turbinaria* spp.) and highly lobed, massive *Porites* (Figure 6.10a). Although rigorous quantification of community structure has not yet been completed, visual observations suggest that the coral assemblages at Round Top are likely to be similar to those observed from the fringing reefs of the inshore Whitsunday Islands, and from coral communities near Broad Sound, which are dominated by sediment tolerating species (van Woesik 1992; Kleypas 1996; van Woesik and Done 1997; van Woesik et al. 1999).

Preliminary evidence indicates that the reefs at Keswick and St. Bees Islands may have experienced a recent shift from coral to algal dominance. Like the Calf Island and Pine Island reefs observed by van Woesik et al. (1999), the Keswick and St. Bees fringing reefs were largely covered by macroalgae, particularly *Sargassum* spp. and *Podina* spp. (Figures 6.9d and 6.10b), over a carbonate framework (S. Jupiter, personal observation). Although cores confirming modern carbonate accretion on an underlying Holocene structure have been collected from the reef platforms of nearby Scawfell and Cockermouth Island (Kleypas 1996), no data presently exist from Keswick or St. Bees Islands. Some coral rubble fragments are being dated (by J. Quaintance, University of Queensland) to determine whether recent disturbances may have caused high coral mortality that released algal growth. Although changing water quality is unlikely to have caused any initial disturbance, overfishing of herbivorous stocks combined with elevated sediment and nutrient loads can prevent coral recovery (Scheffer et al. 2001). In nutrient-rich waters, even low levels of sediment tend to form biologically-mediated “marine snow”, with aggregates exceeding 3 mm diameter (Eisma 1986; Wolanski and Gibbs 1995; Ayukai and Wolanski 1997; Wolanski et al. 1998). These aggregates of sediment and transparent exopolymer particles will smother and kill coral recruits (Fabricius et al.

2003). In addition, large macroalgae like *Sargassum* spp. decrease coral resilience by causing mechanical damage to corals and by impeding coral recruitment through shading, allelopathy, sediment trapping, and occupying space (Connell 1997; Hughes and Tanner 2000; Szmant 2002; Fabricius 2005; Schaffelke et al. 2005; Stamski and Field 2006).

At Scawfell Island, mean live hard coral cover (22%) was within range of cover observed by van Woesik and Done (1997) on Cockermouth and Scawfell Islands' reefs (27%), but was considerably lower than mean octocoral cover (35%), which was the highest recorded from all sites (Figures 6.9b and 6.10c; Table 6.2). While hard coral decline after disturbance can release octocorals from competition in some regions (Fabricius 1998), high abundances of octocorals have been documented from both turbid nearshore reefs and clear water offshore sites (Fabricius and De'ath 2001); therefore the present distribution of hard corals versus octocorals cannot necessarily be linked to water quality. Mean hard coral cover at Derwent Island and the Pompey reefs (33-35%) is within the range of live hard coral covers observed by the Australian Institute of Marine Sciences' long-term monitoring surveys of offshore reefs in the Pompey Sector (Sweatman et al. 2005). Coral cover in this region may be reduced by high energy waves propagating through the Capricorn Channel, as evidenced by the highly detrital framework of cored outer reefs (Kleypas and Hopley 1992).

Estimates of current sediment export from the Pioneer catchment range from 50 to > 400 Kt yr^{-1}, which is very minor compared to the total estimated volume of sediments (15-28 Mt yr^{-1}) discharged into the GBR Lagoon (Belperio 1983; Gourlay and Hacker 1986; Hacker 1988; Moss et al. 1992; Neil and Yu 1996; Prosser et al. 2001; Neil et al. 2002; Furnas 2003; McKergow et al. 2005). Even if Pioneer River sediment delivery has increased fourfold over natural rates (Gourlay and Hacker 1986; Hacker 1988), this level of sedimentation alone would not be likely to impact fringing reef development. Larcombe and Woolfe (1999) have argued that sediment supply is irrelevant if turbidity is governed by local hydrodynamics and resuspension. Yet, while reef development between Mackay and Shoalwater Bay has historically been explained as limitation by high resuspension rates from the large (6-10 m) tidal ranges (Kleypas 1996), current reef condition may still be affected by fluvial discharge, if increased sediment delivery is accompanied by increased nutrient loads. Sticky flocs that develop from suspended matter in eutrophic nearshore waters can stress coral colonies and kill small benthic recruits, thus reducing resilience from disturbance (Fabricius and Wolanski 2000; Fabricius et al. 2003). Preliminary $\delta^{15}N$ data from the long-term (~2 m) Round Top Island core suggest an increase in nutrient availability since the 1950s (Marion et al. 2006), while recent sampling of the Pioneer River flood plume following a minor event in 2005 resulted in some values of nitrate, ammonium and filterable reactive phosphorus above thresholds known to adversely impact corals (Rohde et al. 2006). Therefore, even though coral proxies of suspended sediment delivery do not show strong increasing trends since 1946, the combined effects of high sediment availability from resuspension and highly eutrophied nearshore waters could have negatively impacts on reefs near Mackay, and may have encouraged algal dominance at Keswick and St. Bees reefs.

Conclusions

This study has focused on connections between changes in the Pioneer River catchment land cover (and land use) and changes in sediment delivery to the nearshore. Historical records indicate early, extensive land clearing throughout the catchment for sugarcane cultivation and grazing immediately following European settlement in 1862, while changes since 1972 have mostly been due to losses of vegetation on the alluvial plains, as farms encroached on riparian zones (Chapter 2). Losses of riparian vegetation throughout the catchment coincided with losses of mangroves in the estuary, where the area of tidal mangroves had a net decrease of 22% between 1948 and 2002 (Chapter 3). The combination of clearing for agricultural expansion and loss of these buffer zones would be expected to increase sediment delivery from fluvial discharge. However, while proxy records of sediment delivery (Ba/Ca and Y/Ca) were clearly related to discharge and wind (Chapter 4), there was no apparent increase in Ba/Ca normalized to discharge over time. The lags of nearshore coral Ba/Ca peaks to discharge events suggest that Ba availability may be influenced by coastal productivity. Meanwhile, changes in Y/Ca (which had no lags) normalized to discharge may reflect both agricultural expansion and management (e.g. shift to GCTB). The combination of high turbidity and high river nutrient discharge may affect survival of coral recruits, which in turn would affect recovery from disturbance. With increasing frequency of disturbance from coral bleaching, associated with high SSTs (Hughes et al. 2003; Donner et al. 2005), and from crown-of-thorns outbreaks, possibly caused by high nutrient levels that increase juvenile survivorship (Brodie 1992; Brodie et al. 2005), changes in Mackay water quality are of concern for reef health, particularly for reefs like Keswick and St. Bees that may have already experienced declines in coral.

References

Alibert, C., Kinsey, L., Fallon, S.J., McCulloch, M.T., Berkelmans, R. and McAllister, F. 2003. Source of trace element variability in Great Barrier Reef corals affected by the Burdekin flood plumes. Geochimica et Cosmochimica Acta 67: 231-246.

Alongi, D.M., Sasekumar, A., Chong, V.C., Pfitzner, J., Trott, L.A., Tirendi, F., Dixon, P. and Brunskill, G.J. 2004. Sediment accumulation and organic material flux in a managed mangrove ecosystem: estimates of land-ocean-atmosphere exchange in peninsular Malaysia. Marine Geology 208: 383-402.

Amos, K.J., Alexander, J., Horn, A., Pocock, G.D. and Fielding, C.R. 2004. Supply-limited sediment transport in a high discharge event of the tropical Burdekin River, North Queensland, Australia. Sedimentology 51: 145-162.

Anderson, H.W. 1970. Principal components analysis of watershed variables affecting suspended sediment discharge after a major flood. International Association of Scientific Hydrology 96: 404-416.

Ayukai, T. and Wolanski, E. 1997. Importance of biologically mediated removal of fine sediments from the Fly River plume, Papua New Guinea. Estuarine, Coastal and Shelf Science 44: 629-639.

Barnes, D.J. and Lough, J.M. 1999. *Porites* growth characteristics in a changed environment: Misima Island, Papua New Guinea. Coral Reefs 18: 213-218.

Barnes, D.J. and Taylor, R.B. 2001. On the nature and causes of luminescent lines and bands in coral skeletons. Coral Reefs 19: 221-230.

Barnes, D.J. and Taylor, R.B. 2005. On the nature and causes of luminescent lines and bands in coral skeletons: II. Contributions of skeletal crystals. Journal of Experimental Marine Biology and Ecology 322: 135-142.

Barnes, D.J., Taylor, R.B. and Lough, J.M. 2003. Measurement of luminescence in coral skeletons. Journal of Experimental Marine Biology and Ecology 295: 91-106.

Belperio, A.P. 1983. Terrigenous sedimentation in the central Great Barrier Reef Lagoon; a model from the Burdekin region. Bureau of Mineral Resources Journal of Australian Geology and Geophysics 8: 179-190.

Beman, J.M., Arrigo, K.R. and Matson, P.A. 2005. Agricultural runoff fuels large phytoplankton blooms in vulnerable areas of the ocean. Nature 434: 211-214.

Bonnell, M. 1988. Hydrological processes and implications for land management in forests and agricultural areas of the wet tropical coast of north-east Queensland. *In*: Warner, R.F. (ed.), Fluvial Geomorphology in Australia. pp. 41-68. Academic Press Ltd., Sydney, Australia.

Brassington, G.B. 1997. The modal evolution of the Southern Oscillation. Journal of Climate 10: 1021-1034.

Brodie, J. 1992. Enhancement of larval and juvenile survival and recruitment in *Acanthaster planci* from the effects of terrestrial runoff--a review. Marine and Freshwater Research 43: 539-554.

Brodie, J. 2004. Mackay Whitsunday Region State of the Waterways Report 2004. ACTFR Report Number 02/03, Australian Centre for Tropical Freshwater Research, Townsville, Australia.

Brodie, J., Fabricius, K., De'ath, G. and Okaji, K. 2005. Are increased nutrient inputs responsible for more outbreaks of crown-of-thorns starfish? An appraisal of the evidence. Marine Pollution Bulletin 51: 266-278.

Buddemeier, R.W. and Hopley, D. 1988. Turn-ons and turn-offs: causes and mechanisms of the initiation and termination of coral reef growth. *In*: Proceedings of the Sixth International Coral Reef Symposium, Townsville, Australia, pp. 253-261.

Burkham, D.E. 1981. Uncertainties resulting from changing river form. American Society of Civil Engineering Journal of the Hydraulics Division 107: 593-610.

Connell, J.H. 1997. Disturbance and recovery of coral assemblages. Coral Reefs 16: S101-S113.

Cortes, J. and Risk, M.J. 1985. A reef under siltation stress: Cahuita, Costa Rica. Bulletin of Marine Science 36: 339-356.

Costa, M.H., Botta, A. and Cardille, J.A. 2003. Effects of large-scale changes in land cover on the discharge of the Tocantins River, Southeastern Amazonia. Journal of Hydrology 283: 206-217.

Credlin, B.L. 1973. Water resources of Mackay district. Producers Review 63: 9-15.

Done, T.J. 1982. Patterns in the distribution of coral communities across the central Great Barrier Reef. Coral Reefs 1: 95-107.

Done, T.J. 1992. Effects of tropical cyclone waves on ecological and geomorphological structures on the Great Barrier Reef. Continental Shelf Research 12: 859-872.

Donner, S.D., Skirving, W.J., Little, C.M., Oppenheimer, M. and Hoegh-Guldberg, O. 2005. Global assessment of coral bleaching and required rates of adaptation under climate change. Global Change Biology 11: 2251-2265.

Douglas, I. 1967. Man, vegetation and the sediment yields of rivers. Nature 215: 925-928.

Duke, N.C. and Wolanski, E. 2001. Muddy coastal waters and depleted mangrove coastlines--depleted seagrass and coral reefs. *In*: Wolanski, E. (ed.), Oceanographic Processes of Coral Reefs: Physical and Biological Links in the Great Barrier Reef. pp. 77-91. CRC Press, Boca Raton.

Eisma, D. 1986. Flocculation and de-flocculation of suspended matter in estuaries. Netherlands Journal of Sea Research 20: 183-199.

Fabricius, K.E. 1998. Reef invasion by soft corals: which taxa and which habitats? *In*: Greenwood, J.G. and Hall, N.J. (eds.), Proceedings of the Australian Coral Reef Society 75th Anniversary Conference, Heron Island, Australia, pp. 77-90.

Fabricius, K.E. 2005. Effects of terrestrial runoff on the ecology of corals and coral reefs: review and synthesis. Marine Pollution Bulletin 50: 125-146.

Fabricius, K. and Wolanski, E. 2000. Rapid smothering of coral reef organisms by muddy marine snow. Estuarine, Coastal and Shelf Science 50: 115-120.

Fabricius, K. and De'ath, G. 2001. Biodiversity on the Great Barrier Reef: large-scale patterns and turbidity-related local loss of soft coral taxa. *In*: Wolanski, E. (ed.), Oceanographic Processes of Coral Reef: Physical and Biological Links in the Great Barrier Reef. pp. 127-144. CRC Press, Boca Raton.

Fabricius, K.E. and De'ath, G. 2004. Identifying ecological change and its causes: a case study on coral reefs. Ecological Applications 14: 1448-1465.

Fabricius, K.E. and McCorry, D. 2006. Changes in octocoral communities and benthic cover along a water quality gradient in the reefs of Hong Kong. Marine Pollution Bulletin 52: 22-33.

Fabricius, K.E., Wild, C., Wolanski, E. and Abele, D. 2003. Effects of transparent exopolymer particles and muddy terrigenous sediments on the survival of hard coral recruits. Estuarine, Coastal and Shelf Science 57: 613-621.

Fabricius, K., De'ath, G., McCook, L., Turak, E. and Williams, D.M. 2005. Changes in algal, coral and fish assemblages along water quality gradients on the inshore Great Barrier Reef. Marine Pollution Bulletin 51: 384-398.

Furnas, M. 2003. Catchments and Corals. Australian Institute of Marine Science, Townsville, Australia. 334 pp.

Goreau, T.F. 1964. Mass expulsion of zooxanthellae from Jamaican reef communities after Hurrican Flora. Science 145: 383-386.

Gourlay, M.R. and Hacker, J.L.F. 1986. Pioneer River Estuary Sedimentation Studies. University of Queensland, Department of Civil Engineering, St. Lucia, Australia. 207 pp.

Hacker, J.L.F. 1988. Rapid accumulation of fluvially derived sands and gravels in a tropical macrotidal estuary: the Pioneer River at Mackay, North Queensland, Australia. Sedimentary Geology 57: 299-315.

Haynes, D., Bass, D., Brodie, J., Christie, C., Devlin, M., Michalek-Wagner, K., Morris, S., Ramsay, M., Storrie, J., Waterhouse, J. and Yorkston, H. 2001. Great Barrier Reef water quality: current issues. Great Barrier Reef Marine Park Authority, Townsville, Australia.

Hendy, E.J., Gagan, M.K. and Lough, J.M. 2003. Chronological controls of coral records using luminescent lines and evidence for non-stationary ENSO teleconnections in northeast Australia. The Holocene 13: 187-199.

Hendy, E.J., Gagan, M.K., Alibert, C.A., McCulloch, M.T., Lough, J.M. and Isdale, P.J. 2002. Abrupt decrease in tropical Pacific sea surface salinity at end of Little Ice Age. Science 295: 1511-1514.

Hoegh-Guldberg, O. 1999. Climate change, bleaching and the future of the world's coral reefs. Marine and Freshwater Research 50: 839-866.

Hopley, D. 1984. The Holocene 'high energy window' on the central Great Barrier Reef. *In*: Thom, B.G. (ed.), Coastal Geomorphology in Australia. pp. 135-150. Academic Press, Canberra, Australia.

Hopley, D. 1995. Continental shelf reef systems. *In*: Carter, R.W.G. and Woodroffe, C.D. (eds.), Coastal Evolution : Late Quaternary Shoreline Morphodynamics. pp. 303-340. Cambridge University Press, Cambridge, UK.

Hughes, T.P. and Tanner, J.E. 2000. Recruitment failure, life histories, and long-term decline of Caribbean corals. Ecology 81: 2250-2263.

Hughes, T.P., Baird, A.H., Bellwood, D.R., Card, M., Connolly, S.R., Folke, C., Grosberg, R., Hoegh-Guldberg, O., Jackson, J.B.C., Kleypas, J.A., Lough, J.M., Marshall, P., Nystrom, M., Palumbi, S.R., Pandolfi, J.M., Rosen, B. and Roughgarden, J. 2003. Climate change, human impacts, and the resilience of coral reefs. Science 301: 929-933.

Isdale, P. 1984. Fluorescent bands in massive corals record centuries of coastal rainfall. Nature 310: 578-579.

Jiang, N., Neelin, J.D. and Ghil, M. 1995. Quasi-quadrennial and quasi-biennial variability in the equatorial Pacific. Climate Dynamics 12: 101-112.

Johnson, A.K.L., Bramley, R.G.V. and Roth, C.H. 2001. Landcover and water quality in river catchments of the Great Barrier Reef Marine Park. *In*: Wolanski, E. (ed.), Oceanographic Processes of Coral Reef: Physical and Biological Links in the Great Barrier Reef. pp. 19-35. CRC Press, Boca Raton.

Jokiel, P.L., Hunter, C.L., Taguchi, S. and Watarai, L. 1993. Ecological impact of a freshwater "reef kill" in Kaneohe Bay, Oahu, Hawaii. Coral Reefs 12: 177-184.

Kleypas, J.A. 1996. Coral reef development under naturally turbid conditions: fringing reefs near Broad Sound, Australia. Coral Reefs 15: 153-167.

Kleypas, J.A. and Hopley, D. 1992. Reef development across a broad continental shelf, southern Great Barrier Reef, Australia. *In*: Proceedings of the Seventh International Coral Reef Symposium, Guam, pp. 1129-1141.

Kleypas, J.A., Buddemeier, R.W., Archer, D., Gattuso, J.-P., Langdon, C. and Opdyke, B.N. 1999. Geochemical consequences of increased atmospheric carbon dioxide on coral reefs. Science 284: 118-120.

Larcombe, P. and Woolfe, K.J. 1999. Increased sediment supply to the Great Barrier Reef will not increase sediment accumulation at most coral reefs. Coral Reefs 18: 163-169.

Lawrence, P.A. and Thorburn, P.J. 1989. Changes in hydrology, soil fertility and productivity of brigalow catchments following clearing. QDPI Report RQR89002, Queensland Department of Primary Industries, Brisbane, Australia.

Likens, G.E., Bormann, F.H., Johnson, N.M., Fisher, D.W. and Pierce, R.S. 1970. Effects of forest cutting and herbicide treatment on nutrient budgets in the Hubbard Brook watershed-ecosystem. Ecological Monographs 40: 23-47.

Lough, J.M. 1994. Climate variation and El Nino-Southern Oscillation events on the Great Barrier Reef: 1958 to 1987. Coral Reefs 13: 181-195.

Lough, J.M. and Fritts, H.C. 1985. The Southern Oscillation and tree rings: 1600-1961. Journal of Climate and Applied Meteorology 24: 952-966.

Lough, J.M., Barnes, D.J. and McAllister, F.A. 2002. Luminescent lines in corals from the Great Barrier Reef provide spatial and temporal records of reefs affected by land runoff. Coral Reefs 21: 333-343.

Loya, Y. 2004. The coral reefs of Eilat--past, present, and future: three decades of coral community structure studies. *In*: Rosenberg, E. and Loya, Y. (eds.), Coral Health and Disease. pp. 1-34. Springer, Berlin, Germany.

Mallela, J., Perry, C.T. and Haley, M.P. 2004. Reef morphology and community structure along a fluvial gradient, Rio Bueno, Jamaica. Caribbean Journal of Science 40: 299-311.

Marion, G.S., Hoegh-Guldberg, O., McCulloch, M.T. and Jupiter, S.D. 2006. Coral isotopic records ($\delta^{15}N$) of unprecedented land-use stress in Great Barrier Reef coastal communites. Eos Transactions of AGU, 87(36), Ocean Science Meeting Suppl., Abstract OS520-04.

McCulloch, M.T., Gagan, M.K., Mortimer, G.E., Chivas, A.R. and Isdale, P.J. 1994. A high-resolution Sr/Ca and $\delta^{18}O$ coral record from the Great Barrier Reef, Australia, and the 1982-1983 El Nino. Geochimica et Cosmochimica Acta 58: 2747-2754.

McCulloch, M., Fallon, S., Wyndham, T., Hendy, E., Lough, J. and Barnes, D. 2003. Coral record of increased sediment flux to the inner Great Barrier Reef since European settlement. Nature 421: 727-730.

McKergow, L.A., Prosser, I.P., Hughes, A.O. and Brodie, J. 2005. Regional scale nutrient modelling: exports to the Great Barrier Reef World Heritage Area. Marine Pollution Bulletin 51: 186-199.

McMahon, T.A., Finlayson, B.L., Srikanthan, R. and Haines, A.T. 1992. Global Runoff: Continental Comparisons of Annual Flows and Peak Discharges. Catena Verlag, Cremlingen-Destedt, Germany.

Mitchell, C., Brodie, J. and White, I. 2005. Sediments, nutrients and pesticide residues in event flow conditions in streams of the Mackay Whitsunday Region, Australia. Marine Pollution Bulletin 51: 23-36.

Moberg, F., Nystrom, M., Kautsky, N., Tedengren, M. and Jarayabhand, P. 1997. Effects of reduced salinity on the rates of photosynthesis and respiration in the hermatypic corals *Porites lutea* and *Pocillipora damicornis*. Marine Ecology Progress Series 157: 53-59.

Moss, A.J., Rayment, G.E., Reilly, N. and Best, E.K. 1992. A preliminary assessment of sediment and nutrient exports from Queensland coastal catchments. Queensland Department of Primary Industries, Brisbane, Australia.

Neil, D.T. and Yu, B. 1996. Fluvial sediment yield to the Great Barrier Reef Lagoon: spatial patterns and the effect of land use. *In*: Hunter, H.M., Eyles, A.G. and Rayment, G.E. (eds.), Downstream Effects of Land Use. pp. 281-286. Queensland Department of Natural Resources, Brisbane, Australia.

Neil, D.T., Orpin, A.R., Ridd, P.V. and Yu, B. 2002. Sediment yield and impacts from river catchments to the Great Barrier Reef lagoon. Marine and Freshwater Research 53: 733-752.

Nugues, M.M. and Roberts, C.M. 2003. Partial mortality in massive reef corals as an indicator of sediment stress on coral reefs. Marine Pollution Bulletin 46: 314-323.

Ogston, A.S., Storlazzi, C.D., Field, M.E. and Presto, M.K. 2004. Sediment resuspension and transport patterns on a fringing reef flat, Molokai, Hawaii. Coral Reefs 23: 559-569.

Ohlhorst, S.L., Liddell, W.D., Taylor, R.J. and Taylor, J.M. 1988. Evaluation of reef census techniques. *In*: Proceedings of the Sixth International Coral Reef Symposium, Townsville, Australia, pp. 319-324.

Pickup, G. and Warner, R.F. 1976. Effects of hydrologic regime on magnitude and frequency of dominant discharge. Journal of Hydrology 29: 51-75.

Pimentel, D., Allen, J., Beers, A., Guinand, L., Hawkins, A., Linder, R., McLaughlin, P., Meer, B., Musonda, D., Perdue, D., Poisson, S., Salazar, R., Siebert, S. and

Stoner, K. 1993. Soil erosion and agricultural productivity. *In*: Pimentel, D. (ed.), World Soil Erosion and Conservation. pp. 277-292. Cambridge University Press, Cambridge, UK.

Pimentel, D.P., Harvey, C., Resosudarmo, K., Sinclair, K., Kurz, D., McNair, M., Crist, S., Shpritz, L., Fitton, L., Saffouri, R. and Blair, R. 1995. Environmental and economic costs of soil erosion and conservation benefits. Science 267: 1117-1123.

Power, S., Casey, T., Folland, C., Colman, A. and Mehta, V. 1999. Interdecadal modulation of the impact of ENSO on Australia. Climate Dynamics 15: 319-324.

Power, S., Haylock, M., Colman, R. and Wang, X. 2005. Asymmetry in the Australian response to ENSO and the predictability of inter-decadal changes in ENSO teleconnections. BMRC Research Report No. 113 Australian Government, Bureau of Meteorology, Melbourne, Australia.

Prosser, I.P., Rutherfurd, I.D., Olley, J.M., Young, W.J., Walbrink, P.J. and Moran, C.J. 2001. Large scale patterns of erosion and sediment transport in river networks, with examples from Australia. Marine and Freshwater Research 52: 81-99.

QDNRM 2001. Pioneer Valley Water Resource Plan -- Current environmental conditions and impacts of existing water resource development. Queensland Department of Natural Resources and Mines, Brisbane, Australia.

Rasmusson, E.M., Wang, X. and Ropelewski, C.F. 1990. The biennial component of ENSO variability. Journal of Marine Systems 1: 71-96.

Rayment, G.E. and Neil, D.T. 1997. Sources of material in river discharge. *In*: Proceedings of the Great Barrier Reef: Science, Use and Management, Townsville, Australia, pp. 42-58. Great Barrier Reef Marine Park Authority.

Restrepo, J.D., Zapata, P., Díaz, J.M., Garzón-Ferreira, J. and García, C.B. 2006. Fluvial fluxes into the Caribbean Sea and their impact on coastal ecosystems: The Magdalena River, Colombia. Global and Planetary Change 50: 33-49.

Risk, M.J., Sammarco, P.W. and Edinger, E.N. 1995. Bioerosion in *Acropora* across the continental shelf of the Great Barrier Reef. Coral Reefs 14: 79-86.

Rogers, C.S. 1990. Responses of coral reefs and reef organisms to sedimentation. Marine Ecology Progress Series 62: 185-202.

Rohde, K., Masters, B., Brodie, J., Faithful, J., Noble, R. and Carroll, C. 2006. Fresh and marine water quality in the Mackay Whitsunday region 2004/2005. Mackay Whitsunday Natural Resource Management Group, Mackay, Australia.

Rolleston, F. 1987. The Defiance. North Eton Co-operative Sugar Milling Association Limited, North Eton, Australia.

Rose, C.S. and Risk, M.J. 1985. Increase in *Cliona delitrix* infestation of *Montastrea cavernosa* heads on an organically polluted portion of the Grand Cayman fringing reef British West-Indies. Marine Ecology 6: 345-364.

Sahin, V. and Hall, M.J. 1996. The effects of afforestation and deforestation on water yields. Journal of Hydrology 178: 293-309.

Sammarco, P.W. and Risk, M.J. 1990. Large-scale patterns in internal bioerosion of *Porites*: cross continental shelf trends on the Great Barrier Reef. Marine Ecology Progress Series 59: 145-156.

Schaffelke, B., Mellors, J. and Duke, N.C. 2005. Water quality in the Great Barrier Reef region: responses of mangrove, seagrass and macroalgal communities. Marine Pollution Bulletin 51: 279-296.

Scheffer, M., Carpenter, S., Foley, J.A., Folkes, C. and Walker, B. 2001. Catastrophic shifts in ecosystems. Nature 413: 591-596.

Sinclair, D.J. 1999. High spatial-resolution analysis of trace elements in corals using laser ablation ICP-MS. Ph.D. Thesis. The Australian National University, Canberra, ACT, Australia.

Sinclair, D.J. and McCulloch, M.T. 2004. Corals record low mobile barium concentrations in the Burdekin River during the 1974 flood: evidence for limited Ba supply to rivers? Palaeogeography, Palaeoclimatology, Palaeoecology 214: 155-174.

Smith, S.V., Kimmener, W.J., Laws, E.A., Brock, R.E. and Walsh, T.W. 1981. Kaneohe Bay sewerage diversion experiment: perspectives on ecosystem response to nutritional perturbation. Pacific Science 35: 279-395.

Smithers, S.G., Hopley, D. and Parnell, K.E. 2006. Fringing and nearshore coral reefs of the Great Barrier Reef: episodic Holocene development and future prospects. Journal of Coastal Research 22: 175-187.

Stamski, R.E. and Field, M.E. 2006. Characterization of sediment trapped by macroalgae on a Hawaiian reef flat. Estuarine, Coastal and Shelf Science 66: 211-216.

The State of Queensland and Commonwealth of Australia (2003). Reef Water Quality Protection Plan: for catchments adjacent to the Great Barrier Reef World Heritage Area. Brisbane, Australia. 42 pp.

Sweatman, H., Burgess, S., Cheal, A., Coleman, G., Delean, S., Emslie, M., McDonald, A., Miller, I., Osborne, K. and Thompson, A. 2005. Long-term monitoring of the Great Barrier Reef. Status Report Number 7 Australian Institute of Marine Sciences, Townsville, Australia.

Szmant, A.M. 2002. Nutrient enrichment on coral reefs: is it a major cause of coral reef decline? Estuaries 25: 743-766.

Thornes, J.B. 1980. Erosional processes of running water and their spatial and temporal controls: a theoretical viewpoint. *In*: Kirkby, M.J. and Morgan, R.P.C. (eds.), Soil Erosion. pp. 129-182. John Wiley and Sons Ltd., Chichester, UK.

Tribollet, A. and Golubic, S. 2005. Cross-shelf differences in the pattern and pace of bioerosion of experimental carbonate substrates exposed for 3 years on the northern Great Barrier Reef, Australia. Coral Reefs 24: 422-434.

van Woesik, R. 1992. Ecology of coral assemblages on continental islands in the southern section of the Great Barrier Reef, Australia. Ph.D. Thesis. James Cook University, Townsville, Australia.

van Woesik, R. and Done, T.J. 1997. Coral communities and reef growth in the southern Great Barrier Reef. Coral Reefs 16: 103-115.

van Woesik, R., Tomascik, T. and Blake, S. 1999. Coral assemblages and physico-chemical characteristics of the Whitsunday Islands: evidence of recent community changes. Marine and Freshwater Research 50: 427-440.

Verdon, D.C., Wyatt, A.M., Kiem, A.S. and Franks, S.W. 2004. Multidecadal variability of rainfall and streamflow: Eastern Australia. Water Resources Research 40, W10201, doi:10.1029/2004WR003234, 2004.

Veron, J.E.N. 1995. Corals in Space and Time: The Biogeography and Evolution of the Scleractinia. Comstock/Cornell, Ithaca, USA. 321 pp.

Vorosmarty, C.J., Meybeck, M., Fekete, B., Sharma, B., Green, K. and Syvitski, J.P.M. 2003. Anthropogenic sediment retention: major global impact from registered river impoundments. Global and Planetary Change 39: 169-190.

Wainright, S.A. 1965. Reef communities visited by the Israel South Red Sea expedition, 1962. Sea Fisheries Research Station (Haifa) Bulletin 38: 40-53.

Walling, D.E. 2000. Linking land use, erosion and sediment yields in river basins. Hydrobiologia 410: 223-240.

Walling, D.E. and He, Q. 1999. Using fallout lead-210 measurements to estimate soil erosion on cultivated land. Soil Science Society of America Journal 63: 1404-1412.

Wolanski, E. and Gibbs, R.J. 1995. Flocculation of suspended sediment in the Fly River Estuary, Papua New Guinea. Journal of Coastal Research 11: 754-762.

Wolanski, E., Spagnol, S. and Ayukai, T. 1998. Field and model studies of the fate of particulate carbon in mangrove-fringed Hinchinbrook Channel, Australia. Mangroves and Salt Marshes 2: 205-221.

Woolfe, K.J. and Larcombe, P. 1999. Terrigenous sedimentation and coral reef growth: a conceptual framework. Marine Geology 155: 331-345.

Yu, B. and Neil, D.T. 2000. Empirical catchment-wide rainfall erosivity models for two rivers in the humid tropics of Australia. Australian Geographer 31: 115-132.

Zhang, X.-G. and Casey, T.M. 1992. Long-term variations in the Southern Oscillation and relationships with Australian rainfall. Australian Meteorological Magazine 40: 211-225.

Table 6.1. Details of benthic habitat surveys.

Site	# Transects	Distance from Pioneer R. (km)	Depth Range (m)	Lat (^{O}S)	Long (^{O}E)
Round Top Island	6	5	3.5 - 6.0 m	-21.1715559	149.2639205
Keswick and St. Bees Islands	14	32	1.2 - 5.1 m	-20.9307626	149.4227693
Scawfell Island (Refuge Bay)	6	51	1.0 - 4.4 m	-20.8570345	149.5996082
Derwent Island	6	61	2.0 - 2.5 m	-20.9898814	149.7873472
Pompey Complex (Big and Little Kindemar Reefs)	12	128	2.5 - 7.0 m	-21.0864519	150.4495846

Table 6.2. Mean proportion cover (± SD) of each benthic cover category at the coral community and reef sites (6-13 March 2006) along an inshore (Round Top) to offshore (Pompey Complex) gradient from Mackay.

Site	**Live Hard Coral**	**Octocoral**	**Turf Algae and CCA**	**Macroalgae**	**Rubble and Sand**	**Other**
Round Top	0.082 ± 0.090	0.021 ± 0.017	0.263 ± 0.107	0.024 ± 0.028	0.609 ± 0.278	0.001 ± 0.001
Keswick-St. Bees	0.072 ± 0.074	0.011 ± 0.011	0.076 ± 0.081	0.667 ± 0.658	0.172 ± 0.172	0.003 ± 0.004
Scawfell	0.224 ± 0.082	0.351 ± 0.156	0.408 ± 0.094	0.003 ± 0.006	0.008 ± 0.014	0.008 ± 0.014
Derwent	0.348 ± 0.170	0.011 ± 0.012	0.500 ± 0.071	0.013 ± 0.026	0.015 ± 0.026	0.113 ± 0.109
Pompey Complex	0.331 ± 0.100	0.096 ± 0.060	0.446 ± 0.152	0.003 ± 0.006	0.141 ± 0.118	0.012 ± 0.011

Figure 6.1. Schematic model of ecosystem connectivity in the context of land use change. (a) Catchment in “natural” state: periodic pulses of sediments delivered by rivers are subject to resuspension and longshore transport, creating turbid nearshore waters. (b) “Disturbed” catchment with (considerable land clearing): the quantity, quality and dispersal of suspended matter are modified, affecting coral communities and reefs over a larger area.

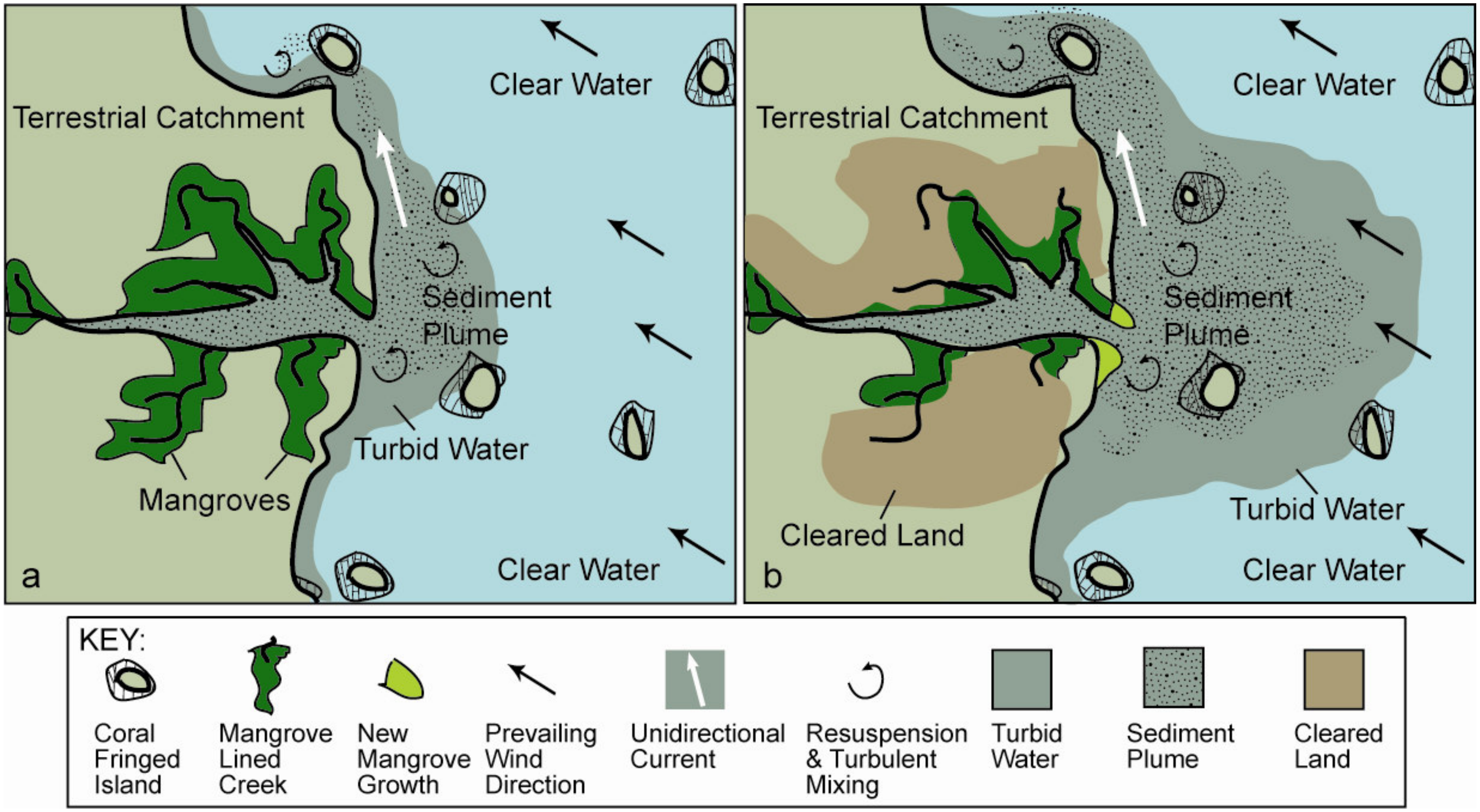
Terrestrial Catchment
Clear Water
Sediment Plume
Turbid Water
Mangroves
Clear Water
a
Terrestrial Catchment
Clear Water
Sediment Plume
Cleared Land
Turbid Water
Clear Water
b
KEY:
Coral Fringed Island
Mangrove Lined Creek
New Mangrove Growth
Prevailing Wind Direction
Unidirectional Current
Resuspension & Turbulent Mixing
Turbid Water
Sediment Plume
Cleared Land

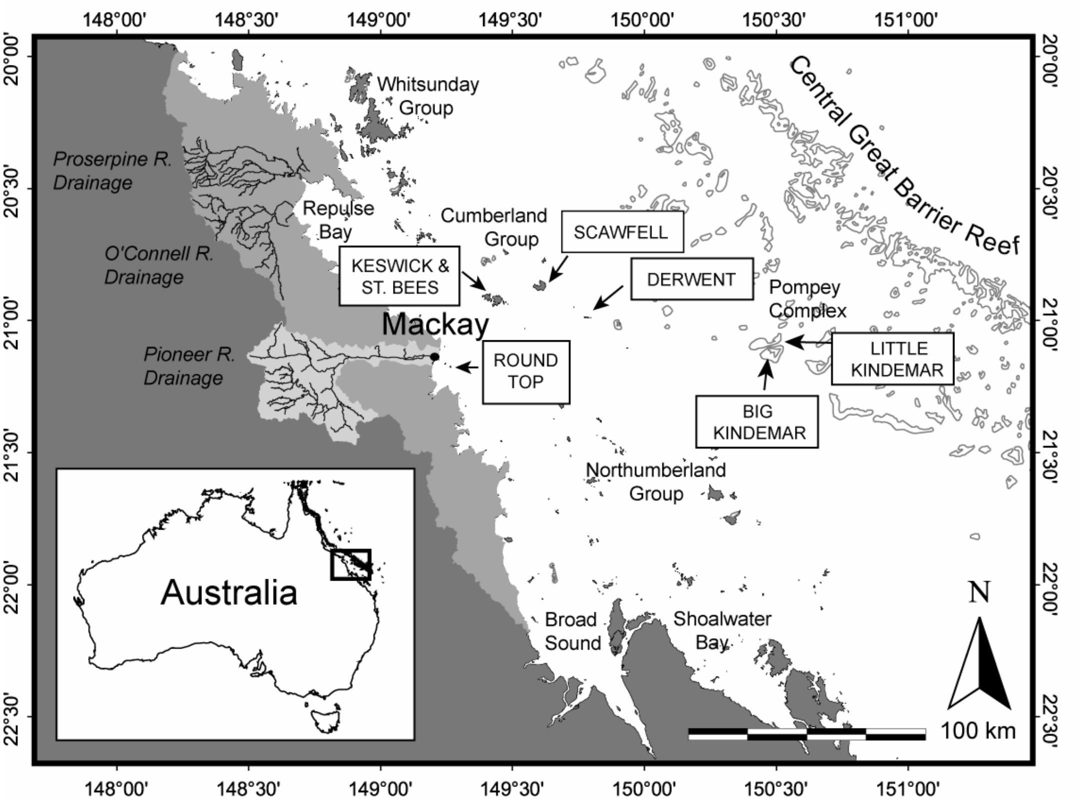

Figure 6.2. The Mackay-Whitsunday region (medium grey) showing the Pioneer River and catchment (light grey), adjacent rivers and catchments, turbid bays and nearshore to midshelf island groups. Arrows from boxes point to benthic habitat sampling locations.

Figure 6.3. Variation in Pioneer River discharge and rainfall in the Pioneer catchment. (a) Ratio of annual discharge to Mackay rainfall between 1916 and 2002. (b) Annual discharge versus Mackay rainfall (1917-2002). (c) Annual discharge versus Dalrymple Heights rainfall (1939-2002). Red years follow several years of below average rainfall; blue years follow years or series of years of high rainfall.

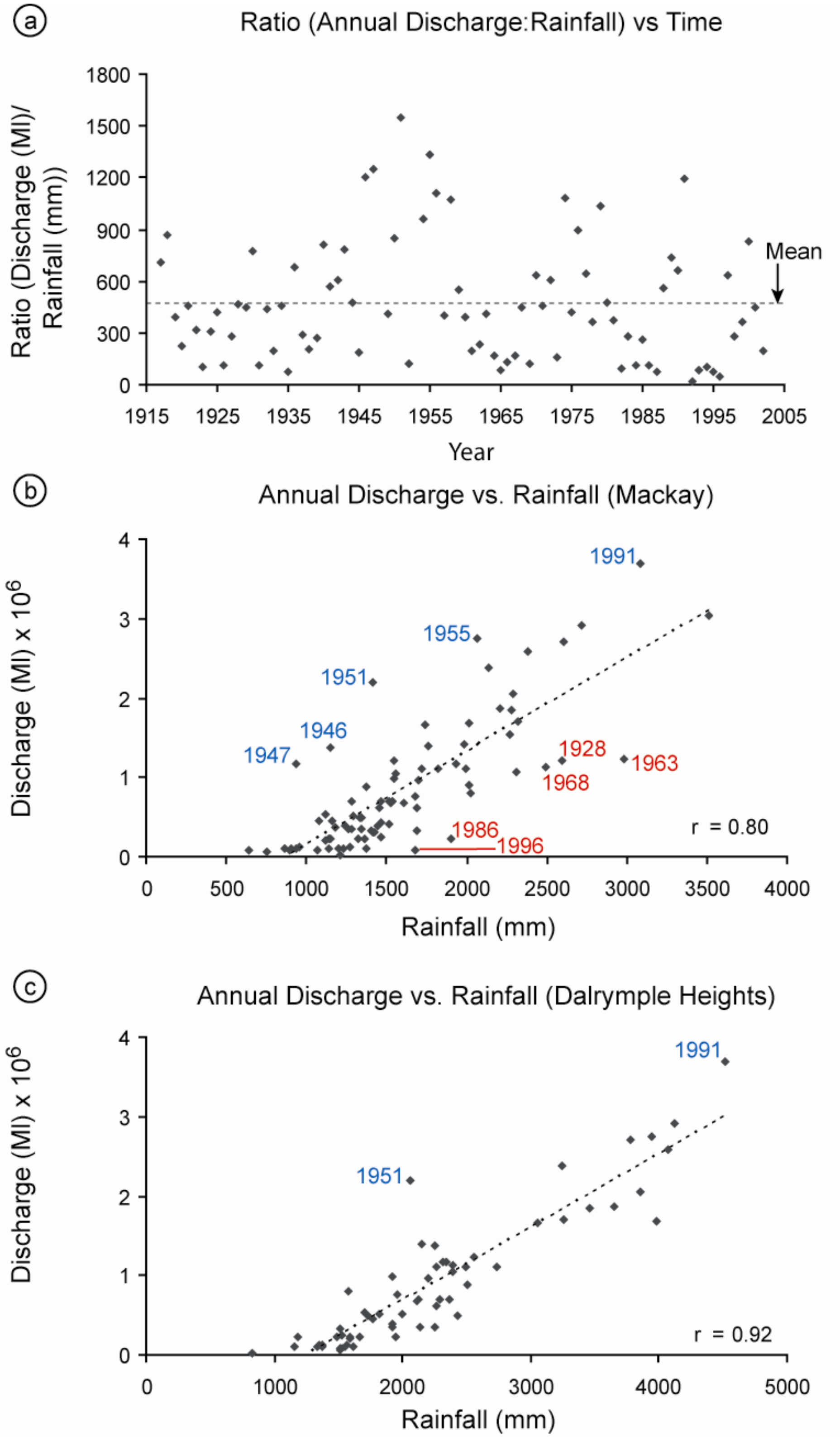
a
Ratio (Annual Discharge:Rainfall) vs Time
Ratio (Discharge (Ml)/ Rainfall (mm))
1800
1500
1200
900
600
300
0
1915
1925
1935
1945
1955
1965
1975
1985
1995
2005
Year
Mean
b
Annual Discharge vs. Rainfall (Mackay)
Discharge (Ml) x 10^6
4
3
2
1
0
1991
1955
1951
1946
1947
1928
1963
1968
1986
1996
r = 0.80
0
500
1000
1500
2000
2500
3000
3500
4000
Rainfall (mm)
c
Annual Discharge vs. Rainfall (Dalrymple Heights)
Discharge (Ml) x 10^6
4
3
2
1
0
1991
1951
r = 0.92
0
1000
2000
3000
4000
5000
Rainfall (mm)

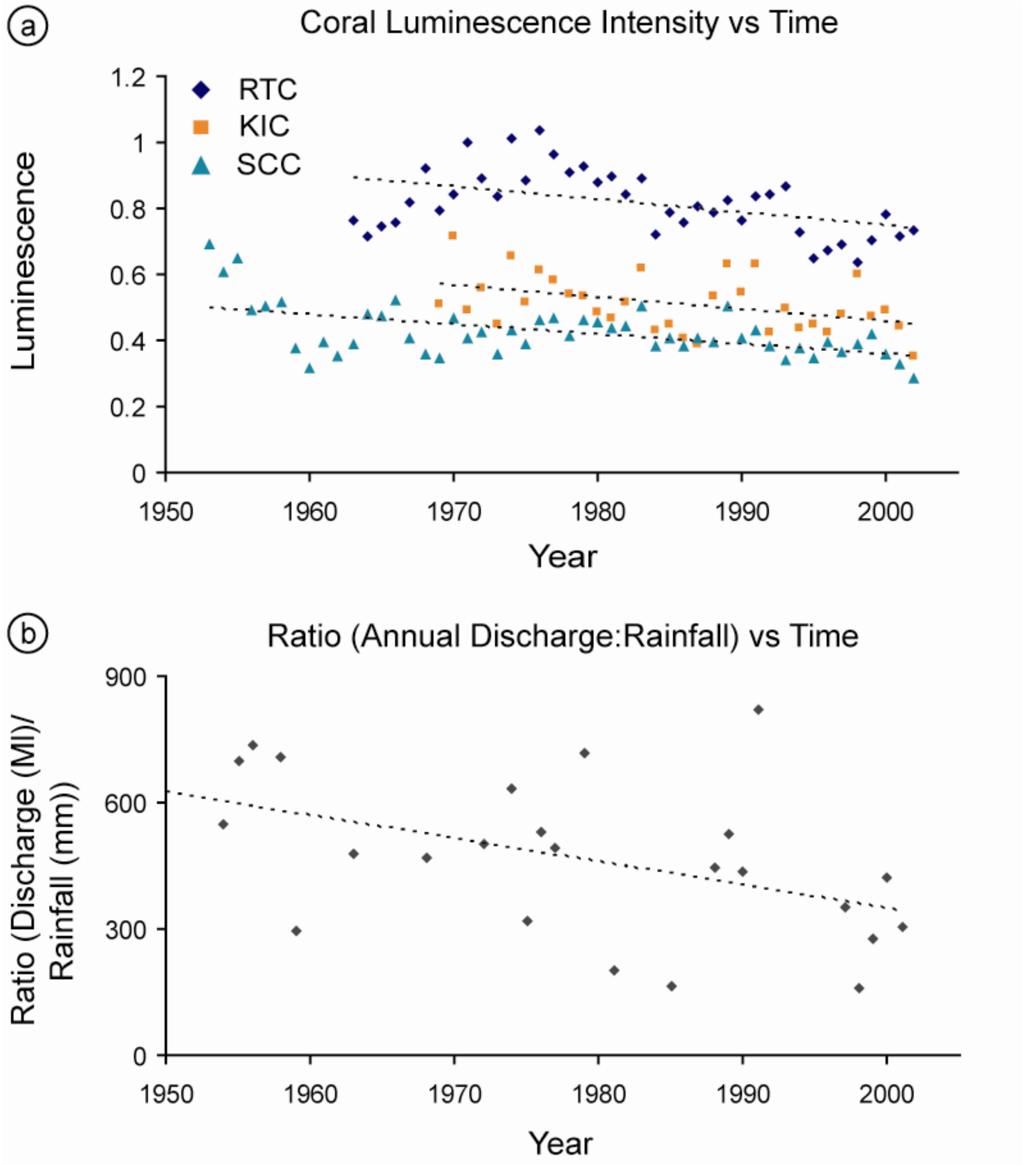

Figure 6.4. Records of Pioneer River discharge since 1952. (a) Proxy records of freshwater delivery from annual luminescence maxima in coral skeletons at 5 km (RTC: dark blue diamonds), 32 km (KIC: orange squares) and 51 km (SCC: aqua triangles) from the Pioneer River mouth. (b). Ratios of Pioneer River discharge to annual Dalrymple Heights rainfall for 24 wet years (> 2000 mm).

Figure 6.5. Power spectra analyses for (a) inshore core RTF Ba/Ca; (b) Mackay wind speed; (c) Pioneer River discharge; (d) and RTF Y/Ca. The numbers above spectral density peaks are dominant periodicities (in years).

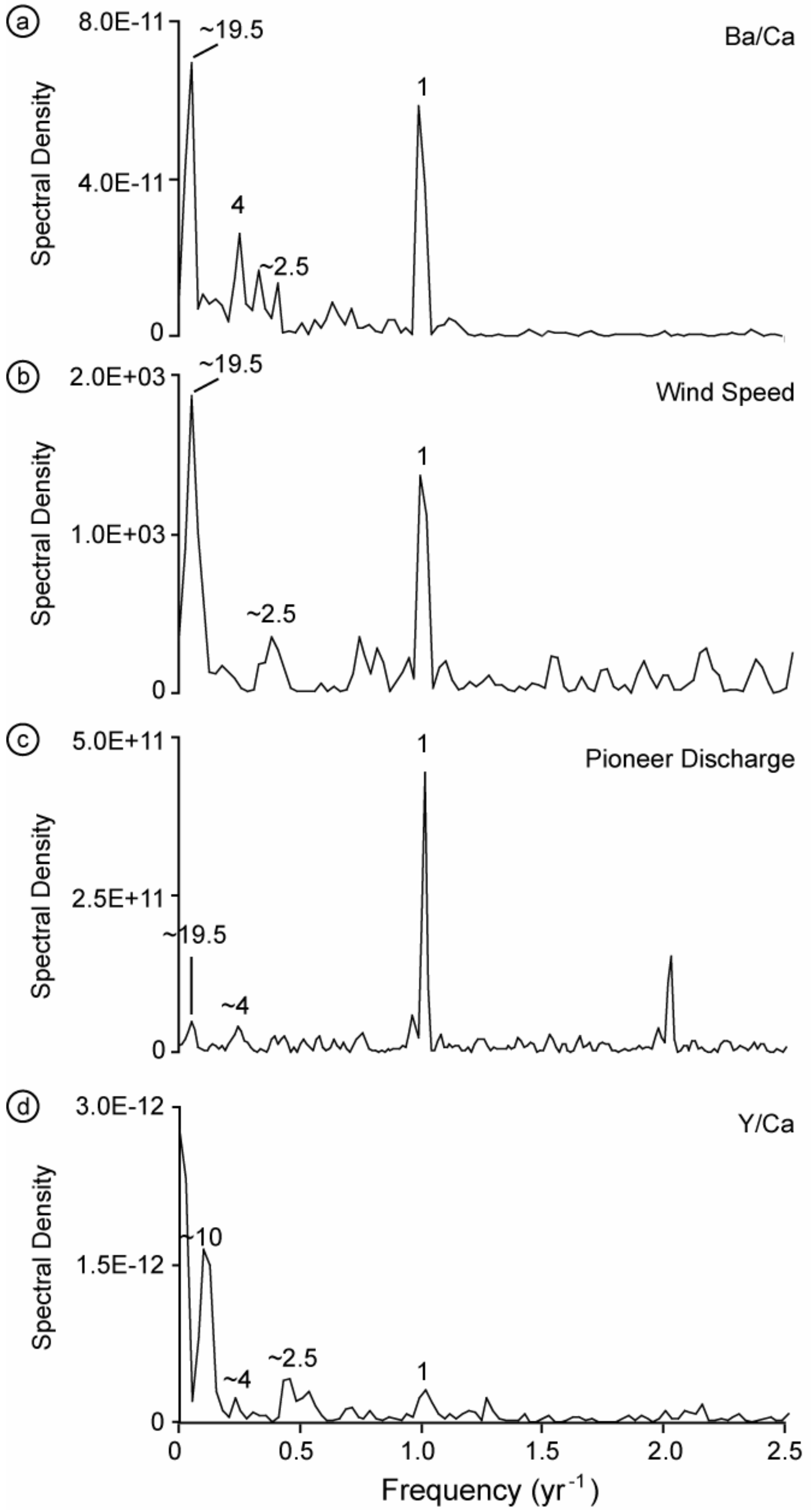
a
8.0E-11
4.0E-11
0
~19.5
1
4
~2.5
Ba/Ca
Spectral Density
b
2.0E+03
1.0E+03
0
~19.5
1
~2.5
Wind Speed
Spectral Density
c
5.0E+11
2.5E+11
0
1
~19.5
~4
Pioneer Discharge
Spectral Density
d
3.0E-12
1.5E-12
0
~10
~4
~2.5
1
Y/Ca
Spectral Density
0
0.5
1.0
1.5
2.0
2.5
Frequency (yr⁻¹)

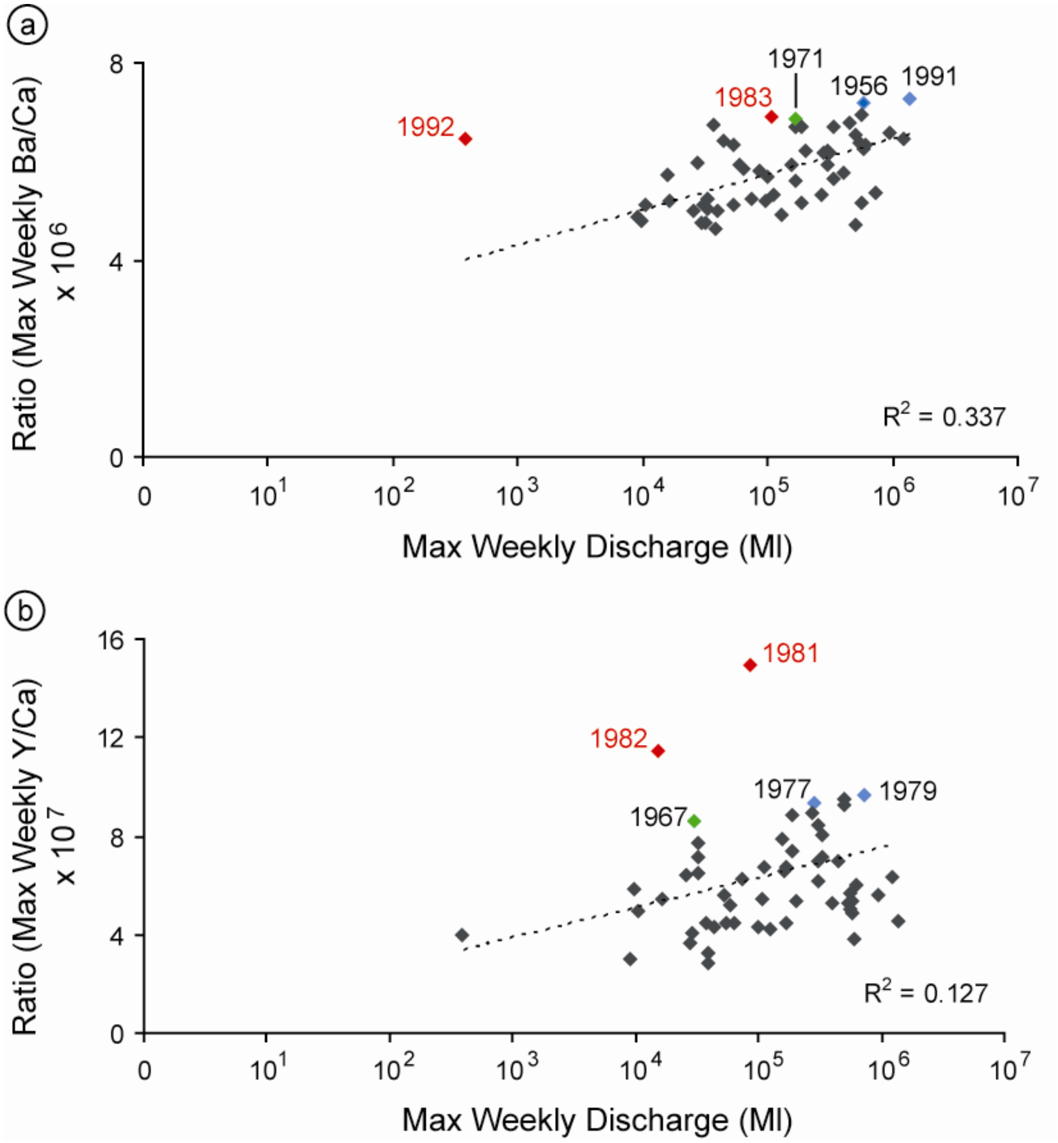

Figure 6.6. Relationships between trace element proxies of suspended sediment delivery and Pioneer River discharge from a Round Top Island core (RTF) between 1946 and 2002. (a) Maximum weekly Ba/Ca and (b) maximum weekly Y/Ca plotted against log maximum weekly discharge for each year of record. Red dates are anomalous years that were excluded from the regression analyses. Blue dates are years that follow major floods or flood periods. Green dates are relatively dry years with early seasonal rains.

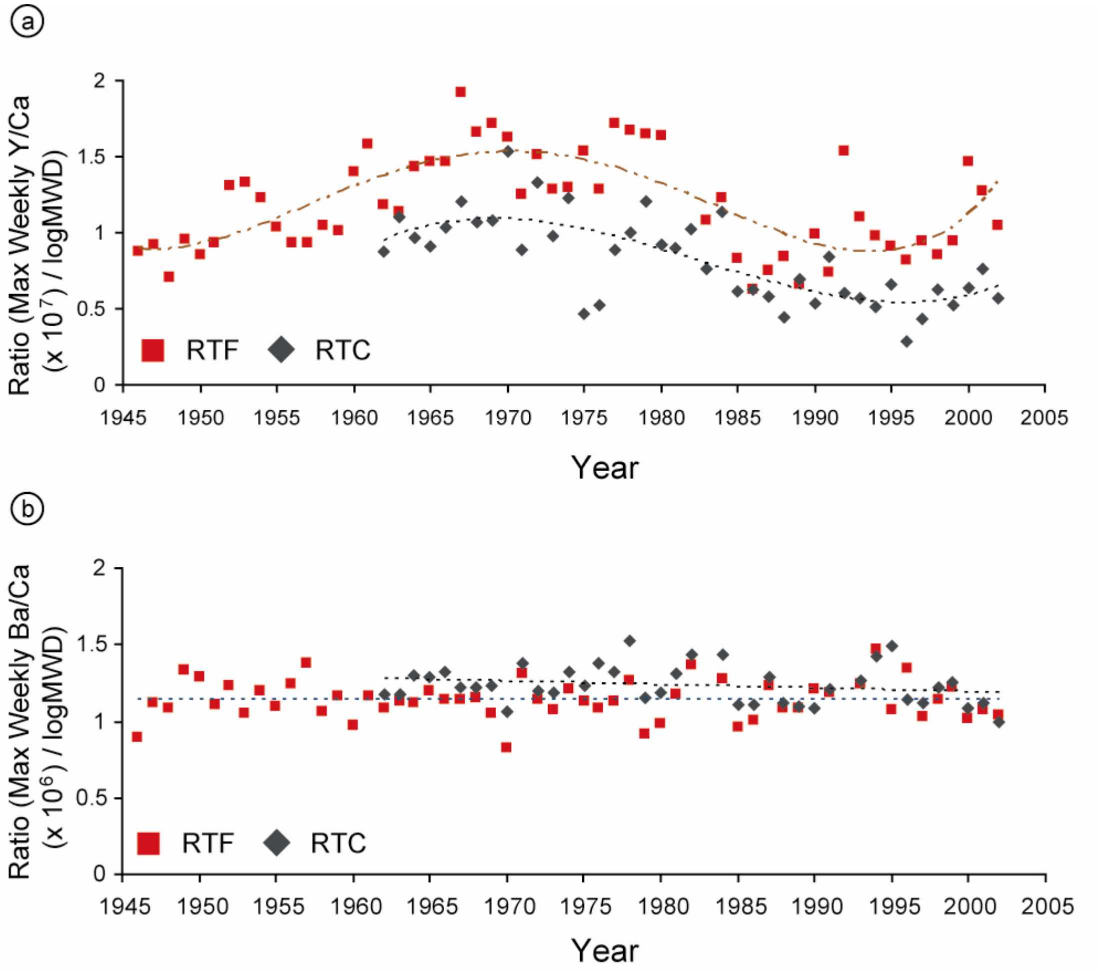

Figure 6.7. Temporal trends in ratios of maximum weekly trace element to calcium (E/Ca) relative to the log of maximum weekly Pioneer River discharge (MWD) in Round Top Island coral cores (RTF: red squares; RTC: black diamonds) for each year between 1946 and 2002. (a) Ratios of Y/Ca to logMWD were fit with fourth order polynomial curves (RTF: $r^2 = 0.53$; RTC: $r^2 = 0.54$). (b) Ratios of Ba/Ca to logMWD were fit with linear regression lines (RTF: $r^2 = 0.04$; RTC: $r^2 < 0.001$).

Figure 6.8. Trends in Pioneer catchment land cover, compared with records of Pioneer River discharge and coral elemental records between 1946 and 2004. (a) Pioneer discharge. (b) Riparian forested area mapped from Landsat satellite data (Chapter 2). (c) Tidal mangrove area mapped from aerial photographs and Landsat data (Chapter 3). (d) Round Top Island coral records of maximum weekly Y/Ca (red squares) and Ba/Ca (black diamonds) normalized to the log of maximum weekly discharge (MWD) (x 10^7 for Y/Ca:logMWD; x10^6 for Ba/Ca:logMWD). (e) Total REY measured from annual samples of Round Top Island (dark blue diamonds) and Keswick Island (light blue squares) corals.

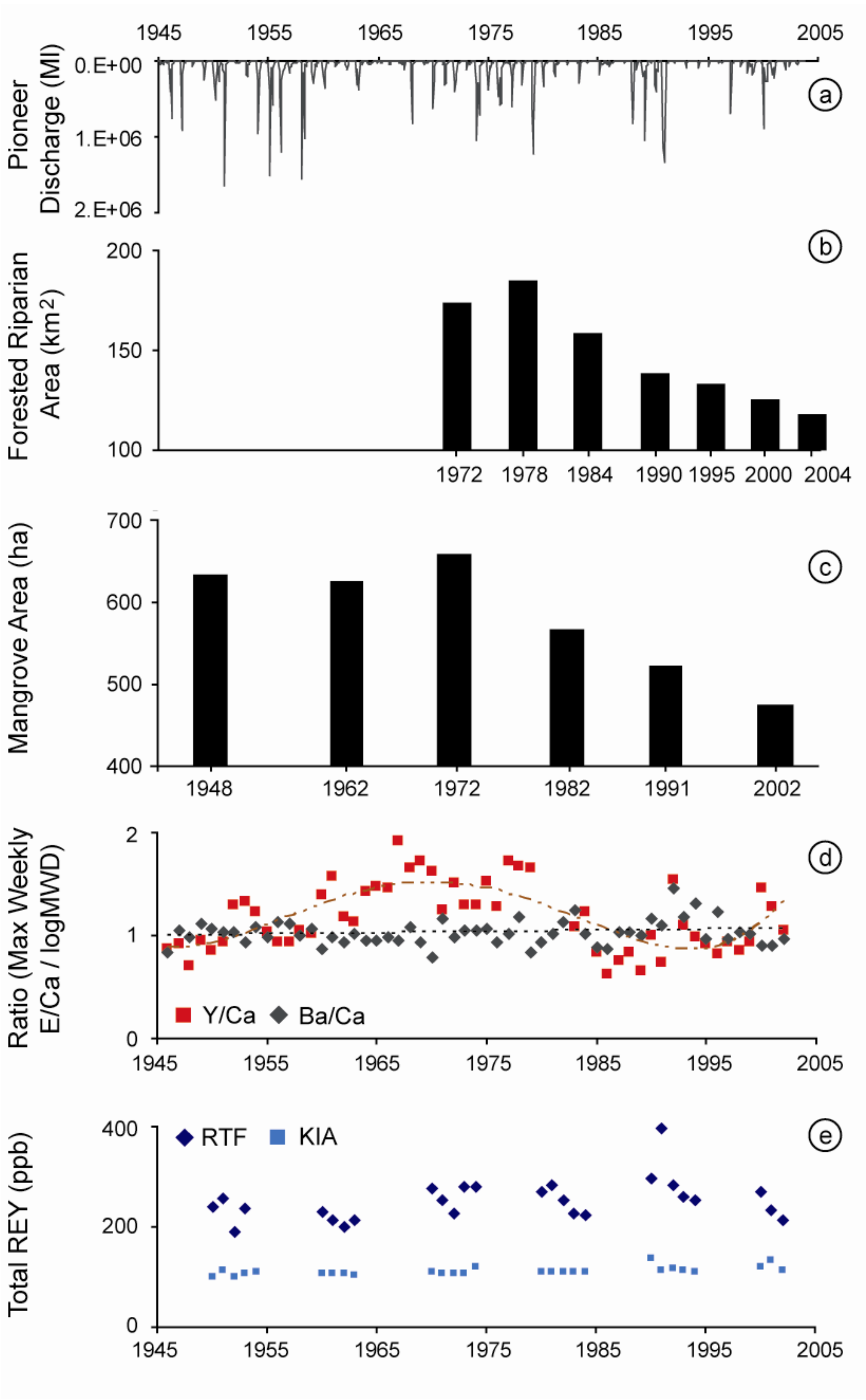

Pioneer Discharge (Ml)
0.E+00
1.E+06
2.E+06
1945
1955
1965
1975
1985
1995
2005
ⓐ
Forested Riparian Area (km^2)
200
150
100
1972
1978
1984
1990
1995
2000
2004
ⓑ
Mangrove Area (ha)
700
600
500
400
1948
1962
1972
1982
1991
2002
ⓒ
Ratio (Max Weekly E/Ca / logMWD)
2
1
0
■ Y/Ca
◆ Ba/Ca
1945
1955
1965
1975
1985
1995
2005
ⓓ
Total REY (ppb)
400
200
0
◆ RTF
■ KIA
1945
1955
1965
1975
1985
1995
2005
ⓔ

Figure 6.9. Proportions of benthic cover by (a) live hard corals, (b) soft corals, (c) crustose coralline algae (CCA) and turf algae, (d) macroalgae, (e) rubble and sand, and (f) other for five study sites (RT = Round Top Island; KS = Keswick and St. Bees Islands; SC = Scawfell Island; DR = Derwent Island; PO = Big and Little Kindemar Reefs in the Pompey Complex). The length of the box represents the range of the 25th to 75th percentiles of values with the median value denoted by the horizontal line. The bars show the range of values that fall within ± 1.5 times the difference between the top and bottom of the box. Asterisks represent outlier values above or below this range.

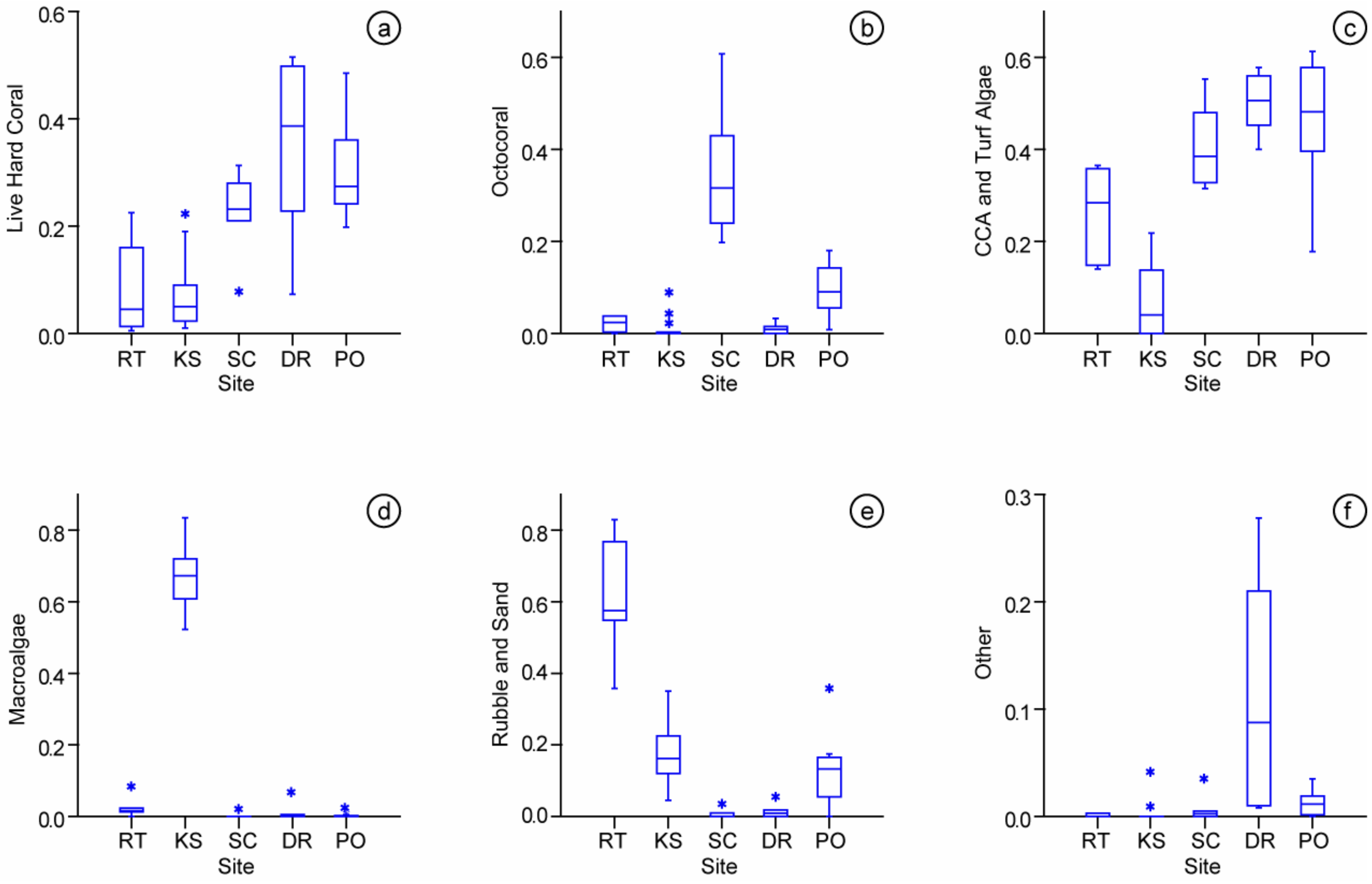
a
Live Hard Coral
0.0
0.2
0.4
0.6
RT
KS
SC
DR
PO
Site
b
Octocoral
0.0
0.2
0.4
0.6
RT
KS
SC
DR
PO
Site
c
CCA and Turf Algae
0.0
0.2
0.4
0.6
RT
KS
SC
DR
PO
Site
d
Macroalgae
0.0
0.2
0.4
0.6
0.8
RT
KS
SC
DR
PO
Site
e
Rubble and Sand
0.0
0.2
0.4
0.6
0.8
RT
KS
SC
DR
PO
Site
f
Other
0.0
0.1
0.2
0.3
RT
KS
SC
DR
PO
Site

Figure 6.10. (a) Coral assemblage off the northwestern corner of Round Top Island, dominated by *Turbinaria* spp. (19 September 2003). (b) *Sargassum* spp. dominating reef structure at Keswick Island. (7 March 2006). (c) High octocoral cover in Refuge Bay, Scawfell Island. (12 March 2006).

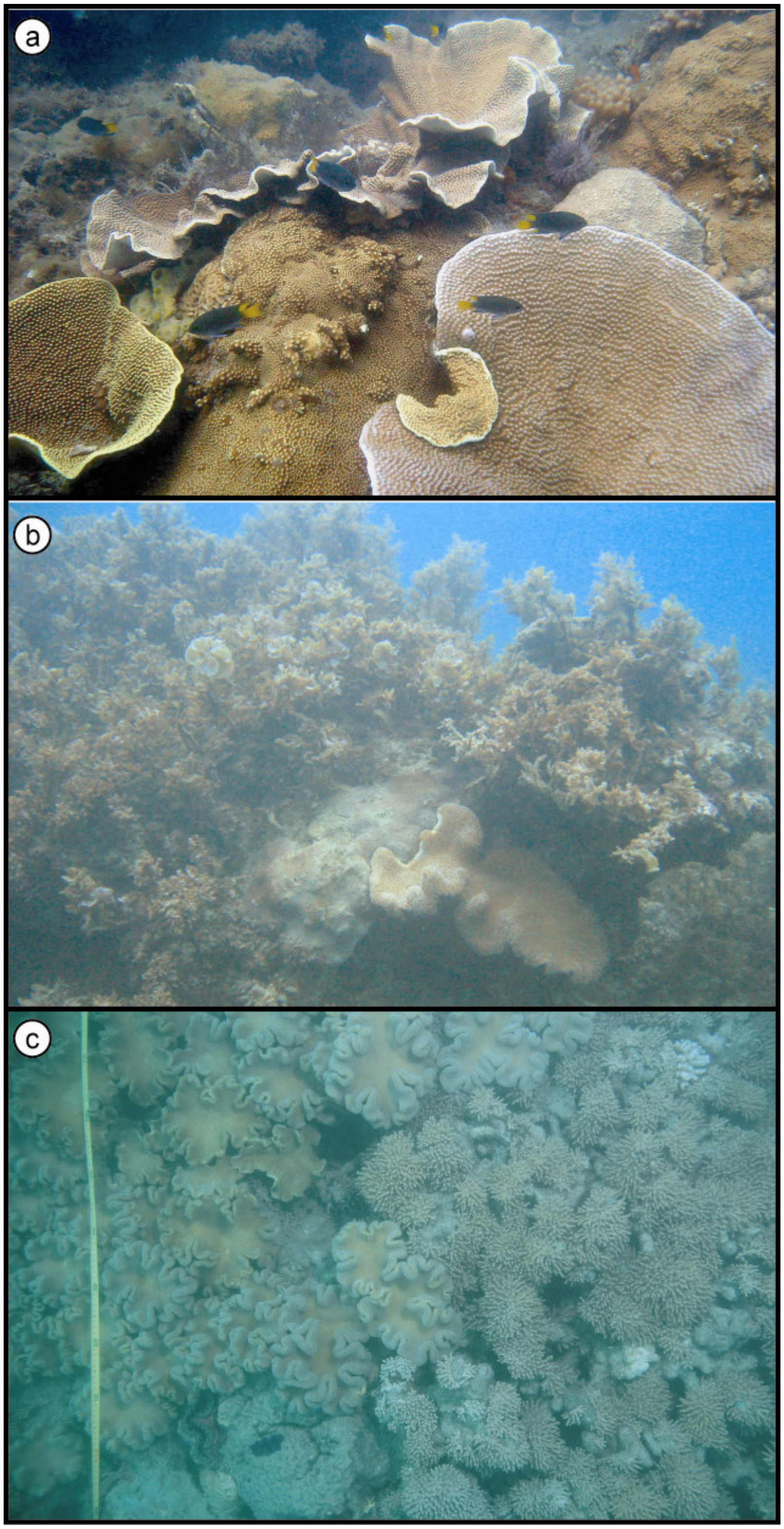
a
b
c

Appendix A. Regional Ecosystems of the Pioneer River Catchment

Regional ecosystem (RE) class codes and descriptions were assigned by QEPA based on their regional ecosystem description database (QEPA 2005). Total estimated pre-clear and mapped 2001 areas are reported, as well as the % remnant for REs that have been reduced over time. Because polygons containing several REs were merged with the dominant RE class (see Chapter 2), the totals reported here for some classes are larger than those reported in the QEPA attribute tables for pre-clearing and 2001 distributions.

Regional Ecosystem	Dominant vegetation, land form and rock type	Pre-clear area (ha)	2001 area (ha)	% remnant
8.1.1	Mangrove vegetation of marine clay plains and estuaries. Estuarine wetland	973.2	729.3	74.9
8.1.2	Samphire open forbland to isolated clumps of forbs on saltpans and plains adjacent to mangroves	12.9	12.6	97.8
8.1.3	*Sporobolus virginicus* grassland on marine sediments. Estuarine wetland	48.4	41.8	86.4
8.1.4	*Paspalum* spp. and *Fimbristylis ferruginea* sedgeland/grassland (estuarine wetland). Includes areas of deep open water with clumps of *Schoenoplectus littoralis* ± *Eleocharis dulcis*	199.8	128.1	64.2
8.2.1	*Casuarina equisetifolia* open forest to woodland with *Ipomoea pes-caprae* and *Spinifex sericeus* dominated ground layer on foredunes	0.0	43.9	
8.2.2	Microphyll vine forest on coastal dunes	0.0	10.0	
8.2.6a*	*Corymbia tessellaris* + *Acacia leptocarpa* + *Banksia integrifolia* + *Melaleuca dealbata* + beach scrub species open forest on coastal parallel dunes	99.0	38.7	39.1
8.2.7a	*Melaleuca* spp. and/or *Lophostemon suaveolens* and/or *Eucalyptus robusta* open woodland to open forest in wetlands associated with parabolic dunes	64.8	55.6	85.9
8.2.9	*Heteropogon triticeus* , *Imperata cylindrica* and *Themeda triandra* grassland on coastal dunes	226.4	87.2	38.5
8.2.13a	*Corymbia tessellaris*, *Melaleuca* spp., *Livistona decipiens* and/or *Acacia* spp. and/or *Lophostemon suaveolens* open to closed forest on dune sands mixed with alluvial material ± marine sediments	430.4	28.9	6.7
8.3.1a	Semi-deciduous notophyll/mesophyll vine forest fringing watercourses on alluvial plains	3416.2	1768.4	51.8
8.3.2	*Melaleuca viridiflora* woodland often with emergent eucalypts and grassy/herbaceous ground layer, on seasonally inundated alluvial plains with impeded drainage	2618.6	90.1	3.4

* Letters (a, b, or c) are vegetation communities within the listed RE. They could be mapped as separate classes on a larger scale (QEPA 2005).

(Appendix A cont.)

Regional Ecosystem	Dominant vegetation, land form and rock type	Pre-clear area (ha)	2001 area (ha)	% remnant
8.3.3a,x1**	*Melaleuca leucadendra* or *M. fluviatilis* ± *Casuarina cunninghamiana* open forest to woodland, fringing watercourses	2199.3	3000.0	136.4
8.3.4	Freshwater wetlands with permanent water and aquatic vegetation including *Phragmites australis*, *Nymphaea gigantea*, *Nymphoides indica*, *Eleocharis* spp., *Cyperus* spp., and *Juncus* spp.	18.3	8.1	44.3
8.3.5	*Corymbia clarksoniana* + *Lophostemon suaveolens* + *Eucalyptus platyphylla* woodland, or *E. platyphylla* woodland on alluvial plains	24661.3	1375.4	5.6
8.3.6a	*Eucalyptus tereticornis*, *Corymbia intermedia* and *Lophostemon suaveolens* (or *C. tessellaris* dominant) open forest on alluvial levees and lower terraces	11078.4	1038.2	9.4
8.3.10	Notophyll vine forest with variable dominants, on gently to moderately sloping alluvial fans adjacent to ranges	300.3	27.1	9.0
8.3.11	*Melaleuca* spp. aff. *viridiflora* closed forest to woodland in broad drainage areas (wetlands)	1155.2	70.7	6.1
8.3.12	Grassland on alluvial and old marine plains	1621.8	25.2	1.6
8.3.13a	*Eucalyptus tereticornis* and/or *Corymbia tessellaris* and/or *Melaleuca* spp. open woodland to open forest on alluvial and old marine plains, often adjacent to estuarine areas	5.6	5.6	100.0
8.8.1a,b	Complex notophyll (feather palm) vine forest on Tertiary basalt	1088.6	1085.8	99.7
8.11.1	*Eucalyptus drepanophylla* and *E. platyphylla* woodland on hills formed from metamorphosed sediments	533.3	364.4	68.3
8.11.2	Notophyll/microphyll vine forest ± *Araucaria cunninghamii* on low ranges on Permian sediments ± volcanics	16.5	16.5	100.0
8.11.3a	Mixed eucalypt including *Corymbia intermedia*, *Eucalyptus portuensis*, *C. clarksoniana*, *E. platyphylla* and *E. drepanophylla* woodland to open forest on low hills, on metamorphosed sediments	1368.0	950.4	69.5

** Although 8.3.3a and 8.3.3x1 were merged, the "x1" notation means that this is probably a new ecosystem which has not yet been described in the regional ecosystem description database (QEPA 2005).

(Appendix A cont.)

Regional Ecosystem	Dominant vegetation, land form and rock type	Pre-clear area (ha)	2001 area (ha)	% remnant
8.11.4	*Eucalyptus platyphylla* , *Corymbia clarksoniana* , and *E. drepanophylla* woodland on low undulating areas on metamorphosed sediments	419.9	51.0	12.1
8.11.5a	*Corymbia tessellaris* and *Eucalyptus tereticornis* ± *E. drepanophylla* woodland on low hills formed from metamorphosed sediments or conglomerate	73.8	73.8	100.0
8.12.11a	Semi-deciduous microphyll vine forest/thicket with emergent *Araucaria cunninghamii* in coastal areas including islands, on Mesozoic to Proterozoic igneous rocks and Tertiary acid to intermediate volcanics and granite	7.6	7.6	100.0
8.12.12a	Variable *Corymbia* spp. ± *Eucalyptus tereticornis* ± *E. platyphylla* ± *E. drepanophylla* ± *E. portuensis* woodland on lower and mid-slopes of ranges on Mesozoic to Proterozoic igneous rocks	35319.2	30958.0	87.7
8.12.13a	*Xanthorrhoea latifolia* subsp. *latifolia* or *Imperata cylindrica* grassland, including some areas recently colonised by *Timonius timon* shrubland, on slopes of islands and headlands, on Mesozoic to Proterozoic igneous rocks and Tertiary acid to intermediate volcanics	16.6	16.6	100.0
8.12.17a	Notophyll mossy evergreen vine forest on mountain slopes and summits subject to regular mist cover, on Mesozoic to Proterozoic igneous rocks	721.5	721.5	100.0
8.12.1a	Complex notophyll (feather palm) vine forest often with *Acmena resa* and *Syzygium wesa* , of wet uplands on Mesozoic to Proterozoic igneous rocks	1932.3	1915.1	99.1
8.12.2	Notophyll to complex notophyll vine forest often with *Argyrodendron actinophyllum* subsp. *diversifolium* ± *A. polyandrum* , on drier uplands and coastal ranges on Mesozoic to Proterozoic igneous rocks	18543.4	18368.7	99.1
8.12.3a	Notophyll rainforest/microphyll rainforest often with *Argyrodendron polyandrum* and *Paraserianthes toona* , ± *Araucaria cunninghamii* , on low to medium ranges on Mesozoic to Proterozoic igneous rocks	5429.1	5307.5	97.8
8.12.5a	*Corymbia intermedia* , *E. portuensis* ± *Lophostemon* spp. ± *Syncarpia glomulifera* ± *Banksia integrifolia* , open forest on Mesozoic to Proterozoic igneous rocks	1145.0	1130.4	98.7

(Appendix A cont.)

Regional Ecosystem	Dominant vegetation, land form and rock type	Pre-clear area (ha)	2001 area (ha)	% remnant
8.12.7a,c	*Corymbia citriodora* ± *Eucalyptus portuensis* ± *E. drepanophylla* (or *E. crebra*) open forest to woodland on hillslopes and undulating plateaus, on Mesozoic to Proterozoic igneous rocks	14287.7	14106.1	98.7
8.12.9	*Eucalyptus tereticornis* ± *Lophostemon suaveolens* ± *Corymbia intermedia* woodland to open forest on undulating uplands, on Mesozoic to Proterozoic igneous rocks	1686.1	1686.1	100.0
8.12.23	*Eucalyptus moluccana* woodland on elevated tablelands on Mesozoic to Proterozoic igneous rocks	4.8	4.8	100.0
8.12.26	*Corymbia tessellaris* and/or *Eucalyptus tereticornis* open forest ± vine thicket understorey on hill slopes of islands and near coastal areas, on Mesozoic to Proterozoic igneous rocks, and Tertiary acid to intermediate volcanics	0.0	13.9	
8.12.27a	*Eucalyptus tereticornis*, *Corymbia tessellaris*, *Livistona decipiens* ± *C. intermedia* ± rainforest pioneering spp. open forest, on low hills on Mesozoic to Proterozoic igneous rocks	2436.8	618.1	25.4
8.12.31a,b	*Corymbia intermedia* and *Allocasuarina* spp. open to closed forest, or *Allocasuarina* spp. closed forest to closed shrubland on moist upper slopes and ridges of ranges, on Mesozoic to Proterozoic igneous rocks	6481.7	6427.8	99.2
8.12.32	*Corymbia intermedia* grassy open forest on extensive plateaus on high ranges, on Mesozoic to Proterozoic igneous rocks	7836.9	6696.8	85.5
11.3.4	*Eucalyptus tereticornis* and/or *Eucalyptus* spp. tall woodland on alluvial plains	8553.5	6834.2	79.9
11.3.25b	*Eucalyptus tereticornis* or *E. camaldulensis* woodland fringing drainage lines	22.6	22.6	100.0
11.12.1a	*Eucalyptus crebra* woodland on igneous rocks	1888.0	1408.3	74.6
11.12.3	*Eucalyptus crebra*, *E. tereticornis*, *Angophora leiocarpa* woodland on igneous rocks especially granite	438.5	109.8	25.0
11.12.6a	*Corymbia citriodora* open forest on igneous rocks (granite)	125.9	116.8	92.7
cleared	Area cleared for agriculture, predominantly on alluvial plains	0.0	50993.3	